Área de Genética,
Departamento de Biología Experimental,
Facultad de Ciencias Experimentales,
Universidad de Jaén.

Análisis funcional de MCPH1 en la condensación cromosómica y el control del ciclo celular

TESIS DOCTORAL

María de la Cabeza Arroyo López

Jaén 2018

Área de Genética
Departamento de Biología Experimental
Facultad de Ciencias Experimentales
Universidad de Jaén

TESIS DOCTORAL

Análisis funcional de MCPH1 en la condensación cromosómica y el control del ciclo celular

MARIA DE LA CABEZA ARROYO LOPEZ

2018

Análisis funcional de MCPH1 en la condensación cromosómica y el control del ciclo celular

Dirigida por los doctores:

J. Alberto Marchal Ortega **Antonio Sánchez Baca**

Memoria presentada por la licenciada María de la Cabeza Arroyo López para optar al Grado de Doctor Internacional en Biología.

Junio, 2018

El presente trabajo ha sido realizado en el Área de Genética del Departamento de Biología Experimental de la Universidad de Jaén durante los años 2014-2018, período durante el cual el Doctorando disfrutó de una *Ayuda para la Formación de Personal Investigador* con cargo al *Plan de Apoyo a la Investigación, Desarrollo Tecnológico e Innovación* de la Universidad de Jaén. Además, parte de este trabajo se ha llevado a cabo en el "Department of Genetics, Cell Biology and Developoment, University of Minnesota", gracias a unas ayudas para estancias breves proporcionadas por la organización EMBO y la Escuela de Doctorado de la Universidad de Jaén. La investigación realizada ha sido financiada en parte por la Universidad de Jaén a través del proyecto UJA/2011/12/36, y la Junta de Andalucía a través del programa "Ayudas a grupos de Investigación (BIO-220).

Parte de los resultados de este estudio han sido recogidos en las siguientes publicaciones científicas: Chromosoma (2015) 124:491–501 DOI 10.1007/s00412-015-0512-2; Scientific Reports (2017) 7: 13019 DOI:10.1038/s41598-017-12793-7. Además, también han sido presentados en el "19th International Chromosome Conference"; en el "EMBO Workshop on Cell Division: Molecular Machineries and Cancer Targeted Therapies"; en el "XL Congreso de la Sociedad Española de Genética"; y en las ediciones VIII y IX del Seminario de Citogenética.

AGRADECIMIENTOS

Quiero expresar mi más sincero agradecimiento:

A los doctores Juan Alberto Marchal Ortega y Antonio Sánchez Baca, porque no habría podido caer en mejores manos. Esta tesis doctoral no habría sido posible sin su apoyo y su dedicada dirección. Con ellos di mis primeros pasos en la ciencia, de ellos he aprendo todo y espero poder seguir aprendiendo aún más. Agradezco y admiro su actitud siempre positiva, amable y humilde, porque no solo me han enseñado protocolos, también me han transmitido sus valores personales y su motivación incansable. Ellos han hecho que la ciencia sea mi principal vocación.

A Duncan J. Clarke y Ryoko Kuriyama. Jamás habría imaginado que al otro lado del mundo iba a encontrar otro laboratorio con dos personas tan dedicadas y amables, que se implicarían tanto en mi trabajo. Su colaboración y su experiencia ha sido fundamental y lo seguirá siendo.

A Jesús Calahorra, por su ayuda y sobre todo su paciencia con los muchos y muchos WB que hemos hecho (y los que nos queden…), siempre buscando el mejor resultado.

A Ana Rosa Cañuelo Navarro, por todo lo que he aprendido de ella, los conocimientos y la buena energía transmitida a nivel personal y profesional.

A Jorge Nicolás Dominguez Macías, por su gran sentido del humor y por crear un buen ambiente de trabajo con esas bromas que a veces tardo en pillar. Y por supuesto por su ayuda y su orientación como el gran profesional que es.

A los doctores Heidemarie Neitzel, Karl Sperling y Marc Trimborn (Charite Hospital, Berlín) por haber cedido las líneas de linfoblastos utilizadas en este trabajo, así como diversos reactivos, anticuerpos y oligos siRNA. Su asesoramiento en la realización de este estudio ha sido imprescindible.

Al doctor Tatsuya Hirano (RIKEN Advanced Science Institute, Japón) por proporcionar el anticuerpo frente a MCPH1, y por los comentarios y sugerencias aportadas.

Al doctor J. Francisco Giménez-Abián (CIB, Madrid), por las ideas y discusiones científicas aportadas, que han sido muy importante en los aspectos relacionados con el ciclo celular.

A todos mis compañeros de la sala de becarios y del labo, a los que están y a los que no. Gracias a Ismael y a Maribel, que fueron los que me dieron la mano durante mis primeros pasos en el laboratorio. Aunque haya llovido mucho, no me olvido de ellos. A Vero, por ser la más simpática

del Área de Genética y ayudarme a socializar con todos, por echarme una mano siempre que he necesitado algo.

A mi pareja, por aguantar tantas charlas de ciencia, agobios a veces, por cruzar el charco conmigo y ayudarme a desconectar siempre que lo necesito. En fin, por estar al pie del cañón las 24 horas. A Armando y Mariloli, que desde que entré en sus vidas me han animado y apoyado, convirtiéndose en una parte fundamental de mi vida.

A mi familia, porque qué sería yo sin mi familia. Los que lo dan todo por mí, los que han estado siempre ahí, pacientemente, aguantando mis malos momentos y mis errores sin esperar nada a cambio.

ÍNDICE

ÍNDICE

RESUMEN/ABSTRACT

RESUMEN

El gen *MCPH1* es uno de los implicados en el síndrome de microcefalia primaria (MCPH), una enfermedad rara consecuencia de una alteración en la neurogénesis que determina una reducción drástica en el tamaño cerebral, con el consiguiente retraso mental asociado. A diferencia de los otros genes MCPH identificados, los pacientes por mutaciones en *MCPH1* muestran una alteración en el ciclo celular que afecta a todos los tipos celulares analizados. Por tanto, la importancia de este gen trasciende su papel como regulador de la neurogenésis humana, siendo un elemento clave para la coordinación del proceso de condensación cromosómica con el resto de mecanismos que participan de la mitosis. Además, su función también es importante en la respuesta celular frente al daño en el ADN. Por todo ello el síndrome asociado al gen *MCPH1* es un modelo experimental interesante para el estudio de las bases moleculares de la división mitótica, y su importancia en los mecanismos reguladores que controlan el desarrollo cerebral humano. En esta tesis doctoral se presentan nuevos resultados sobre la función específica del gen *MCPH1* durante la mitosis y su contribución en las vías moleculares que controlan su puesta en marcha en células humanas.

En primer lugar, se ha demostrado que la estructura de los cromosomas metafásicos está alterada de manera específica en ausencia de función para el gen *MCPH1*. En concreto, en células de pacientes MCPH1 con diferentes tipos de mutaciones el análisis detallado de la morfología cromosómica identificó varias alteraciones, como ejes cromatídicos hiperenrollados con morfología ondulada distintiva (denominada “twisted”), cromátidas hermanas de menor longitud y con problemas de resolución, así como pérdida de la cohesión centromérica. Estos defectos podrían ser consecuencia de un superenrollamiento extremo de los ejes cromatídicos centrales. Estos resultados confirman que la función de MCPH1 es importante en el mecanismo que controlan la organización y formación del cromosoma mitótico. En concreto, algunas de las alteraciones identificadas - resolución de las cromátidas y cohesión centromérica – sugieren la existencia de una nueva función molecular para este gen, aún por definir.

Otro aspecto estudiado ha sido la contribución de *MCPH1* en la dinámica de condensación cromosómica y la progresión del ciclo celular en ausencia de daño en el ADN. Este análisis era de importancia ya que los estudios previos similares se habían focalizado principalmente en el contexto de daño en el ADN. Los resultados obtenidos demuestran que cuando falta la función de este gen la progresión a través de la fase G2 del ciclo celular y la posterior entrada en mitosis no se ve retrasada. Esto concuerda también con otros resultados que muestran que las células con condensación cromosómica prematura en pacientes MCPH1, denominadas PLCs, no son positivas

para varios marcadores mitóticos. Además, la tasa de entrada en mitosis sigue dinámicas similares tanto en controles sanos como en células de pacientes MCPH1. En conjunto, estos resultados confirman que las PLCs corresponden a células en las fases G2 o G1 del ciclo, que surgirían como consecuencia de una descoordinación entre la condensación cromosómica y la progresión normal del ciclo celular.

Además, se ha puesto de manifiesto un nuevo fenotipo celular asociado a la falta de función de este gen. Así, el alineamiento cromosómico completo en la placa metafásica está significativamente retrasado en células sin función para *MCPH1*, lo que indica que este gen es esencial para una eficiente biorientación cromosómica durante mitosis. Este descubrimiento también resulta de especial interés al demostrar que la duración total de la mitosis está incrementada en células sin función para *MCPH1*. Esto podría ser un factor a considerar en el mecanismo patogénico responsable del síndrome de microcefalia primaria. En concreto, un incremento en la duración de la mitosis podría tener un gran impacto en la neurogénesis y afectar a la producción final de neuronas, mientras que en otros tipos celulares dicha alteración no tendría consecuencias tan importantes.

Diversos estudios previos habían demostrado que MCPH1 participa en las vías de señalización del daño en ADN dependientes de ATR, además de en el proceso mismo de reparación del daño. Sin embargo, su importancia en otros puntos de control del ciclo celular que regulan la transición G2/M no había sido analizada hasta ahora. En concreto, hemos investigado la contribución de *MCPH1* en el denominado "*decatenation checkpoint*" (DC), punto de control operativo durante la fase G2 del ciclo que monitoriza la actividad de Topoisomerasa II sobre el ADN. Los resultados obtenidos demuestran que MCPH1 no participa en la activación de este punto de control; sin embargo, su función si es requerida para la adaptación celular al mismo. Así, cuando carecen de la función de este gen las células no son capaces de adaptarse espontáneamente al DC e iniciar la división celular, permaneciendo paradas en G2 de modo permanente. Además, la habilidad de cafeína, un conocido inhibidor de las quinasas ATR/ATM, para inducir una adaptación celular forzada al DC también está comprometida.

A la vista de estos resultados, se realizaron más análisis experimentales para caracterizar en detalle la vía de señalización que regula esta respuesta adaptativa y el papel concreto de *MCPH1* en la misma. En este contexto, se ha demostrado que la función de CHK1 es necesaria para que la activación del DC de lugar a una parada del ciclo celular en G2 eficiente. Además, CHK1 estaría localizado por debajo de MCPH1 en la vía de señalización que controla la adaptación celular a este punto de control. La función de PLK1, al igual que MCPH1, también es esencial para esta respuesta adaptativa. En ausencia de función para PLK1 el DC produce una parada permanente en G2 tanto

en células control como en células sin función para MCPH1 y/o CHK1, lo que emplazaría a PLK1 por debajo de MCPH1 y CHK1 en la vía de señalización que controla la adaptación celular. WEE1 también es otro factor que confiere robustez a la parada del ciclo celular inducida por el DC, aunque aún está por discernir cuál es su papel concreto en la vía de señalización comentada.

En conjunto, estos resultados ayudan a comprender mejor cuales son los factores genéticos que confieren adaptación celular a los puntos de control, un proceso aún no bien entendido y que tiene una implicación importante, entre otros, en la biología del cáncer. La participación de MCPH1 en este mecanismo, así como su contribución en la señalización y reparación del daño en el ADN son de importancia también en este contexto y podrían explicar en parte las evidencias recientes que señalan a *MCPH1* como posible diana terapéutica en cáncer.

ABSTRACT

MCPH1 is one of the genes mutated in primary microcephaly, a rare syndrome consequence of alterations during neurogenesis that result in a drastic reduction of brain size and mental retardation. Unlike the rest of MCPH genes identified, patient cells with mutations in MCPH1 show alterations during the cell cycle observable in all cell types. Therefore, the importance of this gene goes beyond its role as regulator of human neurogenesis, being a key element for coupling chromosome condensation with other processes involved in mitosis. In addition, MCPH1 function is important for the cellular response to DNA damage. According to these evidences, MCPH1 syndrome is an interesting model to get new insights into the molecular basis of mitotic cell division and its importance for human brain development. In this Phd. thesis it is presented new data about the specific functions of MCPH1 during mitosis and its contribution into the molecular pathways controlling mitosis onset in human cells.

First it is demonstrated that the organization and structure of mitotic chromosomes is altered in a specific manner when MCPH1 function is loss. In particular, the detailed analyses of chromosome morphology in MCPH1 patients with different type of mutations led to the identification of several alterations as hypercoiled chromatid axes of distinctive morphology (named as “twisted”), sister chromatids with length reduction and resolution problems, as well as loss of centromeric cohesion. These defects might be consequence of an extreme hypercoiling of central chromatid axes. These results confirm that MCPH1 function is important for the mechanism controlling the shaping of mitotic chromosomes. In particular, some of these alterations – sister chromatids resolution and centromeric cohesion – point to a novel molecular function of this gene that remains to be elucidated.

Other investigated issue was how MCPH1 contributes to chromosome condensation dynamic and cell cycle progression during undamaging cell division cycles. This analysis was important to establish since previous studies were focused into the role of MCPH1 during cell cycle progression under conditions where DNA is damaged. Our results clearly demonstrate that cells lacking MCPH1 function progress through G2 phase of cell cycle and enter into mitosis without delay compared with controls. These data agree with others results showing that cells with premature chromosome condensation, characteristic of MCPH1 syndrome and named as PLCs, are negative for mitotic markers. Moreover, the rate of mitosis onset follows similar dynamics in both healthy controls and MCPH1 patient cells. Altogether, these results confirm that PLCs correspond with

cells in G2 or G1 phase of cell cycle that arise as consequence of chromosome condensation being uncoupled from normal cell cycle progression.

Our analyses have revealed a new cellular phenotype linked to MCPH1 loss of function. Thus, full chromosome alignment in the metaphase plate is significantly delayed in cells lacking the function of this gene, pointing out its importance for the process of chromosome biorentation during mitosis. This finding is of special interest since, as consequence, the timing of mitosis is increased in cells without MCPH1 function. A lengthened mitosis is an important factor to consider for the current discussions about the pathogenic mechanisms of MCPH1 primary microcephaly. Even a subtle increase in the duration of mitosis could deeply impact the final production of neurons during neurogenesis, while in other tissues types it would not induce noticeable alterations.

Several studies demonstrate that MCPH1 is involved in the ATR- dependent pathway signaling DNA damage, as well as in the DNA repair process itself. However, its importance for others cell cycle checkpoints regulating G2/M transition is less known. In particular, we have investigated MCPH1 contribution to the decatenation checkpoint (DC), a less understood pathway which monitors Topoisomerase II activity on the DNA during G2 phase of cell cycle. The results obtained clearly demonstrate that MCPH1 is not involved in the DC activation pathway; however, its function is required during cellular adaptation to this checkpoint. Thus, cells lacking MCPH1 function have no capacity of spontaneously adapt to the DC, being permanently arrested in the G2 phase of the cell cycle. Moreover, the ability of caffeine, a well-known inhibitor of ATM/ATR kinases, to induce adaptation is strongly perturbed in MCPH1 depleted cells

Considering these evidences we have performed further analyses in order to get a detailed characterization of the pathway regulating this adaptive response as well as the exact role of MCPH1 within it. In this context, our analyses have demonstrated that CHK1 function is required for the DC to achieve an efficient cell cycle arrest in G2. Furthermore, CHK1 might act downstream of MPCH1 in the pathway that controls cellular adaptation to this checkpoint. PLK1 function, similarly to MCPH1, is also essential for the adaptive response. If PLK1 is inhibited, the DC triggers a permanent G2 arrest in control and either MCPH1 and/or CHK1 depleted cells. These results suggest that PLK1 is downstream of MCPH1 and CHK1 in the pathway that controls cellular adaptation to the DC. WEE1 is another factor that restrains spontaneous adaptation to the decatenation checkpoint; however its specific role in this pathway is still not well characterized.

Taking together, these results are of importance to better understand the genetic requirements of cells to allow adaptation to G2 checkpoints, a poorly understood process with direct implications in

cancer biology. The contribution of MCPH1 to this mechanism, as well as its importance for DNA damage signaling and repair, might explain recent evidences pointing to MCPH1 as therapeutic target in cancer.

INTRODUCCIÓN

INTRODUCCIÓN

1. Microcefalia primaria autosómica recesiva (MCPH)

1.1 Bases clínicas

El síndrome de microcefalia primaria (MCPH, OMIM 606858) es una enfermedad con patrón de herencia autosómica recesivo caracterizada por un trastorno en el desarrollo neuronal que produce una pronunciada microcefalia y retraso mental moderado, estando ausentes en la mayoría de los casos otras malformaciones congénitas severas o déficits neurológicos significativos (Jackson et al., 2002; Woods, 2004). La reducción en el tamaño cerebral, que es aproximadamente un tercio del tamaño normal, afecta principalmente a la región del córtex mientras que la arquitectura del cerebro se mantiene aparentemente inalterada (Bond et al., 2002). La microcefalia suele ser evidente a partir de la 32ª semana de gestación, se observa claramente desde el nacimiento y no es progresiva, a diferencia de la microcefalia secundaria, en la cual el tamaño del cerebro es el esperado al nacer, pero falla en su crecimiento posterior (Woods, 2004).

El síndrome MCPH pertenece al grupo de las enfermedades raras, con una incidencia estimada en las poblaciones que varía entre 1/30,000 a 1/250,000 (Van Den Bosch, 1959; Mochida et al., 2001; Kumar et al., 2002). Sin embargo, este síndrome es mucho más frecuente en poblaciones con un elevado grado de consanguineidad, como ocurre en algunas regiones de Turquía, Norte de Paquistán e India (incidencia 1/10,000) (Suri, 2003; Kaindl et al., 2010). Entre los criterios para su diagnóstico clínico se incluyen una circunferencia occipital-frontal reducida (-3 SD, al menos tres unidades por debajo de la desviación estándar de la media correspondiente por edad y sexo), cara de tamaño normal y frente muy inclinada, cerebro de pequeño tamaño con patrón gyral normal o simplificado, retraso mental medio o moderado a partir del primer año de vida y personalidad afable (Woods, 2004). En la mayoría de los casos no existen reseñas en estos pacientes de otras alteraciones clínicas que afecten al crecimiento o metabolismo, si bien algunos pueden presentar cierto retraso en el crecimiento (Trimborn et al., 2004; Woods et al., 2005; Mahmood et al., 2011; Liu et al., 2016).

Se han propuesto varias hipótesis para explicar el desarrollo de este síndrome. Una de ellas plantea la existencia de algún tipo de alteración mitótica durante la neurogénesis como desencadenante de su desarrollo anómalo (Woods, 2004; Klingseisen y Jackson, 2011). En concreto, las células progenitoras neuronales siguen procesos de división diferenciales, uno simétrico, que da lugar a dos

nuevas células progenitoras, y otro asimétrico, en el que se origina una neurona postmitótica y una nueva célula progenitora (Finlay y Darlington, 1995; Rakic, 1988; Mochida et al., 2001; Woods y Bond, 2005). Según este escenario, pequeñas alteraciones en la ejecución coordinada de ambas divisiones durante el desarrollo podrían desembocar en una drástica disminución del número de neuronas y, consecuentemente, en una masa cerebral reducida (Thornton y Woods, 2009; Leroy y Frias, 2005). Otras hipótesis alternativas plantean incrementos en el nivel de apoptosis y/o senescencia celular como origen para la microcefalia en pacientes MCPH (Kumar et al., 2009). También se ha propuesto que la aparición de algún tipo de alteración en los mecanismos de reparación del ADN, frente a los cuales serían más sensibles las células neuroprogenitoras, podría contribuir al desarrollo de esta patología (O'Driscoll y Jeggo, 2008). Las causas propuestas en las distintas hipótesis no serían mutuamente excluyentes, y queda aún por demostrar la influencia real de cada una como desencadenantes de esta enfermedad.

Hay una relación directa entre tamaño cerebral e inteligencia medible entre diferentes especies de homínidos y otros mamíferos (Evans et al., 2004A; 2004B; Mochida y Walsh 2001; Rushton et al., 2007). En casi todas las condiciones en las que el tamaño del cerebro está reducido significativamente, la capacidad intelectual también se ve afectada, como es el caso de los pacientes MCPH. Una cuestión llamativa es que el cerebro de estos pacientes es similar en tamaño al que presentaban las primeras especies de homínidos (400 cm^3), lo que ha llevado a algunos investigadores a considerar el síndrome MCPH como un modelo de estudio sobre los mecanismos reguladores responsables de la expansión cerebral en humanos (Evans et al., 2005; Ponting y Jackson 2005; Lancaster et al., 2013). En el linaje de las diferentes especies de homínidos hay evidencias descritas de selección evolutiva y cambios genéticos acumulados en el tiempo en la mayoría de los genes implicados en el síndrome de microcefalia primaria (Wang et al., 2008; Leroy y Frias, 2005; Roberts et al., 2002; Woods et al., 2005; Vallender y Lahn, 2004). Este proceso acumulativo podría haber determinado que en un intervalo de 3-5 millones de años el cerebro de algunos de nuestros ancestros triplicara su tamaño en comparación con otras especies cercanas (Thornton y Woods, 2009).

1.2 Bases genéticas

La microcefalia primaria es un síndrome monogénico con un elevado grado de heterogeneidad génica. El primero de los genes implicados, denominado *MCPH1* (también conocido como *MICROCEPHALIN* o *BRIT1*), fue identificado en el año 2002 (Jackson et al., 2002). Desde esa

fecha hasta hoy se han identificado mutaciones en otros 19 genes más que dan lugar a la aparición de este síndrome (Tabla I-1).

El síndrome MCPH es un ejemplo de cómo han evolucionado los métodos de identificación de genes implicados en enfermedades durante los últimos 20 años. Así, en los primeros genes MCPH la identificación se basaba en la localización primero del locus, mediante mapeo fino de homocigosidad con SNPs o microsatélites. Posteriormente, los genes incluidos en el locus eran priorizados y analizados por secuenciación "Sanger" hasta encontrar alguna mutación patogénica. Esta estrategia, de elevado coste y esfuerzo, empezó a reemplazarse a finales de la primera década del siglo XXI por otras, que no requieren de un mapeo previo del locus, basadas en técnicas NGS ("*Next Generation Sequencing*"), principalmente la secuenciación exómica masiva (WES, "*Whole Exome Sequencing*"). En el caso del síndrome MCPH, mientras que en 2010 solo cinco de los genes habían sido identificados, actualmente el número de genes MCPH caracterizados alcanza los 20.

1.2.1 Genes MCPH y fenotipo clínico

El fenotipo clínico que presentan la mayoría de los pacientes con mutaciones en estos genes es muy similar, y en algunos casos indistinguible (Woods et al., 2005; Passemard et al., 2009; 2011A; Kaindl et al., 2010). Sin embargo, al ser un síndrome con elevada heterogeneidad génica y alélica, su espectro clínico muestra alguna variabilidad según el gen implicado y las diferentes mutaciones del mismo (Venkatesh et al., 2014). Por ejemplo, una de las variaciones más común es el grado de reducción del tamaño cerebral, que puede ser desde ligera a muy severa. A continuación, se comentan las variaciones en el fenotipo clínico que se han descrito en pacientes con mutaciones en los genes de los distintos locus implicados.

Si bien la estructura del cerebro en la mayoría de los casos se mantiene normal, cuando está mutado el gen *WDR62* (locus MCPH2) el espectro de manifestaciones clínicas es más amplio e incluye lisencefalia y polimicrogiria (Bilgüvar et al., 2010) o alteraciones en el cuerpo calloso (Yu et al., 2010). En el caso de mutaciones en el gen *CDK5RAP2* (MCPH3) se ha descrito afectación de las habilidades sensoriales como ceguera o audición reducida (Pagnamenta et al., 2012; Lancaster et al., 2013), mientras que los pacientes asociados a mutaciones de *COPB2* (MCPH19) muestran ceguera cortical con cuerpo calloso anormalmente delgado, poca expansión ventricular y mielinización retardada (DiStasio et al., 2017). También hay casos de pacientes con microcefalia primaria que sufren de ataxia, como en las mutaciones del gen *STIL* (MCPH7) (Darvish et al.,

2010), o muertes prematuras o a corta edad, en el caso de MCPH10 (Kakar et al., 2015). Éstos últimos se caracterizan por tener una circunferencia occipital extremadamente reducida (-9 SD) y muerte prematura normalmente con un año de edad. Para el síndrome asociado a este locus, los estudios neuropatológicos mostraron una severa pérdida de neuronas, así como menor polaridad de las mismas, acompañado de una maduración dendrítica anormal. En estos individuos, el córtex cerebral era más pequeño que el cráneo, lo que apunta a una posible degeneración secundaria, y el cerebelo estaba afectado de forma similar. Los individuos afectados también mostraban bajo peso y talla en el nacimiento, lo que indica cierta afectación de las células somáticas (Yang et al., 2012). Esto último también es común al locus MCHP13 (Mirzaa et al., 2014) y MCPH14, en el que algunos afectados son incapaces de andar y además presentan otras malformaciones cerebrales (Khan et al., 2014).

Entre las variantes con síntomas clínicos más graves destaca el del locus MCPH15, ya que los pacientes muestran una reducción del tamaño cerebral progresiva (hasta -6.2 SD), severo retraso en el desarrollo psicomotor, y otros déficits neurológicos como cuadriplejía espástica, la forma más grave de parálisis cerebral (Guemez-Gamboa et al., 2015). MCPH17 es otro ejemplo de microcefalia primaria que parece ser degenerativa, reduciéndose el tamaño cerebral a lo largo del tiempo de vida del individuo (hasta -12 SD). En los casos más severos aparece lisencefalia con hipoplasia en el bulbo raquídeo y cerebelo (Harding et al., 2016).

1.2.2 Genes MCPH: función molecular

De los veinte genes identificados actualmente en el síndrome MCPH, casi todos ellos tienen en común el estar implicados en la mitosis y/o bien expresarse de forma específica en tejido nervioso. A continuación, se resumen las principales evidencias acerca del papel molecular y la contribución de los mismos al desarrollo de microcefalia.

Los análisis celulares demuestran que muchos de los productos de los genes implicados en el síndrome MCPH se localizan en el centrosoma durante mitosis (Guernsey et al., 2010; Bond et al., 2005; Kouprina et al., 2005; Zhong et al., 2006). Durante la división celular, el centrosoma es el responsable de la organización de los microtúbulos en las células animales y contribuye a la unión eficiente y posicionamiento de las fibras del huso. Su ciclo de duplicación está coordinado con la replicación del ADN para evitar que haya más de dos centrosomas en una célula (Morris-Rosendahl et al., 2015).

Los productos de varios genes implicados en MCPH, están relacionados con la función centrosómica. Así, el gen MCPH1 coordina el ciclo de duplicación centrosómica con la entrada en mitosis (Gruber et al., 2011), mientras que otros codifican proteínas esenciales en la duplicación centrosómica (como *SAS-6, STIL, CPAP, CEP63, CEP135, y CEP152*) o bien constituyen proteínas centrosómicas per se, como *CDK5RAP2*, cuya función es localizar/señalizar los polos del huso durante mitosis (Hassan et al., 2007; Lizarraga et al., 2010).

Otro elemento esencial en el proceso de división celular es el huso mitótico. Esta estructura está formada por microtúbulos, fibras dinámicas polares, y cientos de proteínas que funcionan juntas orquestando la segregación cromosómica.

Durante la neurogénesis temprana, las células madre neuronales y las progenitoras se dividen simétricamente para incrementar su población, para lo que el huso tiene que estar orientado con precisión para permitir la segregación simétrica de factores pluripotentes entre las dos células resultantes. Una disposición anómala del huso supone una segregación asimétrica de estos factores, lo que produce una diferenciación prematura de la célula y una disminución en el número de células progenitoras neuronales (Woods y Basto, 2014). Dos de los genes que aparecen mutados más frecuentemente en pacientes MCPH, *ASPM* y *WDR62*, codifican para proteínas del huso mitótico (Bond et al., 2002; Bilguvar et al., 2010). ASPM es una proteína de gran tamaño que une a los extremos del huso mitótico y participa en el ensamblaje del mismo (do Carmo-Avides et al., 2001; Bond et al., 2002; Bond et al., 2003). WDR62 interactúa con la quinasa mitótica Aurora A, lo que también regula el ensamblaje del huso mitótico (Chen et al., 2014). A la luz de estos datos, algunos autores consideran que la disposición anormal del huso mitótico podría ser el mecanismo patológico causante del síndrome MCPH (Bilguvar et al., 2010; Yu et al., 2010).

El análisis de los ortólogos para algunos genes causantes del síndrome MCPH en *Drosophila* y/o pez cebra también sugieren un papel importante de dichos genes en la función centrosómica, la organización de los microtúbulos y la función del huso mitótico (Do Carmo-Avides y Glover 1999; Pfaff et al., 2007; Rickmyre et al., 2007). En ratón, los mutantes para *Wdr62* muestran un fenotipo característico de microcefalia en el que las células progenitoras neuronales presentan defectos en el ensamblaje del huso, lo que produce un enlentecimiento de la mitosis, parada del ciclo celular, y finalmente muerte celular (Woods y Basto, 2014). Sin embargo, el ortólogo de *ASPM* en moscas (*Asp*) interactúa con miosina-II regulando la migración nuclear interquinética y la morfogénesis del

cerebro, lo que indicaría una función no mitótica para *Asp* y, posiblemente también para *ASPM*, en el cerebro.

Los estudios de expresión génica en embriones de ratón y fetos humanos demuestran que los genes causantes de MCPH se expresan durante la división neurogénica (Kumar et al., 2009; Nicholas et al., 2010). Los resultados sugieren la existencia de algún tipo de mecanismo encargado de regular y coordinar la orientación espacial del huso mitótico durante el conjunto de divisiones simétricas y asimétricas en la neurogénesis (Fish et al., 2006; Gruber et al., 2011; Lancaster et al., 2013; Insolera et al., 2014). Este mecanismo resultaría fundamental para el correcto desarrollo del cerebro y su alteración podría originar la aparición de microcefalia primaria (Thornton y Woods, 2009). Según esta hipótesis, las células progenitoras neuronales serían más susceptibles que otros tipos de células progenitoras a las mutaciones en genes que codifican proteínas centrosómicas o del huso mitótico, como es el caso de muchos de los genes implicados en la aparición de microcefalia primaria.

Algunos de los genes causantes del síndrome MCPH identificados más recientemente tienen otras funciones, como *ZNF335*, codificante de un componente del complejo remodelador de cromatina que regula la expresión de genes neuronales y muerte celular (Yang et al., 2012). Otros ejemplos son *PHC1*, miembro del complejo represivo de genes polycomb 1 (Awad et al., 2013); MFSD2A, una proteína transmembrana que se localiza en células endoteliales vasculares del cerebro y forma parte de la barrera hematoencefálica (Guemez-Gamboa et al., 2015; Alakbarzade et al., 2015); *ANKLE2*, con un papel crítico en el ensamblaje de la envoltura nuclear al final de anafase (Asencio et al., 2012); CIT, una quinasa que actúa en diferentes rutas de señalización (Madaule et al., 1995); WDFY3, proteína que interactúa con P62 y regula la ubiquitinación proteica (Clausen et al., 2010); y finalmente *COPB2*, codificante de una subunidad del complejo de Golgi necesaria para su transporte hasta el retículo endoplasmático (DiStasio et al., 2017).

En el caso de *ANKLE2*, se han identificado mutaciones en su homólogo en Drosophila en los que en el tercer estado larvario el tamaño del cerebro se reduce progresivamente, mostrando un menor número de neuroblastos, menor proliferación celular e incremento de la apoptosis (Yamamoto et al., 2014).

Tabla I-1: Relación de locus y genes MCPH caracterizados hasta la fecha.

Locus	Cromosoma	Gen	Función	Referencia
MCPH1	8p23	*MCPH1* (microcefalina)	Reparación del daño en el ADN, condensación cromosómica	Jackson et al., (2002), Trimborn et al., (2004)
MCPH2	19q13.12-q13.2	*WDR62*	Orientación del huso mitótico	Nicholas et al., (2010)
MCPH3	9q33.2	*CDK5RAP2*	Regulación de la función de los microtúbulos, desarrollo del centrómero	Bond et al., (2005)
MCPH4	15q15-q21	*CASC5*	Ensamblaje del cinetocoro con el huso mitótico	Jamieson et al., (1999), Genin et al., (2012)
MCPH5	1q31.1	*ASPM*	Orientación de los husos mitóticos durante la neurogénesis embrionaria	Shen et al., (2005)
MCPH6	13q12.12	*CENPJ*	Control de la longitud del centriolo, función de los microtúbulos	Bond et al., (2005)
MCPH7	1p33	*STIL*	Organización de los husos, progresión del ciclo celular	Kumar et al., (2009)
MCPH8	4q12	*CEP135*	Control del número de centrosomas	Hussain et al., (2012)
MCPH9	15q21.1	*CEP152*	Proteína centrosómica	Guernsey et al., (2010)
MCPH10	20q13.12	*ZNF335*	Regulación de la actividad del complejo encargado de la metilación de histona H3K4	Yang et al., (2012)
MCPH11	12p13.31	*PHC1*	Regulación de la expresión génica	Awad et al., (2013)
MCPH12	7q21.2	*CDK6*	Progresión de ciclo celular, organización de microtúbulos	Hussain et al., (2013)
MCPH13	4q24	*CENPE*	Elongación del huso mitótico, movimiento de los cromosomas	Mirzaa et al., (2014)
MCPH14	1p21.2	*SASS6*	Duplicación del centriolo	Khan et al., (2014)
MCPH15	1p34.2	*MFSD2A*	Células endoteliales vasculares del cerebro	Guemez-Gamboa et al., (2015)
MCPH16	12q24.33	*ANKLE2*	Reconstrucción de la membrana nuclear al final de anafase	Yamamoto et al., (2014)
MCPH17	12q24.23	*CIT*	Proteína-quinasa	Li et al., (2016)
MCPH18	4q21.23	*WDFY3*	Marcaje de estructuras citoplasmáticas para autofagia (se expresa únicamente en tejido neuronal)	Kadir et al., (2016)
MCPH19	3q23	*COPB2*	Subunidad del aparato de Golgi	DiStasio et al., (2017)
MCPH20	1q32.1	*KIF14*	Perteneciente a la superfamilia de las quinesinas, proteína motora asociada a microtúbulos	Makrythanasis et al., (2018)

A pesar de que se han hecho grandes progresos en nuestro conocimiento sobre el desarrollo del cerebro y las bases genéticas del síndrome MCPH, todavía no se dispone de una respuesta concreta a la pregunta principal: ¿por qué las mutaciones en los genes causantes de MCPH afectan exclusivamente al neuroepitelio? Queda patente que estos genes controlan una amplia gama de procesos celulares, muchos de ellos directamente relacionados con la mitosis como la maduración de los centrosomas, y la organización y funcionamiento del huso mitótico. Ligeras perturbaciones en la función de los mismos podrían alterar el equilibrio entre proliferación y muerte celular, división simétrica y asimétrica o diferenciación normal o anormal, teniendo como consecuencia principal una reducción en el número total de células neuroprogenitoras y neuronas diferenciadas en el cerebro en desarrollo, lo que en conjunto se manifestaría como microcefalia (Barbelanne y Tsang, 2014). Además, las divisiones celulares neurogénicas en el cerebro ocurren en su mayor parte durante un periodo de tiempo concreto en el desarrollo embrionario, aunque también ocurren de forma minoritaria en regiones muy concretas en el cerebro adulto (Woods et al., 2004). Probablemente, esto contribuya a las diferencias observadas entre el desarrollo embrionario del cerebro y otros órganos y partes del cuerpo, al ser éstos últimos menos susceptibles a mutaciones en alguno de los genes causante de MCPH por abarcar su desarrollo un periodo de tiempo más amplio.

1.3 Bases ambientales

Además de cómo síndrome genético, la microcefalia primaria también puede ocurrir por causas externas ambientales que alteren la neurogénesis embrionaria durante el embarazo, tales como consumo de alcohol, derivados opiáceos o infección por toxoplasma (Krauss et al., 2003; Woods y Bond, 2005). Estos agentes externos ambientales podrían alterar la expresión de genes clave durante la neurogénesis embrionaria, bien de manera directa o indirectamente al afectar el intercambio normal de factores de origen materno a través de la placenta.

La implicación final de los genes relacionados con el síndrome MCPH en este escenario está aún por demostrar, aunque ya hay algunos estudios que muestran una relación causal directa, en concreto para el gen *MCPH1*. Durante el desarrollo embrionario en ratón, el uso de antagonistas del péptido vasoactivo intestinal (VIP), un conocido factor materno inductor de crecimiento embrionario (Gressens et al., 1993), inhibe la expresión del gen *Mcph1*, lo que determina la aparición de microcefalia primaria (Passemard et al., 2011B).

2. Microcefalia primaria MCPH1

El gen *MCPH1* (también denominado "*microcephalin*"), está localizado en 8p23.1 y contiene una pauta de lectura abierta (ORF) de 8,032 pb. Este gen está compuesto por 14 exones y codifica una proteína de 835 aminoácidos denominada microcefalina o BRIT1. Esta proteína contiene tres dominios BRCT ("*BReast cáncer gene Carboxy-Terminal domain*"), uno N-terminal y dos C-terminales, además de una secuencia señal de localización nuclear (*Nuclear Localization Signal*) (Figura I-1 B). Los dominios BRCT están presentes en proteínas que participan en la señalización del daño en el ADN (Gavvovidis et al., 2012), y median interacciones de tipo proteína-proteína y proteína-ADN (Huyton et al., 2000). En humanos, sus genes homólogos más cercanos son la proteína de unión a Topoisomerasa II tipo 1 (TOPBP1) y BRCA1 (Ponting y Jackson, 2005).

Mientras que los tres dominios BRCT de la proteína y las regiones cercanas a éstos están muy conservados, las secuencias centrales son altamente variables en la mayoría de los vertebrados, lo que implica que MCPH1 es una proteína que ha sufrido una rápida evolución (Yamashita et al., 2011). Así, *MCPH1* muestra un 57% de identidad total con su gen ortólogo en ratón, mientras que en las regiones más conservadas correspondientes a los dominios BRCT la identidad es del 80% (Jackson et al., 2002). El gen *Mcph1* en ratón tiene una organización similar a la observada en humanos y codifica para una proteína con un tamaño de 822 aminoácidos (Koonin et al., 1996; Huyton et al., 2000). La estructura de esta proteína está conservada evolutivamente en metazoos, habiéndose descrito genes que codifican una proteína con estructura equivalente en dos modelos animales de invertebrados, *Drosophila melanogaster* y *Caenorhabditis elegans* (Ponting y Jackson, 2005).

En humanos se ha documentado la existencia de al menos seis isoformas de la proteína MCPH1, codificadas por diferentes transcritos originados por "*splicing"* alternativo (Figura I-1 A). De todas ellas, los análisis sobre los niveles y el patrón de expresión sugieren que solo dos isoformas tienen relevancia funcional, mientras que las demás probablemente sean subproductos de "*splicing"* (Gavvovidis et al., 2012). La isoforma denominada "*Full Lenght*" (MCPH1-FL), está codificada por un transcrito que contiene los 14 exones del gen y que da lugar a la proteína completa (835 aminoácidos). La otra isoforma con relevancia funcional es de menor tamaño (610 aminoácidos) al estar codificada por un transcrito que carece de los últimos seis exones (MCPH1-Δe9-14). En esta isoforma están ausentes los dos dominios BRCT C-terminales incluidos en la isoforma MCPH1-FL (Gavvovidis et al., 2012). Ambas isoformas difieren en el patrón de expresión en cerebro fetal,

siendo ésta cinco veces mayor para la isoforma MCPH1-Δe9-14, mientras que sus niveles de expresión son más similares en otros tejidos fetales y adultos. Por otro lado, la expresión de ambas isoformas está sujeta a una regulación diferencial durante el ciclo celular. Mientras que los niveles de MCPH1-FL disminuyen desde mitad de la fase S a la G2, para MCPH1-Δ9-14 disminuyen en la fase S temprana, pero se incrementan al final de la fase S y durante G2. También existen evidencias de funciones diferenciales para cada una de las isoformas, en concreto en los procesos de reparación del ADN y en la condensación cromosómica (Gavvovidis et al., 2012) (ver más adelante).

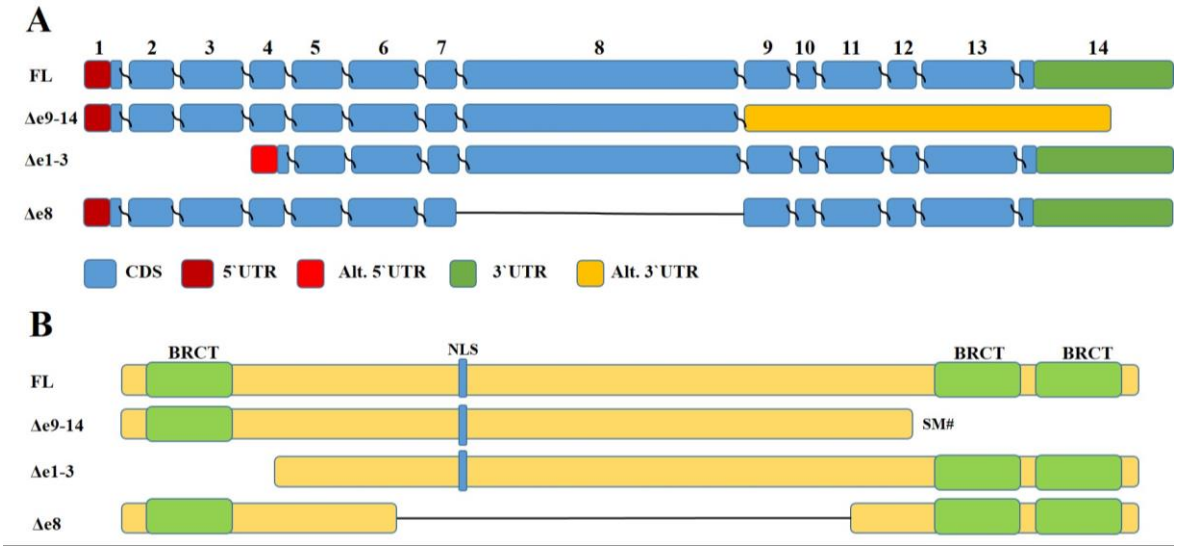

Figura I-1: Estructura de los diferentes transcritos descritos del gen *MCPH1* generados por "splicing" alternativo y las isoformas generadas a partir de los mismos A) Transcrito para la isoforma "*Full-Length"* (FL) y los transcritos alternativos Δe9-14, Δe1-3, y Δe8 difieren en la composición de exones y la región 3'UTR; Los rectángulos numerados representan exones, los coloreados en azul indican regiones codificantes (CDS), los rojos regiones 5´UTR y los verdes 3`UTR. La región 3`UTR de la isoforma Δe9-14 difiere de las demás y está resaltada en amarillo. B) Polipéptidos esperados generados a partir de los diferentes transcritos de MCPH1. Los rectángulos verdes indican la posición de los dominios BRCT, los azules marcan la posición de la señal de localización nuclear (NLS). Dos aminoácidos adicionales, S y M, se incluyen en MCPH1-Δe9-14, debido al cambio en la pauta de lectura que origina finalmente la terminación prematura (#).

2.1 MCPH1 y microcefalia primaria: mutaciones descritas

Se han descrito un total de 14 mutaciones distintas en homocigosis para este gen en pacientes con microcefalia primaria tipo MCPH1. Ocho de ellas dan lugar a proteínas incompletas: dos mutaciones sin sentido en el exón 2 (Jackson et al., 2002) y en el exón 4 (Farooq et al., 2010); dos inserciones de una base en el exón 5 y en el exón 6 (Trimborn et al., 2004; Darvish et al., 2010); y una deleción de una base en el exón 8 (Hussain et al., 2013). También se han descrito dos mutaciones que alteran el patrón de "*splicing"* (Darvish et al., 2010; Ghafouri-Fard et al., 2015); cuatro mutaciones no sinónimas (Trimborn et al., 2005; Darvish et al., 2010; Leung et al., 2011; Darvish et al., 2010) y siete grandes deleciones (Garshasbi et al., 2006; Darvish et al., 2010; Pfau et al., 2013; Hemmat et al., 2017; Ahmad et al., 2017) (Figura I-2, Tabla I-2).

La mutación en homocigosis en una secuencia de *splicing* del intrón 4 resulta en un fallo de procesamiento del ARN. Curiosamente, dentro de la misma familia esta mutación da lugar a diferentes fenotipos según el sexo: a pesar de que en el hombre se observó un notable retraso mental, la mujer afectada presentaba inteligencia normal, al igual que sus habilidades motoras y lingüísticas. Esto podría explicarse por variaciones sexuales específicas durante el desarrollo del cerebro o por otros mecanismos como genes modificadores (Ghafouri-Fard et al., 2015; Shi et al., 2015). Las deleciones que involucran a varios exones también parecen causar un fenotipo de microcefalia más severo que las mutaciones puntuales (Hemmat et al., 2017).

La mayoría de las mutaciones no sinónimas en el gen *MCPH1* han sido descritas en pacientes con un fenotipo clínico moderado, en comparación con las mutaciones sin sentido o las que inducen cambios en la fase de lectura (Woods et al., 2005; Trimborn et al., 2004; Gharshasbi et al., 2006). Por ejemplo, la mutación Thr27Arg altera la polaridad y carga en un residuo de la proteína altamente conservado, ya que se localiza dentro del dominio BRCT N-terminal (Huyton et al., 2000; Trimbron et al., 2005). De este modo, el análisis de mutaciones no sinónimas que inducen pérdida de función de la proteína es de importancia para la identificación de regiones con especial relevancia funcional dentro de la mismo (Ghani-Kakhi et al., 2012).

Tabla I-2: Mutaciones descritas para el gen MCPH1 en pacientes con microcefalia primaria. Los asteriscos señalan las mutaciones concretas que contienen las líneas celulares de pacientes empleadas en nuestro trabajo.

Mutación	**Alteración molecular y fenotipo**	**Referencia**
Transversión 74C-G en el exón 2, Sustitución S25X (c.74G>C, Ser25X)*****	Mutación en el primer dominio BRCT. Expresión residual de proteína con pérdida del dominio BRCT N-terminal. Reducción del tamaño cerebral -5 a -10 SD	Jackson et al., (2002); Alderton et al., (2006)
Inserción de 1 base en exón 5, 427insA, generando codón de parada prematura en exón 6 y proteína truncada de 146 aa (c.427_428insA)*****	Pérdida funcional de la proteína. Pacientes con condensación cromosómica prematura.	Neitzel et al., (2002) Trimborn et al., (2004)
Transición c80C>G, T27R	Microcefalia primaria moderada (-2.5 SD) y fracción de PLCs reducida en comparación con la fracción encontrada para mutaciones sin sentido.	Trimborn et al., (2005)
Deleción de 150- a 200-kb que incluyen el promotor y los primeros 6 exones del gen	Afectados con retraso mental, microcefalia moderada (-3 SD) y condensación cromosómica prematura (10-15% de las células).	Garshasbi et al., (2006)
Inserción de 1 base en exón 6, 566insA (c.566_567insA)	Afectados con microcefalia (-6 SD), retraso mental moderado y condensación cromosómica prematura.	Darvish et al., (2010)
Transversión 147C-G en el exón 3, sustitución H48Q	Afectados con microcefalia (-7 a -9 SD), retraso mental moderado y condensación cromosómica prematura. Afecta al primer dominio BRCT.	Darvish et al., (2010)
Transición 215C-T en exón 3, sustitución S72L	Afectados con microcefalia (-6 a -7 SD), retraso mental moderado y condensación cromosómica prematura. Afecta al primer dominio BRCT.	Darvish et al., (2010)
Transversión 302C-G en exón 4, sustitución S101X(c.302C>G, Ser101X)	Afectado con microcefalia, craneosinostosis, ptosis, micrognatia, y alta sensibilidad al daño en ADN. Pérdida de los dos dominios BRCT C-terminales.	Tommerup et al., (1993), Farooq et al., (2010)
Mutación en lugar de *splicing* c.436+16>T, exón 5	Microcefalia severa, -9 SD.	Darvish et al., (2010)
Mutación de cambio de sentido c.149T>G, Val50Gly	Alteración en los dominios BRCT N-terminales. Microcefalia moderada.	Leung et al., (2011)
Mutación de cambio de sentido c.215C>T, Ser72Leu	Exón 3, cambio en la polaridad del aminoácido, -6.2 SD	Ghani-Kakhki et al., 2012
Mutación de cambio de sentido c.223T>C, Trp75Arg*	Exón 3, cambio en la polaridad del aminoácido, -5.7 SD	Ghani-Kakhki et al., 2012
Deleción de una base, c.1179delG en el exón 8, R393S	Microcefalia de moderada a severa, -8 to -10 SD.	Hussain et al., (2013)
Mutación en lugar de *splicing* c.322-2A>T	Deleción de 15 nucleótidos en el exón 5 del transcrito de ARN mensajero (r.322_336del15, R108_Q112del5).	Ghafouri-Fard et al., (2015)
Microdeleciones de 160 kb y 570 kb	Afectan a los dos o a los once primeros exones del gen respectivamente	Ahmad et al., (2017)
Microdeleción de 250 kb	Descrita en una familia consanguínea de origen hispano, abarca los ocho primeros exones de *MCPH1*.	Hemmat et al., (2017)

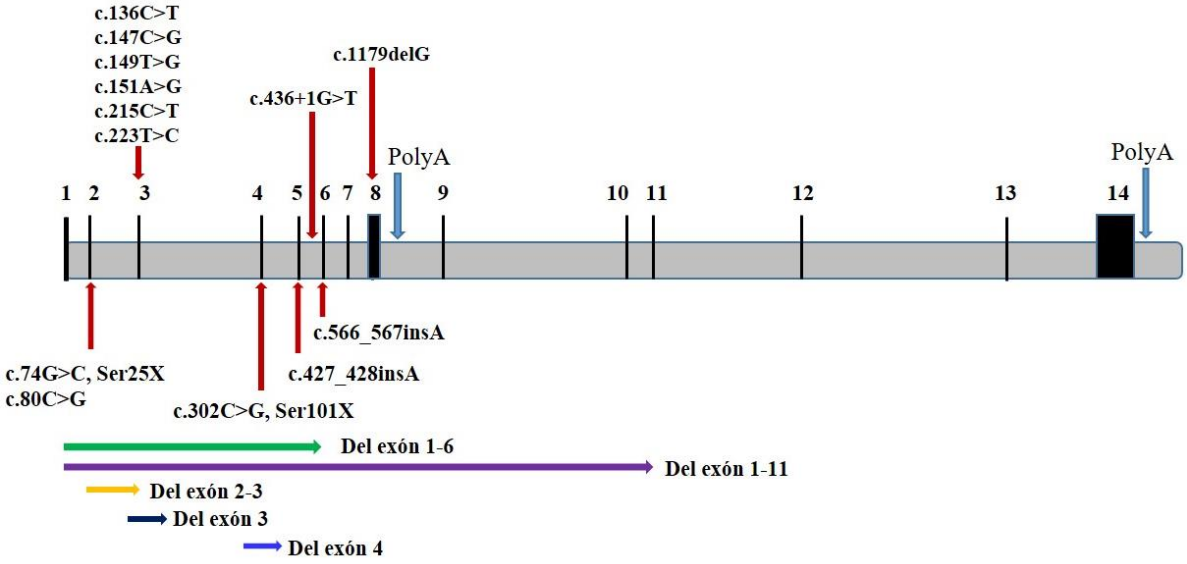

Figura I-2: Representación esquemática del gen MCPH1 y las posiciones de las mutaciones descritas para el mismo en pacientes con microcefalia primaria. La extensión de las deleciones se indica con flechas horizontales coloreadas bajo la estructura del gen. Los 14 exones del gen se corresponden con las líneas o rectángulos negros. Entre éstos, las regiones no codificantes en gris.

2.2 Expresión y localización subcelular de MCPH1

Una cuestión llamativa es que la expresión de algunos genes relacionados con MCPH no es exclusiva del neuroepitelio. *MCPH1* es un ejemplo representativo ya que se expresa en la mayoría de tipos celulares analizados, lo que es indicativo de un papel más general en otras funciones celulares además de controlar la mitosis neuroepitelial. Así, este gen se expresa de manera generalizada en todos los tejidos humanos adultos, siendo sus niveles más elevados en cerebro, testículo, páncreas e hígado (Lin et al., 2010). Durante la etapa embrionaria en humanos, muestra niveles altos en el cerebro fetal, riñón e hígado, y niveles más bajos en el corazón embrionario y pulmones (Jackson et al., 2002). En embriones de ratón, se ha detectado la expresión de *Mcph1* en los ventrículos laterales del prosencéfalo (Jackson et al., 2002). Igualmente, se han detectado transcritos de este gen durante todo el desarrollo embrionario de *Drosophila*, desde embriones a adultos (Brunk et al., 2007). La proteína MCPH1 se localiza en el centrosoma en la línea celular humana U2OS (osteosarcoma) y en la DT-40 de pollo (Zhong et al., 2006; Jeffers et al., 2008). También se localiza en "*hot-spots*" de reparación del ADN en células U2OS, HeLa (carcinoma

cervical), y líneas celulares de linfoblastos derivadas de pacientes MCPH1 (Rai et al., 2006; Wood et al., 2007; Gavvovidis et al., 2010).

Además de en estas líneas celulares, en cultivos primarios realizados a partir de tejido ovárico y en el tejido mamario la localización de MCPH1 es citoplasmática y nuclear, concretamente en puntos o *foci* nucleares (Bruning-Richardson et al., 2011). En el contexto fisiológico, la localización de MCPH1 ha sido estudiada también en *Drosophila*, donde se encuentra en el ADN de células interfásicas en embriones de esta especie, estando ausente en el ADN de las células desde prometafase a telofase (Brunk et al., 2007).

3. Funciones moleculares de MCPH1

3.1 Condensación cromosómica

Los análisis citogenéticos en pacientes con microcefalia primaria por mutaciones en el gen MCPH1 han permitido identificar un fenotipo celular llamativo con importantes implicaciones funcionales. Así, en las preparaciones mitóticas obtenidas de estos pacientes siempre se observa una fracción muy elevada (10-20%) de células con cromatina condensada similares a profases mitóticas ((Trimborn et al., 2005; Garshasbi et al., 2006; Darvish et al., 2010; Farooq et al., 2010; Leung et al., 2011; Hussain et al., 2013; Ghafouri-Fard et al., 2015; Ahmad et al., 2017; Hemmat et al., 2017 (Figura I-3). Este fenotipo, denominado PLCs ("*Prophase-like cells*"), es consecuencia de un inicio prematuro del proceso de condensación cromosómica y un retraso en la descondensación cromosómica al final de mitosis (Neitzel et al., 2002).

La frecuencia de este fenotipo celular está directamente relacionada con el tipo concreto de mutación, y guarda también relación con el grado de microcefalia que muestra el paciente. Por ejemplo, en pacientes con mutaciones que dan lugar a la aparición de codones de parada prematuros en el gen *MCPH1* (S25X, T143NfsX5), la fracción de PLCs es muy elevada (7-17%) y la microcefalia es severa (entre -5 y -10 SD) (Neitzel et al., 2002; Trimborn et al., 2004). Por el contrario, en un paciente con una mutación no sinónima para este gen (T27A) la fracción de PLCs (3-4%) y el grado de microcefalia (-2.4 SD al nacer) son menos acusados (Trimborn et al., 2005). Otras mutaciones no sinónimas para este gen (S72L; T74A) originan un fenotipo clínico y celular mucho más severo dado que se localizan dentro de la región del gen que codifica para el dominio BRCT N-terminal (Ghani-Kakhki et al., 2012). Estos datos sugieren que ambos aspectos, tanto el

defecto celular en la condensación cromosómica como el fenotipo clínico, están correlacionados con el tipo de mutación y la localización de la misma dentro del gen *MCPH1*.

La implicación del gen *MCPH1* en el proceso de condensación cromosómica se ha demostrado también mediante análisis funcionales por RNAi en líneas celulares humanas HeLa y U2OS. Así el silenciamiento transitorio de su expresión era suficiente para originar la aparición del fenotipo PLC (Trimborn et al., 2004). Además, este fenotipo celular también se observó en un modelo de ratón "*knock-out*" para *Mcph1* (Trimborn et al., 2010). Curiosamente, aunque su ratio de supervivencia estaba reducida, estos animales no mostraban un fenotipo que recapitulara la microcefalia primaria humana ni presentaban problemas de fertilidad (Trimborn et al., 2010). Teniendo en cuenta estos datos, es evidente que la falta de función del gen *MCPH1* altera de manera clara y reproducible el proceso de condensación cromosómica no solo en diferentes tipos celulares sino también en distintas especies de mamíferos.

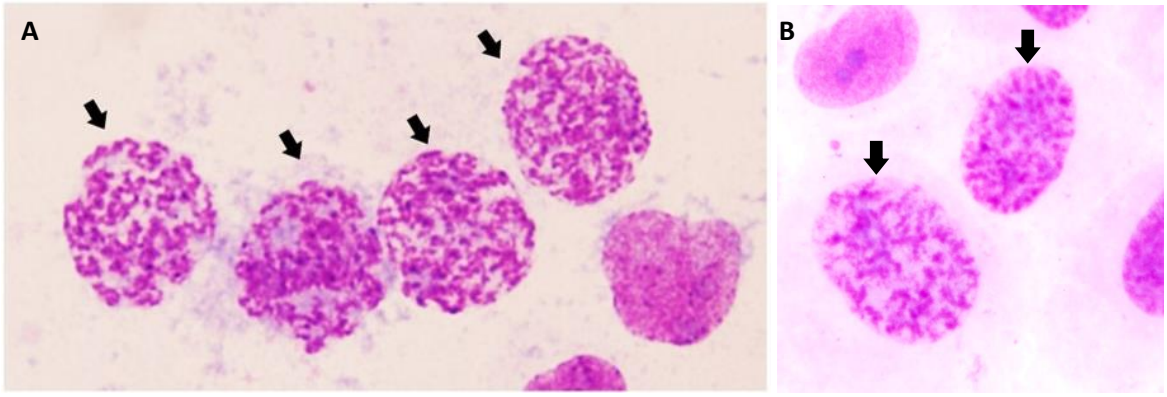

Figura I-3: Fotos ilustrativas del fenotipo PLC en: (A) células de pacientes con mutaciones en MCPH1, y (B) celulas U2OS (osteosarcoma) con silenciamiento temporal de la expresión de MCPH1. Las células que exhiben el fenotipo PLC (*Prophase-like cells*) se muestran señaladas con flechas.

3.1.1 Bases moleculares del proceso de condensación cromosómica

El proceso de condensación cromosómica implica la reorganización de todo el genoma en un conjunto de estructuras citológicas distinguibles denominadas cromosomas (Shintomi y Hirano, 2010). El conocimiento de este proceso ha ido avanzando conforme se han ido descubriendo algunos de los genes reguladores del mismo, aunque todavía no se conocen en detalle todos los mecanismos moleculares implicados.

Unos de los reguladores principales son los complejos condensina I y condensina II, que se unen al ADN e inducen su condensación (Hirano et al., 1997; Ono et al., 2003). Ambos están compuestos por una unidad estructural central formada por las subunidades ATPasa CAP-E/SMC2 y CAP-C/SMC4 (*Structural maintenance of chromosomes protein* 2 y 4), y por varias subunidades reguladoras de tipo no SMC que son diferentes para cada uno de ellos (CAP-D2, CAP-G y CAP-H en condensina I, y CAP-D3, CAP-G2 y CAP-H2 en condensina II) (Hirano, 2006). La actividad de ambos complejos de condensinas está regulada diferencialmente a lo largo del ciclo celular. Así, condensina I se localiza mayoritariamente en el citoplasma, y solo se une a la cromatina tras la rotura de la envoltura nuclear. Sin embargo, condensina II es nuclear durante todo el ciclo celular y se asocia a la cromatina al inicio de mitosis (Hirota et al., 2004; Ono et al., 2004). Estas diferencias parecen reflejar también una función específica en la arquitectura del cromosoma mitótico. Según esta visión, condensina II facilitaría uniones entre tramos de cromatina distanciados, algo fundamental para establecer un eje cromosómico, mientras que la condensina I llevaría a cabo la unión de bucles de ADN próximos sobre dicho eje (Ono et al., 2003; Green et al., 2012).

Además de la condensación progresiva que producen las condensinas, también es indispensable una organización concreta que permita la disposición paralela de las cromátidas hermanas a lo largo del eje cromosómico. Este proceso, denominado "resolución de cromátidas hermanas", implica la correcta formación de un armazón o eje en cada una de ellas y la pérdida simultánea de la cohesión que las mantiene próximas físicamente (Shintomi y Hirano, 2010; Losada et al., 2005A; Nasmyth y Haering, 2005). La cohesión entre cromátidas hermanas está mediada por dos tipos de fuerzas. Una la determina el grado de concatenación y superenrollamiento de la cromatina, y la otra es consecuencia de la actividad del complejo cohesina, responsable de mantener físicamente asociadas ambas cromátidas hermanas (Shintomi y Hirano, 2010).

El complejo multiproteico cohesina está muy conservado desde levaduras a humanos. Está compuesto por un heterodímero de las subunidades SMC1 y SMC3, y dos unidades adicionales no-SMC llamadas SCC1/MCD1/RAD21 y SCC3 (Guacci et al., 1997; Losada et al., 1998; Michaelis et al., 1997). La disociación de cohesina de la cromatina tiene lugar en dos fases consecutivas. En primer lugar, al inicio de profase comienza su disociación gradual de los brazos cromosómicos. Esta pérdida está determinada por la fosforilación directa de las quinasas PLK1 (*Polo-like kinase 1*) y Aurora B, de manera que al alcanzar metafase solo queda cohesina unida a la cromatina en el centrómero, quedando las cromátidas hermanas totalmente resueltas e independientes (Kitajima et al., 2006). La disociación final de cohesina de la cromatina centromérica, requisito indispensable para la segregación anafásica, es debida a la escisión de la subunidad RAD21/SCC1 mediada por

Separasa, la cual se activa una vez pasado el punto de control del huso mitótico (Waizenegger et al., 2000). El mantenimiento de una fracción residual de cohesina unida al centrómero es fundamental, y se consigue mediante fosfatasas que revierten los niveles de cohesina fosforilada (Kitajima et al., 2006; Tang et al., 2006).

Los superenrollamientos y concatenaciones en el ADN suponen un segundo factor implicado en la cohesión cromosómica y son consecuencia del proceso de replicación en sí mismo, que origina entrelazamientos entre las dos cadenas de ADN replicadas en las regiones donde convergen horquillas de replicación adyacentes (Roca y Wang 1994; Roca, 1995; Berger et al., 1996). La enzima encargada de eliminar los superenrollamientos que se establecen entre las cromátidas hermanas es Topoisomerasa II (Coelho et al., 2008). Se trata de una enzima homodimérica en la que cada monómero contiene tres dominios distintos (Lynn et al., 1986): un dominio N-terminal que contiene secuencias consenso de unión a ATP, un dominio central que contiene el sitio activo con un residuo de tirosina que se une covalentemente al ADN, y finalmente, un dominio C-terminal que constituye la región más variable de la enzima (Cortes et al., 2003). Puede mostrar dos configuraciones, de abrazadera abierta o de abrazadera cerrada en ausencia o presencia de ATP, respectivamente. Se diferencia de las Topoisomerasas tipo I por la reacción enzimática que llevan a cabo: mientras que éstas últimas producen roturas en una sola hebra del ADN y liberan la tensión asociada a superenrollamientos, las Topoisomerasas tipo II producen roturas transitorias en las dos hebras del ADN (DSBs, "*Double Strand Breaks*") y son capaces de pasar un dúplex intacto de ADN a través de otro dúplex asociado a la proteína y que contiene la rotura, por lo que son las únicas que pueden separar moléculas de ADN entrelazadas (Bower et al., 2010A; 2010B; Austin y Marsh, 1998; Burden y Osheroff, 1998).

En mamíferos existen dos isoformas de Topoisomerasa II, denominadas α y β, ambas codificadas por genes diferentes y con unas secuencias de aminoácidos con una similitud del 70% (Gromova et al., 1998; Wang et al., 2002; Watt et al., 1994; Austin et al., 1998; Biersack et al., 1996). Sin embargo, la actividad de ambas isoformas difiere bastante. Así, Topoisomerasa IIα es una proteína esencial que se expresa fundamentalmente en fase G2 y M, y está involucrada principalmente en la replicación del ADN y la segregación cromosómica. Por el contrario, Topoisomerasa IIβ no es esencial y se expresa de forma constitutiva durante todo el ciclo celular, teniendo un papel principal como reguladora de la transcripción (Goswami et al., 1996; Heck et al., 1988; Akimitsu et al., 2003; Ju et al., 2004, 2006; Kitagawa et al., 2003).

Además de sus funciones generales en el metabolismo del ADN, Topoisomerasa II tiene también funciones importantes en la condensación y organización de los cromosomas mitóticos. Este papel

recae fundamentalmente en Topoisomerasa IIα, ya que la contribución de Topoisomerasa IIβ parece ser necesaria únicamente en las etapas iniciales del acortamiento cromosómico axial (Vos et al., 2011; Nitiss et al., 2009). Topoisomerasa IIα parece tener también un importante papel estructural, ya que está presente en altos niveles en la matriz nuclear y en el armazón cromosómico (Laemli et al., 1992). Aunque su papel concreto en la arquitectura del cromosoma es motivo de cierta controversia, su presencia es crucial para la compactación del mismo, probablemente promoviendo la formación de concatenaciones dentro del propio cromosoma, siendo responsable de desenlazar el ADN entre las hebras hermanas replicadas (in trans) mientras que también produce la compactación en la misma molécula de DNA (in cis) (Farr et al., 2014).

Las concatenaciones entre las cromátidas tienen que ir resolviéndose conforme avanza la profase, mientras que las concatenaciones centroméricas deben mantenerse hasta la transición metafase/anafase (Diaz-Martínez et al., 2006; Santamaría et al., 2007). La actividad de Topoisomerasa IIα durante la condensación y segregación cromosómica está a su vez regulada por las condensinas y la cohesina (Piskadlo y Oliveira 2017). Topoisomerasa IIα juega un papel fundamental en el mantenimiento de la cohesión centromérica, bien de modo directo permitiendo la compactación y ensamblaje correcto del cinetocoro, o indirectamente mediando en la decatenación de las cromátidas hermanas en dicha región (Wang et al., 2008; Coelho et al., 2008; Maeshima et al., 2005). Este papel es indispensable para la posterior segregación anafásica: si su función es bloqueada tras la condensación cromosómica, las células quedan bloqueadas en metafase produciéndose fallos en la separación de las cromáticas (Clarke et al., 1993).

3.1.2 Papel del gen MCPH1 en la condensación cromosómica

La implicación del gen *MCPH1* en el proceso de condensación cromosómica podría ocurrir por diferentes vías moleculares. Por un lado, se ha demostrado que la falta de función de este gen origina condensación cromosómica prematura debido a una alteración de la función de la condensina II. Esta relación se demostró por silenciamiento temporal con RNAi de la expresión de los complejos condensina I y II en fibroblastos de pacientes con mutaciones en *MCPH1* (Trimborn et al., 2006). Así, mientras que el silenciamiento del complejo condensina I no tenía ningún impacto sobre la dinámica de las PLCs, cuando se silenciaba condensina II se observaba una drástica reducción de su frecuencia. Una reducción similar se obtenía cuando el gen *MCPH1* y la condensina II eran silenciados simultáneamente con oligos de siRNA en células HeLa, mientras que la fracción de PLCs se mantenía elevada cuando el gen *MCPH1* y la condensina I eran silenciados

conjuntamente. Además, estos resultados concordaban con la localización diferencial de ambos complejos de condensina al final de G2, esto es, citoplasmática para la condensina I y nuclear para la condensina II (Hirota et al., 2004; Ono et al., 2004; Trimborn et al., 2006). Posteriormente, estudios in vitro en extractos de *Xenopus* demostraron que *Mcph1* inhibe de modo específico la función de condensina II al competir por los mismos sitios de unión a la cromatina. Esta inhibición depende específicamente de la región N-terminal de la proteína MCPH1, que contiene el primer dominio BRCT (Yamashita et al., 2011).

Las dos isoformas principales de MCPH1 descritas, MCPH1-FL y MCPH1-Δ9-14, tienen la capacidad de complementar la alteración en la condensación cromosómica cuando se sobreexpresan en células de pacientes con mutaciones en el gen MCPH1 (Gavvovidis et al., 2012). Estos resultados apuntan también a que el dominio BRCT N-terminal está implicado en la regulación de la condensación cromosómica, ya que es el único que comparten ambas isoformas. Además, el silenciamiento específico de cada una de las isoformas no daba lugar a la aparición del fenotipo PLC en células HeLa. Sin embargo, este sí aparecía cuando ambas se silenciaban simultáneamente, lo que demuestra que ambas tienen un papel redundante en el control de la condensación cromosómica (Gavvovidis et al., 2012).

También se ha demostrado que la proteína SET, un oncogen nuclear, estaría implicado en el control de la condensación cromosómica a través de su unión al dominio BRCT N-terminal de MCPH1 (Leung et al., 2011). El silenciamiento de la expresión de SET origina condensación cromosómica anormal y, curiosamente, este fenotipo es revertido si al mismo tiempo también es silenciada la condensina II, de modo similar a lo descrito para MCPH1 (Trimborn et al., 2006). De momento se desconoce la función molecular concreta del complejo MCPH1-SET, pero los resultados previos sugieren que la disrupción de la interacción MCPH1-SET puede ser importante en la patogénesis del síndrome de microcefalia primaria (Leung et al., 2011).

Otro escenario, no excluyente con el anterior, explica la influencia de la proteína MCPH1 sobre el proceso de condensación cromosómica a través de su relación con la activación de CDK1 y el control temporal de la mitosis (ver sección siguiente). De este modo, el fenotipo PLC característico de células sin función para el gen *MCPH1* podría ser consecuencia (i) directa debido a una desregulación del proceso de condensación cromosómica y/o (ii) indirecta por una alteración más general en la progresión del ciclo celular. Además, otro aspecto muy interesante relacionado con la alteración en la dinámica de condensación cromosómica asociado a la falta de función para MCPH1 es el posible impacto sobre la organización y morfología del cromosoma metafásico. Así, en los análisis citogenéticos rutinarios realizados sobre pacientes MCPH1 siempre se obtiene un patrón de

bandas G de muy baja calidad, incluso sobre preparaciones cromosómicas de alta resolución (Neitzel et al., 2002; Trimborn et al., 2004; 2005; 2006). Otro indicio es que la disrupción de la unión física entre el dominio central de la proteína MCPH1 y el complejo condensina II produce una alteración en la morfología cromosómica (Yamashita et al., 2011). Estos datos sugieren que la función de MCPH1 podría ser también fundamental para la organización y estructura de los cromosomas durante mitosis, aunque por el momento no se conocen más detalles de esta posible implicación.

4. MCPH1 y control del ciclo celular

Se ha sugerido que MCPH1 participa en el control del ciclo celular a través de la regulación temporal de la activación de CDK1 durante la transición G2/M (Alderton et al., 2006; Tibelius et al., 2009; Gruber et al., 2011). Según esto, el inicio prematuro de la condensación cromosómica asociado a la falta de función para el gen *MCPH1* podría ser consecuencia indirecta de una activación prematura de CDK1.

4.1 Bases moleculares de la entrada en mitosis

En el control del ciclo celular tienen un papel destacado un conjunto de proteínas denominadas "quinasas dependientes de ciclinas" (CDKs, "*Cyclin dependent kinases*"), responsables de controlar la transición entre las fases del ciclo (Malumbres y Barbacid, 2005). La actividad catalítica de estas enzimas requiere de su unión a una subunidad reguladora, siendo estas últimas moléculas sintetizadas y degradadas de manera específica en diferentes etapas del ciclo celular, recibiendo por ello el nombre de "ciclinas" (Malumbres y Barbacid, 2005). En vertebrados, el complejo ciclina B-CDK1 regula en última instancia la entrada en mitosis una vez que la ciclina B es sintetizada durante la fase G2. Cuando los niveles del complejo ciclina B-CDK1 activo sobrepasan un determinado límite en el interior del núcleo, la célula está destinada irreversiblemente a dividirse por mitosis (Pines y Rieder, 2001).

La activación del complejo ciclina B-CDK1 implica una compleja vía de señalización. Esta vía se organiza como un bucle de retroalimentación positiva que permite amplificar la señal de activación de CDK1 de manera rápida y efectiva. Esta retroalimentación ocurre a través de dos vías paralelas, una central directa denominada "*inner feedback loop*", y otra secundaria indirecta conocida como "*outer feedback loop*" (Lindquvist et al., 2009). Si bien los niveles de ciclina B están periódicamente regulados por ciclos de transcripción/traducción y degradación, su unión a CDK1

no es suficiente para formar un complejo activo. La activación completa depende también de modificaciones postraduccionales, principalmente fosforilaciones. Así, CDK1 tiene que ser fosforilada en el residuo T161 dentro del denominado T *loop* para producir actividad quinasa (Tassan et al., 1994; Lindqvist et al., 2009). Además, una vez que la ciclina B se une a CDK1, esta última es inmediatamente fosforilada en dos residuos (T14 e Y15), lo que resulta en una inhibición de su actividad quinasa. Los niveles de fosforilación de CDK1 en T14 y Y15 están controlados por el balance opuesto de las quinadas WEE1/MYT1, responsables de la fosforilación y, por tanto, de su inactivación, y la fosfatasa CDC25, que desfosforila dichos residuos determinado así su activación. Conforme CDK1 se activa, promueve de modo directo tanto la activación de CDC25 como la inactivación de WEE1/MYT1 mediante fosforilaciones específicas en las mismas, lo que amplifica su propia activación, y conformando el denominado "*inner feedback loop*" (O'Farrel, 2001; Tuck et al., 2013; Lindqvist et al., 2009; Murray et al., 1993).

El tráfico subcelular de ciclina B es otro factor que condiciona la activación del complejo ciclina B-CDK1. Al igual que otros reguladores de ciclo celular, la ciclina B se transfiere continuamente entre el núcleo y el citoplasma (Lindqvist et al., 2009). Durante la fase S y la mayor parte de G2, la exportación nuclear sobrepasa su importación al núcleo, lo que resulta en una localización predominantemente citoplasmática (Hagting et al., 1998; Toyoshima et al., 1998; Yang et al., 1998). Conforme la fase G2 avanza, la ciclina B comienza a acumularse en los centrosomas según estos maduran, hasta alcanzar niveles elevados al final de esta fase (Jackman et al., 2003). La fosforilación de la ciclina B en los centrosomas hace inaccesible una secuencia de exportación nuclear y promueve su transporte al núcleo, lo que favorece la acumulación del complejo ciclina B-CDK1 en el mismo (Li et al., 1997; Hagting et al., 1999). La propia activación del complejo ciclina B-CDK1 estimula también la autofosforilación de ciclina B, favoreciéndose la importación al núcleo del complejo activo (Lindqvist et al., 2009). En este momento, el complejo ciclina B-CDK1 puede llevar a cabo la fosforilación de sus dianas nucleares, como lamininas estructurales, dando lugar entre otros sucesos a la rotura de la envoltura nuclear (Jackman et al., 2003; Lindqvist et al., 2007).

La activación de CDK1 también está regulada por otras vías indirectas en las que tiene un papel importante la quinasa PLK1. Su función está regulada directamente por el complejo ciclina B-CDK1, que fosforila múltiples dianas, incluidas WEE1, MYT1 y CDC25, creando así sitios de unión ("*docking sites*") para PLK1 (Elia et al., 2003a, b). La unión de PLK1 a dichos sustratos provoca una nueva ronda de activación/inactivación a través de nuevas fosforilaciones, que en última instancia amplifican los niveles finales del complejo ciclina B-CDK1 activo. PLK1 también

fosforila directamente a la ciclina B, lo que coincide con la fosforilación autocatalítica del complejo ciclina B-CDK1 (Toyoshima et al., 2001; Yuan et al., 2002; Jackman et al., 2003). Además, PLK1 y Aurora A incrementan la concentración local de ciertas proteínas en el material pericentriolar, aumentando la concentración de los componentes de la vía de señalización que controla la entrada en mitosis (Barr y Gergely, 2007; Hachet et al., 2007; Portier et al., 2007). Ambos bucles de retroalimentación, tanto "*inner feedback*" o como "*outer feedback*", no solo promueven una activación eficiente del complejo ciclina B-CDK1, sino que además aseguran que otros factores reguladores necesarios para la correcta división celular se activen de modo coordinado. Esto parece ser esencial para la coordinación de los múltiples eventos que ocurren simultáneamente durante la mitosis (Lindqvist et al., 2009). Finalmente, la inactivación de los complejos ciclina B-CDK1 es necesaria para la finalización de la división celular, e implica la degradación de la ciclina B mediante ubiquitinación gracias a la regulación del ciclosoma/APC ("*anaphase-promoting complex*") (Harper et al., 2002).

4.2 MCPH1 y control de la entrada en mitosis

Desde un punto de vista bioquímico, las células de pacientes con mutaciones en el gen *MCPH1* presentan niveles elevados de CDC25A activo y niveles reducidos de CDK1 inactivo durante las fases S tardía y G2 (Alderton et al., 2006). Esta alteración podría condicionar un inicio prematuro de la condensación cromosómica, ya que en condiciones normales el complejo regulador ciclina B1-CDK1 no se activa hasta el inicio de profase, tras su desfosforilación en Y15 por CDC25A. Además, la función centrosómica de MCPH1 también podría estar relacionada con el inicio prematuro de la condensación cromosómica. Así, a través de su interacción con PCNT (pericentrina) MCPH1 regularía la distribución de la quinasa CHK1 en el centrosoma, dónde ésta tiene un papel fundamental en la sincronización de los eventos nucleares y citoplasmáticos que ocurren durante la progresión mitótica (Tibelius et al., 2009).

A la vista de estos datos, se ha propuesto que la función de las quinasas ATR y CHK1, reguladoras de la activación de CDC25A, estaría modulada de algún modo por *MCPH1* (Gruber et al., 2011). Sin embargo, niveles anormalmente elevados de CDC25A activo durante G2 también se han observado en células de pacientes con el síndrome ATR-Seckel (Alderton et al., 2006), y en pacientes con mutaciones en el gen *PCNT* (Tibelius et al., 2009). No obstante, mientras que microcefalia y niveles alterados de CDC25 son dos alteraciones compartidas por los pacientes MCPH1, ATR-Seckel y PCNT, la condensación cromosómica prematura es una alteración

exclusiva del síndrome en pacientes MCPH1. Por tanto, el papel del gen *MCPH1* como regulador de la condensación cromosómica no parece ejecutarse a través de la modulación de ATR y CDC25, o al menos no exclusivamente.

Estos estudios demuestran que en condiciones fisiológicas normales, es decir, en ausencia de daño grave en el ADN, MCPH1 contribuye a que la condensación cromosómica, la maduración centrosómica y la mitosis ocurran de modo coordinado. Por tanto, la función de este gen se considera clave para el control del ciclo celular, en concreto la transición G2-M (Gruber et al., 2011). En ausencia de función para MCPH1 las vías de señalización que controlan la transición entre G2 y M estarían desreguladas, lo que resulta evidente por una activación prematura de CDK1 y CDC25A, así como por la pérdida de CHK1 en el centrosoma durante G2 (Alderton et al., 2006; Tibelius et al., 2009; Gruber et al., 2011). Según algunos autores, esta desregulación determinaría finalmente que la célula inicie mitosis de manera prematura. Siguiendo esta idea MCPH1 sería un factor clave que controla la progresión celular por G2 y el inicio en tiempo de la mitosis. Sin embargo, el único dato experimental que apoya esta afirmación es el incremento significativo en la fracción de células mitóticas que se observa tanto en líneas celulares humanas con silenciamiento temporal de la expresión del gen *MCPH1* como en líneas celulares de pacientes (Tibelius et al., 2009; Gruber et al., 2011). Por tanto, si bien en ausencia de función para MCPH1 algunas vías de señalización durante G2 están desreguladas, aún falta por conocer más en profundidad como afecta esta alteración a la dinámica del ciclo celular. En este sentido, estudios detallados sobre la dinámica del ciclo celular en células sincronizadas sin expresión de MCPH1 serían de gran importancia para definir el papel funcional de este gen en el control temporal de la mitosis.

4.3 Papel de MCPH1 en el control del daño en el ADN

Durante el ciclo celular las células transitan por diferentes puntos de control o "*checkpoints*" encargados de monitorizar su estado fisiológico y coordinar su progresión por el ciclo con otros eventos como, por ejemplo, la reparación del daño en el ADN, la organización estructural de la cromatina o el ensamblaje del huso mitótico. Estos "*checkpoints*" constituyen mecanismos mediante los cuales las células detienen activamente su progresión en un punto del ciclo celular hasta que el proceso asociado que los activa ha sido completado satisfactoriamente (Doll et al., 1981). Durante la fase G2 del ciclo es fundamental que las células detecten y reparen los daños en el ADN antes de iniciar mitosis, a fin de mantener la estabilidad genómica, por lo que estos puntos de control están enfocados a la señalización y reparación de dichos daños (O`Driscoll et al., 2006; Lukas et al.,

2004; Terzoudi et al., 2005). La activación y el funcionamiento correcto de los puntos de control requiere de la actuación de tres componentes principales: sensores y mediadores del problema, transductores de señal y reparadores del daño (Kastan y Barket, 2004).

Cada tipo de daño o estrés concreto activa un conjunto específico de vías de señalización que son necesarias para responder eficientemente frente a la naturaleza del daño. De los puntos de control operativos en G2 el más conocido y estudiado es el que señaliza roturas en la doble hélice del ADN (comentado a continuación). Sin embargo, existen otros puntos de control menos conocidos que también están activos durante dicha fase como el "*antephase checkpoint*", que bloquea la entrada en mitosis y revierte la condensación cromosómica en respuesta a un amplio rango de agentes estresantes (Chin y Yeong, 2010; Matsusaka y Pines, 2004); o el "*decatenation checkpoint*", que monitoriza la actividad de Topoisomerasa II sobre la topología de la cromatina (Downes et al., 1994; Damelin y Bestor, 2007).

4.3.1 Punto de control por roturas en ADN dependiente de ATR/ATM

ATM ("*Ataxia Telangiectasa Mutated kinase*") y ATR ("*Ataxia Telangiectasa and RAD3-related kinase*") son dos proteínas pertenecientes a la familia de las PI3 quinasas, y tienen un papel clave en la señalización del daño en el ADN (Iliakis et al., 2003). ATM se activa primariamente en respuesta a roturas de cadena doble en el ADN, denominadas DSBs ("*Double Strand Breaks*"), asociadas frecuentemente a la radiación ionizante (IR, "*ionizing radiation*"). También pueden formarse DSBs por horquillas de replicación colapsadas, o de un modo programado durante meiosis para iniciar procesos de recombinación entre cromosomas homólogos (Shiloh y Kastan, 2001; Abraham, 2001; Bartek et al., 2001A; 2001B). Por otro lado, ATR responde principalmente a daños producidos por radiación ultravioleta (UV) o a fallos por paradas en las horquillas de replicación (Osborn et al., 2002). Estos originan principalmente huecos o "*gaps*" en una sola hebra del ADN, denominados *ssDNA* (*single-stranded DNA*), o bien roturas de cadena simple, denominadas *SSBs ("Single-Strand Breaks")* (Ray et al., 2016; Ray et al., 2013). Esta situación canónica no siempre se cumple. Así, estudios recientes demuestran que el daño en el ADN inducido por radiación UV y por estrés replicativo también pueden activar ATM (Yajima et al., 2009; Ray et al., 2013).

ATR y ATM fosforilan y activan a las quinasas CHK1 y CHK2 respectivamente, y éstas a su vez fosforilan e inactivan a CDC25, entre otras dianas. De este modo, CDK1 no se activa al no defosforilar CDC25 en su residuo Y15, quedando las células paradas en G2 temporalmente (Xiao et al., 2003; Bartek y Lukas, 2007) (Figura I-4). Tanto ATM como ATR fosforilan también a la

histona H2AX en S139 (γH2AX). Esta variante de histona se distribuye por todo el ADN cada 200-400 kb y ayuda a reclutar proteínas de reparación del daño y activación del punto de control (Rogakou et al., 1998; Stucki y Jackson, 2006; Ray et al., 2009). Dichas proteínas reparadoras forman agregados o "*foci*" nucleares observables al microscopio. Recientemente, se ha demostrado que los agregados de γH2AX se distribuyen espacialmente en el núcleo de las células según un patrón dependiente de la progresión temporal de la respuesta al daño en el ADN. Dicho patrón muestra una tendencia jerárquica de eucromatina a heterocromatina motivado por su estado de compactación: las regiones de cromatina que se encuentra en estado relajado serían reparadas en primer lugar, mientras que las regiones más compactadas requieren una remodelación estructural antes de que la maquinaria de reparación pueda actuar (Natale et al., 2017). CTCF (*CCCTC-binding factor*) (Baniahmad et al., 1990; Lobanenkov et al., 1990; Ong y Corces, 2014) parece tener un papel crucial en la formación y distribución espacial de los agregados de γH2AX, y su ausencia retrasa la vía de respuesta al daño en el ADN disminuyendo la capacidad de reparación del daño, a pesar de la activación eficiente de otros señalizadores y efectores como ATM (Natale et al., 2017).

4.3.2 Papel de MCPH1 en los puntos de control dependientes de ATR y ATM

Diversos estudios previos demuestran que MCPH1 participa en la respuesta celular al daño en el ADN. Así, MCPH1 se localiza preferentemente en regiones de ADN con roturas de cadena doble, actividad dependiente de sus dominios BRCT C-terminales (Wood et al., 2007; Jeffers et al., 2008; Gavvovidis et al., 2012). Según algunos autores, MCPH1 sería fundamental para relajar la estructura de la cromatina y facilitar el acceso del resto de proteínas de reparación a la zona dañada mediante su interacción con el complejo remodelador de cromatina SWI/SNF (Peng y Lin, 2009) (Figura I-5). Esta función de MCPH1 parece ser necesaria para la actuación de los mecanismos de reparación, tanto los basados en recombinación homóloga (HR) como los dependientes de recombinación no homóloga (NHEJ) (Peng et al., 2009; Liang et al., 2010, 2015; Zhuo et al., 2012). Este requerimiento podría explicar el descenso en la viabilidad celular que experimentan células sin función para *MCPH1* tras radiación ionizante (Peng et al., 2009; Liang et al., 2010, 2015; Zhou et al., 2013). Donde existe alguna controversia es en la supuesta implicación de MCPH1 en la formación de *foci* nucleares de señalización y reparación. Los dominios BRCT están presentes en proteínas que controlan el daño en el ADN y reparación, como *BRCA1, 53BP1* y *NFBD1/MDC1,* y confieren capacidad de formar agregados o "*foci*" nucleares tras la aparición del daño en el ADN (Kastan y Bartek, 2004). Mientras que análisis basados en células de pacientes MCPH1 (Gavvovidis et al., 2010) o células de ratón Mcph1 -/- (Zhou et al., 2013) apuntan a que la

formación de "*foci*" nucleares de reparación es normal, otros estudios sugieren que dicha capacidad sí está afectada (Rai et al., 2006; Liang et al., 2010, 2015).

MCPH1 también participa en la vía de señalización de los puntos de control del daño en el ADN. Estudios previos han demostrado que las células de pacientes sin función para MCPH1, al igual que se observa en el síndrome ATR, presentan una parada en G2 defectiva en respuesta al daño que activa específicamente la vía dependiente de ATR, como radiación UV o estrés replicativo (Alderton et al., 2006). En concreto, los niveles de CDC25A activo no se reducen a pesar de que tanto la activación de ATR como la de su diana CHK1 es normal, lo que explicaría la ausencia de una parada efectiva en G2. Según estos autores, MCPH1 funcionaría en algún punto por debajo de CHK1 y por encima de CDC25 en la vía de señalización dependiente de ATR (Alderton et al., 2006) (Figura I-4).

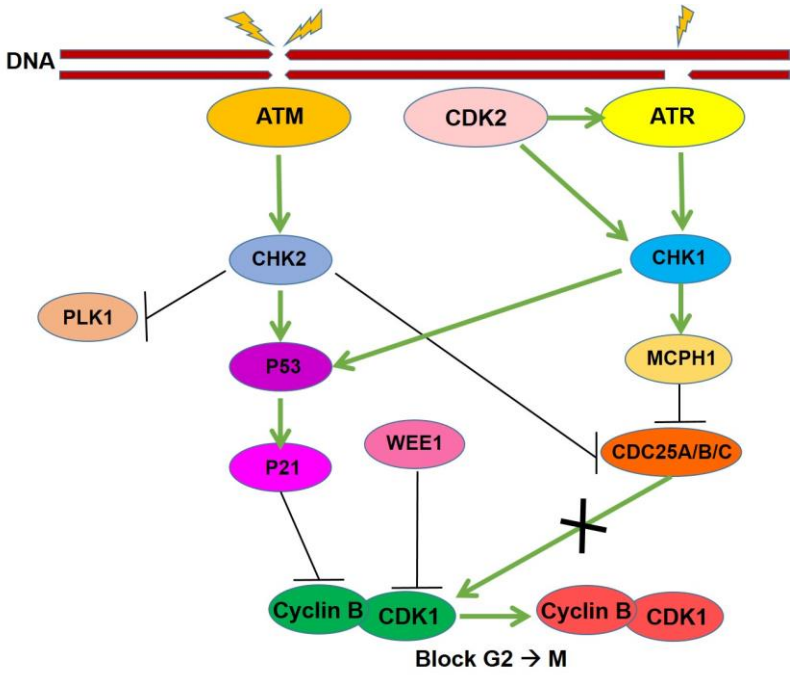

Figura I-4: Esquema simplificado que muestra los principales componentes de las vías de señalización del daño en el ADN durante la fase G2 del ciclo celular. Según Alderton et al. 2006, MCPH1 participa en la transducción de la señal desde CHK1 hasta CDC25 en la vía dependiente de ATR. Las flechas verdes indican activación, las líneas negras inactivación. Las versiones activa e inactiva del complejo ciclina B-CDK1 se indican con los colores verde y rojo respectivamente.

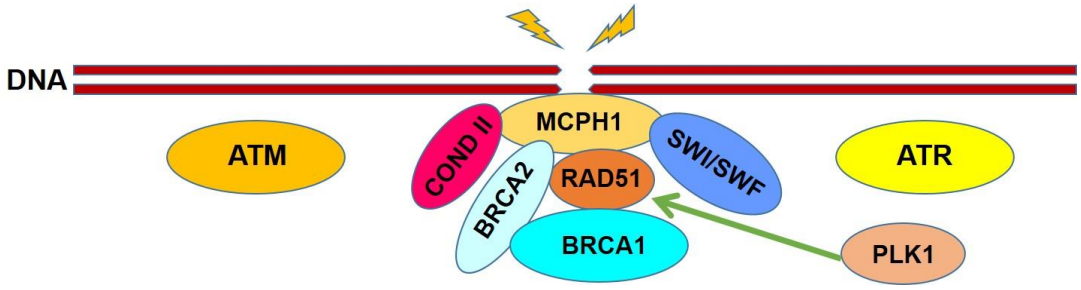

Figura I-5: Papel de MCPH1 en la señalización del daño en el ADN, dónde ayudaría al reclutamiento de múltiples proteínas a los sitios dañados y relajaría la compactación de la cromatina a través de su interacción con SWI/SNF y/o condensina II.

La implicación de MCPH1 en la vía de señalización dependiente de ATM es sin embargo más controvertida. Diversos estudios basados en células de pacientes (Gavvovidis et al., 2010), líneas celulares aviares DT40 knock-out (Brown et al., 2010) y células de ratón Mcph1 -/- (Gruber et al., 2011; Zhou et al., 2013) coinciden en señalar que este punto de control es operativo y determina una parada eficiente en G2 en respuesta a IR. Sin embargo, algunos estudios basados en silenciamiento de la expresión de *MCPH1* por siRNAs, sugerían que dicho punto de control era deficiente (Xu et al., 2004; Rai et al., 2006, 2008). Esta aparente discrepancia podría explicarse por una pérdida incompleta de la función de este gen y/o una hiperactivación compensatoria de vías señalizadoras redundantes en alguno de los modelos celulares citados. En cualquier caso, los datos en su conjunto apuntan a que el gen *MCPH1* no interviene directamente en el punto de control por daño en el ADN. Sin embargo, es interesante destacar que la recuperación celular del bloqueo provocado por el punto de control dependiente de ATM ocurre de modo más lento cuando falta la función de MCPH1 (Gavvovidis et al., 2010; Brown et al., 2010). Recientemente, se ha propuesto que esta recuperación más tardía estaría motivada por un aumento incontrolado de la señal inhibitoria de CHK1 en el centrosoma tras IR (Antonczak et al., 2016). Estos datos sugieren que la recuperación y/o adaptación a este punto de control podría estar regulada de algún modo por MCPH1.

4.4 Otros puntos de control en G2: "Decatenation Checkpoint"

La actividad de la Topoisomerasa II es fundamental durante la condensación y segregación cromosómica debido a su capacidad para eliminar las concatenaciones y superenrollamientos de la cromatina que se establecen entre cromátidas hermanas y no hermanas cuando termina la replicación. Además, la resolución de concatenaciones inter-cromosómicas es un requisito para que

los cromosomas se puedan individualizar. En contraposición, ciertas concatenaciones organizadas en el centrómero permanecerían sin resolver hasta el inicio de anafase, asegurando un grado de cohesión suficiente (Díaz-Martínez et al., 2006). Según esto, la topología que adquiere el ADN en el núcleo durante G2 es determinante para el resultado de la división posterior. Estudios previos han demostrado la existencia de un punto de control específico operativo durante la fase G2 del ciclo que se encarga de monitorizar la actividad de Topoisomerasa II sobre el ADN. Esta vía de señalización, denominada "*decatenation checkpoint*", retrasa el inicio de la mitosis hasta que las concatenaciones en el ADN cromosómico se eliminan en grado suficiente (Downes et al., 1994). A pesar de su importancia, este punto de control es menos conocido y estudiado en comparación con el que responde al daño en el ADN, e incluso ha sido puesto en duda por algunos autores (Damelin et al., 2005; Doherty et al., 2003).

Su identificación se llevó a cabo tras el descubrimiento de inhibidores catalíticos de Topoisomerasa II, como ICRF-193 (meso-4,4´-(3,2-butanediyl)-bis-(2,6-piperazinedione)) y otros tipos de bisdioxopiperazinas (Roca et al., 1994). Así, la incubación tanto de células humanas como de otros mamíferos con estos inhibidores daba lugar a un bloqueo temporal en G2 (Kalwinsky et al., 1983; Kaufmann y Kies, 1998; Downes et al., 1994; Deming et al., 2001; Damelin et al., 2005). La Topoisomerasa II forma con el ADN un complejo covalente reversible enominado complejo de rotura (Burden y Osheroff, 1998; Cortes et al., 2003). Los inhibidores catalíticos atrapan y bloquean este complejo en su conformación de abrazadera cerrada, lo que evita la inducción masiva de DSBs en el ADN (Downes et al., 1994; Roca et al., 1994). En contraposición, otros compuestos denominados inhibidores clásicos o "*Topo II poisons*" bloquean este complejo en una fase previa del ciclo catalítico, quedando DSBs en el ADN sin ligar. Así, inhibidores como etoposido (VP-16), amsacrine y doxorubicin generan de modo masivo DSBs en el ADN, y como consecuencia activan el punto de control de daños en el ADN dependiente de ATM. Por tanto, el "*decatenation checkpoint*" conformaría una vía de señalización distinta que no se activa como respuesta a la formación de DSBs en el ADN. Sin embargo, algunos autores cuestionan aún este planteamiento al dudar de la incapacidad de ICRF-193 para producir daños en el ADN (Downes et al., 1994; Deming et al., 2001; Nakawaga et al., 2004; Park y Avraham, 2006; Wang et al., 2002).

En la vía de señalización del "*decatenation checkpoint"* juega un papel importante ATR. Así, el tratamiento con cafeína, un conocido inhibidor de las quinasas ATR/ATM, anula el bloqueo celular en G2 inducido por ICRF-193 (Downes et al., 1994). Además, mientras que la sobreexpresión de una versión inactiva de ATR impide la activación eficiente de este punto de control, en células de

pacientes con mutaciones en ATM esta vía de señalización es funcional, lo que confirma la no implicación de esta quinasa (Deming et al., 2001). Otros elementos de esta vía de señalización bajo control de ATR son BRCA1 y WRN (*Werner helicase*) (Deming et al., 2001; Franchitto et al., 2003) (Figura I-6). La participación de CHK1, sin embargo, está bajo discusión al haberse obtenido resultados contradictorios en algunos estudios (Deming et al., 2001; Robinson et al., 2007). También se ha implicado a PLK1 ya que su actividad aparece reducida tras la incubación con ICRF-193 y, por el contrario, la funcionalidad del punto de control se pierde cuando se sobreexpresa este gen (Deming et al., 2002). También se ha demostrado que Topoisomerasa II participa directamente en la vía de señalización (Gimenez-Abián et al., 2000; Luo et al., 2009). En concreto, su fosforilación en la posición S1524 favorece la unión de la misma con el dominio BRCT de MDC1 (*mediator of DNA damage checkpoint protein-1*) y su posterior reclutamiento a la cromatina, siendo esta asociación indispensable para la activación del "*decatenation checkpoint"*. Algunas hipótesis sugieren que el residuo S1524 fosforilado de Topoisomerasa II quedaría expuesto tras la incubación con ICRF-193, dando lugar a la activación de la vía de señalización (Luo et al., 2009). Finalmente, algunas modificaciones epigenéticas de la cromatina controlan la unión de Topoisomerasa II a la misma y son determinantes para el funcionamiento de este punto de control (Lane et al., 2013).

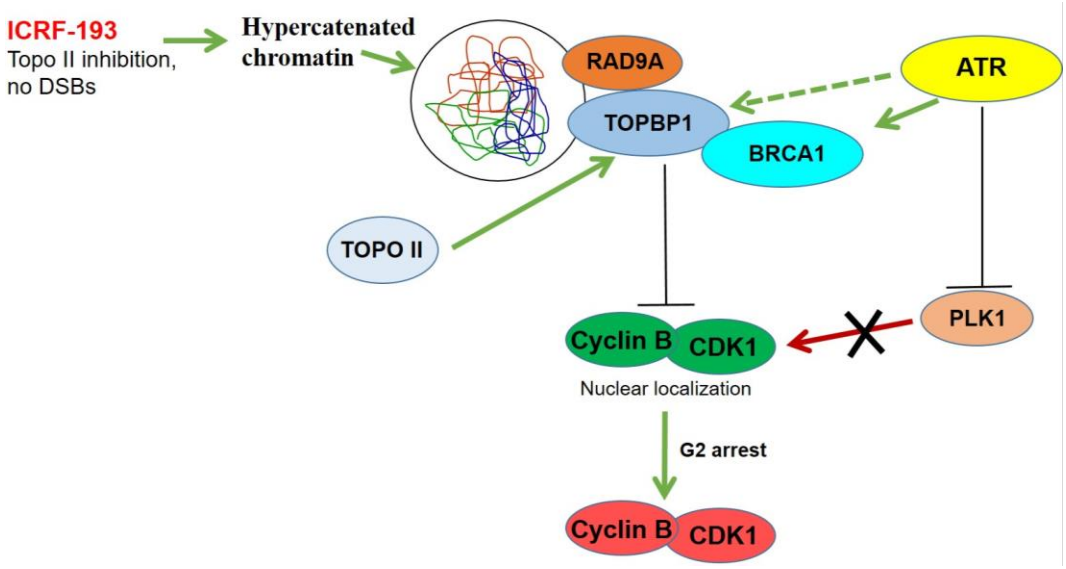

Figura I-6: Esquema simplificado que muestra los principales componentes de la vía de señalización del *"decatenation checkpoint" durante la fase G2 del ciclo celular*. La inhibición de Topoisomerasa II con ICRF-193 produce catenaciones cromosómicas que inducen la activación del punto de control y el retraso en G2 mediado por ATR. ATR actúa por encima de BRCA1 y PLK1 en esta vía de señalización que resulta en la exclusión de la ciclina B del núcleo retrasando el inicio de mitosis. Las flechas verdes indican activación, las líneas negras inactivación. La s versiones activa e inactiva del complejo ciclina B-CDK1 se indican con los colores verde y rojo respectivamente.

Por el momento se desconocen los sensores del "*decatenation checkpoint"*. Éstos podrían detectar perturbaciones en la función de Topoisomerasa II a través de dos posibles mecanismos: medida directa de la actividad catalítica de la enzima o detección de anomalías estructurales en la cromatina que aparecen indirectamente cuando se altera la actividad este enzima (Clarke et al., 2006). Estudios recientes en levaduras apuntan hacia la primera opción, aunque por el momento se desconoce si en organismos superiores ocurre de igual modo (Furniss et al., 2013). En este sentido habría que destacar la función de RAD9A, que actúa en varios puntos de control en G2 como proteína sensora del daño en el ADN gracias a la formación de un anillo nuclear heterodimérico alrededor del ADN conocido como complejo 911 (St. Onge et al., 1999; Volkmer y Karnitz, 1999; Griffith et al., 2002). Recientemente se ha demostrado su importancia en el "*decatenation checkpoint"* mediante su interacción con TOPBP1, una proteína de unión a Topoisomerasa II, siendo necesaria para la detección del nivel de resolución de concatenaciones cromosómicas (Greer Card et al., 2010).

Es importante diferenciar este punto de control, operativo en G2, de otro que también monitoriza el grado de concatenación entre cromátidas hermanas pero que se activa durante prometafase y metafase (Skoufias et al., 2004). Éste último da lugar a un parada o retraso en la transición metafase/anafase si la actividad de Topoisomerasa II se ve comprometida en ese punto, y para el que se requiere MAD2 y PKCε (Brownlow et al., 2014). Si bien sus vías de señalización son distintas, ambos puntos de control muestran cierta interrelación al monitorizar un mismo proceso, aunque en dos momentos distintos. Así, en aquellas líneas celulares que son deficientes para el "*decatenation checkpoint"* en G2, como las descritas para algunos modelos tumorales (Damelin y Bestor, 2007), el punto de control mitótico dependiente de PKCε permanece activo mucho más tiempo en un intento de corregir la topología de los cromosomas antes de su segregación (Brownlow et al., 2014).

Si bien se ha investigado a fondo el papel de *MCPH1* en la respuesta al daño en el ADN, hasta la fecha no se conocen datos sobre su posible participación en otros puntos de control operativos en la fase G2 del ciclo celular, como por ejemplo el mencionado "*decatenation checkpoint"*. A favor de este planteamiento estarían algunos datos preliminares. Por ejemplo, la señalización de la quinasa ATR, esencial para transducir la señal del "*decatenation checkpoint"* (Deming et al., 2001), requiere de la función de *MCPH1* para inducir una parada efectiva del ciclo celular la respuesta al daño en el ADN por radiación UV (Alderton et al., 2006). Además, el hecho de que la cromatina está hipercondensada durante parte de la fase G2 en células sin función para

MCPH1 podría ser un factor que alterara la respuesta de este punto de control, ya que responde a alteraciones en la topología del ADN.

4.5 Adaptación celular al punto de control

La señal de parada del ciclo producida por cualquier punto de control debe ser silenciada una vez que se repara el daño (Langerak y Russell, 2011; Alvarez-Fernandez y Medema, 2010). La reentrada en el ciclo celular, denominada recuperación del punto de control ("*checkpoint recovery*") es factible gracias a que la parada producida por el punto de control es reversible, a menos que el daño producido sea excesivo o de naturaleza irreparable, en cuyo caso determina senescencia o muerte celular programada (Bartek y Lukas, 2007, Jackson y Bartek, 2009). Sin embargo, una respuesta celular alternativa menos conocida y estudiada es la adaptación celular a un punto de control. Este fenómeno fue descubierto inicialmente en *Sacharomyces cerevisiae*, y se refiere a la capacidad para dividirse tras una parada del ciclo celular por un punto de control sostenido, en presencia de daño en el ADN irreparable (Sandell y Zakian, 1993). La adaptación a un punto de control también se ha observado posteriormente en células de organismos superiores, incluidas las humanas (Toczyski et al., 1997; Yoo et al., 2004; Syljuasen et al., 2006). Aunque las células que experimentan el fenómeno de adaptación frecuentemente mueren en los siguientes ciclos de división debido a daños excesivos en su genoma, algunas células muestran la capacidad de proliferación a pesar de presentar daños persistentes en el ADN. De ahí, que la capacidad de adaptación al punto de control potencialmente pueda promover inestabilidad genómica ligada a cáncer (Syljuasen, 2007). Este proceso implica el inicio de mitosis aun existiendo daño en el ADN, y se distingue por tres características: en primer lugar, el daño en el ADN debe producir una parada en G2/M eficiente; en segundo lugar, las células deben sobrepasar esta parada; y, por último, iniciar la mitosis en presencia del daño (Toczyski et al., 1997).

Los mecanismos moleculares subyacentes a los procesos de recuperación y adaptación a un punto de control concreto no son idénticos como podría pensarse (Harrison y Haber, 2006). PLK1 controla la recuperación del punto de control por daños en el ADN dependiente de ATM (Van Vugt et al., 2005). Esta quinasa fosforila e inactiva a WEE1, lo que resulta en una menor fosforilación inhibitoria sobre el complejo ciclina B-CDK1. Además, la actividad específica de la fosfatasa CDC25B, pero no la de CDC25A o CDC25C, es requerida para la activación de esta vía de recuperación (Van Vugt et al., 2004). De este modo, las vías de señalización que determinan la entrada en mitosis se vuelven críticamente dependientes de la función de PLK1 tras una situación

de daño en el ADN (Van Vugt et al., 2004). También se ha descrito un papel importante en este mecanismo para otros reguladores como son Aurora A o TLK1 (Macurek et al., 2008; Bruinsma et al., 2016)

Estudios previos muestran que la función de PLK1 también es necesaria en el proceso de adaptación al punto de control en G2 dependiente de ATM que responde a IR en células humanas. Así, su falta de expresión impide que las células escapen del bloqueo inducido por dicho punto de control, incluso si la proteína señalizadora del mismo – ATM – se inactiva con cafeína (Syljuasen et al., 2006, 2007). Esta regulación también depende de CHK1, aunque aún no estaría claro si sería a través de la inactivación de esta última por PLK1 o bien ambas proteínas actúan de forma paralela en vías de señalización que convergen en el complejo ciclina B-CDK1 (Syljuasen et al., 2006, 2007). Dado que tanto PLK1 como CHK1 se localizan en los centrosomas (Arnaud et al., 1998; Kramer et al., 2004), la señalización centrosómica podría jugar un papel importante en el proceso de adaptación al punto de control (De Souza et al., 2000). A pesar de los estudios realizados, los mecanismos que intervienen en la adaptación celular a puntos de control en G2 son bastante desconocidos aún, habiéndose estudiado principalmente solo en el contexto de agentes causantes de DSBs en el ADN. En este sentido, la contribución de MCPH1 en las vías de señalización que regulan este proceso podría ser relevante ya que la recuperación del punto de control que señaliza la presencia de DSBs está ligeramente comprometido cuando falta su función (Gavvovidis et al., 2010; Brown et al., 2010).

4.6 MCPH1 y control del ciclo celular: importancia en cáncer

En los últimos años varios trabajos de investigación señalan una implicación del gen *MCPH1* en carcinogénesis. Por el momento, existen 37 mutaciones descritas en la base de datos COSMIC (Forbes et al., 2011). La expresión de este gen aparece significativamente reducida en muestras de cáncer de mama (Rai et al., 2008; Bruning-Richardson et al., 2011), colorectal y gástrico (Jo et al., 2017), y carcinoma renal (Wang et al., 2014). También se ha observado una pérdida de heterocigosidad en muestras de cáncer epitelial de ovario y carcinoma escamoso oral respectivamente (Rai et al., 2006; Venkatesh et al., 2014). Además, otro estudio ha identificado una mutación en heterocigosis de pérdida de función en *MCPH1* asociada con cáncer de mama en una población de origen finlandés (Mantere et al., 2016). También existen dos SNPs descritos para *MCPH1* asociados con un incremento en el grado de patogénesis del tumor de mama (Jo et al.,

2013). En un modelo de ratón mutante para *Mcph1* se ha descrito una mayor incidencia de linfomas y granulomas (Liang et al., 2015).

La implicación de *MCPH1* en la señalización y reparación del ADN, así como su posible participación en otros puntos de control del ciclo celular, aún por determinar, podría explicar estos datos ya que son numerosos los ejemplos de genes que participan en estas rutas cuyo funcionamiento alterado contribuye al desarrollo tumoral. La incorrecta regulación de la división celular es clave en la aparición de un tumor, de ahí la importancia del correcto funcionamiento de los diferentes puntos de control o "*checkpoints*", que en respuesta a un determinado daño dan lugar a una parada temporal del ciclo celular para permitir la reparación del mismo (Hartwell y Kastan, 1994; Nurse, 1997). En este contexto, es de interés también estudiar la contribución de MCPH1 en las vías de señalización que regulan la adaptación a los puntos de control operativos en G2, algo por el momento desconocido. Estos análisis ayudarían a comprender mejor la propuesta inclusión de *MCPH1* como posible diana terapéutica en cáncer (Venkatesh y Sures, 2014)

OBJETIVOS

OBJETIVOS

El síndrome de microcefalia primaria por mutaciones en el gen MCPH1 se caracteriza por un fenotipo celular muy característico como consecuencia de una descoordinación entre la condensación cromosómica y el ciclo celular, observable en todos los tipos celulares. Por tanto, este gen tiene un papel importante en el proceso de división mitótica, aunque por el momento son muchos los interrogantes sobre las funciones concretas que realiza en este contexto. En el presente trabajo pretendemos avanzar en el conocimiento sobre la contribución específica de MCPH1 en el control y ejecución de la mitosis, con vistas a avanzar en las bases moleculares y celulares de este proceso y su implicación en la neurogénesis humana.

Los objetivos concretos de esta Tesis Doctoral son:

1. Identificar y caracterizar en detalle las alteraciones en la organización y estructura de los cromosomas mitóticos en células humanas sin función para MCPH1.
2. Determinar si MCPH1 es un regulador temporal de la mitosis en células humanas.
3. Analizar la función de MCPH1 en el punto de control del ciclo celular dependiente de Topoisomerasa II que controla la transición G2/M.

AIMS

Mutations in the MCPH1 gene result in primary microcephaly in combination with a unique cellular phenotype of defective chromosome condensation observable in all cell types. Therefore, MCPH1 function is required for coupling chromosome condensation with cell cycle progression. However, several questions about the particular contribution of MCPH1 into the mechanisms orchestrating cell entrance and progression through mitosis remain open. In the present study we provide novel insights about the molecular and cellular basis of these mechanisms and the consequences for human neurogenesis.

The specific aims of this Phd thesis are:

1. To identify and characterize in detail the alterations related to the organization and structure of mitotic chromosomes in human cells lacking MCPH1 function.
2. To establish if MCPH1 is a temporal regulator of mitosis in human cells.
3. To analyze if MCPH1 function is required for the cell cycle checkpoint related to Topoisomerase II activity that controls G2/M transition in human cells.

CHAPTER I

Chromosoma
DOI 10.1007/s00412-015-0512-2

RESEARCH ARTICLE

Chromosome structure deficiencies in MCPH1 syndrome

M. Arroyo[1] · M. Trimborn[2] · A. Sánchez[1] · T. Hirano[3] · H. Neitzel[2] · J.A. Marchal[1]

Received: 6 February 2015 / Revised: 6 March 2015 / Accepted: 16 March 2015

Abstract Mutations in the MCPH1 gene result in primary microcephaly in combination with a unique cellular phenotype of defective chromosome condensation. MCPH1 patient cells display premature chromosome condensation in G2 phase of the cell cycle and delayed decondensation in early G1 phase, observable as an increased proportion of cells with prophase-like appearance. MCPH1 deficiency thus appears to uncouple the chromosome cycle from the coordinated series of events that take place during mitosis such as some phases of the centrosome cycle and nuclear envelope breakdown. Here, we provide a further characterization of the effects of MCPH1 loss-of-function on chromosome morphology. In comparison to healthy controls, chromosomes of MCPH1 patients are shorter and display a pronounced coiling of their central chromatid axes. In addition, a substantial fraction of metaphase chromosomes shows apparently unresolved chromatids with twisted appearance. The patient chromosomes also showed signs of defective centromeric cohesion, which become more apparent and pronounced after harsh hypotonic conditions. Taking together, the observed alterations indicate additional so far unknown functions of MCPH1 during chromosome shaping and dynamics.

✉ J.A. Marchal
jamaor@ujaen.es

[1] Department of Experimental Biology, University of Jaén, Paraje Las Lagunillas s/n, E-23071, Jaén, Spain

[2] Institute of Medical Genetics and Human Genetics, Charite Virchow-Klinikum Hospital, Berlin, Germany

[3] Chromosome Dynamics Laboratory, RIKEN, Wako, Saitama, Japan

Introduction

The accurate segregation of sister chromatids in anaphase requires the transformation of the interphase chromatin into the highly condensed and organized structure of metaphase chromosomes beforehand. This transformation is a progressive and dynamic process that finally shapes the chromatin into the well-known microscopic chromosomes. It encompasses the ≈10^4-fold linear condensation of the DNA and, simultaneously, the resolution of sister chromatids by decatenation of DNA entanglements. Before anaphase, the cohesion of the chromatid arms and centromeres has to be released in coordination with the centrosome cycle and the spindle apparatus. Despite the importance of the process and a long history of research, the molecular mechanisms regulating these astonishing processes are still not completely understood.

Different experimental approaches contributed to our knowledge on how mitotic chromosomes are formed during the last five decades. A series of early pioneering studies analysed the architecture of mitotic chromosomes by a combination of techniques including electron microscopy, histone depletion by high-salt extraction protocols and nuclease treatments (Wray and Stubblefield 1970; Stubblefield and Wray 1971; Paulson and Laemmli 1977; Laemmli 1978; Earnshaw and Laemmli 1983). These analyses resulted in the detection of an axial proteinaceous core, the so-called scaffold, which might function as a backbone for chromatin folding during the chromosome condensation process.

The major components of the scaffold, named as Sc1 and Sc2, were later shown by biochemical approaches to be topoisomerase II and the structural maintenance of chromosomes (SMC2) subunit of the condensin complexes, respectively (Earnshaw et al. 1985; Gasser et al. 1986; Saitoh et al. 1994). The development of the *Xenopus* egg cell-free system allowed further biochemical characterization of the protein

Published online: 07 April 2015

components of metaphase chromosomes under defined and controlled conditions (Hirano and Mitchison 1994). The subunits of the condensin complexes CAP-C, CAP-E, CAP-D2, CAP-G and CAP-H, as well as chromokinesin (CAP-D/Klp1) and the chromatin remodelling ATPase ISWI (CAP-F), were identified by this method (Hirano and Mitchison 1994; Hirano et al. 1997; Vernos et al. 1995; MacCallum et al. 2002). Moreover, this experimental system has been crucial to dissect the functional role of many of these proteins in chromosome architecture. For example, the observation of a mass of chromatin without signs of chromosome individualization after specific depletion of condensin I and not in condensin II-depleted *Xenopus* egg extracts leads to the idea of a differential contribution of both condensin complexes in chromosome condensation (Ono et al. 2003). Further studies using the *Xenopus* cell-free system demonstrated that balanced levels of condensin I, condensin II and cohesin complexes are critically important for their primary actions during chromosome assembly, that is lateral compaction and axial shortening for condensin I and II, respectively, while cohesin counteracts the action of condensin II (Shintomi and Hirano 2011).

A useful approach to the functional delineation of the molecular components of the vertebrate mitotic machinery is the cell biological analysis of certain genetic disorders. For example, the analysis of disorders as Cornelia de Lange syndrome, or Roberts syndrome, both caused by mutations in cohesion-related genes, resulted in a better understanding of the mechanisms regulating chromatid cohesion and the clinical impact of the functional disruption of the respective gene functions (reviewed in Liu and Krantz 2008). Another remarkable example is primary microcephaly (MCPH), a rare congenital disorder characterized by a significant reduction of brain size, which mainly affects the cerebral cortex (Jackson et al. 2002). The head circumference of affected individuals is usually at least three standard deviations below that of unaffected individuals of the same age and sex (Cox et al. 2006). MCPH patients display largely normal brain architecture, are mentally retarded and lack other malformations or neurological defects (Woods 2004; Cox et al. 2006). MCPH is genetically heterogeneous, with 14 genes identified up to date (partially reviewed in Mahmood et al. 2011; Barbelanne and Tsang 2014; Khan et al. 2014). Patients cannot be distinguished clinically (Barbelanne and Tsang 2014).

Interestingly, cytogenetic analyses demonstrated that patients with mutations in MCPH1 gene display a unique cellular phenotype. Proliferating cell cultures of MCPH1 patients show dramatically increased rates of prophase-like cells (PLCs). This increase of PLCs is due to premature chromosome condensation (PCC) in early G2 phase of the cell cycle and delayed decondensation post mitosis (Neitzel et al. 2002; Trimborn et al. 2004). This observation resulted in the alternative name of MCPH1 primary microcephaly, that is premature chromosome condensation syndrome (PCC syndrome, OMIM 608585) and identified MCPH1 gene as a regulator of chromosome condensation. Thus, the thorough microscopical analysis of chromatin morphology of the patient cells assigned a novel function to a so far uncharacterised protein and added a new component to the complex network regulating chromosome condensation and mitosis.

Subsequently, it could be shown that the condensation defects in MCPH1 cells are caused by misregulation of the condensin II protein complex. Condensin II is negatively regulated by MCPH1 for a timely coordination of chromosome condensation (Trimborn et al. 2006; Yamashita et al. 2011). MCPH1 associates with chromatin through its N-terminal domain on the same binding sites as condensin II, inhibiting the loading of condensin II to the chromatin. Other studies have reported increased Cdc25A and reduced Cdk1 phosphorylation and centrosomal Chk1 levels to correlate with the premature chromosome condensation in MCPH1 patient cells (Alderton et al. 2006; Tibelius et al. 2009). Thus, cell cultures of patients with MCPH1 syndrome represent a unique opportunity to study the mechanisms underlying chromosome condensation and the coordination of the shaping of metaphase chromosomes and cell cycle progression.

We provide here further detailed morphological analyses of mitotic MCPH1 patient cells. Our results refine the description of the chromosome condensation defect typical for these cells and suggest additional functions of MCPH1 in the resolution and cohesion of metaphase chromosomes. These observations may provide a basis for a further delineation of the molecular processes regulating the preparation of chromosomes for segregation.

Material and methods

Cell lines and chromosome analyses

Conventional cytogenetic analyses were performed on lymphoblast cell lines (LCLs) from five MCPH1 patients (mutations S25X, T143nfsX5, W75R), as well as from healthy control subjects. LCLs were grown under usual conditions in RPMI medium supplemented with 10 % foetal bovine serum. For siRNA analyses, we used U2OS cells growing under standard conditions in DMEM medium. Chromosome preparations were obtained following standard protocols, with variations in the length of the hypotonic treatment (either 10 or 45 min using KCl 0.4 % at room temperature). Also, in some cases, the hypotonic incubation was done according to Gimenez-Abian et al. (2005), which better preserve chromosome morphology by incubating the cells during 6 min at room temperature in a solution 40 % medium/60 % tap water. Chromosome preparations were fixed using Carnoy's solution (methanol/glacial acetic acid, 3:1), stained with Giemsa (10 %) and finally visualized at microscope. The fraction of

"prophase-like cells" (PLCs) was determined after counting 1000 nuclei from coded slides. As previously described, we found the typical increased fraction of PLCs in all patient samples. For analyses of chromosome morphology, at least 70 metaphases were counted and classified. Representative images were captured with a CCD camera (Olympus DP70) coupled to a microscope (Olympus BX51) and finally managed with ImageJ software.

For irradiation, analyses LCLs were treated using the Muller MG 150 X ray apparatus (U_A, 100 kV; I, 10 mA; filter, 0.3 mm Ni; dose rate, 2.1 Gy/min; Seifert, Hamburg, Germany) with doses of 0.5 and 1.0 Gy. Chromosomes were prepared 6 h after irradiation as described above.

Immunofluorescence

Metaphase chromosome spreads from SV-40-transformed fibroblasts from one MCPH1 patient (mutation T143nfsX5) and one health control were prepared as described previously (Ono et al. 2003) with minor modifications. In brief, colcemid was added to the culture medium at a final concentration of 0.05 μg/ml 3 h before harvesting cells. Mitotic cells were collected by tapping culture dishes, treated with 75 mM KCl at 37 °C for 30 min, and then centrifuged onto coverslips at 1200 rpm for 5 min in a cytocentrifuge (Cytospin 4; Thermo Shandon). The cytospin preparations were fixed with 2 % paraformaldehyde for 15 min, permeabilized in 0.5 % Triton X-100 for 5 min and postfixed with 100 % methanol at −20 °C for 10 min. After counterstaining with 4′,6-diamidino-2-phenylindole (DAPI), coverslips were mounted with VECT ASHIELD and examined with a Zeiss Axioskop microscope equipped with a cooled charge-coupled device (CCD) camera. Grayscale images were pseudocolored and merged using ImageJ. Rabbit polyclonal antibodies used were anti-human CAP-E (Ono et al. 2003), anti-human TOPO-II (Topogen), anti-human CAP-H2 (Ono et al. 2003) and anti-human CAP-G (Kimura et al. 2001)..

siRNA and QRT-PCR

U2OS cells were grown in six-well-plates or T25 cell culture flasks and transfected with 120 nM siRNA duplexes using Lipofectamine (Invitrogen), at 0 and 24 h, at 50 % confluence. OptiMEM medium (Invitrogen) was used for cell transfection. The transfected cells were processed for cytological preparations or RT-PCR at 48 h after the first round of transfection. siRNA duplexes were purchased from Qiagen (Hilden, Germany). The sequences of the siRNAs used to deplete MCPH1 were directed against both main isoforms of MCPH1 mRNA, based on the previous study of Gavvovidis et al. (2012). The sequences of the sense strands were as follows: AGGAAGUUGGAAGGAUCCA (oligo-1) and GAUAAG AGAUUUCAGAAGA (oligo-2). A non-silencing oligo from Qiagen was used as control.

Total RNA was isolated using the RNeasy mini kit (Qiagen). First-strand cDNA synthesis was performed using the QuantiTect Reverse Transcription kit (Qiagen). A total of 0.5 μl of each first-stranded sample was used for real-time PCR, which was performed using SsoFast EvaGreen Supermix (BIO-RAD) on the CFX-384 real-time PCR system (BIO-RAD) according to the manufacturer's recommendations. All samples were analysed in triplicate in a final volume of 10 μl. The data were analysed using the comparative Ct method (ΔΔCt). HPRT- and PPIA-specific primers were used as endogenous controls. Primer sequences are available from the authors.

Results

As reported before, the chromosomes of MCPH1 patients display reduced banding resolution in routine cytogenetic analyses (Neitzel et al. 2002; Trimborn et al. 2006; Ghani-Kakhki et al. 2012). We hypothesized that this reduction in banding resolution is due to a hypercondensation of the metaphase chromosomes. To test this hypothesis, we measured the chromosomal length in Giemsa-stained cytogenetic preparations obtained from three MCPH1 patients (truncating mutations S25X, T143nfsX5) and compared it to three healthy controls. We analysed two of the longest human chromosomes, chromosome 2 and 3. Both chromosomes can be easily identified in plainly Giemsa-stained chromosomes and are not known to have heterochromatic polymorphisms that may bias the length measurements. We determined the length of the longitudinal axis of these chromosomes with the computer program ISIS3 V3.05 (MetaSystems). The length distribution and mean length were calculated on the basis of the length measurements of 50 chromosomes 2 and 3 in each sample, respectively (Fig. 1). On average, the length of chromosome 2 was 7.2 μm (S.D. 1.1) in controls and 5.4 μm (S.D. 0.6) in patients, while for chromosome 3, the observed dimension was 6.0 μm (S.D. 0.9) in controls and 4.5 μm (S.D. 0.5) in patients. These results demonstrate that the patient's metaphase chromosomes are shorter, with their length significantly reduced by approximately 25 %.

In addition to hypercondensation, the chromatids of the patient chromosomes have a characteristic wavy or coiled form (Fig. 2a). It was described that hypercondensed chromosomes after prolonged metaphase arrest are characterized by hypercoiled central chromosome axes (Maeshima and Laemmli 2003). We therefore stained the central chromatid axes of MCPH1 patient chromosomes (mutation T143NfsX5) with antibodies against hCAP-E (Fig. 2b), which is one of the two subunits of the condensin core that is shared by both condensin complexes, and with antibodies against topoisomerase IIα (TOPO-II) (Fig. 2c). Both proteins localize to the central chromatid axes of metaphase chromosomes. The

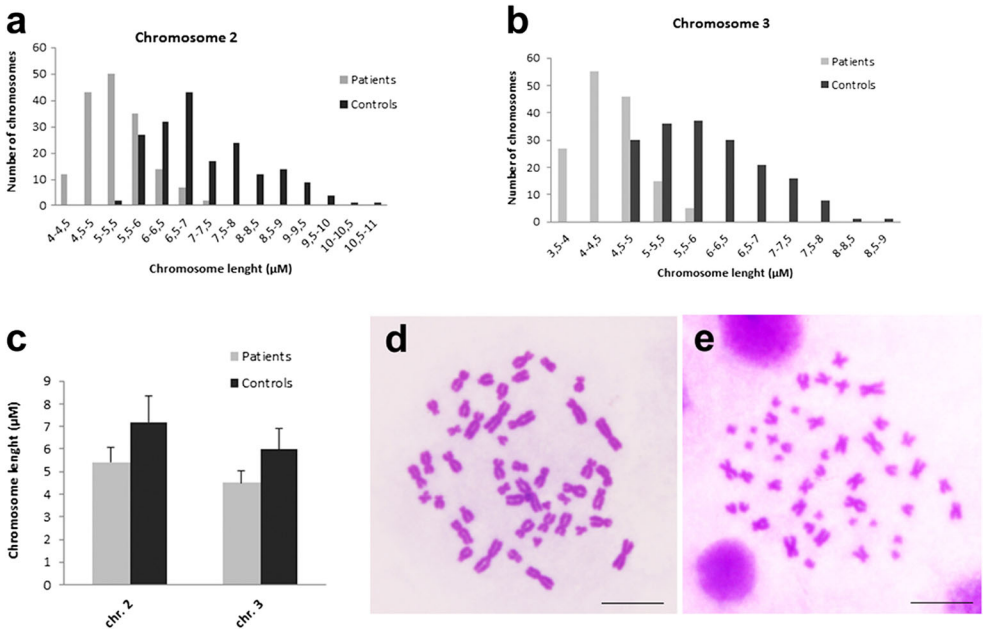

Fig. 1 Analyses of chromosome length in MCPH1 syndrome. **a**, **b** Length of chromosome 2 (**a**) and 3 (**b**) in patients and controls. Measurements were realized in chromosome preparations from three patients (mutations S25X and T143NfsX5) and three controls. A total number of 150 metaphases were analysed in patients and controls, respectively, and the estimated length of chromosome 2 and 3 was plotted. **c** Mean length of chromosomes 2 and 3 in patients and controls from the data presented in **a** and **b**. *Error bars* denote S.D. for each chromosome. **d**, **e** Representative images from a normal sized metaphase (**d**) and a metaphase with hypercondensed chromosomes, frequently observed in MCPH1 patients (e). **e** Images are from chromosome preparations stained with Giemsa. *Bar* 10 µm

chromatid axes of the patient chromosomes had a distinctly hypercoiled appearance with both antibodies (Fig. 2b, c). We also have simultaneously examined the particular distribution of both condensin complexes on the chromatid axes using simultaneously antibodies against CAP-G (subunit of condensin I) and CAP-H2 (subunit of condensin II). In our analyses, both proteins were loaded along the entire length of the chromatid axes in metaphases of patient cells. The labelling revealed an interspersed pattern similar to the one observed in control cells (Fig. 2d). This alternate distribution of both condensin complexes along the chromosomes has been described in previous studies (Ono et al. 2003). Again, the chromatid axes of the patient chromosomes appeared strongly hypercoiled.

Our morphological analyses further revealed another so far undescribed alteration in the chromosome morphology of the patient cells. Standard cytogenetic preparations from five MCPH1 patients (mutations S25X, T143NfsX5 and W75R) showed a high incidence of wavy chromosomes with apparently unresolved, "twisted" chromatids (see inset from Fig. 3d). By unresolved, we make here reference to the process of sister chromatid resolution, by which undistinguished sister chromatids become visible as two discrete paired units during prophase or early prometaphase (Sumner 1991; Shintomi and Hirano 2010). We refer to these wavy chromosomes with apparently unresolved sister chromatids as "twisted" chromosomes in the subsequent text. On average, the frequency of metaphases showing this atypical chromosome morphology was 8.2 % (S.D. 3.4) in control individuals and 29.6 % (S.D. 6.6) in patients (Fig. 3a, b). The differences were statistically significant ($p<0.001$, X^2 test). The highest rate was observed in patients bearing truncating mutations (S25X, T143nfsX5) while in the patient containing a missense mutation (W75R), the phenomenon was less marked but its frequency still significantly increased compared with controls. Additionally, we also performed a morphological study on cytogenetic preparations obtained following the protocol described by Gimenez-Abian et al. (2005), which better preserve mitotic morphology. In patient cells, we observed again a high incidence of metaphases with unresolved twisted chromosomes which demonstrate that the occurrence of this type of alteration is not biased by particular conditions during the methodological procedures.

It was demonstrated that MCPH1 has crucial functions in DNA damage response (e.g. Xu et al. 2004; Alderton et al. 2006; Singh et al. 2012). Although the patient cells do not show dramatic defects in response to DNA damage, we could show before that ionizing irradiation increases the fraction of cells with condensed chromatin in cultures of MCPH1-deficient cells (Gavvovidis et al. 2010). On this context, we asked whether irradiation would have an influence in the incidence of twisted chromosomes in patient cells. Cells from two MCPH1 patients (mutations S25X, T143nfsX5) were irradiated with 0.5 and 1.0 Gy, and cytogenetic slides were prepared 6 h later. These preparations were coded, and metaphases were microscopically screened for unresolved twisted

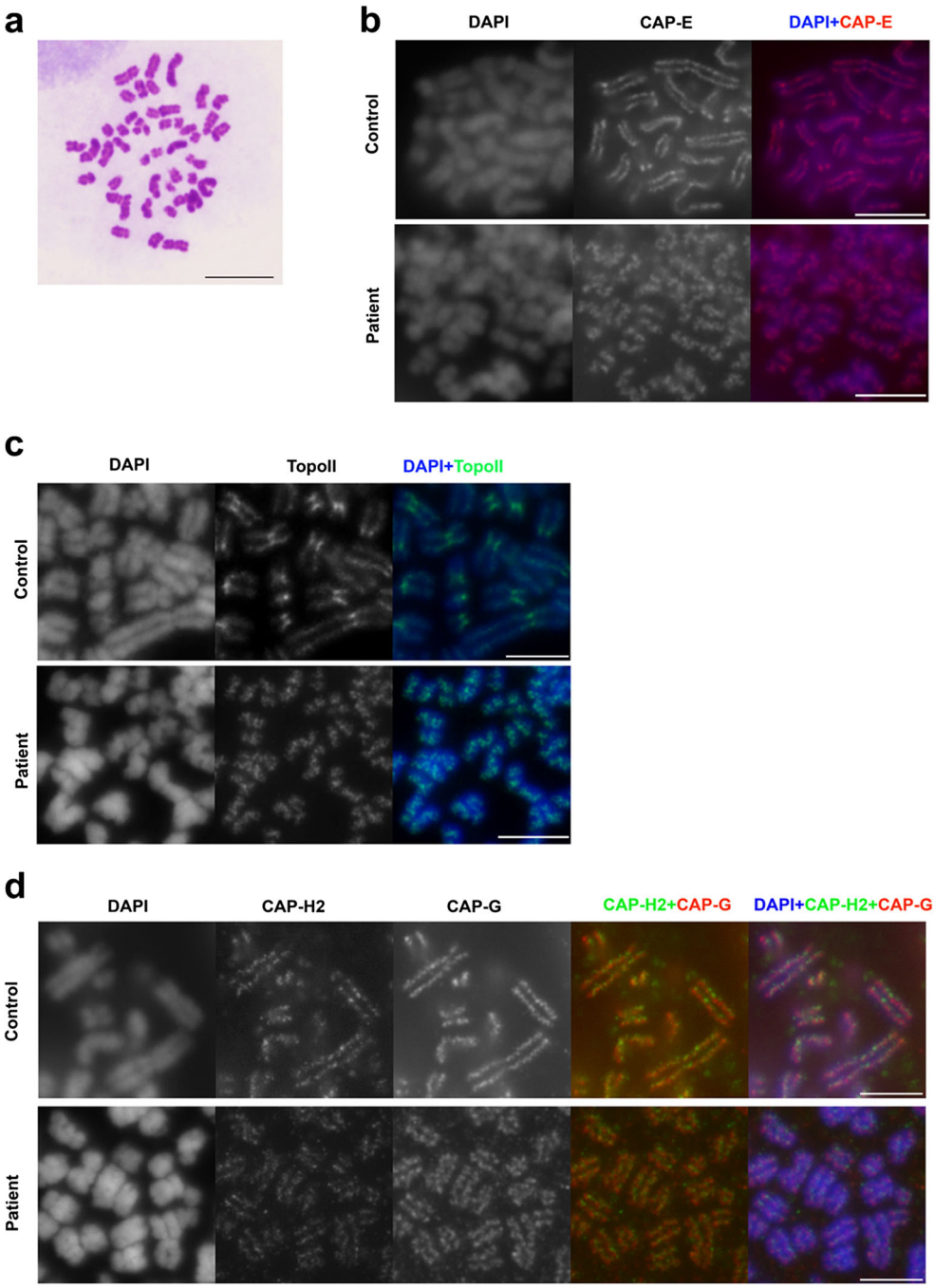

Fig. 2 **a** A metaphase showing hypercondensed chromosomes with a wavy morphology, frequently observed in MCPH1 patient cells. **b–d** Immunostaining analyses of condensin and topoisomerase II on MCPH1 patient and control chromosomes. Chromosome spreads obtained by cytospin from control and MCPH1 patient cells were stained with DAPI and anti-hCAP-E, a common subunit of both condensin complexes (**b**), anti-Topo-II (**c**), and simultaneously with anti-hCAP-H2 and anti-hCAP-G, specific subunits from condensin II and condensin I, respectively (**d**). Grayscale images were pseudocolored and merged using ImageJ. *Bar* 10 μm

chromatids (Fig. 3c). Our analyses showed an increase in the fraction of metaphases with unresolved twisted chromosomes after irradiation from 31 % (S.D. 1.41) in the unirradiated cells to 64 % (S.D. 5.36) and 68.9 % (S.D. 15.63) after doses of 0.5 and 1.0 Gy, respectively. This result suggests that DNA damage produced by irradiation increase the structural deficiency of patient chromosomes.

During our analyses of MCPH1 patient cells, we noticed metaphase chromosomes where the centromeres of sister chromatids had already separated. Premature centromere division (PCD) was observed and described for other genetic disorders such as mosaic variegated aneuploidy (MVA) or Cornelia de Lange syndrome (Kaur et al. 2005; Gerkes et al. 2010). To investigate a possible defect in centromeric cohesion in MCPH1, we quantitatively analysed chromosome preparations from lymphoblastoid cell lines of patients and controls and classified the metaphases as follows: without premature centromere division (no PCD), when the centromeres of all chromosomes of a metaphase were connected; with partial premature centromere division (partial PCD), if some but not all chromosomes showed premature centromere division; or with complete premature centromere division

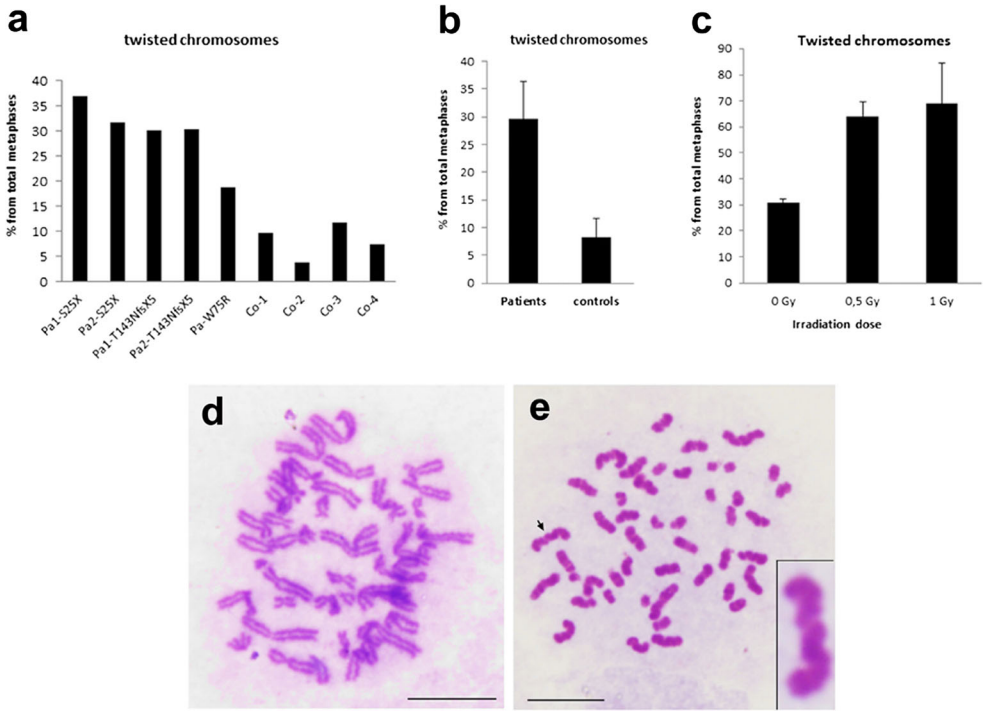

Fig. 3 Analyses of chromosome morphology in MCPH1 patient cells. **a** Fraction of metaphases with "twisted" appearance in chromosome preparations from five MCPH1 patients (mutations indicated) and four healthy controls. A total of 70 metaphases were analysed in each sample, and the fraction of twisted metaphases was determined by microscopic classification of their morphology after Giemsa staining. **b** Mean fraction of metaphases with "twisted" appearance in patients and controls from the data presented in **a**. *Error bars* denote S.D. The differences were statistically significant ($p<0.001$, X^2 test). **c** Rate of twisted chromosomes in MCPH1 patient cells after DNA damage. Lymphoblastoid cells from two MCPH1 patients (S25X, T143NfsX5) were irradiated with 0, 0.5 and 1 Gy, and the fraction of twisted metaphases was estimated in chromosome spreads prepared 6 h after irradiation. The mean fraction is presented, and *error bars* denotes S.D. of samples. **d**–**e** Representative images of Giemsa-stained chromosomes with normal morphology (**d**) and with "twisted" shaped chromosomes (**e**). The chromosome pointed with an *arrow* is three times magnified on the right side. *Bar* 10 μm

(PCD complete), if all chromosomes of a metaphase showed centromere division (representative images in Fig. 4c). In cytogenetic preparations obtained under standard hypotonic conditions, we observed an increased fraction of metaphases with partial PCD in patients (mean=24.5 %, S.D.=9.7) compared with controls (mean=3.2 %, S.D.=3.2) (Fig. 4a). The differences were statistically significant ($p<0.001$, X^2 test). The rate of complete PCD was negligible in all those samples. We next repeated these analyses on chromosome preparations obtained after prolonged incubation in hypotonic treatment (45 min), based on the demonstrated susceptibility to the hypotonic effects of chromosomes with cohesion defects (Ikeuchi et al. 2004). The results confirm the defect in centromere cohesion in MCPH1 cells. Under strong hypotonic conditions, the fraction of metaphases showing PCD increased to 66.7 % (S.D. 17.4) in MCPH1 patient cells compared to 8.5 % (S.D. 8.6) in control cells (Fig. 4b). Furthermore, the fraction of metaphases displaying complete PCD was 32.3 % (S.D. 13.25) in patients and only 5.5 % (S.D. 6.40) in controls. Both differences were statistically significant ($p<0.001$, X^2 test). Our results demonstrate that MCPH1 patient cells apart from their well-described defect in chromosome condensation also show defective centromeric cohesion.

In order to recapitulate our previous findings in patient cells, we performed cytogenetic analyses in cells depleted of MCPH1 function by RNAi. This approach was successfully used before to demonstrate the role of MCPH1 in the regulation of chromosome condensation (Trimborn et al. 2004, 2006; Gavvovidis et al. 2012). Our results show that the morphology of metaphase chromosomes in MCPH1-siRNA-treated cells is affected to a similar extend as in MCPH1 patient cells. Most metaphases in cells treated with siRNAs against MCPH1 showed hypercondensed chromosomes with wavy or coiled morphology (mean=90.9 %, S.D.=5.9), while in cells treated with control siRNAs, chromosomes showed a normal morphology (mean=97.4 %, S.D.=0.3) (Fig. 5a, b). Furthermore, in some metaphases of the MCPH1-depleted cells, we observed twisted chromosomes with apparently unresolved chromatids (Fig. 5b). Similar results were obtained when using an alternative siRNA to deplete MCPH1. We also observed an increased rate of metaphases with PCD in cells treated with MCPH1 siRNAs compared to controls. Under standard hypotonic conditions, the fraction of nocodazole-arrested metaphases displaying partial PCD was increased in MCPH1-depleted cells (mean=20.3 %, S.D.=4.7) compared to control cells (mean=5.5 %, S.D.=2.5) (Fig. 5c). The differences were statistically

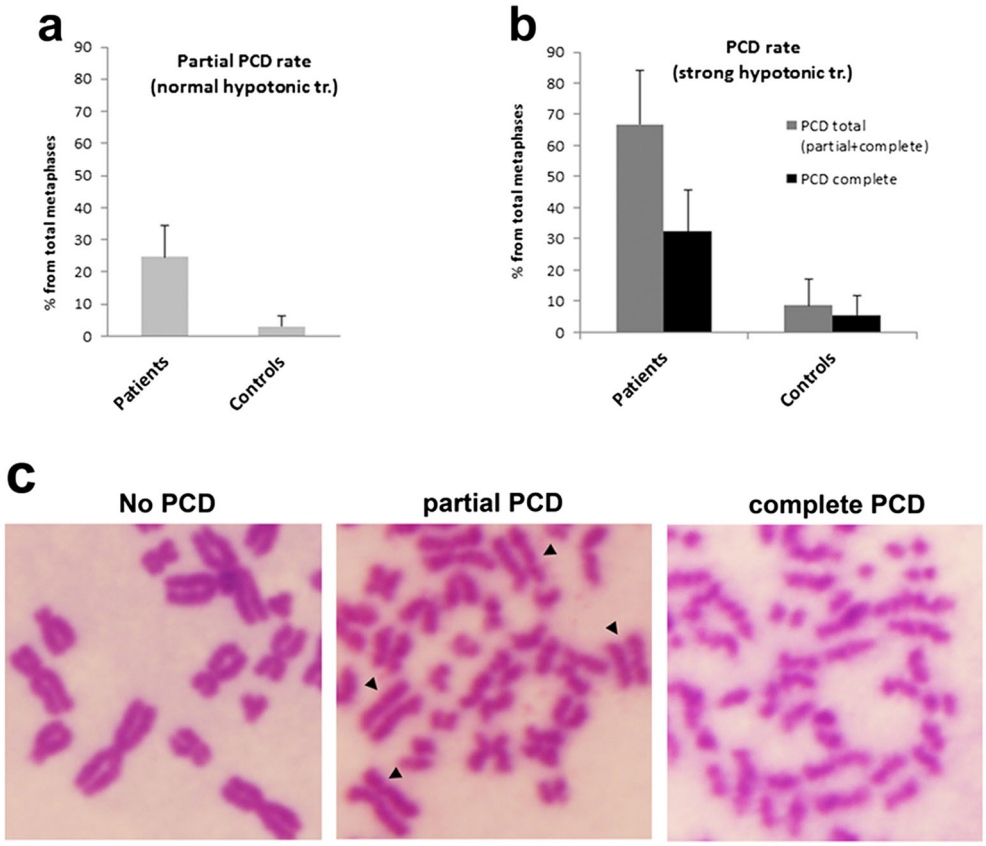

Fig. 4 Analyses of centromere cohesion in MCPH1 patient cells. Metaphases chromosomes from five MCPH1 patients (mutations S25X, T143NfsX5 and W75R) and four healthy controls were classified in three categories according to their cohesion status: without premature centromere separation (no PCD), with partial premature centromere separation (partial PCD) or with complete premature centromere separation (complete PCD). Seventy metaphases were analysed and scored in all samples. **a** Fraction of metaphases with partial PCD in patient and control samples obtained after normal hypotonic conditions. Differences were statistically significant ($p<0.001$, X^2 test). **b** Fraction of metaphases with PCD in patient and control samples obtained after strong hypotonic conditions. The fraction of metaphases showing complete PCD and also the proportion of metaphases presenting either partial or complete PCD are shown. Differences were statistically significant in both cases ($p<0.001$, X^2 test). **c** Representative images of chromosomes without PCD, or with either partial or complete PCD. Chromosomes pointed with *arrowheads* are good examples of partial PCD, showing slightly separated chromatids and reduced centromeric constrictions. Note the difference to the complete PCD category, where the chromatids and the centromeres are fully separated and distanced each other

significant ($p<0.001$, X^2 test). The efficiency of the MCPH1-siRNAs was confirmed by determining the incidence of cells with condensed chromatin ("prophase-like cells" (PLCs)), which is the cellular phenotype that correlates with MCPH1 lack of function (Trimborn et al. 2004, 2006; Gavvovidis et al. 2012). As expected, we observed an increased rate of PLCs in cells treated with siRNAs against MCPH1 (mean= 7.5 %, S.D.=2.12) than in cells treated with control siRNAs (mean=1.4 %, S.D.=1.7) (Fig. 5d). The differences were statistically significant ($p<0.001$, X^2 test). Also, the mRNA levels of MCPH1 were efficiently reduced after RNAi (Fig. 5e).

Discussion

The thorough analysis of cytogenetic preparations from patients with MCPH1 mutations led to the identification of MCPH1 as an important regulator of chromosome condensation. MCPH1-deficient cells condense their chromatin prematurely shortly after the completion of replication at the beginning of G2 phase of the cell cycle and decondense their chromatin delayed in G1 phase (Neitzel et al. 2002; Trimborn et al. 2004). MCPH1 deficiency appears thus to uncouple the chromosome cycle from the coordinated series of events that take place during mitosis, such as some phases of the centrosome cycle or nuclear envelope breakdown. Subsequently, it could be shown that MCPH1 regulates chromosome condensation and shaping as a composite modulator of condensin II (Trimborn et al. 2006; Yamashita et al. 2011). While the N-terminal domain of MCPH1 appears to regulate the onset of mitotic chromosome condensation via condensin II, its central domain plays an additional role in shaping the metaphase chromosomes (Yamashita et al. 2011). Thus, the cytomorphological analysis of MCPH1-deficient cells not only identified the

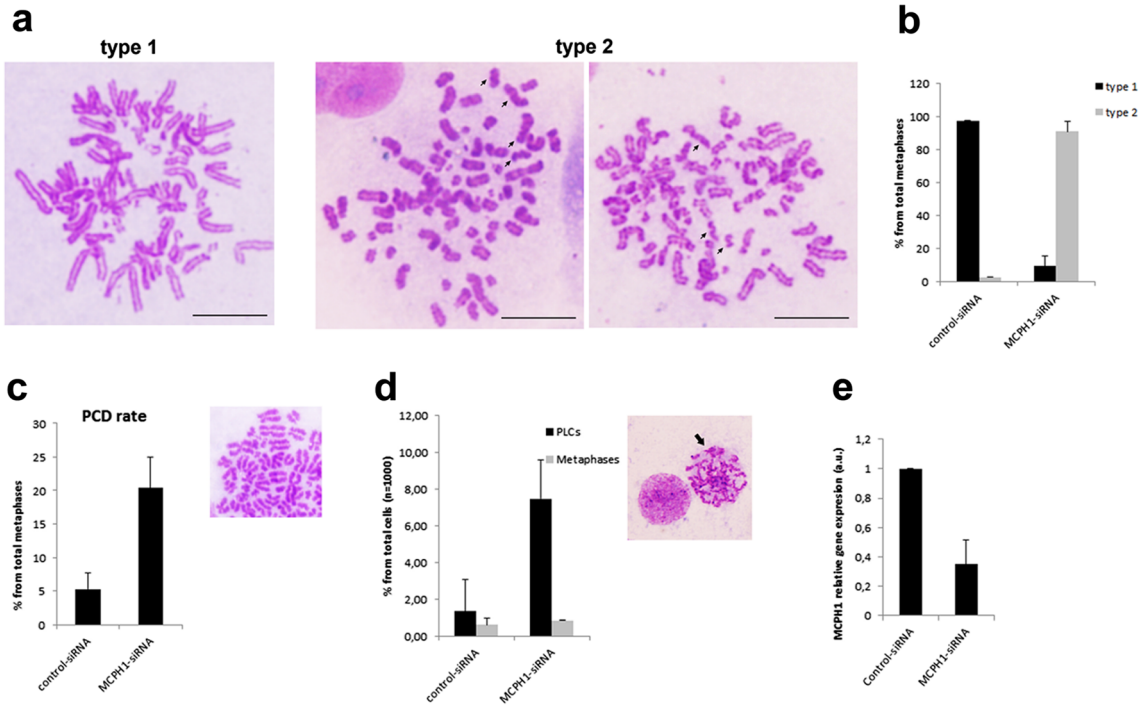

Fig. 5 Analyses of chromosome structure in U2OS cells treated with control or MCPH1-directed siRNAs oligos. **a** Representative images of the main chromosomal morphologies observed in our experiments. In type 1, chromosomes present straight and well-resolved chromatids, while in type 2 chromosomes are all hypercompacted and with wavy appearance. Note that some of them (indicated by *arrows*) show unresolved twisted chromatids comparable to the patient chromosomes shown in Fig. 3e. *Bar* 10 μm. **b** Fraction of metaphase chromosomes showing either type 1 or type 2 chromosomal morphologies after the indicated siRNA treatments. Analyses were done in coded slides as explained in Fig. 3. Data represent the mean and S.D. from two independent experiments. **c** Fraction of metaphases showing partial premature centromeric division after normal hypotonic conditions (analyses performed as explained in Fig. 4). A representative image of chromosomes with partial PCD is shown. Data represent the mean and S.D. from two independent experiments. The differences were statistically significant ($p<0.001$, X^2 test). **d** Fraction of "prophase-like cells" (PLCs) and metaphases observed after the indicated siRNA treatments. A total of 1000 cells were classified on Giemsa-stained coded slides. A representative image of a PLC (pointed by *arrow*) is presented. Data represent the mean and S.D. from two independent experiments. The differences were statistically significant ($p<0.001$, X^2 test). **e** Relative quantification of MCPH1-mRNA levels in cells after the indicated siRNA treatments. Mean and S.D. from two independent experiments

function of MCPH1 in chromosome condensation but also paved the way to the identification of a so far unknown molecular pathway regulating metaphase chromosome condensation and shaping. Therefore, we decided that a further detailed morphological description of MCPH1 patient cells may provide additional clues about how exactly MCPH1 effects chromosome condensation or maybe even indicate further functions.

Our analyses demonstrate that the patient's metaphase chromosomes are approximately 25 % shorter than the chromosomes of controls. Giemsa-stained patient chromosomes also have a distinctive wavy morphology which—like the length reduction—may be explained by an extreme hypercoiling of the central chromatid axes as shown by immunostaining of key components of that structure. It is a well-known phenomenon that prolonged metaphase arrest induced by spindle poisons results in chromosome hypercondensation. These hypercondensed metaphase chromosomes are characterized by a hypercoiled central chromatid axis (Maeshima and Laemmli 2003). Remarkably, the extent of the longitudinal compression of the patient's chromosomes is similar to that of chromosomes of cells in prolonged nocodazole arrest during 12 h, which are on average 20 % shorter (Naumova et al. 2013). This may indicate that after the initial priming of the process of chromosome condensation, the longitudinal compaction proceeds to a maximum level as long as the chromosomes are not segregated in anaphase. Thus, for the occurrence of the phenomenon of hypercondensed metaphase chromosomes, it may not matter whether the condensation timing is prolonged by a premature entry into chromosome condensation as in MCPH1-deficient cells or by a prolonged continuation of the process as in metaphase arrest induced by spindle poisons.

Currently, we are unable to explain the significance of our observation of metaphase chromosomes with apparently unresolved twisted chromatids in cell cultures of MCPH1 patient cells. During an unperturbed prophase in metazoan cells, the replicated genome is not only condensed but also resolved into two microscopically discernible chromatids. Sister chromatid resolution is a dynamic and complex process that requires the formation of the chromatid axes, the release of

chromatid-bound cohesin and the decatenation of the DNA strands of the sister chromatids. This process is fundamental for the accurate segregation of sister chromatids in subsequent anaphase and, therefore, in animal cells is completed by early prometaphase (Losada et al. 2002; Shintomi and Hirano 2010). Although, we cannot decide whether the appearance of the twisted chromosomes is due to defective regulation of cohesion or decatenation, or even represents a completely unrelated phenomenon, it is remarkable that they resemble some of the intermediary stages of chromosome organization during early mitosis proposed by Giménez-Abián et al. (1995). The authors suggested that at the boundary of prophase to prometaphase, the cores of the two sister chromatids remain closely associated. These structures, however, seem to be extremely transient and difficult to observe, as the decatenation and separation into discernible chromatids are rapidly achieved (Giménez-Abián et al. 1995). The functional significance of twisted chromosomes has to be backed up by molecular investigations of chromatid cohesion and decatenation process in MCPH1-deficient cells.

A relation has been established between DNA damage and the defective condensation behaviour of MCPH1 patient cells. Here, we have observed a dramatic increase in the occurrence of unresolved twisted chromosomes following ionizing irradiation in the patient cells. MCPH1 gene presents a key function in DNA damage response and checkpoint control (Xu et al. 2004; Lin et al. 2005; Rai et al. 2006). Direct testing of cell lines from MCPH1 patients showed unexpectedly a G2/M-proficient checkpoint in response to irradiation, followed by a slight delay during subsequent entrance into mitosis (Gavvovidis et al. 2010). Despite the efficient DNA damage checkpoint, patient cells do not decondense their chromatin completely after irradiation, which is in agreement with the role of MCPH1 as regulator of the activity of SWI-SNF chromatin remodelling complex during DNA repair (Peng et al. 2009; Gavvovidis et al. 2010). Instead of decondensation, 6 h after irradiation, patient cells showed a rise into the number of prophase-like cells (PLCs), which is explained as a result of the premature chromosome condensation behaviour combined with the proficient G2/M checkpoint, which forced patient cells to accumulate in G2 phase after DNA damage but with condensed chromatin (Gavvovidis et al. 2010). In spite of better understanding their functional significance, it is tempting to speculate that twisted chromosomes rise after irradiation indirectly as consequence of the prolonged timing of chromatin condensation triggered by DNA damage.

We were surprised by our observation of defective centromeric cohesion in the patients' cells. Metaphase cells of the patients showed increased rates of premature centromeric division (PCDs). Although the defect was not prominent under normal hypotonic conditions, it was statistically significant. Moreover, it became more pronounced following harsher hypotonic treatment. Severe loss of chromosome cohesion is a hallmark of some genetic disorders among others Roberts syndrome (RBS), mosaic variegated aneuploidy (MVA) and Cornelia de Lange syndrome (CdLS) (Tomkins et al. 1979; Kajii et al. 1998; Kaur et al. 2005). While RBS and CdLS are cohesinopathies caused by mutations in genes regulating chromosome cohesion (Vega et al. 2005; Tonkin et al. 2004), MVA represents a defect of the spindle checkpoint (Hanks et al. 2004). However the loss of cohesion in MCPH1 mutant cells is less dramatic and rather resemble the scenario described for patients with microcephalic osteodysplastic primordial dwarfism type II syndrome (MOPDII), harbouring mutations in PCNT gene (Rauch et al. 2008), or patients affected by alpha-thalassemia/mental retardation X-linked by mutations in ATRX gene (Ritchie et al. 2008). In both syndromes, comparable to our observation in MCPH1 patient cells, the centromeric cohesion is reduced but not completely loss and was only detected after extended hypotonic treatment (longer than 20 min). Both PCNT and ATRX genes code for chromatin remodelling complexes influencing chromatid cohesion through different proposed pathways, spindle assembly checkpoint for PCNT and cohesin loading for ATRX (Rauch et al. 2008; Ritchie et al. 2008). It is noteworthy that chromatin remodelling function is also involved in the pathogenesis of MCPH syndrome since mutations in PCH1 gene, a chromatin remodelling factor, were identified in a family affected by primary microcephaly (Awad et al. 2013). No reports on cohesion defect for these patients were presented. In conclusion, our observation of PCDs in patient cells could originate from a so far unknown function of MCPH1 in centromeric cohesion or indirectly from the altered structure of the hypercondensed chromatin. Since MCPH1 condition leads to uncoupling of chromosome cycle from the coordinated events that occur during mitosis, another different origin for PCDs would be early release of centromere cohesion during chromosome division in cells lacking MCPH1 function.

So far, there are no reports of increased aneuploidy levels in MCPH1 patient cells (Neitzel et al. 2002). Accordingly, the reduced centromeric cohesion appears not to disturb subsequent chromosome segregation in MCPH1-mutated cells. Although the number of known elderly patients is extremely small, this observation could in part explain the lack of evidence for an elevated cancer incidence among them. Cancer predisposition is also not reported in CdLS (Liu and Krantz 2008), RBS (Van den Berg and Francke 1993), MOPDII (Rauch et al. 2008) or ATRX syndromes (Gibbons et al. 1995). Increased aneuploidy levels are occurring among some of them as RBS or MOPDII but the incidence is much lower compared with MVA patients, who are inevitably suffering of higher rates of childhood cancer (Callier et al. 2005). Nevertheless, the correlation of MCPH1 mutations with cancer still has to be elucidated as deregulation of MCPH1 expression has been noticed in different tumours during the last years (reviewed in Venkatesh and Suresh 2014). Moreover, a

recent study using a mouse model shows that MCPH1 deficiency promotes genomic instability and increases cancer susceptibility (Liang et al. 2014).

In conclusion, our present study demonstrates that MCPH1 mutations disturb the shape of mitotic chromosomes in a specific manner. Detailed morphological analyses of patient cells harbouring different types of mutations (both protein truncating and missense mutations) revealed hypercoiling of the chromatid axes, longitudinal length reduction and unresolved chromatids. Moreover, we observed defective centromere cohesion in the patient cells. These chromosomal defects were recapitulated in cells depleted of MCPH1 by siRNAs. Interestingly, the two latter alterations, unresolved chromatids and defective centromere cohesion, may point towards so far unknown novel functions of the MCPH1 protein.

Acknowledgments We are indebted to the patients, their parents and the clinicians for their cooperation. We thank S. Niehage for her excellent technical assistance in some analyses. Technical and human support provided by CICT of Universidad de Jaén (UJA, MINECO, Junta de Andalucía, FEDER) is gratefully acknowledged.

Conflict of interest The authors declare no conflict of interest.

Ethical approval All procedures were in accordance with the ethical standards of the institutional and/or national research committee and with the 1964 Helsinki declaration and its later amendments or comparable ethical standards.

Funding This work was supported by Universidad de Jaén (grant UJA2011/12/36), Junta de Andalucía (Funding program "Ayudas a grupos de investigación", reference BIO220) and by Deutsche Forschungsgemeinschaft (grant NE531/5-3).

References

Alderton GK, Galbiati L, Griffith E, Surinya KH, Neitzel H, Jackson AP, Jeggo PA, O'Driscoll M (2006) Regulation of mitotic entry by microcephalin and its overlap with ATR signalling. Nat Cell Biol 8:725–733

Awad S, Al-Dosari MS, Al-Yacoub N, Colak D, Salih MA, Alkuraya FS, Poizat C (2013) Mutation in PHC1 implicates chromatin remodeling in primary microcephaly pathogenesis. Hum Mol Genet 22(11): 2200–2213. doi:10.1093/hmg/ddt072

Barbelanne M, Tsang WY (2014) Molecular and cellular basis of autosomal recessive primary microcephaly. Biomed Res Int 2014: 547986. doi:10.1155/2014/547986

Callier P, Faivre L, Cusin V, Marle N, Thauvin-Robinet C, Sandre D, Rousseau T, Sagot P, Lacombe E, Faber V, Mugneret F (2005) Microcephaly is not mandatory for the diagnosis of mosaic variegated aneuploidy syndrome. Am J Med Genet A 137(2):204–207

Cox J, Jackson AP, Bond J, Woods CG (2006) What primary microcephaly can tell us about brain growth. Trends Mol Med 12:358–366

Earnshaw WC, Laemmli UK (1983) Architecture of metaphase chromosomes and chromosome scaffolds. J Cell Biol 96(1):84–93

Earnshaw WC, Halligan B, Cooke CA, Heck MM, Liu LF (1985) Topoisomerase II is a structural component of mitotic chromosome scaffolds. J Cell Biol 100(5):1706–1715

Gasser SM, Laroche T, Falquet J, Boy de la Tour E, Laemmli UK (1986) Metaphase chromosome structure. Involvement of topoisomerase II. J Mol Biol 188(4):613–629

Gavvovidis I, Pöhlmann C, Marchal JA, Stumm M, Yamashita D, Hirano T, Schindler D, Neitzel H, Trimborn M (2010) MCPH1 patient cells exhibit delayed release from DNA damage-induced G2/M checkpoint arrest. Cell Cycle 9(24):4893–4899

Gavvovidis I, Rost I, Trimborn M, Kaiser FJ, Purps J, Wiek C, Hanenberg H, Neitzel H, Schindler D (2012) A novel MCPH1 isoform complements the defective chromosome condensation of human MCPH1-deficient cells. PLoS One 7(8):e40387. doi:10.1371/journal.pone.0040387

Gerkes EH, van der Kevie-Kersemaekers AM, Yakin M, Smeets DF, van Ravenswaaij-Arts CM (2010) The importance of chromosome studies in Roberts syndrome/SC phocomelia and other cohesinopathies. Eur J Med Genet 53(1):40–44. doi:10.1016/j.ejmg.2009.10.005

Ghani-Kakhki M, Robinson PN, Morlot S, Mitter D, Trimborn M, Albrecht B, Varon R, Sperling K, Neitzel H (2012) Two missense mutations in the primary autosomal recessive microcephaly gene MCPH1 disrupt the function of the highly conserved N-terminal BRCT domain of microcephalin. Mol Syndromol 3:6–13

Gibbons RJ, Picketts DJ, Villard L, Higgs DR (1995) Mutations in a putative global transcriptional regulator cause X-linked mental retardation with alpha-thalassemia (ATR-X syndrome). Cell 80(6): 837–845

Giménez-Abián JF, Clarke DJ, Mullinger AM, Downes CS, Johnson RT (1995) A postprophase topoisomerase II-dependent chromatid core separation step in the formation of metaphase chromosomes. J Cell Biol 131(1):7–17

Gimenez-Abian JF, Diaz-Martinez LA, Wirth KG, De la Torre C, Clarke DJ (2005) Proteasome activity is required for centromere separation independently of securin degradation in human cells. Cell Cycle 4: 1558–1560

Hanks S, Coleman K, Reid S, Plaja A, Firth H, Fitzpatrick D, Kidd A, Méhes K, Nash R, Robin N, Shannon N, Tolmie J, Swansbury J, Irrthum A, Douglas J, Rahman N (2004) Constitutional aneuploidy and cancer predisposition caused by biallelic mutations in BUB1B. Nat Genet 36(11):1159–1161

Hirano T, Mitchison TJ (1994) A heterodimeric coiled-coil protein required for mitotic chromosome condensation in vitro. Cell 79(3): 449–458

Hirano T, Kobayashi R, Hirano M (1997) Condensins, chromosome condensation protein complexes containing XCAP-C, XCAP-E and a Xenopus homolog of the Drosophila Barren protein. Cell 89(4): 511–521

Ikeuchi T, Yang ZQ, Wakamatsu K, Kajii T (2004) Induction of premature chromatid separation (PCS) in individuals with PCS trait and in normal controls. Am J Med Genet A 127A:128–132

Jackson AP, Eastwood H, Bell SM, Adu J, Toomes C, Carr IM, Roberts E, Hampshire DJ, Crow YJ, Mighell AJ, Karbani G, Jafri H, Rashid Y, Mueller RF, Markham AF, Woods CG (2002) Identification of microcephalin, a protein implicated in determining the size of the human brain. Am J Hum Genet 71:136–142

Kajii T, Kawai T, Takumi T, Misu H, Mabuchi O, Takahashi Y, Tachino M, Nihei F, Ikeuchi T (1998) Mosaic variegated aneuploidy with multiple congenital abnormalities: homozygosity for total premature chromatid separation trait. Am J Med Genet 78(3):245–249

Kaur M, DeScipio C, McCallum J, Yaeger D, Devoto M, Jackson LG, Spinner NB, Krantz ID (2005) Precocious sister chromatid separation (PSCS) in Cornelia de Lange syndrome. Am J Med Genet A 138:27–31

Khan MA, Rupp VM, Orpinell M, Hussain MS, Altmüller J, Steinmetz MO, Enzinger C, Thiele H, Höhne W, Nürnberg G, Baig SM, Ansar M, Nürnberg P, Vincent JB, Speicher MR, Gönczy P, Windpassinger C (2014) A missense mutation in the PISA domain of HsSAS-6 causes autosomal recessive primary microcephaly in a large

consanguineous Pakistani family. Hum Mol Genet 23(22):5940–5949. doi:10.1093/hmg/ddu318

Kimura K, Cuvier O, Hirano T (2001) Chromosome condensation by a human condensin complex in Xenopus egg extracts. J Biol Chem 276:5417–5420

Laemmli UK (1978) Levels of organization of the DNA in eucaryotic chromosomes. Pharmacol Rev 30(4):469–476

Liang Y, Gao H, Lin SY, Goss JA, Du C, Li K (2014) Mcph1/Brit1 deficiency promotes genomic instability and tumor formation in a mouse model. Oncogene. doi:10.1038/onc.2014.367

Lin SY, Rai R, Li K, Xu ZX, Elledge SJ (2005) BRIT1/MCPH1 is a DNA damage responsive protein that regulates the Brca1-Chk1 pathway, implicating checkpoint dysfunction in microcephaly. Proc Natl Acad Sci U S A 102(42):15105–15109

Liu J, Krantz ID (2008) Cohesin and human disease. Annu Rev Genomics Hum Genet 9:303–320. doi:10.1146/annurev.genom.9.081307.164211

Losada A, Hirano M, Hirano T (2002) Cohesin release is required for sister chromatid resolution, but not for condensin-mediated compaction, at the onset of mitosis. Genes Dev 16(23):3004–3016

MacCallum DE, Losada A, Kobayashi R, Hirano T (2002) ISWI remodeling complexes in Xenopus egg extracts: identification as major chromosomal components that are regulated by INCENP-aurora B. Mol Biol Cell 13(1):25–39

Maeshima K, Laemmli UK (2003) A two-step scaffolding model for mitotic chromosome assembly. Dev Cell 4(4):467–480

Mahmood S, Ahmad W, Hassan MJ (2011) Autosomal recessive primary microcephaly (MCPH): clinical manifestations, genetic heterogeneity and mutation continuum. Orphanet J Rare Dis 6:39. doi:10.1186/1750-1172-6-39

Naumova N, Imakaev M, Fudenberg G, Zhan Y, Lajoie BR, Mirny LA, Dekker J (2013) Organization of the mitotic chromosome. Science 342(6161):948–953. doi:10.1126/science.1236083

Neitzel H, Neumann LM, Schindler D, Wirges A, Tonnies H, Trimborn M, Krebsova A, Richter R, Sperling K (2002) Premature chromosome condensation in humans associated with microcephaly and mental retardation: a novel autosomal recessive condition. Am J Hum Genet 70:1015–1022

Ono T, Losada A, Hirano M, Myers MP, Neuwald AF, Hirano T (2003) Differential contributions of condensin I and condensin II to mitotic chromosome architecture in vertebrate cells. Cell 115:109–121

Paulson JR, Laemmli UK (1977) The structure of histone-depleted metaphase chromosomes. Cell 12(3):817–828

Peng G, Yim EK, Dai H, Jackson AP, Iv B, Pan MR, Hu R, Li K, Lin SY (2009) BRIT1/MCPH1 links chromatin remodelling to DNA damage response. Nat Cell Biol 11(7):865–872. doi:10.1038/ncb1895

Rai R, Dai H, Multani AS, Li K, Chin K, Gray J, Lahad JP, Liang J, Mills GB, Meric-Bernstam F, Lin SY (2006) BRIT1 regulates early DNA damage response, chromosomal integrity, and cancer. Cancer Cell 10(2):145–157

Rauch A, Thiel CT, Schindler D, Wick U, Crow YJ, Ekici AB, van Essen AJ, Goecke TO, Al-Gazali L, Chrzanowska KH, Zweier C, Brunner HG, Becker K, Curry CJ, Dallapiccola B, Devriendt K, Dörfler A, Kinning E, Megarbane A, Meinecke P, Semple RK, Spranger S, Toutain A, Trembath RC, Voss E, Wilson L, Hennekam R, de Zegher F, Dörr HG, Reis A (2008) Mutations in the pericentrin (PCNT) gene cause primordial dwarfism. Science 319:816–819. doi:10.1126/science.1151174

Ritchie K, Seah C, Moulin J, Isaac C, Dick F, Bérubé NG (2008) Loss of ATRX leads to chromosome cohesion and congression defects. J Cell Biol 180(2):315–324. doi:10.1083/jcb.200706083

Saitoh N, Goldberg IG, Wood ER, Earnshaw WC (1994) ScII: an abundant chromosome scaffold protein is a member of a family of putative ATPases with an unusual predicted tertiary structure. J Cell Biol 127(2):303–318

Shintomi K, Hirano T (2010) Sister chromatid resolution: a cohesin releasing network and beyond. Chromosoma 119:459–467

Shintomi K, Hirano T (2011) The relative ratio of condensin I to II determines chromosome shapes. Genes Dev 25:1464–1469

Singh N, Basnet H, Wiltshire TD, Mohammad DH, Thompson JR, Héroux A, Botuyan MV, Yaffe MB, Couch FJ, Rosenfeld MG, Mer G (2012) Dual recognition of phosphoserine and phosphotyrosine in histone variant H2A.X by DNA damage response protein MCPH1. Proc Natl Acad Sci U S A 109(36):14381–14386. doi:10.1073/pnas.1212366109

Stubblefield E, Wray W (1971) Architecture of the Chinese hamster metaphase chromosome. Chromosoma 32(3):262–294

Sumner AT (1991) Chromosoma 100(6):410–418

Tibelius A, Marhold J, Zentgraf H, Heilig CE, Neitzel H, Ducommun B, Rauch A, Ho AD, Bartek J, Krämer A (2009) Microcephalin and pericentrin regulate mitotic entry via centrosome-associated Chk1. J Cell Biol 185(7):1149–1157. doi:10.1083/jcb.200810159

Tomkins D, Hunter A, Roberts M (1979) Cytogenetic findings in Roberts-SC phocomelia syndrome(s). Am J Med Genet 4(1):17–26

Tonkin ET, Wang TJ, Lisgo S, Bamshad MJ, Strachan T (2004) NIPBL, encoding a homolog of fungal Scc2-type sister chromatid cohesion proteins and fly Nipped-B, is mutated in Cornelia de Lange syndrome. Nat Genet 36:636–641

Trimborn M, Bell SM, Felix C, Rashid Y, Jafri H, Griffiths PD, Neumann LM, Krebs A, Reis A, Sperling K, Neitzel H, Jackson AP (2004) Mutations in microcephalin cause aberrant regulation of chromosome condensation. Am J Hum Genet 75:261–266

Trimborn M, Schindler D, Neitzel H, Hirano T (2006) Misregulated chromosome condensation in MCPH1 primary microcephaly is mediated by condensin II. Cell Cycle 5:322–326

Van Den Berg DJ, Francke U (1993) Roberts syndrome: a review of 100 cases and a new rating system for severity. Am J Med Genet 47(7):1104–1123

Vega H, Waisfisz Q, Gordillo M, Sakai N, Yanagihara I, Yamada M, van Gosliga D, Kayserili H, Xu C, Ozono K, Jabs EW, Inui K, Joenje H (2005) Roberts syndrome is caused by mutations in ESCO2, a human homolog of yeast ECO1 that is essential for the establishment of sister chromatid cohesion. Nat Genet 37:468–470

Venkatesh T, Suresh PS (2014) Emerging roles of MCPH1: expedition from primary microcephaly to cancer. Eur J Cell Biol 93(3):98–105. doi:10.1016/j.ejcb.2014.01.005

Vernos I, Raats J, Hirano T, Heasman J, Karsenti E, Wylie C (1995) Xklp1, a chromosomal Xenopus kinesin-like protein essential for spindle organization and chromosome positioning. Cell 81(1):117–127

Woods CG (2004) Human microcephaly. Curr Opin Neurobiol 14:112–117

Wray W, Stubblefield E (1970) A new method for the rapid isolation of chromosomes, mitotic apparatus, or nuclei from mammalian fibroblasts at near neutral pH. Exp Cell Res 59(3):469–478

Xu X, Lee J, Stern DF (2004) Microcephalin is a DNA damage response protein involved in regulation of CHK1 and BRCA1. J Biol Chem 279:34091–34094

Yamashita D, Shintomi K, Ono T, Gavvovidis I, Schindler D, Neitzel H, Trimborn M, Hirano T (2011) MCPH1 regulates chromosome condensation and shaping as a composite modulator of condensin II. J Cell Biol 194:841–854

CHAPTER II

SCIENTIFIC REPORTS

OPEN

MCPH1, mutated in primary microcephaly, is required for efficient chromosome alignment during mitosis

Received: 9 June 2017
Accepted: 14 September 2017
Published online: 12 October 2017

M. Arroyo[1], R. Kuriyama[2], M. Trimborn[3], D. Keifenheim[2], A. Cañuelo[1], A. Sánchez[1], D. J. Clarke[2] & J. A. Marchal[1]

MCPH1 gene, mutated in primary microcephaly, regulates cell progression into mitosis. While this role has been extensively investigated in the context of DNA damage, its function during unperturbed cell cycles has been given less attention. Here we have analyzed the dynamics of chromosome condensation and cell cycle progression in MCPH1 deficient cells under undamaging conditions. Our study demonstrates that chromosome condensation is uncoupled from cell cycle progression when MCPH1 function is lacking, resulting in cells that prematurely condense their chromosomes during mid G2-phase and delay decondensation at the completion of mitosis. However, mitosis onset occurs on schedule in MCPH1 deficient cells. We also revealed active Cdk1 to be mandatory for the premature onset of chromosome condensation during G2 and the maintenance of the condensed state thereafter. Interestingly, a novel cellular phenotype was observed while monitoring cell cycle progression in cells lacking MCPH1 function. Specifically, completion of chromosome alignment at the metaphase plate was significantly delayed. This deficiency reveals that MCPH1 is required for efficient chromosome biorientation during mitosis.

MCPH1 primary microcephaly (OMIM 608585) is a rare human syndrome that results in pronounced reduction of the cerebral cortex, mental retardation and delayed growth[1,2]. While the clinical phenotype is identical to the other genetic variants of MCPH syndrome (MCPH1-MCPH14) described so far[3–5], from a cellular perspective MCPH1 syndrome revealed a unique altered pattern of chromosome condensation. Routine cytogenetic analysis in MCPH1 patients first reported an increased frequency of cells with condensed chromatin with an intact nuclear envelope, named "prophase-like cells" (PLCs)[6–9]. PLCs are observed due to both premature onset of chromosome condensation in G2-phase and delayed decondensation in early G1 cells following nuclear division[6,7]. Chromosome condensation at these inappropriate cell cycle stages has also been observed in human cells transiently depleted of MCPH1 by siRNAs and in Mcph1−/− mouse models[10,12–14]. This phenotype is therefore considered a cellular hallmark of MCPH1 deficiency.

Mechanistically, MCPH1-related premature chromosome condensation is a result of the premature loading of condensin II onto the chromatin during G2[14,15]. Cell-free assays demonstrated that MCPH1 associates with chromatin through its N-terminal domain at the same binding sites as condensin II, thus inhibiting the loading of the condensin II complex[15]. Other studies have provided indirect evidence that unscheduled activation of Cdk1 kinase directly contributes to the premature onset of chromosome condensation. In MCPH1 mutant cells released from early S-phase synchrony, the levels of inactive Cdk1, phosphorylated at tyrosine 15 (PY15-Cdk1), become drastically reduced as soon as 4 h after release. This correlates temporally with the onset of premature condensation[16,17]. Other data indicate that premature activation of Cdk1 in MCPH1 syndrome relies on inappropriately high levels of active Cdc25A[16,18]. Since Cdc25 activation is normally regulated by the checkpoint kinases Chk1 and ATR, the data potentially place the Cdc25-Chk1-ATR pathway under MCPH1 control[16,18].

[1]Departamento de Biología Experimental, Universidad de Jaén, Jaen, Spain. [2]Department of Genetics, Cell Biology and Development, University of Minnesota, Minneapolis, USA. [3]Institute of Medical Genetics and Human Genetics, Charite Virchow-Klinikum Hospital, Berlin, Germany. Correspondence and requests for materials should be addressed to J.A.M. (email: jamaor@ujaen.es)

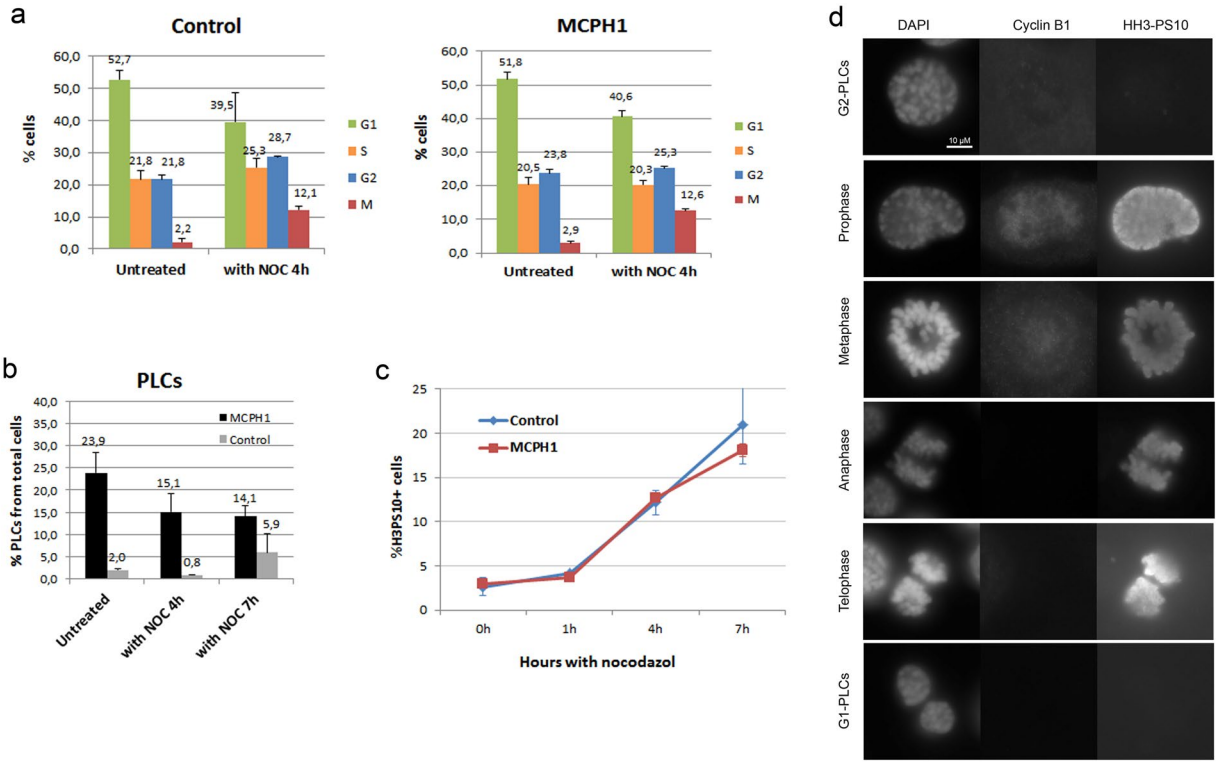

Figure 1. Cell cycle progression and dynamics of prophase like-condensation in control and MCPH1 patient cells. (**a**) Graphs comparing the cell cycle distribution, determined by FACS analyses, in untreated cell samples or cell samples incubated with nocodazole for 4 hours to induce M arrest. (**b**) For each sample from A, we determined in parallel the fraction of PLCs (prophase-like cells) by microscopic analyses of cytogenetic preparations. We also included cells incubated with nocodazole for 7 hours in these analyses. More than 500 cells were scored per sample. As expected, PLC frequency was negligible in control cells. Mean and S.D. data from at least 3 independent experiments are shown. Mean values are indicated. (**c**) Rate of H3PS10 positive cells in control and MCPH1 patient cells, determined by FACS after incubation with nocodazole for the indicated time points. Data from two independent experiments are presented. (**d**) Immunolocalization using antibodies against Cyclin B and Histone H3-PS10 proteins in proliferating cells from one MCPH1 patient. PLCs ("Prophase-like cells") refers to cells with condensed chromatin inside a retained nuclear envelope, either as a consequence of premature onset of chromosome condensation or delayed decondensation at the end of mitosis. Note that G2-PLCs and real prophases are indistinguishable by DAPI staining but showed different IF patterns for both markers. G1-PLCs are also negative for both markers. Only a minor fraction of the observed cells with the typical morphology of prophase cells contained nuclear signals for both Cyclin B and Histone H3-PS10 proteins.

MCPH1 is a multi-functional protein with proposed roles in telomere maintenance, DNA repair, centrosome function and tumor suppression[19]. While a large collection of studies have delineated the role of MCPH1 during cell cycle progression under conditions where DNA is damaged, its function during unperturbed cell division has seen less attention. In relation to this, some studies suggest that MCPH1 deficiency leads to premature entrance into mitosis[17,18]. This conclusion was mainly supported by the increased frequency of H3PS10 positive cells observed in either siRNA-MCPH1 treated cells or patient cell cultures. However, no studies have carefully measured the timing of mitosis and cell cycle transitions in cells with deficient MCPH1. Therefore, it is currently unknown whether the defect lies exclusively in the regulation of chromosome condensation or whether other key events of mitotic progression are also altered.

In the present work we have tracked in real time the dynamics of chromosome condensation and cell cycle progression in MCPH1 deficient cells during unperturbed cell division cycles. This analysis revealed that cells without MCPH1 prematurely condense their chromosomes during mid G2-phase and decondense them subject to a delay at the completion of mitosis. However the onset of mitosis, based on nuclear levels of mitotic markers and the timing of nuclear envelope breakdown, occurs on schedule in MCPH1 deficient cells. We also provide evidence that active Cdk1 is mandatory for the premature onset of chromosome condensation in MCPH1 syndrome. Interestingly, our analysis demonstrates that, in addition to regulating the timing of chromosome condensation, MCPH1 is also required for efficient chromosome alignment during prometaphase.

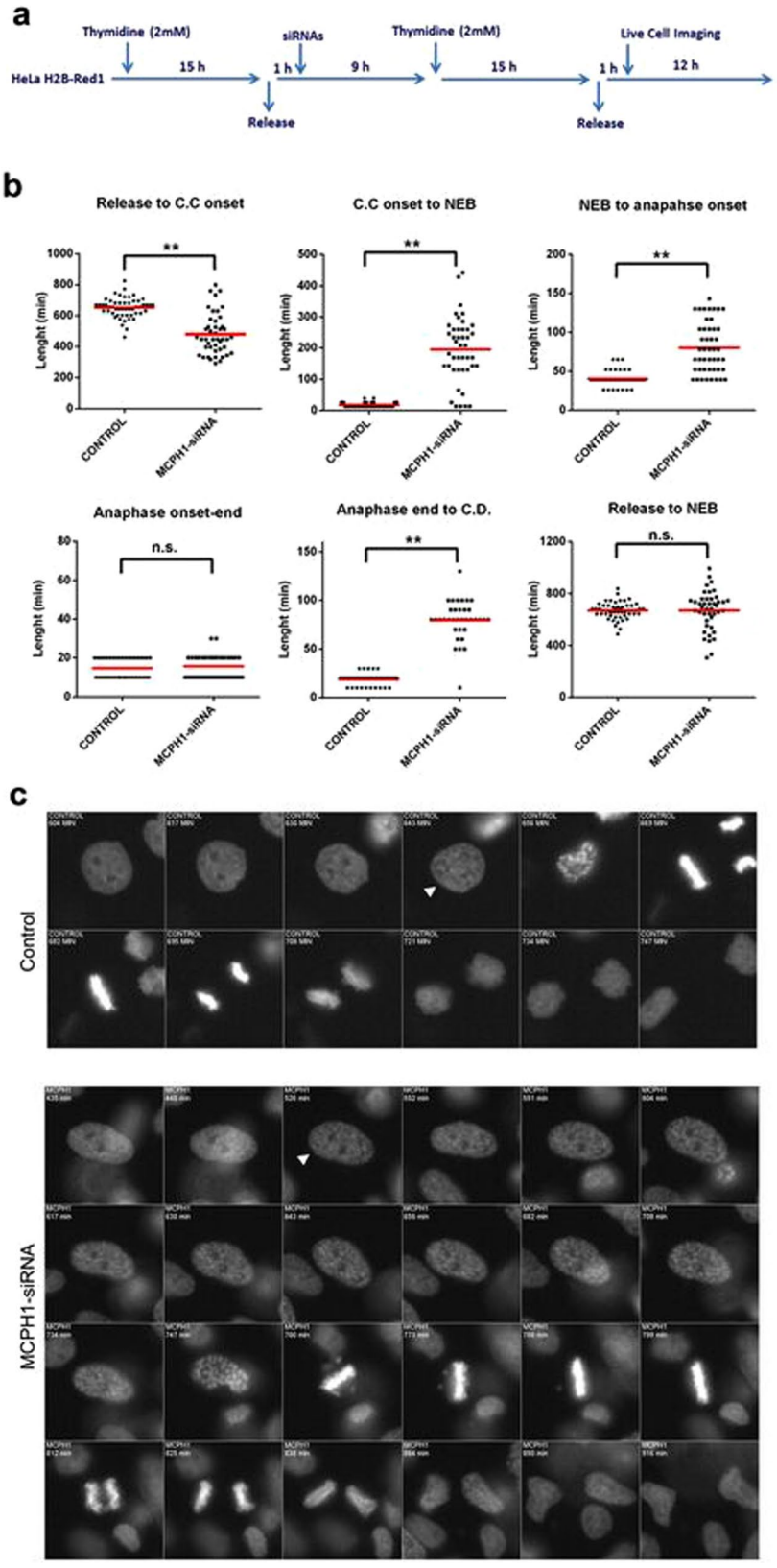

Figure 2. Analyses of mitosis progression by live-cell microscopy in cells depleted of MCPH1 function by siRNAs. (**a**) A brief description of the experimental procedure: HeLa cells stably expressing fluorescent histone H2B fused to Red1 were synchronized at the G1/S border by double thymidine block. MCPH1 depletion was achieved by transfection with siRNAs (oligo siRNA-MCPH1-3) during the release from the first thymidine block. Time-lapse images were collected using "Nikon Biostation IM Cell incubator" one hour after the release from the second thymidine block. (**b**) Dot-plots showing the time interval between different key mitotic events

in minutes for untreated and MCPH1 depleted cells. The red line indicates the mean value. C.C. = chromosome condensation; NEB = nuclear envelope breakdown; C.D. = chromosome decondensation. At least 40 cells were analyzed in each case. Statistical comparisons for the mean and median data were done by T-student and Wilcoxon (W) tests respectively. **$p < 0.01$; N.S. not significant. (**c**) Selected frames showing the mitosis progression of representative HeLa H2B/Red1 cells from both untreated and MCPH1-depleted cell samples. Time from release is indicated in minutes. Arrow heads point to the first time point when chromosome condensation is clearly observable after release. Full movies are included in videos 1 and 2.

Results

Tracking PLC dynamics and mitosis progression in cells lacking MCPH1 function. We first determined the frequency of "Prophase-like cells" (PLCs) in log-phase cultures of MCPH1 patient lymphoblasts, identified through cytomorphological analysis (Fig. 1a and b). In parallel we determined the mitotic index by FACS analysis of mitotic markers (phosphorylation of histone H3). The FACS data revealed that only 2.9% (±0.5%) of MCPH1 patient cells were histone H3PS10 positive (Fig. 1a), while within the same sample 23.9% (±4.5%) of the cells were PLCs (Fig. 1b). Therefore, most PLCs could not have been mitotic cells. In order to gain direct evidence that this is the case, we used immunofluorescence staining to simultaneously observe histone H3PS10, cyclin B and chromosome morphology (Fig. 1d). This analysis revealed only a minor fraction of total PLCs (11%) that were positive for both markers and could, therefore, be defined as mitotic cells. Both markers showed the expected staining patterns in cells that were in prometaphase or beyond (Fig. 1d). Similar results were obtained when we observed histone H3PS28 and cyclin B proteins (Supplementary Figure 1). Interestingly, the fraction of H3PS10 positive cells was slightly although not significantly increased in MCPH1 patient cells (2.9 ± 0.5%) compared with control cells (2.2 ± 1.1%), consistent with previous reports[16,18]. Finally, we compared the dynamics of mitotic entry in both control and MCPH1 patient cells by determining the frequency of H3PS10 positive cells versus time after adding the spindle poison nocodazole to the cultures (Fig. 1c). This revealed that mitotic cells accumulate at similar rates in both samples, suggesting no significant differences in the rate of progression into mitosis in control and MCPH1 patient cells.

Since PLCs are evidently a consequence of premature condensation in G2 and delayed decondensation at the completion of mitosis[6], we also compared their frequency within the G2 and G1 cell populations. As both – G1 and G2 PLCs - are indistinguishable by morphological analysis, we compared the PLC frequency before and after incubation with nocodazole. During this incubation G1 PLCs that decondense their chromosomes are not replaced by new G1 PLCs because progression through mitosis is blocked. Consequently, only G2 PLCs will remain in the population. In untreated patient cells, we observed 23.9% (±4.5%) of the population were PLCs, . After nocodazole incubation for 4 hours this frequency was reduced to 15.1% (±4.2%), and a similar frequency was observed when the incubation was prolonged for 7 hours (14.1 ± 2.5%) (Fig. 1b). In control cells the PLC frequency remained negligible as expected. Thus, we estimate that, in cycling cells from MCPH1 patients, approximately 15% and 9% of total cells are G2 PLCs versus G1 PLCs respectively (Fig. 1b). These data are in agreement with live-cell microscopy studies (see below) and with previous estimations[14]. The FACS analysis showed that G2 and G1 populations represent 23.8% (±1.0%) and 51.8% (± 2.0%) of total cells within the same untreated patient samples (Fig. 1a). Accordingly, we assume that in the MCPH1 patient cells, premature chromosome condensation occurs at mid-G2 phase, as previously proposed[16], while decondensation is delayed at the completion of mitosis, covering approximately 20% of the subsequent G1 phase.

To analyze the dynamics of chromosome condensation and progression through mitosis in individual cells lacking MCPH1 function we performed live-cell fluorescence microscopy using HeLa cells stably expressing histone H2B-Red1. We employed double-thymidine synchronization to arrest cells at the G1/S border then analyzed progression through the subsequent S-phase, G2 and mitosis. MCPH1 depletion was achieved by siRNA transfection using validated siRNA oligos which knocked-down the MCPH1 protein levels efficiently[11] (experimental procedure outlined in Fig. 2a; Supplementary Figure 3). We also confirmed that the cellular phenotypes arising after MCPH1 depletion, that is, the appearance of PLCs and altered chromosome structure in mitosis[6,7,10] were both recapitulated using this protocol (Supplementary Figure 2). Results from live-cell analyses are presented in Fig. 2, and videos 1 and 2 (Supplementary information). We observed that cells depleted of MCPH1 condense their chromosomes 479 (±132) minutes after release from thymidine arrest, and that in these cells the PLC phenotype (with evident chromosome condensation) persisted for an average of 195 (±132) minutes. In control cells chromosome condensation was first evident much later (651 ± 63 minutes after release), and occurred not long (17 ± 7 minutes) before NEB (nuclear envelope breakdown) as expected. Importantly, NEB occurred on schedule in MCPH1 depleted cells, at the same time as in control cells (671 ± 149 minutes in MCPH1, 668 ± 64 minutes in control; time after release). Strikingly, MCPH1 depleted cells required substantially more time to progress from late prophase to the onset of anaphase: the interval from NEB until anaphase onset was 40 ± 9 minutes in control cells and 80 ± 33 minutes in MCPH1 depleted cells. Finally, we determined the timing of progression through late mitosis. While the duration of anaphase was not altered in MCPH1 depleted cells (16 ± 6 minutes) compared with controls (15 ± 5 minutes), the time that cells remained with condensed chromatin once chromosome segregation had been completed was longer. MCPH1 depleted cells required 80 (±20) minutes to complete this last step while control cells required only 19 (±6) minutes. When these analyses were repeated using a second non-overlapping siRNA similar results were obtained (Supplementary Figure 4).

In summary, the data demonstrate that when MCPH1 is depleted, cells condense their chromatin prematurely, in mid-G2 phase, and remain in that state (termed PLCs) for 195 minutes before initiating NEB. Condensation persists for an additional 80 minutes once chromosomes have segregated, covering part of the subsequent G1 phase. Despite the altered condensation dynamics, NEB occurs on time in MCPH1 depleted cells compared

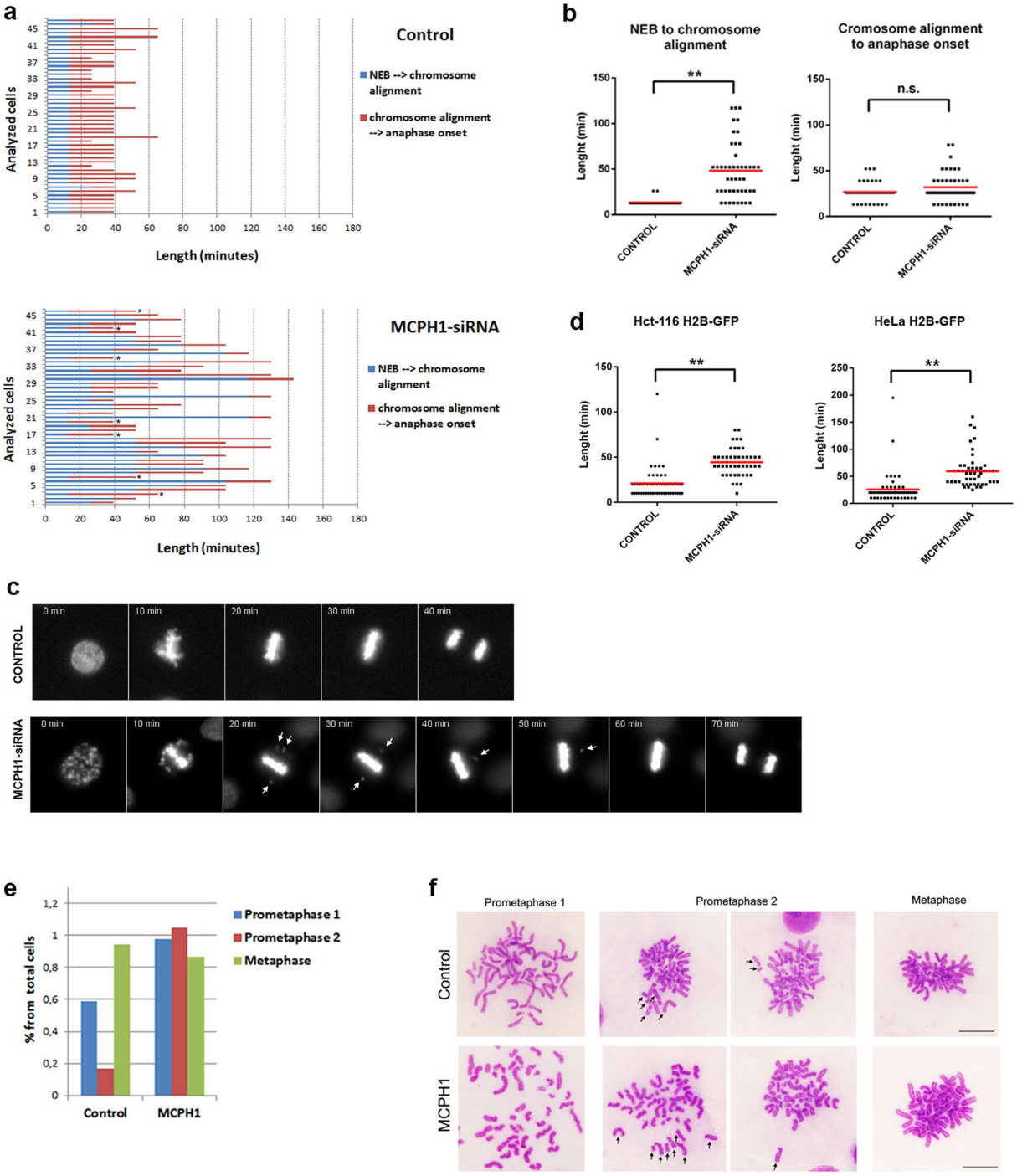

Figure 3. Analyses of prometaphase and metaphase progression in MCPH1 cells lacking MCPH1 function. (**a**) Live-cell microscopy analyses in HeLa H2B-Red1 cells depleted of MCPH1 by siRNAs (oligo siRNA-MCPH1-3). Graphs show the time required in individual control or MCPH1-depleted cells to i) align all the chromosomes at the metaphase plate (blue), ii) initiate chromosome segregation after metaphase alignment (red). Cells marked with an asterisk did not show the PLC phenotype before NEB. (**b**) Dot-plots from the data in A. The red line indicates the mean value. At least 40 cells were analyzed in each case. Statistical comparisons for the mean and median data were done by T-student and Wilcoxon (W) tests respectively. $^{**}p < 0.01$; N.S. not significant. (**c**) Representative cells showing the progression through prometaphase and metaphase from both HeLa untreated and MCPH1-siRNA treated cell samples. Time from nuclear envelope breakdown (first frame) is indicated in minutes. Note that in the MCPH1-depleted cell most chromosomes align at the metaphase plate on time but some require more time to complete the process (pointed by arrows). Once metaphase alignment is fully achieved, cell progresses into anaphase without delay. (**d**) Dot-plots showing the duration of prometaphase in Hct-116 H2B-GFP and HeLa H2B-GFP cells depleted of MCPH1 by siRNAs. Analyses

performed as described in **a** and **b**. (**e**) Percent of the corresponding mitotic stages observed in control and MCPH1 patient lymphoblasts. Analyses were performed by microscopic inspection of cytogenetic preparations obtained following a protocol that preserves the organization of chromosomes on the mitotic spindle[12]. At least 100 mitotic cells were counted and classified according to the alignment stage of their chromosomes as follows: Prometaphase 1, if no signs of metaphase plate conformation is observed; Prometaphase 2, if most chromosomes are already aligned into a plate but few of them remain far; Metaphase, when all chromosomes are finally aligned (representative pictures in **f**; arrows point to chromosomes that remain far from the already formed plate). For better interpretation of our results, the data were adjusted considering the total amount of cells that were in either prometaphase or metaphase in control (1.7%) and patient (2.9%) cells (n = 1000). Representative data from analyses performed by two different persons are presented.

with controls. Condensation is therefore dramatically uncoupled from cell cycle progression. Importantly, similar results were observed when these analyses were repeated using a different isolate of HeLa stably expressing histone H2B-GFP, and also in Hct-116 H2B-GFP cells, a human modified colorectal carcinoma cell line (Supplementary Figure 5; video 8 at supplementary information).

MCPH1 is required for efficient chromosome biorientation in prometaphase. The extended interval between NEB and anaphase onset in MCPH1 depleted cells prompted a closer examination of prometaphase (and metaphase) by live-cell analysis (Fig. 3a–c). This revealed that MCPH1 depleted cells require more time to align all the chromosomes at the metaphase plate compared with controls (14 ± 3 minutes in control, 48 ± 30 minutes in MCPH1). As depicted in Fig. 3c, most chromosomes in MCPH1 depleted cells typically became aligned at the metaphase plate by the first frame after NEB (a time interval of approximately 10 minutes). Despite this, a small number of unaligned chromosomes usually persisted and required more time to complete biorientation. Once full alignment was achieved, cells progressed into anaphase without significant delay (27 ± 10 minutes in control, 32 ± 16 minutes in MCPH1). Similar results were obtained when these analyses were repeated using a second non-overlapping siRNA (Supplementary Figure 4). The observed prolongation of prometaphase was also recapitulated in another HeLa cell line stably expressing Histone H2B-GFP, and also in Hct-116 H2B-GFP cells (Fig. 3d). Importantly, as we could track mitosis and chromosome condensation in individual cells, we observed that only those cells displaying a clear PLC phenotype before NEB (i.e. indicating efficient MCPH1 depletion), then had an extended prometaphase duration (Fig. 3a). On the other hand, rare cells within the MCPH1-siRNA treated population where premature condensation did not occur (i.e. indicative of unsuccessful MCPH1 depletion), did not delay in prometaphase.

In order to confirm these findings that were based on siRNA-mediated loss of MCPH1 function, we next investigated if a similar alteration could be observed during prometaphase in MCPH1 patient cells. This analysis was conducted through detailed microscopic inspection of mitotic preparations obtained from lymphoblast cell cultures following a protocol that preserves the organization of chromosomes on the mitotic spindle[12] (Fig. 3e and f). In both control and patient samples, mitotic cells were counted and scored according to the alignment stage of their chromosomes as follows: prometaphase 1, if no sign of the metaphase plate conformation was observed; prometaphase 2, if most chromosomes were aligned on the metaphase plate but few chromosomes remained away from the plate; and metaphase, where all chromosomes were aligned at the metaphase plate (representative pictures in Fig. 3f). The data obtained are consistent with the process of chromosome alignment taking longer in patient cells compared with controls. While in the MCPH1 patient sample 0.97% and 1.05% of total cells where classified as prometaphase 1 and 2 respectively, in the control sample 0.58% of total cells were in prometaphase 1 and only 0.17% of cells were classified as prometaphase 2. The fraction of cells in metaphase, however, was similar in both samples (0.87% and 0.94% of total cells in control and patient respectively). Remarkably, cells classified as prometaphase 2 and frequently observed in patient cells - and only rarely in controls-, resemble those with an established plate but a few unaligned chromosomes observed by live-cell imaging in MCPH1 depleted HeLa cells (compare Fig. 3c and f). When these analyses were repeated in U2OS cells depleted of MCPH1 function by siRNA, similar results were observed (Supplementary Figure 6). Overall, our data provide clear evidence that MCPH1 is required for efficient chromosome alignment during mitosis, a novel cellular phenotype related to the lack of function of MCPH1.

In the live-cell experiments we did not detect significantly increased frequencies of apoptotic cells or multipolar mitosis in cells depleted of MCPH1 compared with controls. However, we did observe an increased occurrence of anaphase errors including bridged or lagging chromosomes in anaphase (Supplementary Figure 7). Most mis-segregated chromosomes gave rise to micronuclei (data not shown). Although the basal level of these errors clearly differed between the different cell lines that were analyzed, the frequency of anaphase errors was found always to be higher after MCPH1 depletion.

Premature chromosome condensation in MCPH1 syndrome requires active Cdk1. It has been proposed that premature onset of chromosome condensation depends on premature activation of Cdk1 during G2 in MCPH1 deficient cells[16,17]. To test this directly, we examined MCPH1 deficient cells treated with RO-3306, a small-molecule inhibitor of Cdk1 that reversibly arrests human cells at the G2/M border)[20]. We compared the fractions of G2, mitosis (M) and PLCs in control and MCPH1 patient lymphoblast cells incubated with RO-3306 for 4 h and 7 h (Fig. 4). The data reveals that during prolonged incubation with the Cdk1 inhibitor there is a progressive accumulation of G2 cells in both control and MCPH1 cells (Fig. 4a and b). The G2 arrest was confirmed by simultaneous incubation with RO-3306 and nocodazole. In this case, we observed a progressive accumulation of G2 cells but almost no accumulation of mitotic cells despite the treatment with the spindle poison (Fig. 4a and b).

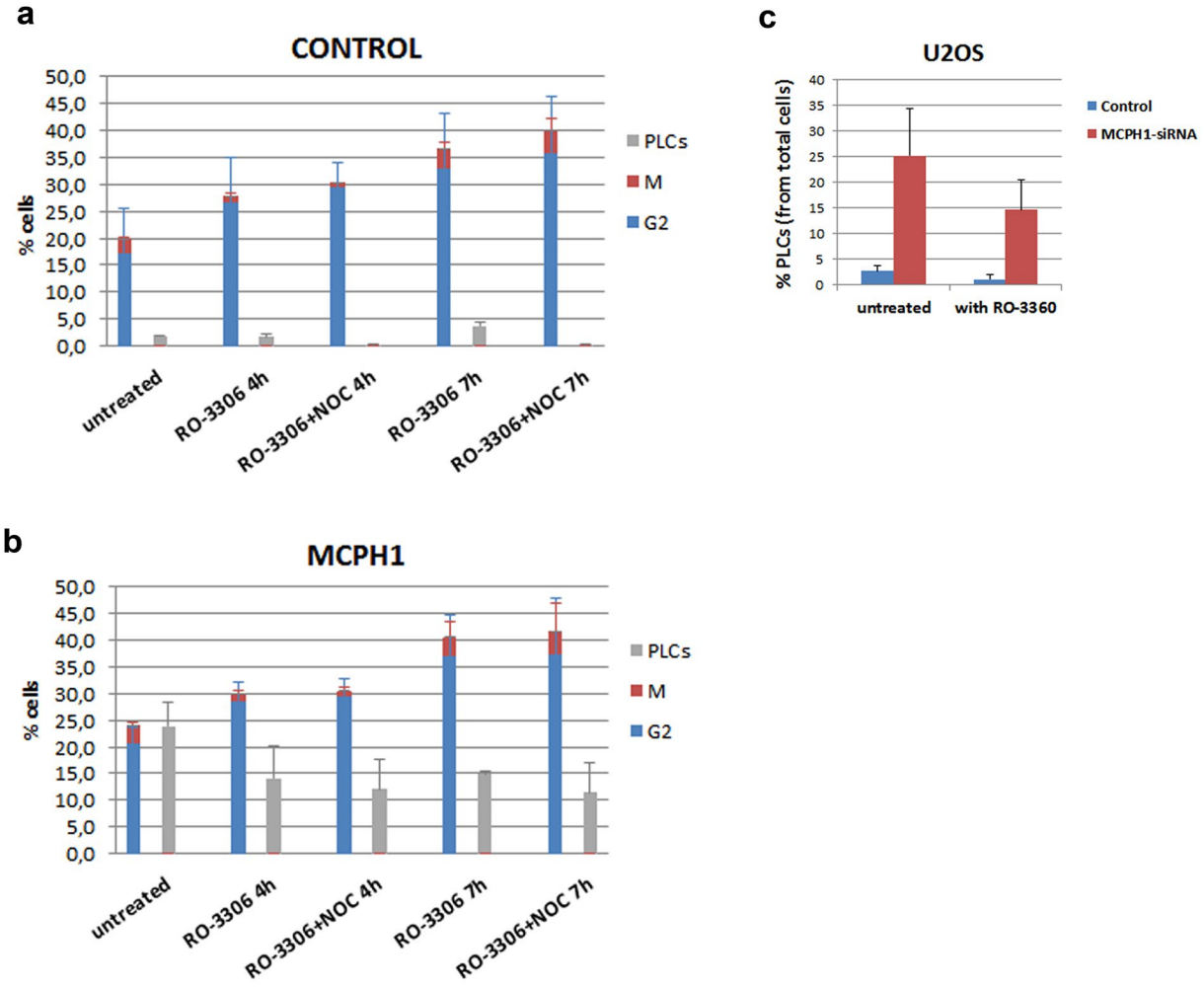

Figure 4. Analyses of cell cycle progression and dynamics of chromosome condensation in control and MCPH1 deficient cells treated with the Cdk1 inhibitor RO-3306. Fraction of M and G2 cells, determined by FACS analyses, in control (**a**) and MCPH1 patient cells (**b**) after either 4 h or 7 h of incubation with RO-3306 alone or combined with nocodazole (NOC), a spindle poison that causes M arrest. For each sample, we determined in parallel the fraction of PLCs by microscopic analyses of cytogenetic preparations. These data confirm that cells do not escape from G2 arrest. The fraction of PLCs is constantly reduced after prolonged incubation with RO-3306 in patient cells. In control cells, as expected, PLCs are nearly abseny. (**c**) Determination of the PLC frequency in U2OS cells depleted of MCPH1 by siRNAs and incubated with the Cdk1 inhibitor RO-3360 for 6 h. Mean and SD data are shown in all cases. Reduction of PLCs rate after RO-3306 treatment in b and c was statistically significant ($p < 0.01$, X^2 test).

Interestingly, in parallel, the PLC frequency progressively diminished in MCPH1 patient cells, both with either RO-3306 alone or in combination with nocodazole (Fig. 4a and b). In control cells, PLCs were rarely observed, as expected. A similar reduction in the PLC frequency was observed in U2OS cells depleted of MCPH1 function by siRNAs then treated with RO-3306 (Fig. 4c).

We next monitored cell cycle progression and the dynamics of chromosome condensation after Cdk1 inhibition by live-cell fluorescence microscopy in HeLa H2B-Red1 cells. Cells were synchronized at G1/S by double-thymidine block and MCPH1 depletion was achieved by transfection with siRNAs. Immediately after release from the second thymidine arrest, RO-3306 was added to the cultures and time-lapse microscopy was performed (videos 3 and 4, supplementary information). This analysis revealed that neither control nor MCPH1 depleted cells were able to enter mitosis during the 20 hours that were recorded following release from the synchrony. Importantly, MCPH1-depleted cells did not undergo chromosome condensation during that time, i.e. no PLCs were observed. Therefore, the onset of premature chromosome condensation during G2 in cells lacking MCPH1 requires active Cdk1. We performed similar analyses using asynchronous cell populations and in agreement we observed that mitotic entry was blocked (data not shown).

We next asked if the maintenance of chromosome condensation in PLCs requires Cdk1 activity. Following MCPH1 depletion and cell synchronization, as described above, we added RO-3306 8 hours after release from the thymidine block, at the time when we observed the peak of PLCs in G2 (based on the data in Fig. 2) (experimental

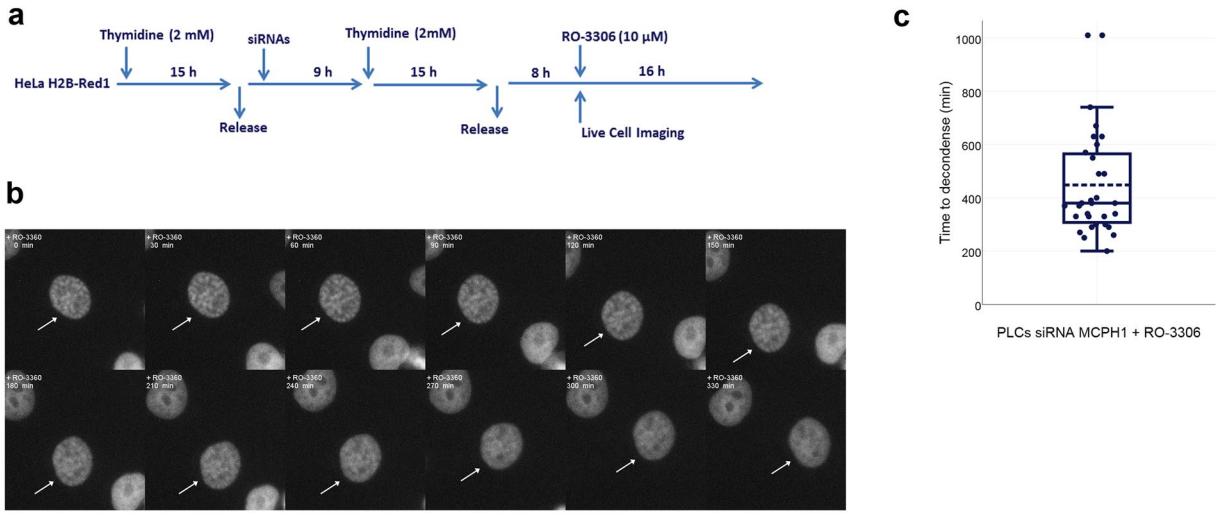

Figure 5. Timing of PLC decondensation after incubation with the Cdk1 inhibitor RO-3360 in HeLa-H2B/Red1 cells. (**a**) Short description of the experimental procedure. RO-3306 was added 8 h after release from the second thymidine block to coincide with the occurrence of PLCs during G2 in the siRNA treated cells. (**b**) Selected frames showing the decondensation of a PLC (pointed by arrows) after incubation with RO-3360. Time after RO-3360 addition is indicated in minutes. (**c**) Combined dot- and box-plot showing the time (in minutes) that PLCs required to completely decondense their chromosomes after adding RO-3360. The broken line indicates the mean value. 30 PLCs were monitored.

outline detailed in Fig. 5a). This revealed that RO-3306 induced a progressive reduction in condensation in most PLCs until these cells had completely decondensed their chromatin (Fig. 5b and video 5). The time required to completely decondense the chromosomes after adding RO-3306 was 409 (±142) minutes (Fig. 5c). These data are in agreement with the PLC dynamics observed in MCPH1 patient cells after Cdk1 inhibition and suggest that PLCs decondense their chromosomes through a slow but progressive process if Cdk1 is inactivated.

Lastly, we asked if RO-3306-induced G2 arrest was reversible in MCPH1 depleted cells. HeLa-H2B-Red1 cells were incubated with the Cdk1 inhibitor for 8 hours, then cells were washed with normal medium and monitored by time-lapse microscopy. MCPH1 depletion was achieved by siRNA transfection 24 hours before the incubation with RO-3306 (Fig. 6a). Strikingly, PLCs were observed soon after the removal of RO-3306 in cells depleted of MCPH1 (25 ± 85 min from removal) and these cells remained in that state with prematurely condensed chromatin for 118 (±95) minutes before NEB (Fig. 6b and c, videos 6 and 7). In contrast, chromosome condensation was initiated later in control cells (241 ± 84 minutes from inhibitor removal) and was visible only 36 (±27) minutes before NEB. Therefore, the onset of NEB occurred with significant delay in control cells (280 ± 93 minutes, from inhibitor removal) compared with PLCs (133 ± 130 minutes, from inhibitor removal). After NEB, MCPH1 depleted cells required more time to align all their chromosomes at the metaphase plate (101 ± 54 minutes in control, 149 ± 101 minutes in MCPH1). However, once aligned, anaphase onset occurred with similar timing in both samples (44 ± 22 minutes in control, 38 ± 28 minutes in MCPH1). The amount of time that cells required to exit from mitosis and completely decondense their chromosomes was increased in MCPH1 depleted cells. Control cells required 22 (±5) minutes to complete this step while MCPH1 depleted cells required 64 (±27) minutes. Together these experiments have provided evidence that inhibition of Cdk1 by RO-3306 induces G2-arrest and chromosome decondensation in MCPH1 depleted cells. After removal of RO-3306, MCPH1 depleted cells condensed their chromosomes prematurely and progressed more quickly into mitosis than controls. The premature onset of NEB after recovery from Cdk1 inhibition could be a consequence of a faster rate of Cdk1 reactivation in MCPH1 depleted cells. Importantly, the mitotic phenotypes observed without prior Cdk1 inhibition were also recapitulated in these experiments: prolonged condensation after anaphase and inefficient prometaphase chromosome alignment.

Discussion

Several studies of MCPH1 function using models including MCPH1 patient cells, depletion of MCPH1 via RNAi and MCPH1 knock-out animals have consistently revealed a key role as a regulator of chromosome condensation. In this paper we have tracked the dynamics of chromosome condensation and cell cycle progression in MCPH1 deficient cells during unperturbed cell division cycles. Our results clearly showed that, in addition to coupling chromosome condensation to other cell division processes, MCPH1 is also required for efficient chromosome alignment during prometaphase.

Our live cell analyses using synchronized cells showed that MCPH1 deficient cells progress through G2 phase and start mitosis on schedule, judged by the timing of NEB. This result was corroborated by our finding that most cells that had undergone premature chromosome condensation (PLCs) in MCPH1 patients were not positive for mitotic markers - nuclear H3PS10 and H3PS28 - and had low levels of nuclear cyclin B, in agreement with previous studies[14,16]. Moreover, we also observed that mitotic cells accumulate at similar rates in control and MCPH1

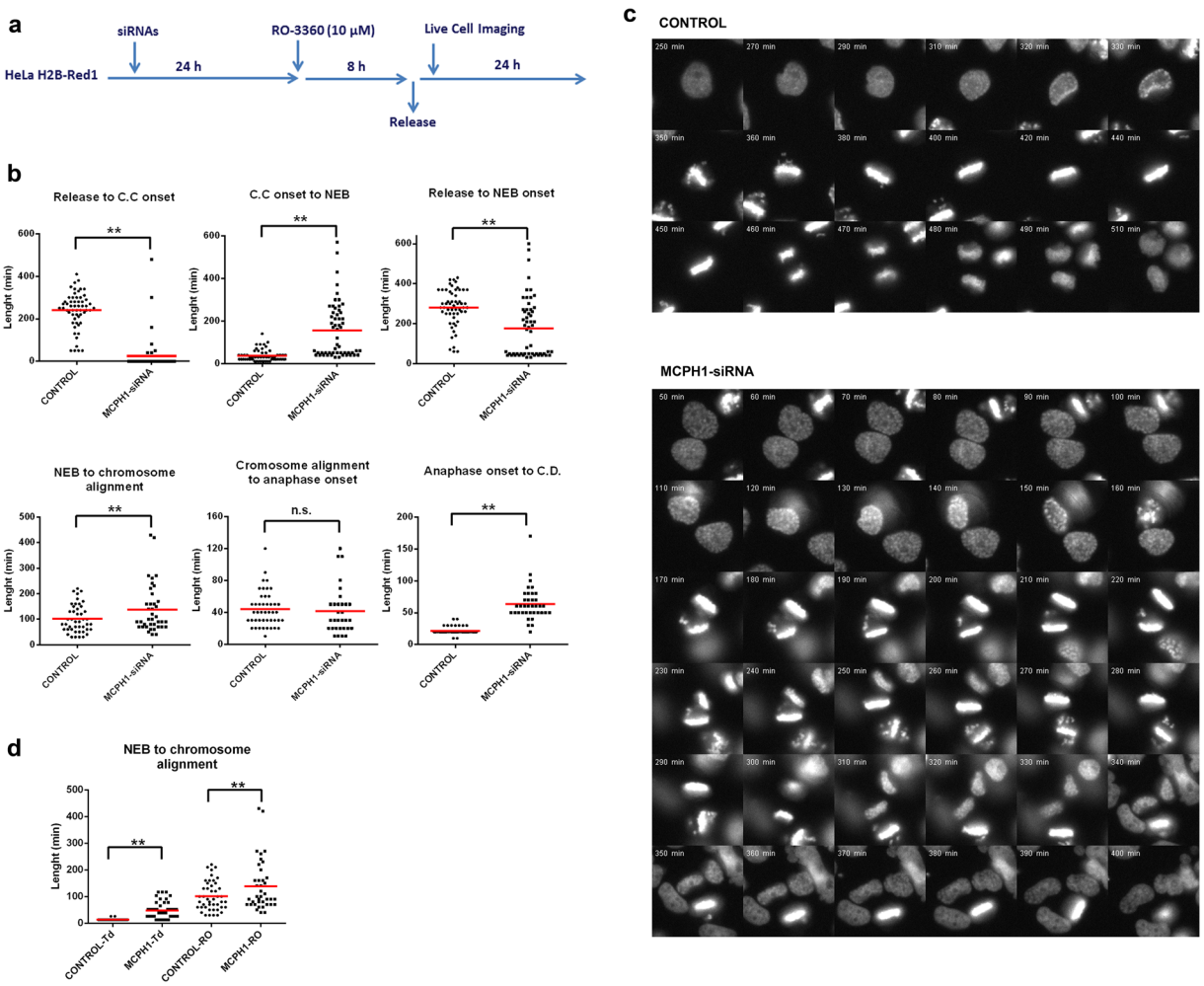

Figure 6. Analyses of mitosis progression by live-cell microscopy in cells depleted of MCPH1 by siRNAs and incubated with the Cdk1 inhibitor RO-3360. (**a**) A brief description of the experimental procedure. HeLa H2B/Red1 cells were arrested in G2 by incubation with RO-3360 for 8 h and then released into normal fresh medium without the inhibitor. MCPH1 depletion was achieved by transfection with siRNAs during the previous 24 hours. Time-lapse recording started 30 minutes after the release from the RO-3360 incubation. Images were analyzed and processed using Image J software. (**b**) Dot-plots showing the time interval between different key mitotic events in minutes for untreated and MCPH1 depleted cells. The red line indicates the mean value. CC = chromosome condensation; NEB = nuclear envelope breakdown; CD = chromosome decondensation. At least 40 cells were analyzed in each case. Chromosome segregation and further decondensation were not analyzed in separate as both occur nearly simultaneously in control cells. Statistical comparisons for the mean and median data were done by T-student and Wilcoxon (W) tests respectively. $^{**}p < 0.01$; N.S. not significant. (**c**) Selected frames showing the mitotic progression of representative HeLa cells from both control and MCPH1-depleted samples. Time from RO-3360 release is indicated in minutes. (**d**) Pairwise comparison of prometaphase timing (duration) in HeLa-H2B/Red1 cells after release from either double block with thymidine (Td) or RO-3360 incubation (RO).

patient cells during time-course analyses. Together the data demonstrate that PLCs are either G2 or G1 cells that arise as a consequence of chromosome condensation being uncoupled from normal cell cycle progression. Since the abnormal condensation pattern is Cdk1 dependent (see below), it is likely to be a regulatory process rather than an aberrant change in chromatin structure. Despite this, the molecular pathways regulating the G2/M transition remain intact in MCPH1 PLCs[21].

It has been proposed that premature onset of chromosome condensation depends on premature activation of Cdk1 during G2 in MCPH1 syndrome[16,17]. Here we revealed by live-cell imaging that inhibition of Cdk1 activity in HeLa cells depleted of MCPH1 induces G2 arrest in the absence of chromosome condensation, a behavior similar to that observed in control cells. Moreover, PLCs require continued Cdk1 activity for the maintenance of chromosome condensation. Both G2 arrest and decondensation of PLCs was also observed in MCPH1 patient cells after prolonged Cdk1 inhibition. Interestingly, chromosome condensation starts immediately after release from prolonged Cdk1 inhibition in MCPH1 deficient cells, while in control cells it occurs significantly later.

Taken together, our results clearly demonstrate that active Cdk1 is required for the premature onset of chromosome condensation and the maintenance of the condensed state in cells lacking MCPH1 function.

The exact role of MCPH1 in Cdk1 regulation and how that modulates chromosome condensation during an unperturbed cell cycle is currently unknown, and seems to occur independently of the ATR pathway[16,20]. Full activation of Cdk1, the key event triggering cell entry into mitosis, relies on a redundant network of interactions that function in feedback loops to guarantee proper coordination of the different mitotic events[22]. Although the bulk of Cdk1 becomes activated at the G2/M border, lower levels of active Cdk1 are detected early in G2[23]. In this context, our data could indicate that MCPH1 prevents, through an unknown pathway, the induction of chromosome condensation by regulating or sustaining the activation threshold of Cdk1 with regard to chromosome condensation. Alternatively, it has not been ruled out that MCPH1 and Cdk1 regulate chromosome condensation independently since a direct relation between both during this process has not been established.

Mechanistically, premature chromosome condensation in cells lacking MCPH1 results from premature loading of condensin II onto chromatin[14,15]. MCPH1 directly inhibits condensin II loading though competitive binding to the same chromatin domains, thus preventing condensation[15]. Condensin II is phosphorylated by Cdk1 at the T1415 residue of CAP-D3 subunit in early mitosis, which is critical for sustaining further Plk1 phosphorylation and, thus, full activation of condensin II[24]. In this scenario it is reasonable to infer that MCPH1 controls condensin II function directly through physical inhibition of its loading onto chromatin and indirectly by temporal control of condensin II activation mediated by Cdk1-Plk1 phosphorylation.

In this study we revealed a novel function for MCPH1 during mitosis. Live-cell analyses showed that MCPH1 deficient cells require more time to align all the chromosomes at the metaphase plate compared with controls. While most chromosomes appeared to have aligned within ten minutes after NEB, a small number of unaligned chromosomes usually persisted and required more time to complete biorientation. When prometaphase and metaphase progression was analyzed in detail in MCPH1 patient cells a similar alteration was noticed. Consequently, the length of prometaphase is extended and the total length of mitosis is increased in MCPH1 deficient cells. This alteration, not previously reported, indicates a function for MCPH1 in chromosome alignment during mitosis. In previous studies it was proposed that MCPH1 deficiency induces premature entry of cells into mitosis. This conclusion was mainly supported by the increased frequency of H3PS10 positive cells observed in either siRNA-MCPH1 treated cells or patient cell cultures[17,18] (our present study, Fig. 1 and Supplementary Figure 1). However, the data presented here reveal that the increased mitotic index can be explained by the extended prometaphase duration in cells lacking MCPH1 function, rather than by an accelerated mitotic entry. One study reported elongated mitosis in cells depleted of MCPH1, based on time-lapse microscopy, but the dynamics of chromosome condensation were not described, and no abnormalities in chromosome alignment were reported[18].

Immunofluorescence analyses in neuroprogenitor cells from a Mcph1 mouse model reported increased frequencies of bipolar spindles with unaligned chromosomes[17]. The occurrence of these errors was explained by uncoupling of centrosome maturation from mitotic processes. We here showed *in vivo* that human cells depleted of MCPH1 require more time to achieve full alignment of chromosomes at the metaphase plate. Taking together our results and previous ones[17], it seems evident that the process of chromosome alignment during prometaphase is compromised by MCPH1 deficiency. Moreover, the resulting mitotic delay may add information to the current discussions about the pathogenic mechanisms of MCPH1 primary microcephaly[25]. Even a subtle increase in the duration of mitosis could deeply impact the final production of neurons during neurogenesis, while in other tissues types it would not induce noticeable alterations.

Currently we do not understand the molecular basis for the deficiency during prometaphase chromosome alignment that is observed. Minor alterations in the dynamics of kinetochore-microtubule attachments and/or chromosome movements towards the spindle equator offer possible explanations. The disturbed maturation of the centrosome reported in Mcph1 −/− mouse cells could be one critical underlying factor[17]. Besides that, it is important to note that mitotic chromosome structure is disturbed by a lack of functional MCPH1[10] (Supplementary Figure 2). Apart from a hypercondensation the resolution of sister chromatids is delayed; a critical process to assure faithful chromosome segregation. Notably, a recent study establishes that decatenation failure is a novel pathogenic mechanism for microcephaly in condensin II-mutated patients[26]. Given the known interaction of condensin II with MCPH1[14,15], the occurrence of unresolved sister chromatids[10] and the extended prometaphase reported here for human cells lacking MCPH1 function, it is interesting to consider that altered decatenation activity during mitosis directly contributes to the occurrence of MCPH1 primary microcephaly. The slight increase in the number of segregation errors observed during anaphase provides additional support to this scenario, as incomplete decatenation is one of the main mechanisms underlying lagging or bridged chromosomes[27–29].

Material and Methods

Cell cultures and treatments. We have used the next standard human cell lines: HeLa modified (H2B-Red1 tagged; H2B-GFP tagged), Hct-116 modified (H2B-GFP tagged) and U2OS. Also we have employed lymphoblast cell lines (LCLs, non-transformed EBV immortalized) from one MCPH1 patient (S25X mutation) and one healthy control subject[6,7]. Adherent cell lines were grown following standard conditions using DMEM medium supplemented with 10% of foetal bovine serum. LCLs were grown under usual conditions in RPMI medium supplemented with 15% foetal bovine serum.

For RNAi treatments cells were transfected with 120 nM siRNA duplexes using Lipofectamine (Invitrogen) at 50% confluency. OptiMEM medium (Invitrogen) was used for cell transfection. RNA oligos were purchased from Qiagen. The sequences of the siRNA duplexes used deplete specifically both major isophorms of MCPH1 mRNA, and were based on a previous study[11]. These validated siRNAs oligos knocked-down the MCPH1

protein levels efficiently [10, 11, 14, Supplementary Figure 3]. Synchronization of cells at G1/S was achieved by a double-thymidine protocol. The inhibitors employed were nocodazole (Sigma-Aldrich, final concentration 1,5 μM) and RO-3306 (Sigma-Aldrich; final concentration 10 μM). Untreated control cells were incubated in all cases with a similar volume of dimethyl sulfoxide.

Live-cell microscopy. Cells were plated onto 35 mm tissue culture dishes fitted with glass cover-slips (MatTek Cultureware). siRNA transfection and thymidine synchrony was performed as described in the results section, except that upon release from the second thymidine arrest or before imaging (when monitoring asynchronous cells) the standard medium containing the thymidine was exchanged for DMEM without phenol red, supplemented with 10% FBS, penicillin/streptomycin and 200 mM Trolox (Calbiochem). The dishes were transferred to a microscope humidified stage incubator containing 5% CO2 at 37 °C. Cells were filmed with three to five z sections using a Nikon Biostation IM microscope fitted with 20x and 40x/0.8 n.a. objectives and coupled with Biostation IM software. Images were stacked and processed using Image J software. Timing data were obtained after visual inspection of a minimum of 40 cells. Statistical comparisons were done using Statgraphics software.

FACS. Flow cytometry analyses were done using lymphoblast cell cultures in log-phase. One million cells approximately were recovered, washed in PBS and fixed in ice-cold Ethanol 70 overnight. Phospho-histone H3 positive cells were detected with a rabbit anti-histone H3PS10 antibody (Abcam) at a dilution of 1/250, and a donkey anti-mouse IgG FITC-conjugated secondary antibody (Santa Cruz). Propidium iodide was used as a counterstain for DNA content. Fluorescence detection was performed using an analytical flow cytometer (LSR Fortessa, BD Bioscience) equipped with BD FACSDiva™ software for data acquisition. Quantitative cell cycle analysis was done with Flowing Software v.2.5.1.

Cytogenetic analyses. Cytogenetic preparations following standard protocols were obtained in parallel from the same log-phase cell cultures analyzed by FACS. Chromosome preparations were fixed using Carnoy's solution (methanol/glacial acetic acid, 3:1), stained with Giemsa (10%) and finally visualized at microscope. The fraction of "prophase-like cells" (PLCs) and metaphases was determined after counting 1000 nuclei from coded slides at microscope. For the detailed analyses of the process of chromosome alignment in prometaphase and metaphase cells we employed cytogenetic preparations obtained following a protocol that preserves the organization of chromosomes on the mitotic spindle[12]. Microscopy images were captured with a CCD camera (Olympus DP70) coupled to a microscope (Olympus BX51) and finally managed with ImageJ software.

Immunofluorescence. SV-40 transformed fibroblasts from one MCPH1 patient (mutation T143nfsX5) and one health control were analyzed as previously described[11]. Cells growing on glass coverslips were fixed with 4% paraformaldehyde in PBS (pH 7.4) for 15 min at room temperature and permeabilized with ice-cold methanol for 30 min on ice. Cells were incubated with PBS containing 20% FBS as a blocking agent for 30 min and then with the indicated antibodies for approximately 1 h at room temperature. After being washed three times with PBS, cells were incubated with the respective secondary antibodies conjugated with fluorescence dyes. After counterstaining with DAPI, coverslips were mounted with VECTASHIELD and examined with a Zeiss Axioskop microscope equipped with a cooled charge-coupled device (CCD) camera. Grayscale images were pseudocolored and merged using ImageJ. Primary antibodies used were mouse anti-Cyclin B1 (Abcam), rabbit anti-H3PS10 (Cell Signaling), rabbit anti-H3PS28 (Upstate).

Immunoblots. For immunoblotting, cells were lysed in 1x SDS sample buffer containing 60 mM Tris-HCl [pH 6.8], 1% SDS, 10% glycerol, 0.01% bromophenol blue, and 0.1 M DTT. 1×10^5 cells were suspended in 100 μl of lysis buffer, sonicated and boiled for 2 min. Proteins were resolved by SDS-PAGE and transferred to Hybond-P PVDF membranes (Amersham). The membrane was blocked with 5% (w/v) dry milk in TBS-T (20 mM Tris-HCl [pH 7.5], 150 mM NaCl, 0.05% Tween 20). Incubation with primary antibodies was performed in TBS-T containing 1% BSA and 0.05% sodium azide for 1 hour at room temperature. Alpha-tubulin (Sigma) was used as loading control. Blots were developed by enhanced chemiluminescence detection system (Amersham). The antibody against human MCPH1 was kindly provided Dr. Tatsuya Hirano (RIKEN, Japan).

Data Availability. All data generated or analyzed during this study are included in this published article (and its Supplementary Information files).

References

1. Woods, C. G., Bond, J. & Enard, W. Autosomal recessive primary microcephaly (MCPH): a review of clinical, molecular, and evolutionary findings. *Am J Hum Genet.* **76**, 717–28 (2005).
2. Thornton, G. K. & Woods, C. G. Primary microcephaly: do all roads lead to Rome? *Trends Genet.* **25**, 501–10, https://doi.org/10.1016/j.tig.2009.09.011 (2009).
3. Mahmood, S., Ahmad, W. & Hassan, M. J. Autosomal Recessive Primary Microcephaly (MCPH): clinical manifestations, genetic heterogeneity and mutation continuum. *Orphanet J Rare Dis.* **6**, 39, https://doi.org/10.1186/1750-1172-6-39 (2011).
4. Barbelanne, M. & Tsang, W. Y. Molecular and cellular basis of autosomal recessive primary microcephaly. *Biomed Res Int.* 2014: 547986, https://doi.org/10.1155/2014/547986 (2014).
5. Khan, M. A. *et al.* A missense mutation in the PISA domain of HsSAS-6 causes autosomal recessive primary microcephaly in a large consanguineous Pakistani family. *Hum Mol Genet.* **23**, 5940–9, https://doi.org/10.1093/hmg/ddu318 (2014).
6. Neitzel, H. *et al.* Premature chromosome condensation in humans associated with microcephaly and mental retardation: a novel autosomal recessive condition. *Am J Hum Genet.* **70**, 1015–22 (2002).
7. Trimborn, M. *et al.* Mutations in microcephalin cause aberrant regulation of chromosome condensation. *Am J Hum Genet* **75**, 261–266 (2004).

8. Trimborn, M. *et al*. The first missense alteration in the MCPH1 gene causes autosomal recessive microcephaly with an extremely mild cellular and clinical phenotype. *Hum Mutat* **26**, 496 (2005).
9. Ghani-Kakhki, M. *et al*. Two Missense Mutations in the Primary Autosomal Recessive Microcephaly Gene MCPH1 Disrupt the Function of the Highly Conserved N-Terminal BRCT Domain of Microcephalin. *Mol Syndromol.* **3**, 6–13 (2012).
10. Arroyo, M. *et al*. Chromosome structure deficiencies in MCPH1 syndrome. *Chromosoma.* **124**, 491–501, https://doi.org/10.1007/s00412-015-0512-2 (2015).
11. Gavvovidis, I. *et al*. A novel MCPH1 isoform complements the defective chromosome condensation of human MCPH1-deficient cells. *PLoS One.* **7**, e40387, https://doi.org/10.1371/journal.pone.0040387 (2012).
12. Giménez-Abián, J. F. *et al*. Regulated separation of sister centromeres depends on the spindle assembly checkpoint but not on the anaphase promoting complex/cyclosome. *Cell Cycle* **4**(11), 1561–75 (2005).
13. Trimborn, M. *et al*. Establishment of a mouse model with misregulated chromosome condensation due to defective Mcph1 function. *PLoS One* **5**, e9242, https://doi.org/10.1371/journal.pone.0009242 (2010).
14. Trimborn, M., Schindler, D., Neitzel, H. & Hirano, T. Misregulated chromosome condensation in MCPH1 primary microcephaly is mediated by condensin II. *Cell Cycle* **5**, 322–6 (2006).
15. Yamashita, D. *et al*. MCPH1 regulates chromosome condensation and shaping as a composite modulator of condensin II. *J Cell Biol.* **194**, 841–54, https://doi.org/10.1083/jcb.201106141 (2011).
16. Alderton, G. K. *et al*. Regulation of mitotic entry by microcephalin and its overlap with ATR signalling. *Nat Cell Biol.* **8**, 725–33 (2006).
17. Gruber, R. *et al*. MCPH1 regulates the neuroprogenitor division mode by coupling the centrosomal cycle with mitotic entry through the Chk1-Cdc25 pathway. *Nat Cell Biol.* **13**, 1325–34, https://doi.org/10.1038/ncb2342 (2011).
18. Tibelius, A. *et al*. Microcephalin and pericentrin regulate mitotic entry via centrosome-associated Chk1. *J Cell Biol.* **185**, 1149–57 (2009).
19. Venkatesh, T. & Suresh, P. S. Emerging roles of MCPH1: expedition from primary microcephaly to cancer. *Eur J Cell Biol.* **93**, 98–105, https://doi.org/10.1016/j.ejcb.2014.01.005 (2014).
20. Vassilev, L. T. *et al*. Selective small-molecule inhibitor reveals critical mitotic functions of human CDK1. *Proc Natl Acad Sci USA.* **103**, 10660–5 (2006).
21. O'Driscoll, M., Jackson, A. P. & Jeggo, P. A. Microcephalin: a causal link between impaired damage response signaling and microcephaly. *Cell Cycle* **5**, 2339–44 (2006).
22. Lindqvist, A., Rodríguez-Bravo, V. & Medema, R. H. The decision to enter mitosis: feedback and redundancy in the mitotic entry network. *J Cell Biol.* **185**, 193–202, https://doi.org/10.1083/jcb.200812045 (2009).
23. Lindqvist, A., van Zon, W., Karlsson Rosenthal, C. & Wolthuis, R. M. Cyclin B1-Cdk1 activation continues after centrosome separation to control mitotic progression. *PLoS Biol.* **5**, e123 (2007).
24. Abe, S. *et al*. The initial phase of chromosome condensation requires Cdk1-mediated phosphorylation of the CAP-D3 subunit of condensin II. *Genes Dev.* **25**, 863–74, https://doi.org/10.1101/gad.2016411 (2011).
25. Woods, C. G. & Basto, R. Microcephaly. *Curr Biol.* **24**, R1109–11, https://doi.org/10.1016/j.cub.2014.09.063 (2014).
26. Martin, C. A. *et al*. Mutations in genes encoding condensin complex proteins cause microcephaly through decatenation failure at mitosis. *Genes Dev.* **30**, 2158–2172 (2016).
27. Germann, S. M. *et al*. TopBP1/Dpb11 binds DNA anaphase bridges to prevent genome instability. *J Cell Biol.* **204**, 45–59, https://doi.org/10.1083/jcb.201305157 (2014).
28. Haarhuis, J. H. *et al*. WAPL-mediated removal of cohesin protects against segregation errors and aneuploidy. *Curr Biol.* **23**, 2071–7, https://doi.org/10.1016/j.cub.2013.09.003 (2013).
29. Brownlow, N., Pike, T., Zicha, D., Collinson, L. & Parker, P. J. Mitotic catenation is monitored and resolved by a PKCε-regulated pathway. *Nat Commun* **5**, 5685, https://doi.org/10.1038/ncomms6685 (2014).

Acknowledgements

This work was supported by Junta de Andalucía (Funding program 'Ayudas a grupos de investigación', reference BIO 220). M. Arroyo PhD is granted by University of Jaén (Spain), and was provided with travelling grants EMBO and "Escuela de Doctorado" (University of Jaén, Spain). The authors express their gratitude to H. Neitzel (Berlin, Germany) for providing the lymphoblast cell lines used in this study; C. Fisher and G. Marques (University of Minnesota, US) for technical assistance; and T. Hirano (RIKEN, Japan) for providing the antibody against MCPH1. Research at laboratory of R. Kuriyama was financially supported by NSF (MCB1140033). Technical and human support provided by CICT of Universidad de Jaén (UJA, MINECO, Junta de Andalucía, FEDER) is gratefully acknowledged.

Author Contributions

J.A.M., D.J.C. and R.K. designed the experiments. M.A., A.C., D.K., M.T. and J.A.M. performed the experiments. M.A., M.T., A.S. and J.A.M. analyzed the results. J.A.M. and D.J.C. wrote the main manuscript text. All authors reviewed the manuscript.

Additional Information

Supplementary information accompanies this paper at https://doi.org/10.1038/s41598-017-12793-7.

Competing Interests: The authors declare that they have no competing interests.

Publisher's note: Springer Nature remains neutral with regard to jurisdictional claims in published maps and institutional affiliations.

Supplementary information: Arroyo *et al*.

MCPH1, mutated in primary microcephaly, is required for efficient chromosome alignment during mitosis

M. Arroyo[1], R. Kuriyama[2], M. Trimborn[3], D. Keifenheim[2], A. Cañuelo[1], A. Sánchez[1], D. J. Clarke[2], J.A. Marchal[1*]

* Corresponding author: Dr. Juan Alberto Marchal Ortega, Departamento de Biología Experimental; Facultad de Ciencias Experimentales, Universidad de Jaén, Paraje Las Lagunillas s/n; Room B3-304, E-23071 Jaén (Spain), Telephone: 0034-953213361; Fax: 0034-953211875, e-mail: jamaor@ujaen.es

Supplementary Figure S1

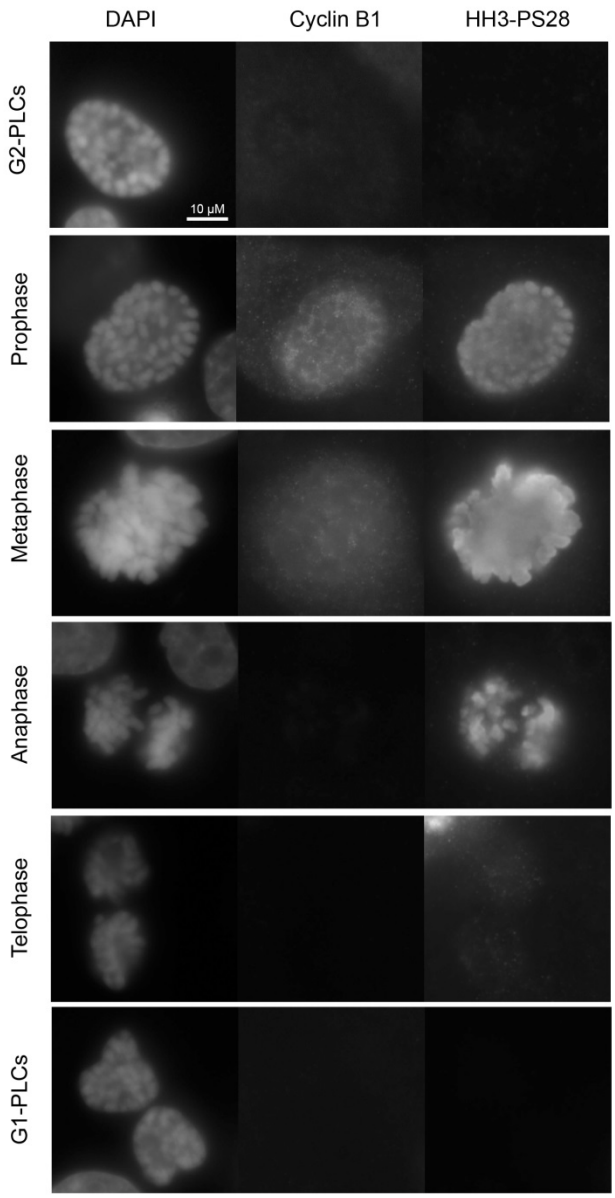

Supplementary figure S1. Immunolocalization using antibodies against Cyclin B and Histone H3-PS28 proteins in proliferating cells from one MCPH1 patient.

Supplementary Figure S2

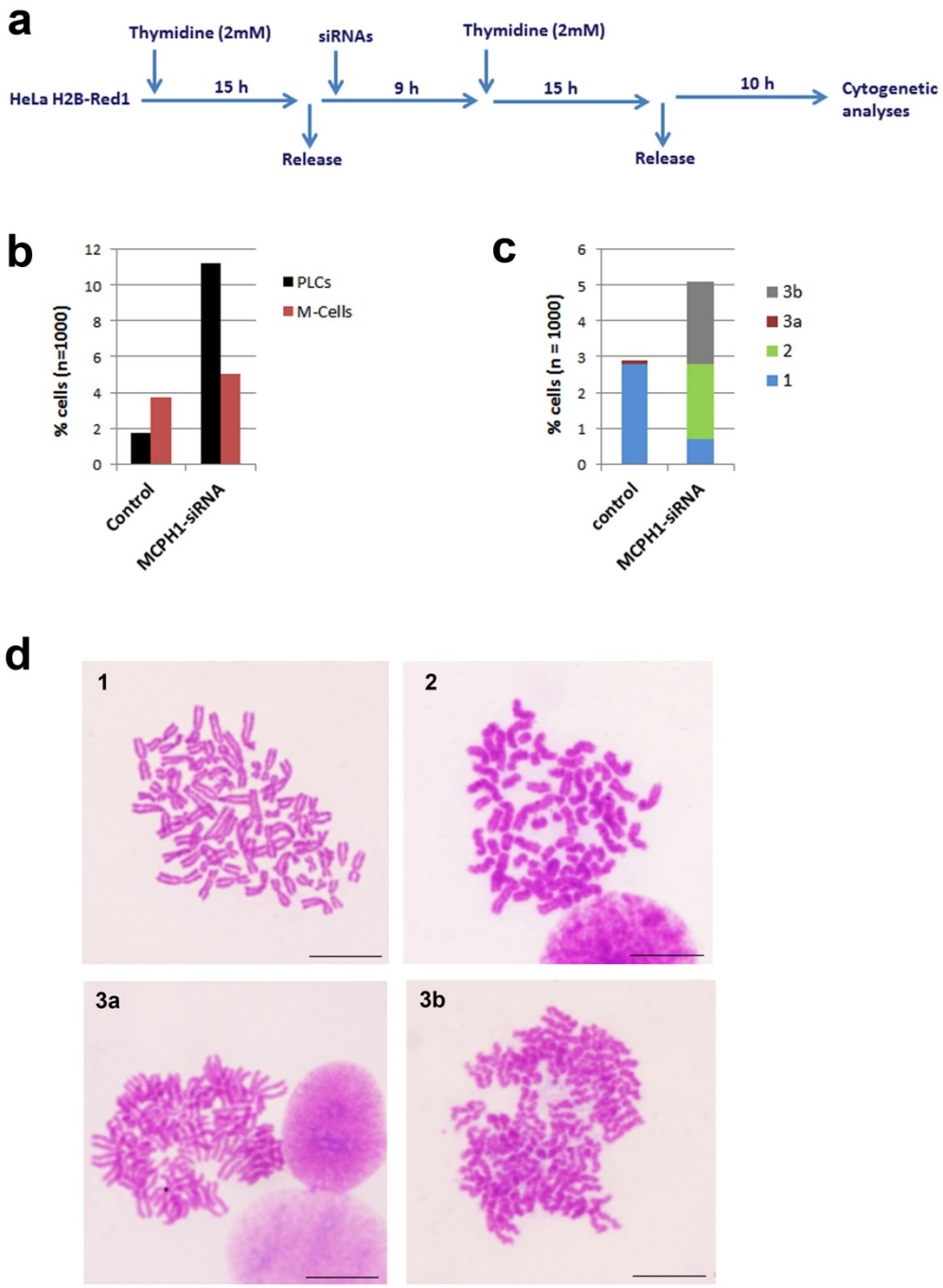

Supplementary figure S2. Cytogenetic analyses of the occurrence of PLCs and chromosome morphology in HeLa H2B-Red1 cells depleted of MCPH1 function by siRNAs. a) A brief diagram of the experimental protocol used. b) Fraction of PLCs and mitotic cells determined by visual inspection by microscopy, n=1000. c) Quantitative analyses of the chromosome morphology observed within the mitotic cells from B. d) Representative images of the main chromosomal morphologies observed in our analyses. As expected, in MCPH1-siRNA treated cells chromosomes with a wavy hypercoiled appearance and unresolved sister chromatids (type 2) or with premature centromeric division (type 3b) were frequently observed. However, in control cells chromosomes present straight, well resolved chromatids that remain connected at the centromeres in most cases (type 1), being premature centromeric division barely observed (type 3a).

Supplementary Figure S3

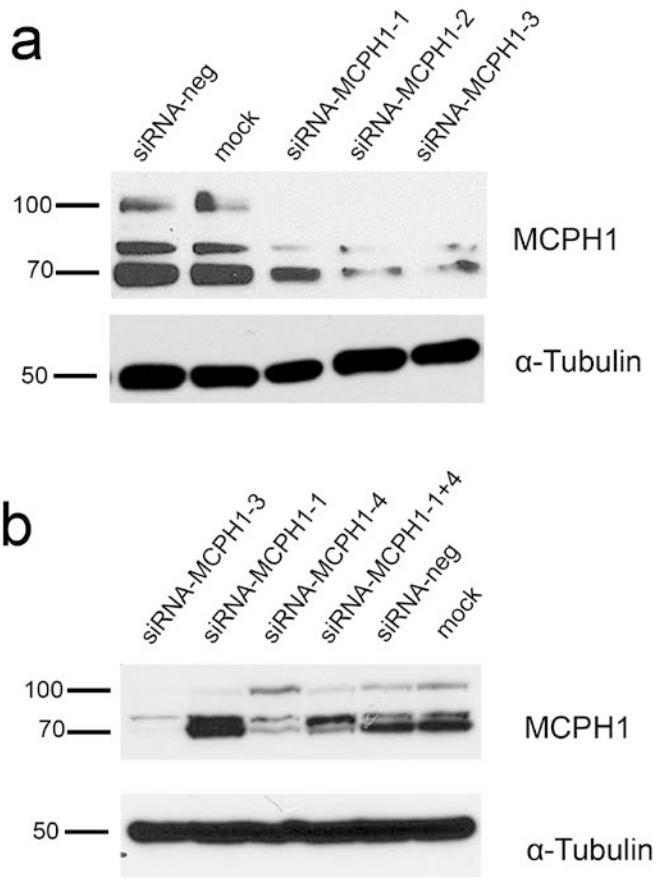

Supplementary figure S3. Immunoblots with an anti-MCPH1 antibody after transfection of HeLa (a) and U2OS (b) cells with different siRNAs showing efficient depletion of MCPH1 protein. Oligos siRNA-2 and siRNA-3 downregulate both described isoforms, full-lenght (93 kDa) and Δ9-14 (70 kDa) (Gavvovvidis et al. 2012). Oligos siRNA-1 and siRNA-4, targeting full-length and Δ9-14 isoforms respectively, specifically downregulate each of them. Non-targeting siRNA (siRNA-neg) or mock-transfected (mock) controls showed no downregulation. Alpha-tubulin served as a loading control. The rabbit polyclonal antiserum against MCPH1 was kindly furnished by Dr. Tatsuya Hirano (RIKEN, Japan).

Supplementary Figure S4

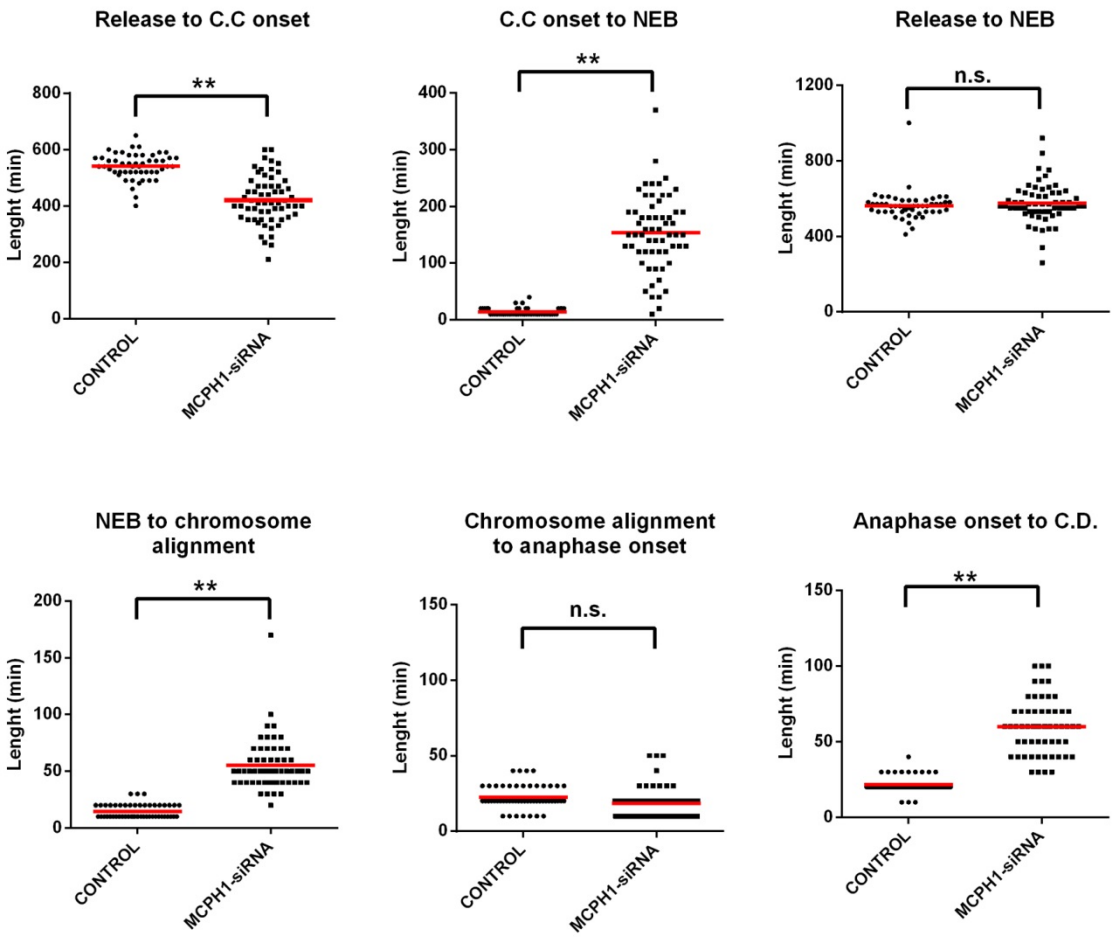

Supplementary figure S4. Dot-plots showing the time interval between different key mitotic events in HeLa-Red1 cells either mock treated or depleted of MCPH1 function with a second non-overlapping siRNA (oligo siRNA-MCPH1-2). Cells were processed as described in Figure 2. The red line indicates the mean value. C.C. = chromosome condensation; NEB = nuclear envelope breakdown; C.D. = chromosome decondensation. More than 50 cells were analyzed in each case. Statistical comparisons for the mean and median data were done by T-student and Wilcoxon (W) tests respectively. ** $p<0.01$; N.S. not significant.

Supplementary Figure S5

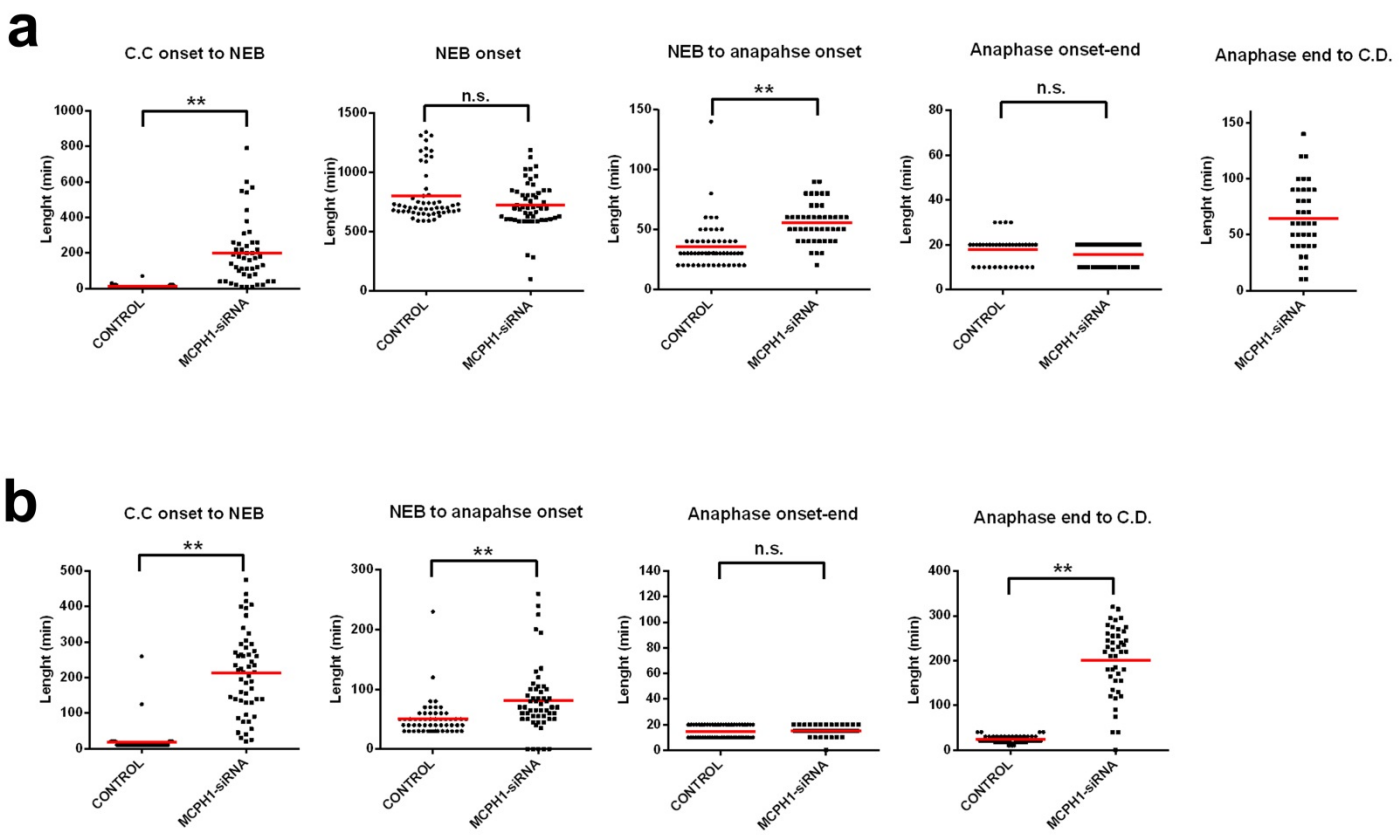

Supplementary figure S5. Dot-plots showing the time interval between different key mitotic events in minutes in Hct-116 (a) and HeLa-GFP (b) cells either mock treated or depleted of MCPH1 function by siRNAs. The red line indicates the mean value. C.C. = chromosome condensation; NEB = nuclear envelope breakdown; C.D. = chromosome decondensation. At least 50 cells were analyzed in each case. In Hct-116 mock control cells chromosome segregation and further decondensation were not analyzed in separate as both occur nearly simultaneously. Statistical comparisons for the mean and median data were done by T-student and Wilcoxon (W) tests respectively. ** $p<0.01$; N.S. not significant.

Supplementary Figure S6

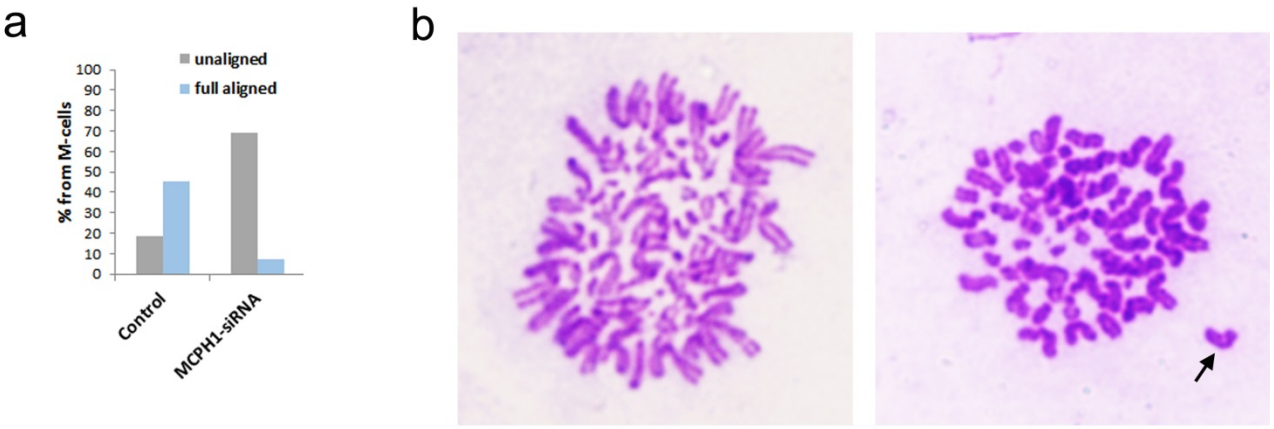

Supplementary figure S6. (a) Fraction of U2OS mitotic cells showing either all chromosomes organized into the metaphase plate or some unaligned chromosomes. Unsynchronized cells either mock treated or depleted of MCPH1 function by siRNAs were used. Analyses were performed by microscopic inspection of cytogenetic preparations obtained following a protocol that preserves the organization of chromosomes on the mitotic spindle [12]. 100 mitotic cells were counted and classified in each case. (b) Representative images of mitotic cells classified in A as aligned (left picture) or displaying some unaligned chromosomes (pointed by arrow, right picture). In MCPH1-siRNA treated cells, this particular phenotype was frequently observed and resemble to the observed by live-cell in HeLa cells (Figure 3C) and in patient cells (Figure 3E).

Supplementary Figure S7

a

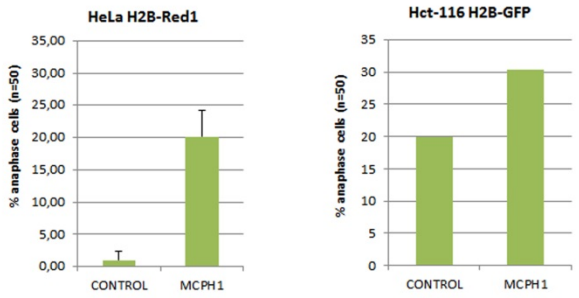

b

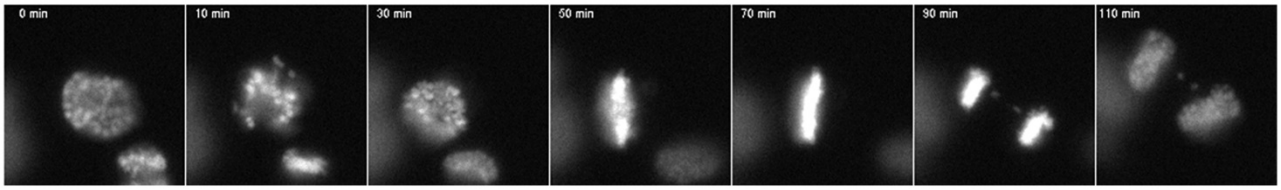

Supplementary figure S7. a) Percent of cells showing bridge or lagging errors during anaphase in either control or MCPH1 depleted cells. Two different cell lines were analyzed. For HeLa cells data from experiments employing either thymidine or RO-3306 synchronization protocols are shown. b) Live-imaging stack from HeLa H2B-Red1 cells depleted of MCPH1 function showing an example of lagging error during anaphase. Time (in minutes) from nuclear envelope breakdown (first frame) is indicated.

Supplementary videos information

Video 1: video showing HeLa H2B-Red1 control cells recorded after release from second thymidine arrest. Time from release (in minutes) is indicated.

Video 2: video showing HeLa H2B-Red1 MCPH1-siRNA treated cells recorded after release from second thymidine arrest. Time from release (in minutes) is indicated.

Video 3: video of HeLa H2B-Red1 control cells released from second thymidine arrest were immediately incubated with RO-3306 and recorded. Time from RO-3306 adding (in minutes) is indicated.

Video 4: video of HeLa H2B-Red1 MCPH1-siRNA treated cells released from second thymidine arrest were immediately incubated with RO-3306 and recorded. Time from RO-3306 adding (in minutes) is indicated.

Video 5: video of a representative PLC showing progressive decondensation after RO-3306 adding. Time from RO-3306 adding (in minutes) is indicated.

Video 6: video of HeLa H2B-Red1 control cells incubated with RO-3306 during 8 hours were released into normal medium and recorded. Time from RO-3306 release (in minutes) is indicated.

Video 7: video of HeLa H2B-Red1 MCPH1-siRNA treated cells incubated with RO-3306 during 8 hours were released into normal medium and recorded. Time from RO-3306 release (in minutes) is indicated.

Video 8: video of HeLa H2B-GFP MCPH1-siRNA treated cells recorded after release from second thymidine arrest. Time from release (in minutes) is indicated. PLCs before NEB and after chromosome segregation are clearly observed.

CHAPTER III

CHAPTER III

TITLE: MCPH1 is essential for cellular adaptation to the G2-phase decatenation checkpoint

AUTHORS: M. Arroyo[1], R. Kuriyama[2], A. Cañuelo[1], Guerrero I[3], A. Sánchez[1], D. J. Clarke[2], J.A. Marchal[1*]

(1) Departamento de Biología Experimental, Universidad de Jaén

(2) Department of Genetics, Cell Biology and Development, University of Minnesota

(3) Instituto de Investigación y Formación Agraria y Pesquera (IFAPA Centro El Toruño)

*** Corresponding author:** Dr. Juan Alberto Marchal Ortega

Departamento de Biología Experimental

Facultad de Ciencias Experimentales

Universidad de Jaén

Paraje Las Lagunillas s/n; Room B3-304

E-23071 Jaén (Spain)

Telephone: 0034-953213361; Fax: 0034-953211875

e-mail: jamaor@ujaen.es

ABSTRACT

Cellular checkpoints controlling entry into mitosis monitor the integrity of the DNA and delay mitosis onset until the DNA damage is fully repaired. However, this canonical response can weaken leading to a spontaneous bypass of the checkpoint, a process referred to as checkpoint adaptation. Here we have investigated the contribution of MCPH1, mutated in primary microcephaly, to the decatenation checkpoint, a less-understood G2 pathway that delays entry into mitosis until chromosomes are properly disentangled. Our results demonstrate that while *MCPH1* function is dispensable for activation and maintenance of the decatenation checkpoint, it is however required for the adaptive response that bypasses it. Furthermore, we demonstrate that CHK1 is required for decatenation checkpoint G2 arrest and functions downstream of MCPH1 to promote recovery. MCPH1 however does not confer adaptation to the G2 arrest triggered by the ATM/ATR-based DNA damage checkpoint. In addition to revealing a new role for MCPH1 in cell cycle control our study provides support to the notion that the DNA damage and the decatenation checkpoints are distinct G2 signaling pathways.

INTRODUCTION

Checkpoints are specialized surveillance mechanisms that ensure coupling and completion of critical processes – such as DNA replication or chromosome segregation – within the cell cycle. Checkpoints controlling entry into mitosis critically monitor the integrity of the DNA. Accordingly, the pathways regulating normal mitosis onset are rewired under damaging conditions, triggering a reversible cell cycle arrest to allow efficient DNA repair before entry into mitosis (Van Vugt et al., 2004). However, cells retain a capacity to spontaneously bypass the checkpoint arrest following a transient G2 delay despite the persistence of the damage that triggered it (Paulovich et al., 1997; Serrano and D'Amours, 2016). Unraveling the molecular requirements of this overlooked mechanism, named checkpoint adaptation, is of importance to better understand the checkpoint control system itself. Checkpoint adaptation mechanisms are also of particular relevance to cancer etiology.

MCPH1, mutated in primary microcephaly, regulates cell progression into mitosis in multiple contexts. During unperturbed cell division it is required for coupling chromosome condensation and centrosome maturation in mitosis (Neitzel et al., 2002; Trimborn et al., 2004; Gruber et al., 2011; Arroyo et al., 2017). The underlying pathways controlling the G2/M transition are also misregulated under undamaging conditions in MCPH1 deficient cells. Unscheduled activation of CDK1 and CDC25A, and loss of centrosomal CHK1 during G2 are all consequences of MCPH1 downregulation (Alderton et al., 2006; Tibelius et al., 2009; Gruber et al., 2011). How MCPH1 modulates CDK1 and CDC25A activation during unperturbed cell division remain to be clarified. Remarkably, those pathways retain sufficient capacity to allow scheduled G2 progression and mitosis onset in cells depleted of *MCPH1* (O'Discoll et al 2006; Arroyo et al., 2017).

A different scenario where MCPH1 function has been explored is cell cycle control in the presence of DNA damage. MCPH1 patient cells, similar to ATR-mutated cells, display defective G2 arrest after treatments that activate the ATR signaling pathway, for example after UV-irradiation induced DNA damage (Alderton et al., 2006). MCPH1 is proposed to function downstream of CHK1 and upstream of CDC25 in the ATR-related pathway (Alderton et al., 2006). Several lines of evidences suggest that MCPH1 is however dispensable for the ATM-related DNA damage checkpoint. A collection of studies using patient cell lines (Gavvovidis et al., 2010), avian DT40 knock-out cells (Brown et al., 2010), or MCPH1-/- mouse cells (Gruber et al., 2011; Zhou et al., 2013), demonstrated a proficient ATM-checkpoint response in each case. Although previous analyses based on RNAi-mediated MCPH1 depletion are discordant

with these findings (Xu et al., 2004; Rai et al., 2006), these discrepancies are likely explained by incomplete loss of MCPH1 function or upregulation of redundant pathways within the cellular models investigated (O'Driscoll et al., 2006). In addition to contributing to G2 checkpoint responses, MCPH1 is a component of the DNA repair machinery. It localizes to sites of double stranded breaks (DSBs) (Wood et al., 2007; Jeffers et al., 2008; Gavvovidis et al., 2012), and its interaction with SWI/SNF chromatin remodeling complexes is required for efficient repair of DSBs (Peng et al., 2009). This function could explain the compromised cell viability after exposure to DSB-inducing agents in cells lacking *MCPH1* (Peng et al., 2009; Liang et al., 2010, 2015; Zhou et al., 2013).

While the contribution of MCPH1 to the DNA damage checkpoint has been extensively investigated, less is known about its potential importance for other G2 checkpoints. Of particular interest is the decatenation checkpoint, a less-understood pathway that delays entry into mitosis until chromosomes are properly disentangled (decatenated) (reviewed in Damelin and Bestor, 2007). This checkpoint is triggered after inhibition of DNA Topoisomerase II with catalytic inhibitors such as ICRF-193 and related bisdioxopiperazines, which block Topo II activity without inducing DSBs (Downes et al., 1994; Deming et al., 2001; Luo et al., 2009). Other studies have revealed that there are key differences in the signaling pathways of the decatenation checkpoint and the DNA damage checkpoint (Damelin and Bestor, 2007; Luo et al., 2009). Interestingly, mitotic cells lacking *MCPH1* function show impaired sister chromatid resolution and chromosome segregation problems (Arroyo et al., 2015; 2017), which could be indicative of a defect in the decatenation checkpoint. That is, if MCPH1-deficient cells have an attenuated decatenation checkpoint, the expected phenotype would be entry into mitosis in the presence of catenated chromatids that cannot be resolved or segregated efficiently. Moreover, ATR signaling, which is essential for the decatenation checkpoint pathway (Deming et al., 2001), requires MCPH1 function to effectively stop the cell cycle in response to UV irradiation (Alderton et al., 2006).

Considering this evidence, we investigated the proficiency of the decatenation checkpoint in cells that lack MCPH1 function. Our results have demonstrated that MCPH1 function is dispensable for the temporary G2 arrest that is triggered by the decatenation checkpoint. Unexpectedly, however, we find that MCPH1 is required for the adaptive response that triggers entry into mitosis despite Topo II catalytic inhibition.

METHODS

Cell cultures and treatments

We have used standard and modified (H2B-Red1 tagged) HeLa cell lines. Also we have employed lymphoblast cell lines (LCLs, non-transformed EBV immortalized) from one MCPH1 patient (S25X mutation) and one healthy control subject (Neitzel et al., 2002; Trimborn et al., 2004). HeLa cell lines were grown following standard conditions using DMEM medium supplemented with 10% of foetal bovine serum. LCLs were grown under usual conditions in RPMI medium supplemented with 15% foetal bovine serum.

For RNAi treatments cells were transfected with 120 nM siRNA duplexes using Lipofectamine (Invitrogen) at 50% confluency. OptiMEM medium (Invitrogen) was used for cell transfection. RNA oligos were purchased from Qiagen. The sequences of the siRNA duplexes used deplete specifically both major isoforms of MCPH1 mRNA, and were based on a previous study (Gavvovidis et al., 2012). These validated siRNA oligos knocked-down the MCPH1 protein levels efficiently (Trimborn et al., 2006; Gavvovidis et al., 2012; Arroyo et al., 2017). Synchronization of cells at G1/S was achieved by a double-thymidine protocol. The inhibitors employed were Nocodazole (final concentration 1,5 μM), ICRF-193 (final concentration 7 μM), etoposide (final concentration 25 μM), caffeine (final concentration 2 mM), SB202190 (final concentration 18 μM) and UCN-01 (final concentration 200 nM). Untreated control cells were incubated in all cases with a similar volume of solvent.

Live-cell microscopy

The procedure was similar to the described in Arroyo et al., 2017. Cells were plated onto 35 mm tissue culture dishes fitted with glass cover-slips (MatTek Cultureware). siRNA transfection and cell synchrony was performed as described in the results section, except that upon release from the second thymidine the standard medium containing the thymidine was exchanged for DMEM without phenol red, supplemented with 10% FBS, penicillin/streptomycin and 200 mM Trolox (Calbiochem). The dishes were transferred to a microscope humidified stage incubator containing 5% CO2 at 37ºC. Cells were filmed with three to five z sections using a Nikon Biostation IM microscope fitted with 20x and 40x/0.8 n.a. objectives and coupled with Biostation IM software. Images were stacked and processed using Image J software. Timing data were obtained after visual inspection of a minimum of 50 cells. Statistical comparisons were done using Statgraphics software.

Flow Cytometry

Flow cytometry analyses were done using lymphoblast cell cultures in log-phase. One million cells approximately were recovered, washed in PBS and fixed in ice-cold Ethanol 70 overnight. Phospho-histone H3 positive cells were detected with a rabbit anti-histone H3PS10 antibody (Abcam) at a dilution of 1/250, and a donkey anti-mouse IgG FITC-conjugated secondary antibody (Santa Cruz). Propidium iodide was used as a counterstain for DNA content. Fluorescence detection was performed using an analytical flow cytometer (LSR Fortessa, BD Bioscience) equipped with BD FACSDiva™ software for data acquisition. Quantitative cell cycle analysis was done with Flowing Software v.2.5.1.

Cytogenetic analyses

Cytogenetic preparations following standard protocols were obtained in parallel from the same log-phase cell cultures analyzed by FACS. Chromosome preparations were fixed using Carnoy's solution (methanol/glacial acetic acid, 3:1), stained with Giemsa (10 %) and finally visualized by bright-field microscopy. The fraction of "prophase-like cells" (PLCs) and metaphases was determined after counting 1000 nuclei from coded slides. Microscopy images were captured with a CCD camera (Olympus DP70) coupled to a microscope (Olympus BX51) and finally managed with ImageJ software.

Immunofluorescence

Control and MCPH1 patient (S25X) lymphoblast cells were treated with the corresponding inhibitors for 3h and attached to glass coverslips pretreated with poly-L-lysine. HeLa cells growing directly in glass cover slips were previously synchronized at G1/S border by double thymidine block, and transfected with siRNAs during the release from the first thymidine block. The corresponding inhibitors were added 6h after release from the second thymidine block, and cells were processed 3h after. Cells were fixed with 4% paraformaldehyde in PBS (pH 7.4) for 15 min at room temperature and permeabilized with ice-cold methanol for 30 min on ice. Cells were incubated with PBS containing 20% FBS as a blocking agent for 30 min and then with mouse anti-γH2AX (Upstate) overnight at 4ºC. After being washed three times with PBS, cells were incubated with donkey anti-mouse IgG FITC-conjugated secondary antibody (Santa Cruz). After counterstaining with DAPI, coverslips were mounted with VECTASHIELD and examined with a Zeiss Axioskop microscope equipped with a cooled charge-coupled device (CCD) camera. Grayscale images were pseudocolored and merged using ImageJ.

Inmunoblots

For immunoblotting, cells were lysed in 1x SDS sample buffer containing 60 mM Tris-HCl [pH 6.8], 1% SDS, 10% glycerol, 0.01% bromophenol blue, and 0.1 M DTT. 1 x 10^5 cells were suspended in 100 µl of lysis buffer, sonicated and boiled for 2 min. Proteins were resolved by

SDS-PAGE and transferred to Hybond-P PVDF membranes (Amersham). The membrane was blocked with 2,5% (w/v) dry milk in TBS-T (20 mM Tris-HCl [pH 7.5], 150 mM NaCl, 0.05% Tween 20). Incubation with primary antibodies was performed in TBS-T containing 1% BSA and 0.05% sodium azide overnight at 4ºC. Alpha-tubulin (Sigma) was used as loading control. For detecting phosphoS345-CHK1 dry milk was replaced by BSA in the blocking solution. Blots were developed by enhanced chemiluminescence detection system (Amersham). Primary antibodies used were anti-total CDK1(ab131450, Abcam), anti-phosphoY15-CDK1 (ab47594, Abcam), and anti-phosphoS345-CHK1(133D3, Cell Signaling).

RESULTS AND DISCUSSION

MCPH1 function is dispensable for activation of the G2 decatenation checkpoint

We first analyzed if cells lacking *MCPH1* function display a functional decatenation checkpoint. In order to do so, we made use of log-phase cultures of control and MCPH1 patient lymphoblasts, and we assayed the dynamics of mitotic entry after incubation with the Topoisomerase II inhibitor ICRF-193 during either 3h or 6h. Nocodazole was also added alone or combined with ICRF-193 to trap those cells entering into mitosis, which were detected by FACS using a mitotic marker (Histone H3PS10). Our data revealed almost no accumulation of mitotic cells during prolonged incubation with ICRF-193 and nocodazole in both control and patient cells, in comparison with the progressive accumulation observed when only nocodazole was added (figure CIII-1A). These results are in accordance with previous studies which demonstrated a proficient decatenation checkpoint in human lymphoblastoid cell lines (Deming et al., 2001; Bower et al., 2010a), and suggest that *MCPH1* function is not required for decatenation checkpoint activation. We next compared the fraction of G2 and mitotic (M) cells, determined by FACS, with the frequency of "Prophase-like cells" (PLCs), determined through microscopic inspection of cytogenetic preparations made in parallel (figure CIII-1B). PLCs are a hallmark of *MCPH1* deficiency and arise as a consequence of premature chromosome condensation during G2 phase, and delayed decondensation following completion of mitosis (Neitzel et al., 2002; Arroyo et al., 2017). Our analyses showed that in patient cells PLCs do not increase in parallel with the G2 fraction during prolonged incubation with ICRF-193. Thus, while the PLC frequency was increased after 3 hours of incubation, it was strikingly reduced after 6 hours with ICRF-193 (figure CIII-1B). Similar results were observed when nocodazole was omitted.

MCPH1 is required for decatenation checkpoint adaptation.

Although cells lacking MCPH1 function arrested in G2 when Topo II was catalytically inhibited, the checkpoint response was unlike controls cells. The decatenation checkpoint is notoriously leaky- G2 cells gradually enter mitosis with catenated, unresolved chromatids after delaying in G2 only transiently. This can be observed in figure CIII-1A where the mitotic index increased slightly in the ICRF-193 treated controls samples over time. However, strikingly, the MCPH1 cells did not leak into mitosis- instead we observed a decrease in mitotic index over time (Figure CIII-1 A). This indicates that MCPH1 deficient cells are defective in the adaptive response that spontaneously bypasses the decatenation checkpoint G2 arrest.

We next investigated the dynamics of mitotic entry after forced bypass of the decatenation checkpoint arrest. In order to do that we made use of caffeine, a well-known inhibitor of ATM/ATR kinases which override the ICRF-193-imposed G2 arrest (Deming et al., 2001). As showed in figure CIII-1A, single incubation with caffeine slightly accelerates the rate of mitotic entry in both control and patient cells. When caffeine was simultaneously combined with ICRF-193, however, we observed a striking inability of MCPH1 patient cells to enter mitosis. In control cells treated with ICRF-193 and caffeine, the mitotic cells increased at a similar rate to untreated samples or caffeine-treated samples. In patient cells, however, inhibition of ATM/ATR with caffeine had only a weak effect on mitotic entry in the presence of ICRF-193, indicating that most G2 cells remained arrest for at least 6 hours (figure CIII-1A and 1C). Moreover, the frequency of PLCs increased during the incubation with ICRF-193 plus caffeine in patient cells (figure CIII-1C).

These dynamics are in sharp contrast to those observed above for PLCs after single incubation with ICRF-193. The caffeine-insensitive nature of the ICRF-193-mediated G2 arrest observed in MCPH1 patient cells was not influenced by the presence of nocodazole in our experiments, as the fraction of G2 and PLCs remain similarly higher – and the mitotic frequency equally reduced - when nocodazole was omitted from the assays (figure CIII-1C). When we analyzed the chromosome structure of control cells treated with ICRF-193 and caffeine we observed a high frequency of mitotic cells with tangled, unresolved and uncondensed chromosomes (figure CIII-1D). Those chromosome alterations, which are a consequence of cells entering mitosis without active Topoisomerase II (Downes et al., 1994; Deming et al., 2002; Giemenz-Abian et al., 2000; Bower et al., 2010a), were not observed in MCPH1 patient cells treated with ICRF-193 and caffeine. Instead, an elevated frequency of PLCs was observed (figure CIII-1D).

MCPH1-depleted HeLa cells are also deficient in G2 decatenation checkpoint adaptation.

The prominent adaptive response of the decatenation checkpoint is not well understood. No cell lines have been examined in which cells permanently arrest in G2 in the presence of Topo II inhibitors. Since MCPH1 patient cells lack this adaptive response, *MCPH1* may be a crucial factor required for decatenation checkpoint bypass. We therefore sought to test directly if MCPH1 is a component of this adaptation response. We employed HeLa cells depleted of MCPH1 function by siRNA because this strategy has been previously characterized (Arroyo et al., 2017). HeLa H2B-Red1 cells synchronized at G1/S using excess thymidine were transfected with siRNAs against *MCPH1* and then monitored by fluorescent live-cell microscopy upon release into the cell cycle (experimental outline in figure CIII-2A). We previously used this approach to demonstrate that the timing of mitotic entry is similar in control and MCPH1

depleted cells following release from the G1/S arrest (Arroyo et al., 2017). Here, ICRF-193 was added 7 hours after release from the thymidine block, at the time when MCPH1 deficient cells start to prematurely condense their chromosomes during G2 (Arroyo et al., 2017). Caffeine was added to parallel samples one hour after ICRF-193. As depicted in figure CIII-2B, control cells efficiently activated the G2 decatenation checkpoint in the presence of ICRF-193 with typical kinetics. That is, Topo II inhibition immediately blocked entry of cells into mitosis and then following three hours, some cells began to spontaneously adapt to the arrest. Therefore, robust decatenation checkpoint activation followed by checkpoint adaptation was readily observed. This was important to establish using the approach because decatenation checkpoint kinetics varies significantly between different human cell lines (Damelin and Bestor 2007). Caffeine efficiently bypassed the G2 decatenation checkpoint as most control cells treated with ICRF-193 entered into mitosis without delay (figure CIII-2B, videos CIII-1-2) Like in control cells, HeLa H2B-Red1 cells depleted of MCPH1 by RNAi efficiently activated the G2 decatenation checkpoint (figure CIII-2B, videos CIII-3-4).

However, unlike the controls, but consistent with the MCPH1 patient cells, the MCPH1 depleted cells did not adapt to the decatenation checkpoint as no spontaneous override was observed. In the presence of caffeine, there was no immediate entry into mitosis as occurred in control cells. Strikingly, in this case a significant number of cells remained arrested in G2 for many hours. Thus, unlike control cells, spontaneous decatenation checkpoint adaptation was severely impaired and the ability of caffeine to induce adaptation in the presence of ICRF-193 was strongly perturbed in MCPH1 depleted cells. As described above for lymphoblast cells, single incubation with caffeine only produced a slight increase in the rate of mitotic entry, especially in MCPH1 depleted HeLa cells (figure CIII-2E).

Overall these results are in line with the findings in lymphoblastoid cells and demonstrate that (1) MCPH1 function is dispensable for decatenation checkpoint activation but (2) MCPH1 is required for decatenation checkpoint adaptation. Our finding that MCPH1 is dispensable for activation and maintenance of the G2 decatenation checkpoint was a surprising outcome. The decatenation checkpoint depends on the ATR-signaling pathway (Deming et al., 2001), and the ATR- pathway requires MCPH1 function to efficiently stop the cell cycle in response to UV irradiation (Alderton et al., 2006). Taken together, these data support the idea that while the pathways responding to UV irradiation and ICRF-193-mediated Topo II catalytic inhibition both depend on ATR, they are nevertheless distinct in their mechanisms of activation and some of their signaling components.

The G2 decatenation checkpoint induces decondensation in PLCs dependent on the ATM/ATR pathway.

MCPH1 deficient cells have a functional decatenation checkpoint. Furthermore, we observed that ICRF-193 treatment induced decondensation of the chromatin in G2- arrested PLCs (Fig 2C-D). PLCs have prematurely condensed chromatin in G2-phase because MCPH1 deficiency results in inappropriate CDK1 activation in G2 (Alderton et al., 2006; Arroyo et al., 2017). That ICRF-193 treatment induced decondensation is consistent with efficient activation of the decatenation checkpoint, which activates the ATM/ATR pathway and thereby inhibits CDK1 activity. In HeLa H2B-Red1 cells depleted of MCPH1, PLCs were visualized from the first frame of the live-cell movies (7hr after release from the G1/S-phase thymidine block). Condensation in PLCs was progressively abolished during the incubation with ICRF-193. Decondensation typically occurred over a period of 386 (±126) minutes, after which PLCs lacked any sign of condensation (Figure CIII-2C and D, video CIII-3). However, when caffeine was added simultaneously with ICRF-193, condensation persisted in the PLCs for much longer (734 ±235 minutes), and many cells remained with condensed chromatin at the end of the movie (>1000 minutes) (Figure CIII-2C and D, video CIII-4). These data are also in agreement with the PLCs dynamic observed in lymphoblast patient cells (figure CIII-1B and C). Taken together these results clearly indicate that PLCs progressively reverse their condensation state while arrested in G2 by decatenation checkpoint activation. Strikingly, decondensation is prevented by caffeine, presumably because the ATR/ATM signaling pathways initiated by the decatenation checkpoint are required for CDK1 inhibition, and thus decondensation, in PLCs.

PLCs have prematurely condensed chromatin in G2-phase because MCPH1 deficiency results in inappropriate CDK1 activation in G2 (Alderton et al., 2006; Gruber et al., 2011). Therefore, chromosome decondensation induced by ICRF-193 treatment in MCPH1 depleted cells would be explained by efficient activation of the decatenation checkpoint, which activates the ATR/ATM pathway and thereby blocks CDK1 activation. This hypothetical scenario would also explain why decondensation will be prevented when the ATR/ATM pathway is inhibited by caffeine. To verify our hypothesis, we compared the protein levels of total and phospho-Y15 (inactive) CDK1 in control and patient samples after prolonged incubation with either ICRF-193 alone or combined with caffeine (figure CIII-2 F). After six hours of ICRF-193 treatment the levels of inactive CDK1 increased in both control and patient cells, while simultaneous adding of caffeine reduced those levels enormously as expected, especially in control samples. In agreement with our assumption, the differences in the amount of inactive CDK1correlated inversely with the condensation dynamic described for the patient cells in each case. On the other hand, the levels of total CDK1 remained quite similar in all cases. Of interest, the levels of phospho-Y15 CDK1 were already increased after three hours of ICRF-193 incubation in patient

cells, while in control cells it still remained reduced as in untreated cells (figure CIII-2 F). However, a robust G2 arrest was equally observed in both control and patient cells (see figure CIII-1A), which indicates that ICRF-193-induced checkpoint response occurs despite substantial CDK1 activity, in line with previous reports (Deming et al. 2001). Moreover, our results could indicate that MCPH1 deficiency favored amplification of the inactive CDK1 signal in response to decatenation checkpoint activation. In line with this, after six hours of incubation with ICRF-193 and caffeine the phosphoY15-CDK1 signal was still detectable in patient but not in control cells.

ICRF-193-induced G2 arrest and PLC decondensation are not dependent on the P38 MAPK pathway in MCPH1 deficient cells.

MCPH1 deficient cells condense their chromosomes in G2 due to premature CDK1 activation to a level that is enough to start condensation but is insufficiently high to induce entry into mitosis. Indeed, MCPH1 deficient cells perform Nuclear Envelop Breakdown (NEBD) and enter prometaphase with the same timing as controls cells (Arroyo et al., 2017; Thesis chapter II). The lack of decatenation checkpoint bypass in the presence of ICRF-193 and caffeine suggest that CDK1 activity does not reach the threshold needed for mitosis, and this indicates that MCPH1 might act between ATM/ATR and CDK1. Another explanation is the possibility that MCPH1 deficiency and Topo II inhibition synergize in a more complex manner, perhaps leading to the activation of another G2 checkpoint pathway. One such pathway is the antephase checkpoint. We considered this in part because PLCs decondense their chromosomes while arrested in G2 in the presence of ICRF-193, and this phenotype resembles the activity of the G2/M "antephase" checkpoint. This checkpoint acts at the end of G2 in response to a variety of cellular stresses including hypotonic shock, UV-irradiation and chromatin topological perturbations, and triggers chromatin decondensation in early prophase cells (Rieder and Cole, 2000; Mikhailov et al., 2004). It is distinct from DNA damage response checkpoints as it does not require ATM or ATR; however, it is critically dependent P38 MAPK signaling (Matsusaka and Pines, 2004; Mikhailov et al., 2004). These facts, together with the caffeine-insensitive nature of the G2 arrest triggered by ICRF-193 in MCPH1 deficient cells, prompted us to examine whether the persistent G2 arrest could be explained by activation of P38 MAPK signaling. In order to test this, we inhibited P38 MAPK with the well-characterized inhibitor SB202190 (Lee et al., 2010) in lymphoblastoid cells from control and a MCPH1 patient, and determined whether checkpoint adaptation is restored. FACS analyses revealed that SB202190 did not abolish the G2 arrest imposed by ICRF-193 in either control or MCPH1 deficient cells (figure CIII-3A and B). Therefore, the G2 arrest is independent of P38 kinase signaling. To corroborate the results in patient cells, experiments were next performed in HeLa-H2B-Red1

cells depleted of MCPH1 using siRNAs. Cells synchronized at the G1/S transition were released and 7 hours later ICRF-193 was added, followed by addition of SB202190 2 hour later (figure CIII-3C). Our results showed that neither control nor MCPH1-siRNA treated cells performed NEBD before the end of the movie (figure CIII-3D and E). Therefore, like in the MCPH1 patient cells, the HeLa cells depleted of MCPH1 did not arrest in G2 dependent on the P38 kinase antephase checkpoint. Importantly, SB202190 alone did not affect the progression through G2 and the rate of mitosis entrance in the lymphobast and HeLa cell models investigated (figure CIII-3A-B, 3F), in accordance with previous reports (Kukkone-Macchi et al., 2010; Lee et al., 2010). Taken together, our results show that P38 MAPK is unlikely to trigger G2 arrest upon ICRF-193 treatment, in agreement with previous studies (Damelin and Bestor, 2007) and in contrast with those previously reported by Mikhailov et al., (2004).

Interestingly, the frequency of PLCs was decreased in MCPH1 patient cells after 7 hours of incubation with ICRF-193 and SB202190 (figure CIII-3B). In MCPH1 depleted HeLa cells condensation was progressively reversed in PLCs in the presence of ICRF-193 and SB202190 (figure CIII-3E), but this process took longer (564 ±133 minutes) than when cells were incubated with ICRF-193 alone (386 ±126) (figure CIII-4F). Therefore, PLC decondensation is delayed but not abolished in the absence of P38 MAPK activity, which suggests that P38 MAPK is not a key regulator of the signaling pathway that triggers chromosome decondensation in MCPH1 depleted cells while arrested at G2. Together the data provide evidence that P38 kinase signaling is not involved in ICRF-193-induced G2 arrest, neither in control nor in MCPH1 deficient cells.

G2 arrest after DNA damage induced by Topo II poisons requires ATR/ATM in MCPH1 deficient cells

ICRF-193 is a catalytic inhibitor of Topo II that blocks the strand passage reaction without causing DNA breakage. In contrast, there are chemicals known as Topo II poisons that inhibit the strand passage reaction by trapping the covalent enzyme-DNA complex in such a way as to generate massive DNA breakage in cells (Damelin and Bestor, 2007). In this way, Topo II poisons arrest cells in G2 exclusively due to DNA damage checkpoint activation that requires ATM/ATR (Clarke et al., 2006; Luo et al., 2009; Bower et al., 2010B). Studies have revealed that the canonical ATM-dependent G2 checkpoint that responds to DNA damage induced by irradiation functions normally in cells lacking *MCPH1* (Gavvovidis et al., 2010; Brown et al., 2010; Gruber et al., 2011; Zhou et al., 2013). Therefore, we sought to determine if MCPH1 deficient cells respond like control cells when treated with Topo II poisons. That is, whether unlike the caffeine-insensitive G2 arrest triggered by ICRF-193, *MCPH1* depleted cells would behave like control cells after incubation with Topo II poisons. To test this, we examined cell

cycle dynamics in control and MCPH1 patient cells incubated with etoposide (alone or combined with caffeine), an extensively studied Topo II poison (Loike et al., 1976) that is used widely as a cancer therapeutic. Nocodazole was included to arrest cells in mitosis. As shown in Figure CIII-4A, both control and patient cells do not enter into mitosis in the presence of etoposide; however, the G2 arrest is efficiently bypassed by caffeine.

Similar results were obtained after live-cell analyses of HeLa H2B-Red1 cells depleted of MCPH1 function by siRNAs (Figure CIII-4C; videos CIII-7-10). Cells synchronized at the G1/S transition were released, and etoposide was added 7 hours later. Caffeine – or an equal volume of medium – was added 1 hour after the etoposide. In this case, caffeine induced rapid entrance into mitosis in control and MCPH1-depleted etoposide-treated cells (figure CIII-4C and D). Without caffeine, etoposide-treated cells remained arrested in G2. Therefore, the DNA damage response induced by a Topo II poison was efficiently activated in *MCPH1* deficient cells and moreover this G2 checkpoint arrest was entirely reliant on the ATM/ATR kinases that are inhibited by caffeine. Consistent with efficient G2 checkpoint activation that inhibits CDK1 activity in MCPH1 depleted cells, PLCs progressively decondensed their chromatin during the G2 arrest triggered by etoposide (figure CIII-4B and E). When monitored by live-cell imaging, PLCs required 606 (±193) minutes to completely decondense (video CIII-9), which is a similar timing to the observed after simultaneous incubation with ICRF-193 and SB202190 (figure CIII-4F).

In order to verify that catalytic inhibition of Topo II with ICRF-193, in contrast to etoposide, did not induce an ATM-based DNA damage response in MCPH1 patient cells we performed immunofluorescence analyses using a well-recognized DNA damage marker, γH2AX, on cells treated with either ICRF-193 or etoposide. As showed in figure CIII-5A, both control and MCPH1 patient cells exhibited an increase in γH2AX positive cells after 3h of etoposide treatment; however, 3h of incubation with ICRF-193 induced no detectable γH2AX staining above background levels. Similar results were also observed in HeLa cells depleted of MCPH1 function by siRNAs (figure CIII-5B). The number of γH2AX foci per cell increased ten-fold in etoposide-treated cells compared with either untreated or ICRF-193-treated cells in both control and patient cells (figure CIII-5C). These results indicate that ICRF-193 does not induce DSBs formation neither in control cells, in agreement with previous reports (Bower et al., 2010b, Luo et al., 2009), nor in cells lacking MCPH1 function. Interestingly, as a reduced number of patient cells exhibited an abnormally higher number of γH2AX foci after ICRF-193 treatment (figure CIII-5C), we next analyzed if this was influenced by the occurrence of prolonged chromosome condensation. Therefore, we compared the number of foci observed in PLCs and non-PLCs from patient cells after the indicated treatments, and we confirmed that the increased number of

γH2AX foci induced by ICRF-193 occurs mostly in PLCs (figure CIII-5D). A similar trend was also observed after etoposide incubation. Further analyses are required to better understand how the condensation state of the nuclei influences the accumulation of γH2AX foci after the indicated treatments.

Together, our results demonstrate that the checkpoint response to DNA damage induced by etoposide is caffeine-sensitive in MCPH1 depleted cells. Thus, while MCPH1 function is essential for G2 checkpoint adaptation in the presence of ICRF-193, it is dispensable for bypass of the ATM-dependent G2 checkpoint that operates in response to etoposide-induced DNA damage. Our results are in accordance with previous irradiation analyses in patient cells (Gavvovidis et al., 2010), and with other studies that reported a canonical ATM-based checkpoint response in MCPH1 depleted cells (Brown et al., 2010; Gruber et al., 2011; Zhou et al., 2013). Importantly, the opposite results observed here with ICRF-193 and etoposide, both specific Topo II inhibitors, provide support to the notion that the G2 DNA damage checkpoint and the decatenation checkpoint are distinct signaling pathways (Damelin and Bestor, 2007; Bower et al., 2010b).

CHK1 is required for decatenation checkpoint G2 arrest and functions downstream of MCPH1 during checkpoint adaptation

There is a substantial body of published evidence, including this study, demonstrating that the G2 checkpoints activated by Topo II poisons versus Topo II catalytic inhibitors are distinct signaling pathways. Though both involve ATM/ATR kinases, other components of these checkpoint mechanisms are unique to each pathway. To gain further insight into the G2 checkpoint that responds to the catalytic Topo II inhibitor, ICRF-193, we examined the potential role of CHK1 kinase. CHK1 is a key element of the ATR signaling pathway but there is no consensus about its contribution at the decatenation checkpoint (Deming et al., 2001; Robinson et al., 2007). However, previous studies have reported that MCPH1 regulates centrosomal CHK1 function during unperturbed cell cycle progression (Tibelius et al., 2009). Interestingly, such interplay was also observed during activation of the DNA damage response, with MCPH1 function being critical to restrict the levels of active CHK1 (Antonczak et al., 2015). Considering these molecular links between MCPH1 and CHK1, we examined if active CHK1 is required to sustain the ICRF-193 mediated G2 arrest in control and MCPH1 patient cells. To do that we incubated lymphoblastoid cells with UCN-01, a well-characterized CHK1 inhibitor (Graves et al., 2000), alone or in combination with ICRF-193 during 4h and 7h treatments in the presence of nocodazole. We determined the rate of mitotic accumulation by FACS analysis (figure CIII-6A). This revealed that CHK1 inhibition bypasses the G2 arrest imposed by ICRF-193 in both control and MCPH1 patient cells. Therefore, CHK1 is required for the G2

decatenation checkpoint induced by Topo II catalytic inhibition. When we analyzed chromosome structure in cells treated with ICRF-193 and UCN-01 we observed a high frequency of mitotic cells with uncondensed and disorganized chromosomes (Figure CIII-6B). These alterations, observed to an equal degree in control and MCPH1 patient cells, are the expected outcome after bypass of the decatenation checkpoint and progression into mitosis without Topo II function (Bower et al., 2010b; Gimenez-Abian et al., 2000).

We next confirmed these results by live-cell microscopy in HeLa H2B-Red1 cells depleted of MCPH1 function by siRNAs. Cells synchronized at the G1/S transition were released and ICRF-193 was added 7h after release while UCN-01 was added after a further hour. As shown in figure CIII-6C, UCN-01 addition induced a massive entrance into mitosis in both control and MCPH1-depleted cells treated with ICRF-193. Further progression through mitosis was similar in both control and MCPH1-siRNA treated cells. In all cases cells completed mitosis aberrantly as chromosome segregation could not occur in the absence of Topo II activity (Figure CIII-6D; videos CIII-11-12). By contrast, cells incubated only with UCN-01 finished mitosis successfully (figure CIII-6E). Since CHK1 activity is essential for the checkpoint response we also investigated if the levels of CHK1 phosphorylated at Ser345, the main hallmark of CHK1 activation, correlates with the cell cycle dynamics observed in our study (figure CIII-4F). Interestingly, an increase in the levels of phospho-CHK1 was observed after prolonged treatment with ICRF-1 in both control and MCPH1 patient cells. However, those levels remained elevated in control cells that bypassed the checkpoint arrest after caffeine addition, while in patient cells, which are unable to override the arrest in the same conditions, the levels of phospho-CHK1 were strikingly diminished. It must be also noted that in our experimental conditions caffeine alone did not reduce as expected the levels of phospho-CHK1. Despite this apparent contradictory observation, which demands further investigations, as overall our results clearly indicate that the contribution of CHK1 to the decatenation checkpoint occurs through a mechanism that does not involve phosphorylation at Ser345. A similar scenario has been previously described in HeLa cells, where a CHK1 dependent mechanism that responds to DNA synthesis inhibition and does not involve phosphorylation of CHK1 at Ser345 exists (Rodriguez-Bravo et al., 2006).

From our results several conclusions can be drawn. First, CHK1 inhibition abrogates the G2 arrest imposed by ICRF-193 in control cells, a clear indication that CHK1 activity is required for the G2 decatenation checkpoint. In line with this, previous studies showed that DT40 CHK1 -/- cells have a defective decatenation checkpoint (Robinson et al., 2007). Secondly, the levels of CHK1 phosphorylated at Ser345 increased after ICRF-193 treatment, unlike previous reports (Deming et al., 2001; Bower et al., 2010); however, these levels remained still elevated after

abrogation of the checkpoint arrest. Therefore, the exact role of CHK1 in this checkpoint remains to be elucidated as it does not depend apparently on its phosphorylation at Ser345, which is considered a hallmark for CHK1 activation (Liu et al., 2000; Zhao et al., 2001). Finally, the defect in decatenation checkpoint adaptation that prevented cells lacking MCPH1 from entering mitosis (either spontaneously or in the presence of caffeine) was rescued by CHK1 inhibition. MCPH1 is likely to act upstream of CHK1 – and downstream of ATR - to promote recovery from decatenation checkpoint arrest.

Previous studies revealed a delayed release from cell cycle arrest after irradiation in cells that lack *MCPH1* function (Gavvovidis et al., 2010; Brown et al., 2010B). Thus, it was proposed that *MCPH1* function is critical for timely inactivation of the CHK1 signal that arises upon the DNA damage response. Notably, in those studies mitotic entry was analyzed after the DNA damage was repaired. Here, we have however investigated the mechanism of cell adaptation to the decatenation checkpoint, that is, the capacity to bypass the checkpoint response despite the persistence of the molecular event (Topo II catalytic inhibition) that triggered the checkpoint (Coats et al., 1999; Gimenez-Abian et al., 2000). These analyses are of importance to better understand the genetic requirements of cells to allow adaptation to G2 checkpoints. For example, PLK1 and TLK1 are required to bypass the DNA damage checkpoint (Van Vugt et al., 2004; Bruinsma et al., 2016). Our current data highlight that G2 cells challenged by DNA catenation present different requirements for mitotic entry compared to either unperturbed cells or cells damaged by UV or IR. Thus, while MCPH1 function seems dispensable for the onset of mitosis in the last two scenarios, it is essential for cell adaptation to the decatenation checkpoint.

ACKNOWLEDGMENTS

This work was supported by Junta de Andalucía (Funding program 'Ayudas a grupos de investigación', reference BIO 220). M. Arroyo PhD is granted by University of Jaén (Spain), and was provided with travelling grants to perform short-term stays at the University of Minnesota by EMBO (and "Escuela de Doctorado" (University of Jaén, Spain), respectively. The authors express their gratitude to H. Neitzel (Berlin, Germany) for providing the lymphoblast cell lines used in this study, G. Marques (University of Minnesota, US) for technical assistance and J. F. Gimenez-Abián for helpful discussions. Research at laboratory of R. Kuriyama was financially supported by NSF (MCB1140033). Technical and human support provided by CICT of Universidad de Jaén (UJA, MINECO, Junta de Andalucía, FEDER) is gratefully acknowledged.

Author's contribution statement

J.A.M., D.J.C. and R.K. designed the experiments. M.A., I. G., and J.A.M. performed the experiments. M.A., A.S. and J.A.M. analyzed the results. J.A.M. and D.J.C. wrote the main manuscript text. All authors reviewed the manuscript.

Additional information

Competing financial interest statement: the corresponding author, on behalf of all authors of the paper, declares no competing financial interest.

REFERENCES

Alderton GK, Galbiati L, Griffith E, Surinya KH, Neitzel H, Jackson AP, et al. (2006). Regulation of mitotic entry by microcephalin and its overlap with ATR signalling. Nat Cell Biol. 8, 725-33.

Antonczak AK, Mullee LI, Wang Y, Comartin D, Inoue T, Pelletier L, Morrison CG. (2016). Opposing effects of pericentrin and microcephalin on the pericentriolar material regulate CHK1 ctivation in the DNA damage response. Oncogene. 2016 Apr 14;35(15):2003-10. doi: 10.1038/onc.2015.257.

Arroyo M, Trimborn M, Sánchez A, Hirano T, Neitzel H, Marchal JA. (2015). Chromosome structure deficiencies in MCPH1 syndrome. Chromosoma. 124, 491-501. doi: 10.1007/s00412-015-0512-2 (2015).

Arroyo M, Kuriyama R, Trimborn M, Keifenheim D, Cañuelo A, Sánchez A, Clarke DJ, Marchal JA. (2017). MCPH1, mutated in primary microcephaly, is required for efficient chromosome alignment during mitosis. Sci Rep. 2017 Oct 12;7(1):13019. doi:10.1038/s41598-017-12793-7.

Bower JJ, Zhou Y, Zhou T, Simpson DA, Arlander SJ, Paules RS, Cordeiro-Stone M, Kaufmann WK. (2010). Revised genetic requirements for the decatenation G2 checkpoint: the role of ATM. Cell Cycle. 2010 Apr 15;9(8):1617-28 (A)

Bower JJ, Karaca GF, Zhou Y, Simpson DA, Cordeiro-Stone M, Kaufmann WK. (2010). Topoisomerase IIalpha maintains genomic stability through decatenation G(2) checkpoint signaling. Oncogene. 2010 Aug 26;29(34):4787-99. doi:10.1038/onc.2010.232 (B)

Brown JA, Bourke E, Liptrot C, Dockery P, Morrison CG. (2010). MCPH1/BRIT1 limits ionizing radiation-induced centrosome amplification. Oncogene. 2010 Oct 7;29(40):5537-44. doi:10.1038/onc.2010.302.

Bruinsma W, van den Berg J, Aprelia M, Medema RH. Tousled-like kinase 2 regulates recovery from a DNA damage-induced G2 arrest. EMBO Rep. 2016 May;17(5):659-70. doi: 10.15252/embr.201540767.

Clarke DJ, Vas AC, Andrews CA, Díaz-Martínez LA, Giménez-Abián JF. Topoisomerase II checkpoints: universal mechanisms that regulate mitosis. Cell Cycle. 2006 Sep;5(17):1925-8.

Coats S, Whyte P, Fero ML, Lacy S, Chung G, Randel E, Firpo E, Roberts JM. A new pathway for mitogen-dependent cdk2 regulation uncovered in p27(Kip1)-deficient cells. Curr Biol. 1999 Feb 25;9(4):163-73.

Damelin M, Bestor TH. The decatenation checkpoint. Br J Cancer. 2007 Jan 29;96(2):201-5.

Deming PB, Cistulli CA, Zhao H, Graves PR, Piwnica-Worms H, Paules RS, Downes CS, Kaufmann WK. The human decatenation checkpoint. Proc Natl Acad Sci U S A. 2001 Oct 9;98(21):12044-9.

Deming PB, Flores KG, Downes CS, Paules RS, Kaufmann WK. ATR enforces the topoisomerase II-dependent G2 checkpoint through inhibition of Plk1 kinase. J Biol Chem. 2002 Sep 27;277(39):36832-8.

Downes CS, Clarke DJ, Mullinger AM, Giménez-Abián JF, Creighton AM, Johnson RT. A topoisomerase II-dependent G2 cycle checkpoint in mammalian cells/. Nature. 1994 Dec 1;372(6505):467-70.

Gavvovidis I, Pöhlmann C, Marchal JA, Stumm M, Yamashita D, Hirano T, Schindler D, Neitzel H, Trimborn M. MCPH1 patient cells exhibit delayed release from DNA damage-induced G2/M checkpoint arrest. Cell Cycle. 2010 Dec 15;9(24):4893-9.

Gavvovidis I, Rost I, Trimborn M, Kaiser FJ, Purps J, et al. (2012). A novel MCPH1 isoform complements the defective chromosome condensation of human MCPH1-deficient cells. PLoS One. 7, e40387. doi: 10.1371/journal.pone.0040387 (2012).

Giménez-Abián JF, Clarke DJ, Devlin J, Giménez-Abián MI, De la Torre C, Johnson RT, Mullinger AM, Downes CS. Premitotic chromosome individualization in mammalian cells depends on topoisomerase II activity. Chromosoma. 2000 Jul;109(4):235-44.

Graves PR, Yu L, Schwarz JK, Gales J, Sausville EA, O'Connor PM, Piwnica-Worms H. The Chk1 protein kinase and the Cdc25C regulatory pathways are targets of the anticancer agent UCN-01. J Biol Chem. 2000 Feb 25;275(8):5600-5.

Gruber R, Zhou Z, Sukchev M, Joerss T, Frappart PO, Wang ZQ. (2011). MCPH1 regulates the neuroprogenitor division mode by coupling the centrosomal cycle with mitotic entry through the Chk1-Cdc25 pathway. Nat Cell Biol. 13, 1325-34. doi: 10.1038/ncb2342.

Jeffers LJ, Coull BJ, Stack SJ, Morrison CG. (2008). Distinct BRCT domains in Mcph1/Brit1 mediate ionizing radiation-induced focus formation and centrosomal localization. Oncogene. 2008 Jan 3;27(1):139-44.

Kukkonen-Macchi A, Sicora O, Kaczynska K, Oetken-Lindholm C, Pouwels J, Laine L, Kallio MJ. (2011). Loss of p38gamma MAPK induces pleiotropic mitotic defects and massive cell death. J Cell Sci. 2011 Jan 15;124(Pt 2):216-27. doi:10.1242/jcs.068254

Lee K, Kenny AE, Rieder CL. P38 mitogen-activated protein kinase activity is required during mitosis for timely satisfaction of the mitotic checkpoint but not for the fidelity of chromosome segregation. (2010). Mol Biol Cell. 2010 Jul 1;21(13):2150-60. doi: 10.1091/mbc.E10-02-0125.

Liang Y, Gao H, Lin SY, Peng G, Huang X, Zhang P, Goss JA, Brunicardi FC, Multani AS, Chang S, Li K. (2010). BRIT1/MCPH1 is essential for mitotic and meiotic recombination DNA repair and maintaining genomic stability in mice. PLoS Genet. 2010 Jan 22;6(1):e1000826. doi: 10.1371/journal.pgen.1000826.

Liang Y, Gao H, Lin SY, Goss JA, Du C, Li K. (2015). Mcph1/Brit1 deficiency promotes genomic instability and tumor formation in a mouse model. Oncogene. 2015 Aug 13;34(33):4368-78. doi: 10.1038/onc.2014.367.

Liu Q, Guntuku S, Cui XS, Matsuoka, Cortez D, Tamai K, Luo G, Carattini-Rivera S, DeMayo F, Bradley A, Donehower LA, Elledge SJ. (2000). Chk1 is an essential kinase that is regulated by Atr and required for the G(2)/M DNA damage checkpoint. Genes Dev. 14:1448–1459.

Loike JD, Horwitz SB, Grollman AP. (1976). Effect of podophyllotoxin and VP-16 on microtubule assembly in vitro and nucleoside transport in HeLa cells.

Luo K, Yuan J, Chen J, Lou Z. (2009). Topoisomerase IIalpha controls the decatenation checkpoint. Nat Cell Biol. 2009 Feb;11(2):204-10. doi: 10.1038/ncb1828. Epub 2008 Dec 21.

Matsusaka T, Pines J. (2004). Chfr acts with the p38 stress kinases to block entry to mitosis in mammalian cells. J Cell Biol. 2004 Aug 16;166(4):507-16.

Mikhailov A, Shinohara M, Rieder CL. (2004). Topoisomerase II and histone deacetylase inhibitors delay the G2/M transition by triggering the p38 MAPK checkpoint pathway. J Cell Biol. 2004 Aug 16;166(4):517-26.

Neitzel H, Neumann LM, Schindler D, Wirges A, Tonnies H, Trimborn M, et al. (2002). Premature chromosome condensation in humans associated with microcephaly and mental retardation: a novel autosomal recessive condition. Am J Hum Genet. 70, 1015-22 (2002).

O'Driscoll, M. Jackson, A. P, Jeggo, P. A. (2006). Microcephalin: a causal link between impaired damage response signaling and microcephaly. Cell Cycle 5, 2339-44.

Paulovich AG, Toczyski DP, Hartwell LH. (1997). When checkpoints fail. Cell 88:315–321.

Peng G, Yim EK, Dai H, Jackson AP, Burgt Iv, Pan MR, Hu R, Li K, Lin SY. (2009). BRIT1/MCPH1 links chromatin remodelling to DNA damage response. Nat Cell Biol. 2009 Jul;11(7):865-72. doi: 10.1038/ncb1895.

Rai R, Dai H, Multani AS, Li K, Chin K, Gray J, Lahad JP, Liang J, Mills GB, Meric-Bernstam F, Lin SY. (2006). BRIT1 regulates early DNA damage response, chromosomal integrity, and cancer. Cancer Cell. 2006 Aug;10(2):145-57.

Rieder CL, Cole R. (2000). Microtubule disassembly delays the G2-M transition in vertebrates. Curr Biol. 2000 Sep 7;10(17):1067-70.

Robinson HM, Bratlie-Thoresen S, Brown R, Gillespie DA. (2007). Chk1 is required for G2/M checkpoint response induced by the catalytic topoisomerase II inhibitor ICRF-193. Cell Cycle. 2007 May 15;6(10):1265-7.

Serrano D, D'Amours D. (2016). Checkpoint adaptation: Keeping Cdc5 in the T-loop. Cell Cycle. 2016 Dec 16;15(24):3339-3340. doi: 10.1080/15384101.2016.1237769.

Trimborn, M. Bell, S. M. Felix, C. Rashid, Y. Jafri, H. et al., (2004). Mutations in microcephalin cause aberrant regulation of chromosome condensation. Am J Hum Genet 75, 261–266.

Trimborn, M. Schindler, D. Neitzel, H. and Hirano, T. (2006). Misregulated chromosome condensation in MCPH1 primary microcephaly is mediated by condensin II. Cell Cycle 5, 322-6.

Tibelius A, Marhold J, Zentgraf H, Heilig CE, Neitzel H, Ducommun B, et al. (2009). Microcephalin and pericentrin regulate mitotic entry via centrosome-associated Chk1. J Cell Biol. 185, 1149-57.

Van Vugt MA, Brás A, Medema RH. (2004). Polo-like kinase-1 controls recovery from a G2 DNA damage-induced arrest in mammalian cells. Mol Cell. 2004 Sep 10;15(5):799-811.

Wood JL, Singh N, Mer G, Chen J. (2007). MCPH1 functions in an H2AX-dependent but MDC1-independent pathway in response to DNA damage. J Biol Chem. 2007 Nov 30;282(48):35416-23.

Xu X, Lee J, Stern DF. (2004). Microcephalin is a DNA damage response protein involved in regulation of CHK1 and BRCA1. J Biol Chem. 2004 Aug 13;279(33):34091-4.

Zhao H, and Piwnica-Worms H. (2001). ATR-mediated checkpoint pathways regulate phosphorylation and activation of human Chk1. Mol. Cell. Biol. 21:4129–4139.

Zhou ZW, Tapias A, Bruhn C, Gruber R, Sukchev M, Wang ZQ. (2013). DNA damage response in microcephaly development of MCPH1 mouse model. DNA Repair (Amst). 2013 Aug;12(8):645-55. doi: 10.1016/j.dnarep.2013.04.017.

FIGURES LEGEND

Figure CIII-1: A) Frequency of histone H3PS10 positive cells in control and MCPH1 patient cells, determined by FACS, after incubation with nocodazole alone or combined with either ICRF-193, caffeine or both for the indicated time points. Data from at least two independent experiments are presented. B) Fraction of mitotic (M) and G2 cells, determined by FACS, in control and MCPH1 patient cells after either 3h or 6h of incubation with ICRF-193 alone or combined with nocodazole, a spindle poison that produce M arrest. For each sample, we determined in parallel the fraction of PLCs (prophase-like cells) by microscopic analyses of cytogenetic preparations. More than 500 cells were scored per sample. Data from at least two independent experiments are presented. C) Similar analyses as in B but adding caffeine to the cell cultures to bypass the ICRF-193-mediated G2 arrest. D) Representative images from cytogenetic preparations of control and MCPH1 patient cells treated simultaneously with ICRF-193 and caffeine. Arrowheads point to mitotic cells showing entangled and disorganized chromosomes, frequently observed in control cells. Arrows point to PLCs, frequently observed in MCPH1 patient cells. Scale bars, 5 μM.

Figure CIII-2: A) Description of the experimental procedure employed: HeLa cells stably expressing fluorescent histone H2B fused to Red1 were synchronized at the G1/S border by double thymidine block. MCPH1 depletion was achieved by transfection with siRNAs during the release from the first thymidine block. ICRF-193 was added 7h after release from the second thymidine block to coincide with the occurrence of PLCs during G2 in the siRNA treated cells. Caffeine (or an equal volume of medium) was added one hour after ICRF-193 treatment. Time-lapse images were collected using "Nikon Biostation IM Cell incubator" immediately after caffeine (or medium) adding. B) Cumulative frequency chart showing the timing (in minutes) of nuclear envelope breakdown (NEB) after the indicated treatments in control and MCPH1-siRNA treated cells monitored as explained in A. Time after caffeine (or mock) addition is shown. At least 50 cells were analyzed in each case. C) Box-plot showing the time (in minutes) that PLCs from MCPH1-siRNA treated cells required to completely decondense their chromosomes after adding ICRF-193 alone or combined with caffeine. The broken line indicates the mean value. 30 PLCs were monitored. Statistical comparisons for the mean and median data were done by T-student and Wilcoxon (W) tests respectively. ** $p<0.01$ D) Selected frames of representative cells from C showing the dynamics of PLCs in MCPH1-siRNA treated cells. Time after caffeine (or mock) addition is indicated in minutes. Note that the PLC phenotype, visible from the first frame, is progressively reduced in ICRF-193 treated cells. However, after incubation with ICRF-193 and caffeine PLCs remain visible up to the end of the recording. E) Cumulative frequency chart showing the timing (in minutes) of nuclear envelope breakdown (NEB) in control and MCPH1-siRNA treated HeLa cells after incubation with

caffeine or mock (untreated). Time after release from the second thymidine block is shown. Caffeine was added 200 minutes after the release. At least 50 cells were analyzed in each case. F) CDK1 and phosphoY15-CDK1 protein levels were visualized by inmunoblotting with anti-CDK1 and anti-phosphoY15-CDK1antibodys in control and patient samples after prolonged incubation with either ICRF-193 alone or combined with caffeine.

Figure CIII-3: A) Frequency of histone H3PS10 positive cells in control and MCPH1 patient cells, determined by FACS, after incubation with nocodazole alone or combined with either SB202190 or SB202190 and ICRF-193 for the indicated time points. B) Fraction of mitotic (M) and G2 cells, determined by FACS, in control and MCPH1 patient cells after either 4h or 7h of incubation with ICRF-193, SB20219 and nocodazole. For each sample, we determined in parallel the fraction of PLCs (prophase-like cells) by microscopic analyses of cytogenetic preparations. More than 500 cells were scored per sample. Data from two independent experiments are presented. C) Experimental procedure employed in HeLa H2B/Red1 cells to monitor cell cycle progression by live-cell miscroscopy after incubation with ICRF-193 and SB202190. D) Cumulative frequency chart showing the timing (in minutes) of nuclear envelope breakdown (NEB) for control and MCPH1 depleted HeLa cells treated as explained in C. Time after SB202190 (or mock) addition is shown. At least 50 cells were analyzed in each case. E) Selected frames showing the condensation dynamic of MCPH1-siRNA treated HeLa cells while incubated with ICRF-193 and SB202190. Note that the PLC phenotype of the cells, visible from the first frames, is progressively reduced. Time from SB202190 addition is indicated in minutes. F) Cumulative frequency chart showing the timing (in minutes) of nuclear envelope breakdown (NEB) in control and MCPH1-siRNA treated HeLa cells after single incubation with SB202190 or mock (untreated). Time after release from the second thymidine block is shown. SB202190 was added 300 minutes after the release. At least 50 cells were analyzed in each case.

Figure CIII-4: A) Fraction of mitotic cells, determined by FACS, in control and MCPH1 patient cells after 4h of incubation with nocodazole alone or combined with either etoposide or etoposide and caffeine. Data from at least two independent experiments are presented. B) Fraction of PLCs (prophase-like cells) in MCPH1 patient cells after prolonged incubation with etoposide. More than 500 cells were scored microscopically per sample. Data from two independent experiments are presented. C). Cumulative frequency chart showing the timing (in minutes) of nuclear envelope breakdown (NEB) for control and MCPH1depleted HeLa H2B-Red1 cells after the corresponding treatments. Time after caffeine (or mock) addition is shown. At least 50 cells were analyzed in each case. Cells were synchronized at G1/S border by double thymidine block and MCPH1 depletion was achieved by transfection with siRNAs during the release from the first thymidine block. Etoposide was added 7h after release from the second thymidine block, which is coincident with the occurrence of PLCs. Caffeine was added 1.5 h

later. Time-lapse phase contrast and fluorescent images were collected using "Nikon Biostation IM Cell incubator" immediately after adding caffeine. D) Selected frames showing the mitotic progression of representative control and MCPH1-depleted HeLa cells treated with etoposide and caffeine as indicated in A. Time from etoposide addition is indicated in minutes. Note that in both cases chromosome segregation is altered probably as consequence of the DNA damage induced. E) Selected frames showing the condensation dynamic of control and MCPH1-siRNA treated HeLa cells while arrested in G2 by etoposide. Note that the PLC phenotype of MCPH1 depleted cells, visible from the first frames, is progressively reduced. Time from etoposide addition is indicated in minutes. F) Box-plots showing the time (in minutes) that PLCs from MCPH1-siRNA treated cells incubated required to completely decondense their chromosomes after adding ICRF-193 alone, combined with SB202190 or after adding etoposide. The red line indicates the mean value. 30 PLCs were monitored. Statistical comparisons for the mean and median data were done by T-student and Wilcoxon (W) tests respectively. ** $p<0.01$; N.S. not significant.

Figure CIII-5: A) Representative images from immunofluorescence analyses using an antibody against γH2AX protein in proliferating lymphoblast from control and MCPH1 patient cells treated with either DMSO (untreated), ICRF-193 or etoposide. Cells were incubated for 3h before being processed. Scale bars, 5 μM. B) Same analyses as in A in HeLa cells either mock or MCPH1 depleted. Cells were synchronized at G1/S border by double thymidine block and MCPH1 depletion was achieved by transfection with siRNAs during the release from the first thymidine block. DMSO (untreated), ICRF-193 or etoposide were added 6h after release from the second thymidine block, and cells were processed 3h after. Scale bars, 10 μM. C) Box-plots showing the number of γH2AX foci per cell from A. At least 200 cells from two independent experiments were analyzed. The red line and the number in red indicate the mean value. D) Box-plots showing the number of γH2AX foci in PLCs and non-PLCs from the patient cells analyzed in C. At least 50 PLCs from two independent experiments were analyzed. The red line and the number in red indicate the mean value. Statistical comparisons for the mean and median data were done by T-student and Wilcoxon (W) tests respectively. **$p<0.01$; N.S. not significant.

Figure CIII-6: A) Frequency of histone H3PS10 positive cells in control and MCPH1 patient cells, determined by FACS, after incubation with either nocodazole alone or combined with UCN-01 or UCN-01 and ICRF-193 for the indicated time points. Data from at least two independent experiments are presented. B) Representative images from cytogenetic preparations of control and MCPH1 patient cells treated simultaneously with ICRF-193 and UCN-01. Arrows point to mitotic cells showing entangled and disorganized chromosomes, typical of cells treated with Topo II inhibitors. Scale bars, 5 μM. C) Cumulative frequency chart showing the

timing (in minutes) of nuclear envelope breakdown (NEB) in control and MCPH1 depleted HeLa H2B-Red1 cells after the indicated treatments. Time from UCN-01 addition is shown. At least 50 cells were analyzed in each case. Cells were synchronized at G1/S border by double thymidine block. MCPH1 depletion was achieved by transfection with siRNAs during the release from the first thymidine block. ICRF-193 was added 7h after release from the second thymidine block, which corresponds in time with the occurrence of PLCs. UCN-01 was added 2 h later. Time-lapse phase contrast and fluorescent images were collected using "Nikon Biostation IM Cell incubator" immediately after adding UCN-01. D) Selected frames showing the mitotic progression of representative control and MCPH1-depleted HeLa cells treated with UCN-01 and ICRF-193. Time from UCN-01 addition is indicated in minutes. Note that cells end mitosis aberrantly as chromosome segregation is prevented. E) Selected frames showing the mitotic progression of representative control and MCPH1-depleted HeLa cells treated only with UCN-01. Time from UCN-01 addition is indicated in minutes. In this case cells progress normally through mitosis. F) PhosphoS345-CHK1 protein levels were visualized by inmunoblotting with anti- phosphoS345-CHK1 antibody in control and patient samples after prolonged incubation with either ICRF-193 alone or combined with caffeine.

VIDEOS LEGEND

Video CIII-1: synchronized HeLa H2B-Red1 control cells were incubated with ICRF-193 and medium (mock) at 7 and 8 hours respectively after release from the second thymidine block. Time from mock adding (in minutes) is indicated.

Video CIII-2: synchronized HeLa H2B-Red1 control cells were incubated with ICRF-193 and caffeine at 7 and 8 hours respectively after release from the second thymidine block. Time from caffeine adding (in minutes) is indicated.

Video CIII-3: synchronized HeLa H2B-Red1 MCPH1-siRNA treated cells were incubated with ICRF-193 and medium (mock) at 7 and 8 hours respectively after release from the second thymidine block. Time from mock adding (in minutes) is indicated.

Video CIII-4: synchronized HeLa H2B-Red1 MCPH1-siRNA treated cells were incubated with ICRF-193 and caffeine at 7 and 8 hours respectively after release from the second thymidine block. Time from caffeine adding (in minutes) is indicated.

Video CIII-5: synchronized HeLa H2B-Red1 control cells were incubated with ICRF-193 and SB202190 at 7 and 9 hours respectively after release from the second thymidine block. Time from SB202190 adding (in minutes) is indicated.

Video CIII-6: synchronized HeLa H2B-Red1 MCPH1-siRNA treated cells were incubated with ICRF-193 and SB202190 at 7 and 9 hours respectively after release from the second thymidine block. Time from SB202190 adding (in minutes) is indicated.

Video CIII-7: synchronized HeLa H2B-Red1 control cells were incubated with etoposide and medium (mock) at 7 and 8,5 hours respectively after release from the second thymidine block. Time from mock adding (in minutes) is indicated.

Video CIII-8: synchronized HeLa H2B-Red1 control cells were incubated with etoposide and caffeine at 7 and 8,5 hours respectively after release from the second thymidine block. Time from mock adding (in minutes) is indicated.

Video CIII-9: synchronized HeLa H2B-Red1 MCPH1-siRNA treated cells were incubated with etoposide and medium (mock) at 7 and 8,5 hours respectively after release from the second thymidine block. Time from mock adding (in minutes) is indicated.

Video CIII-10: synchronized HeLa H2B-Red1 MCPH1-siRNA treated cells were incubated with etoposide and caffeine at 7 and 8,5 hours respectively after release from the second thymidine block. Time from mock adding (in minutes) is indicated.

Video CIII-11: synchronized HeLa H2B-Red1 control cells were incubated with ICRF-193 and UCN-01 at 7 and 9 hours respectively after release from the second thymidine block. Time from mock adding (in minutes) is indicated.

Video CIII-12: synchronized HeLa H2B-Red1 MCPH1-siRNA treated cells were incubated with ICRF-193 and UCN-01 at 7 and 9 hours respectively after release from the second thymidine block. Time from mock adding (in minutes) is indicated.

Figure CIII-1:

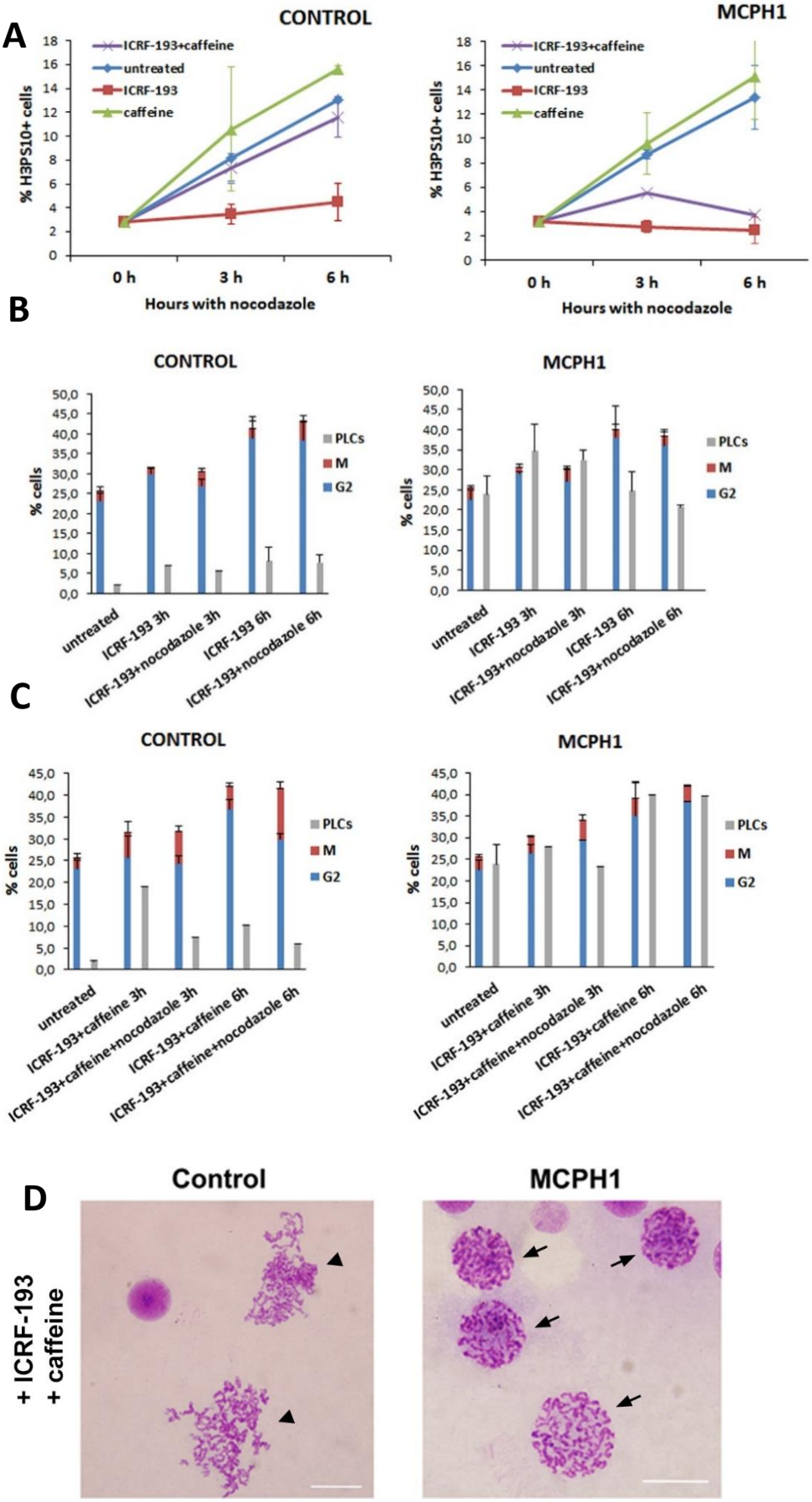

Figure CIII-2:

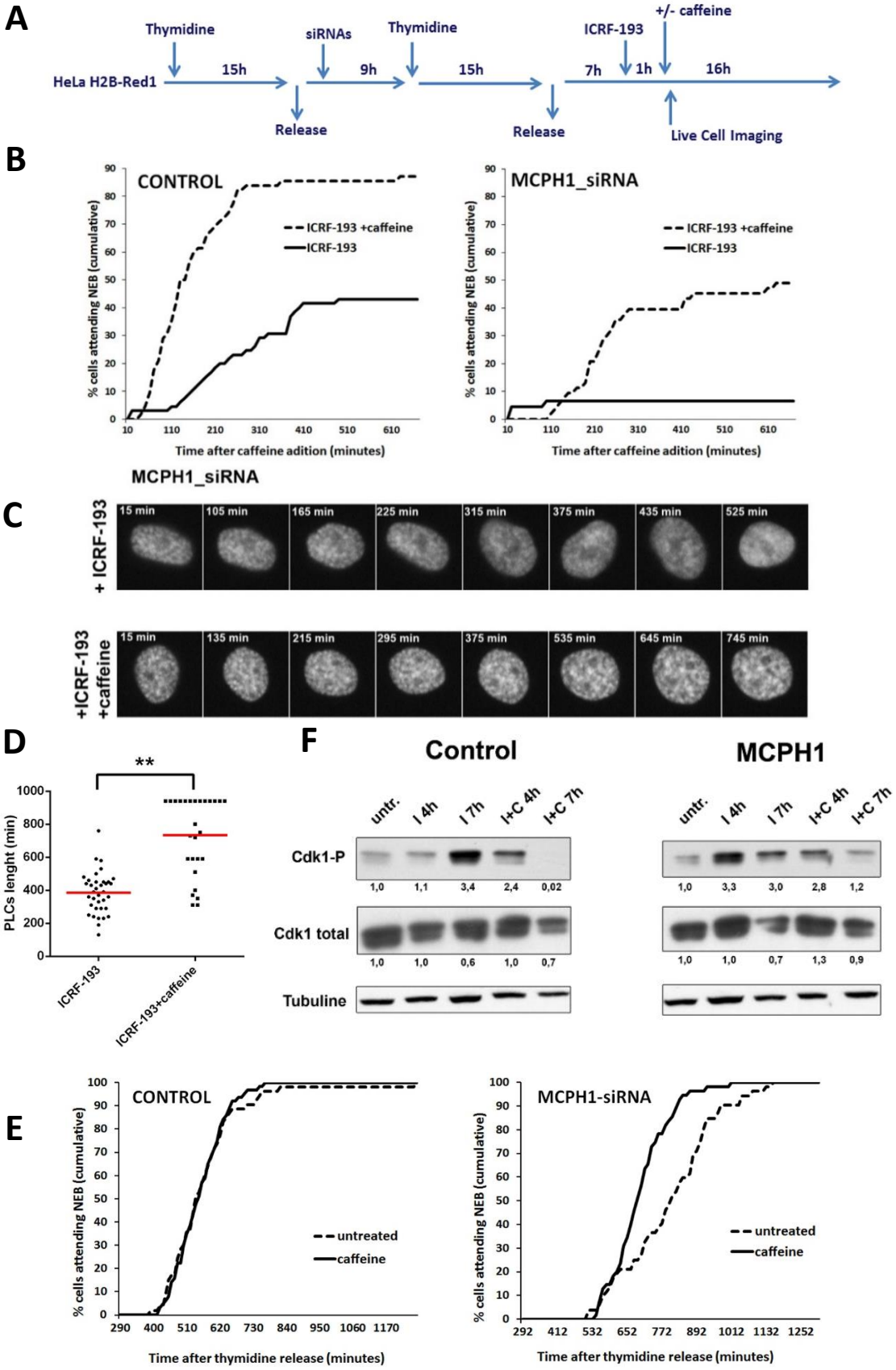

Figure CIII-3:

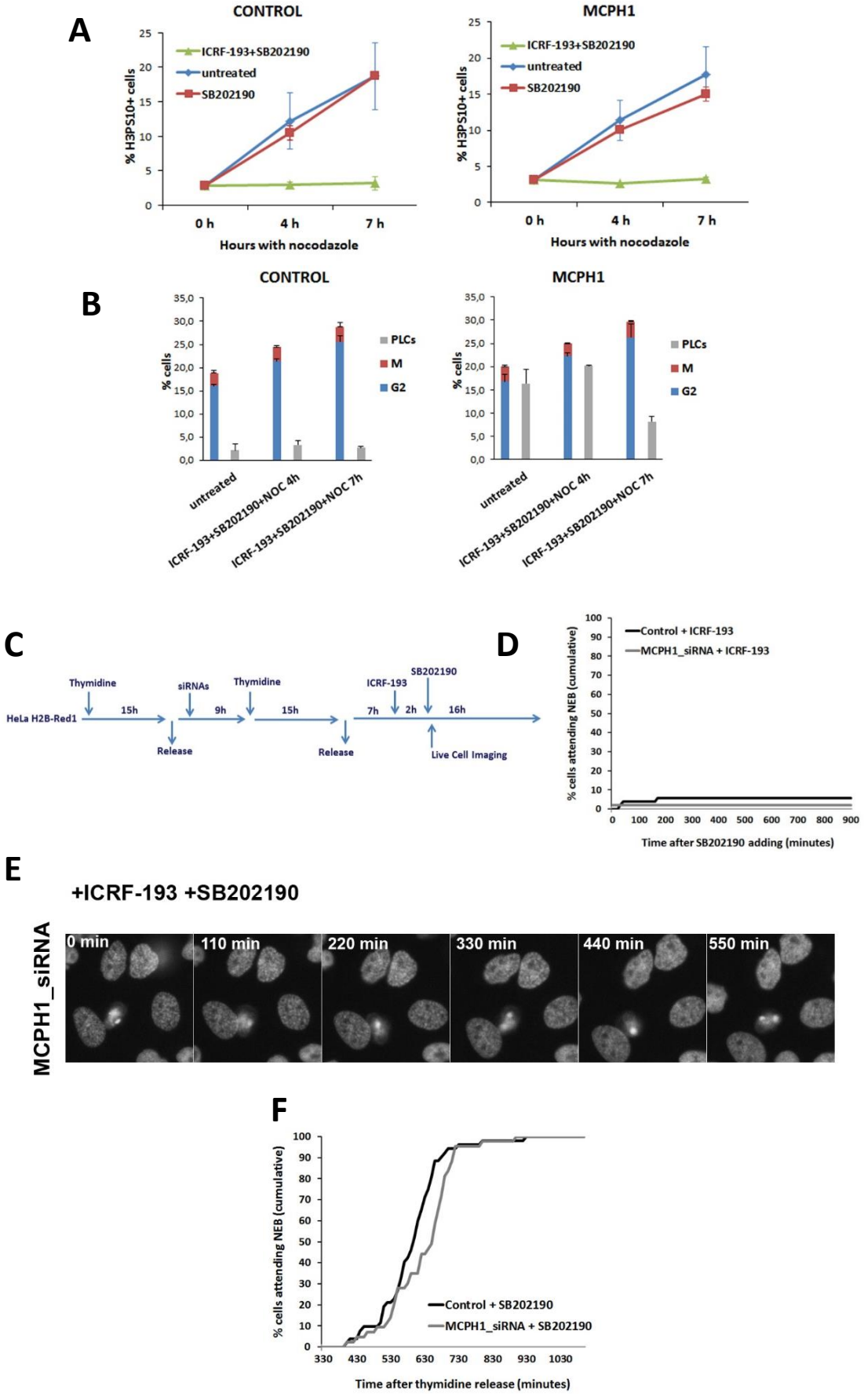

Figure CIII-4:

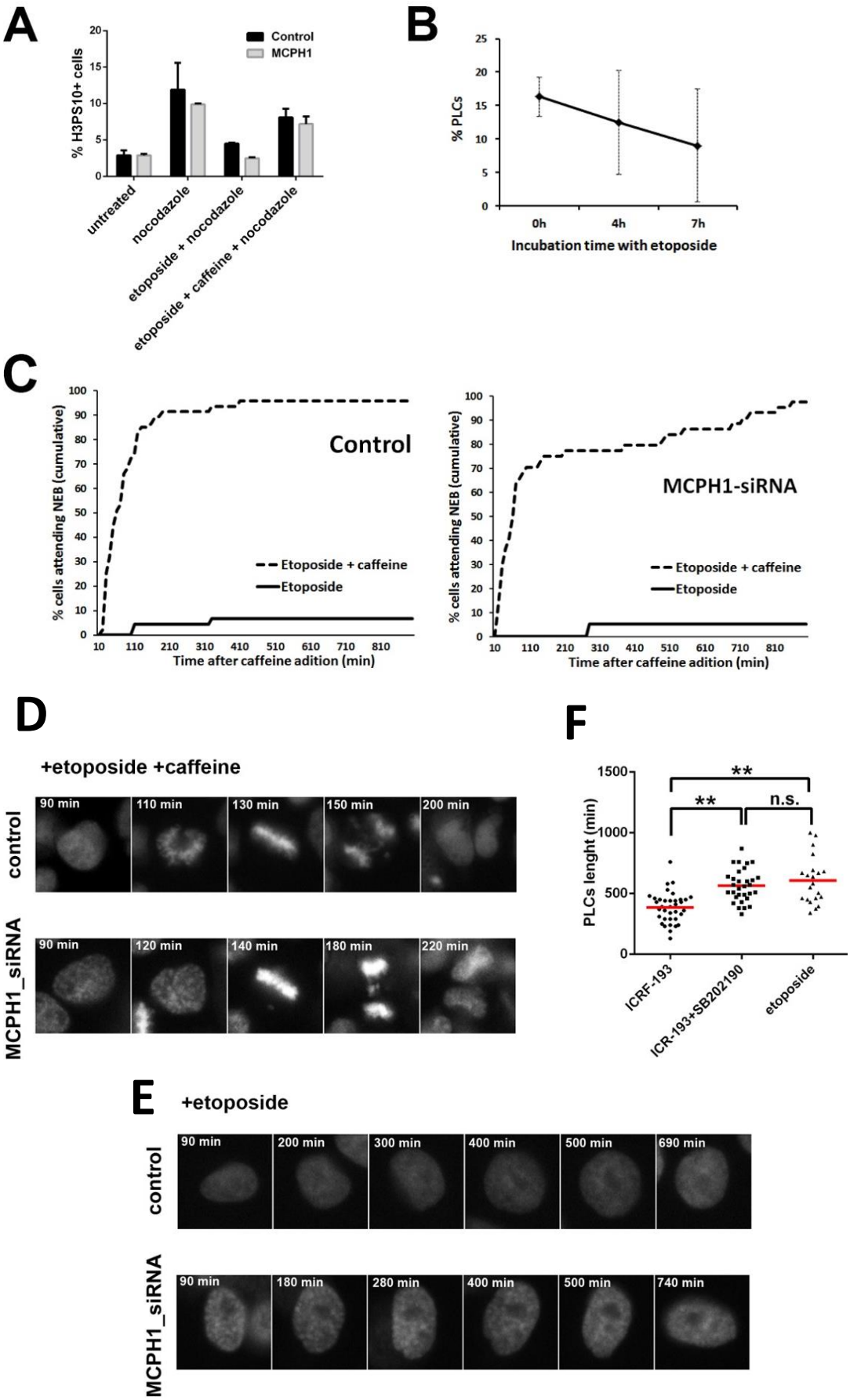

Figure CIII-5:

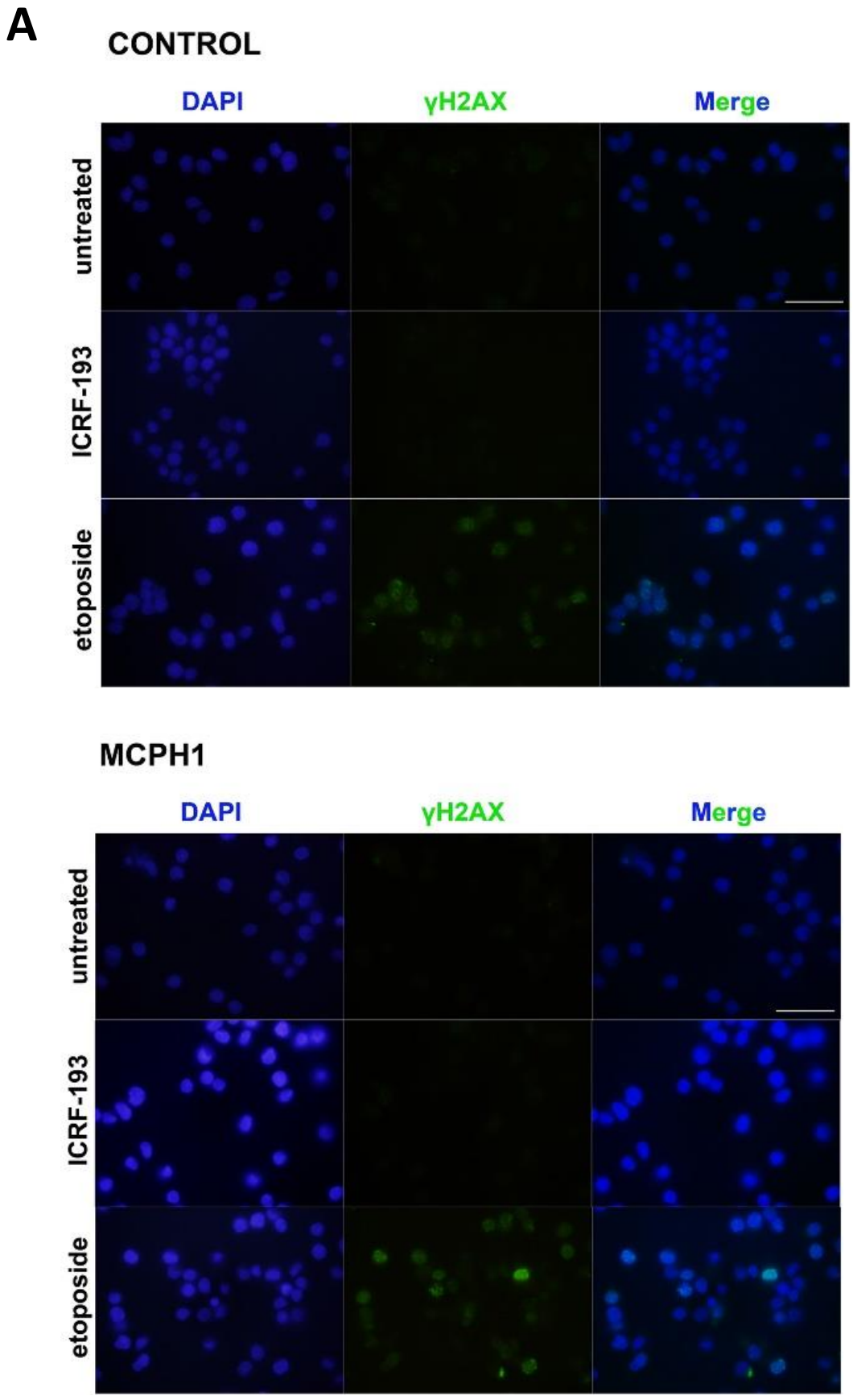

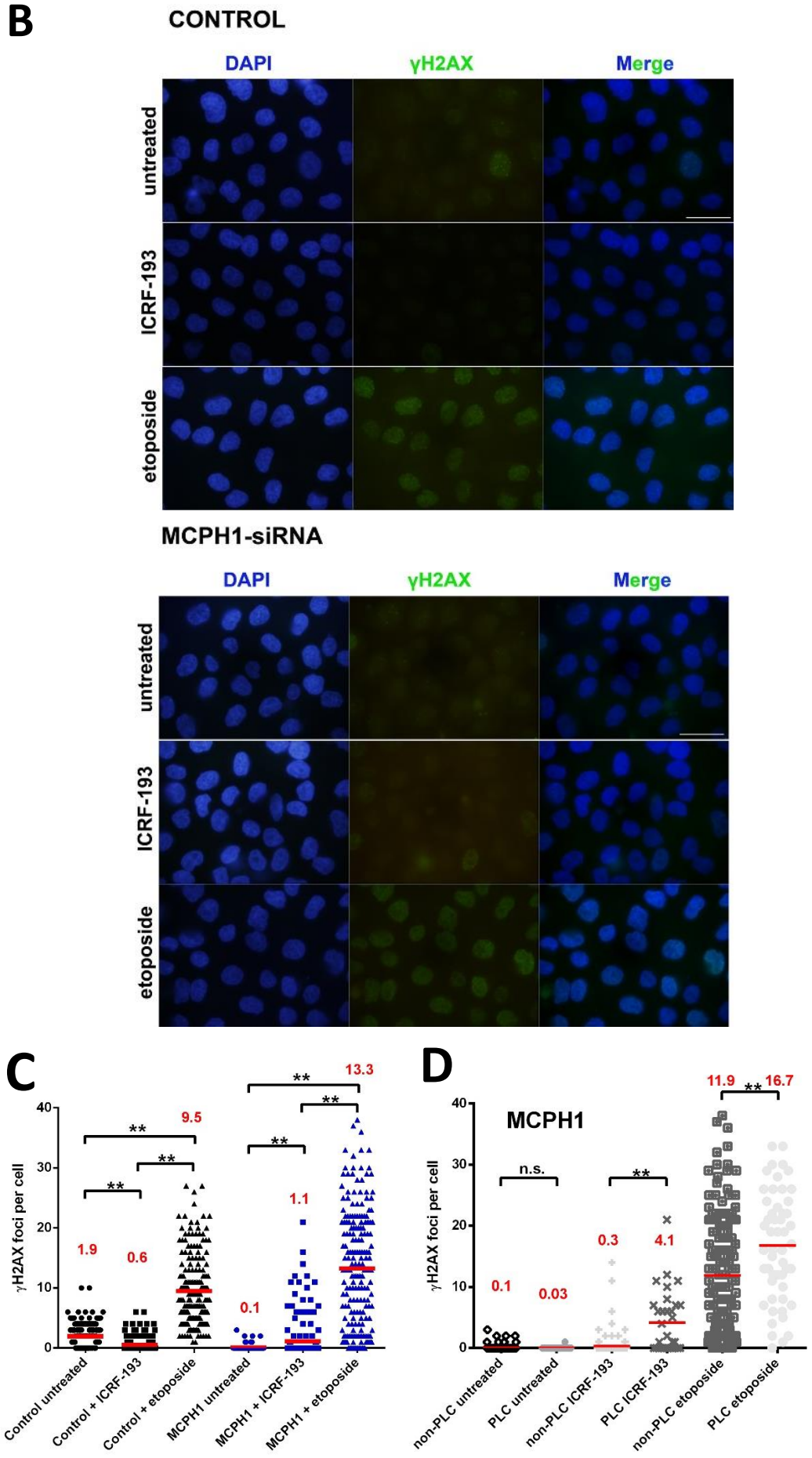
B
CONTROL
DAPI
γH2AX
Merge
untreated
ICRF-193
etoposide
MCPH1-siRNA
DAPI
γH2AX
Merge
untreated
ICRF-193
etoposide
C
γH2AX foci per cell
Control untreated
Control + ICRF-193
Control + etoposide
MCPH1 untreated
MCPH1 + ICRF-193
MCPH1 + etoposide
1.9
0.6
9.5
0.1
1.1
13.3
D
MCPH1
γH2AX foci per cell
n.s.
0.1
0.03
0.3
4.1
11.9
16.7
non-PLC untreated
PLC untreated
non-PLC ICRF-193
PLC ICRF-193
non-PLC etoposide
PLC etoposide

Figure CIII-6:

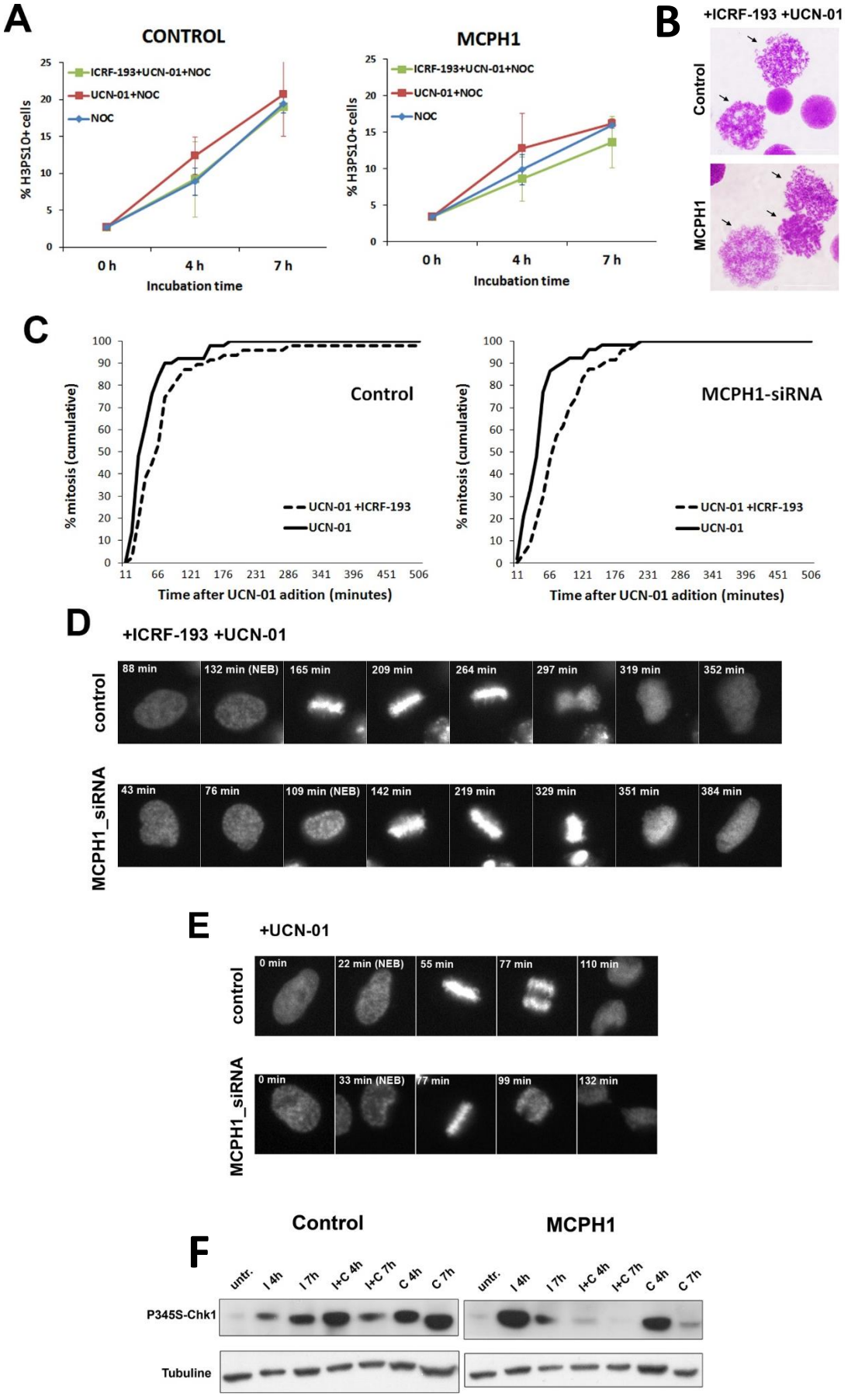

CHAPTER IV

CHAPTER IV

TITLE: PLK1 acts downstream of MCPH1 in a single pathway that confers adaptation to the G2 decatenation checkpoint

M. Arroyo[1], R. Kuriyama[2], A. Cañuelo[1], A. Sánchez[1], D. J. Clarke[2], J.A. Marchal[1*]

(1) Departamento de Biología Experimental, Universidad de Jaén

(2) Department of Genetics, Cell Biology and Development, University of Minnesota

*** Corresponding author:** Dr. Juan Alberto Marchal Ortega

Departamento de Biología Experimental

Facultad de Ciencias Experimentales

Universidad de Jaén

Paraje Las Lagunillas s/n; Room B3-304

E-23071 Jaén (Spain)

Telephone: 0034-953213361; Fax: 0034-953211875

e-mail: jamaor@ujaen.es

ABSTRACT

The molecular basis underlying G2 checkpoint adaptation in human cells is not fully understood. The current knowledge is predominantly derived from analyses about cell response to agents inducing double strand breaks (DSBs) in the DNA. However, the pathways conferring adaptation to other G2 checkpoints are less explored. In a recent study we have demonstrated that *MCPH1* function is required for the spontaneous - and induced - bypass of the decatenation checkpoint, a G2 pathway that delays entry into mitosis in response to excessive DNA catenation. Here, we demonstrate for the first time that PLK1 function is required for the adaptive response that bypasses the checkpoint arrest in response to Topo II catalytic inhibition. Our results also suggest that PLK1 likely acts downstream of MCPH1 and CHK1 in a linear pathway that promote adaptation to the decatenation checkpoint. WEE1 is another factor that restrains spontaneous adaptation to the decatenation checkpoint. This contribution is reinforced if MCPH1 function is simultaneously lacked. These results are of importance to better understand the genetic requirements of cells to allow adaptation to G2 checkpoints.

INTRODUCTION

G2 cell cycle checkpoints are induced in response to agents that alters the DNA and delay mitosis onset to allow repair. The induced arrest is necessarily reversible making possible that cells resume progression once the damage is full repaired. Coupling between checkpoint activation and cell cycle progression is tightly controlled by feedback mechanisms that allow shutting the checkpoint signaling off immediately after completion of the repair (Langerak and Russell, 2011). This fine-tuning relies in the capacity of damaged cells to lessen their pro-mitotic G2 transcriptional program temporally but beyond a level still sufficient to allow recovery from the checkpoint when appropriate (Alvarez-Fernandez and Medema, 2010). Only in those cases where the damage is too extensive or unrepairable, cells will exit from the cycle and undergone senescence or programmed cell death (Bartek and Lukas, 2007; Jackson and Bartek, 2009).

An alternative less-understood cell response is checkpoint adaptation. This process refers to the spontaneous bypass of the checkpoint arrest after a G2 delay despite the damage that triggers it persists. Checkpoint adaptation was initially described in *Saccharomyces cerevisae* and later observed in higher organisms including humans (Sandell and Zakian, 1993; Toczyski et al., 1997; Yoo et al., 2004; Syljuåsen et al., 2006). Since cells entering mitosis with unrepaired damaged DNA are a source of genomic instability, checkpoint adaptation is considered a potential contributor to tumorigenesis and cancer resistance during genotoxic therapy.

The molecular basis underlying G2 checkpoint adaptation in human cells is not fully understood. The current knowledge is predominantly derived from analyses about cell response to agents inducing double strand breaks (DSBs) in the DNA as ionizing irradiation (Toczyski et al., 1997; Yoo et al., 2004; Syljuasen et al., 2006, 2007). A key regulator of checkpoint adaptation in that context is PLK1. Thus, mutations in the yeast orthologous Cdc5 or downregulation of human PLK1 abolish cellular adaptation to IR-induced G2 checkpoint (Toczyski et al., 1997; Syljuasen et al., 2006). Furthermore, CHK1 activity is also required in human cells to sustain the IR-induced checkpoint (Syljuasen et al., 2006, 2007). However, the evidences suggest that both PLK1 and CHK1 control checkpoint adaptation through independent signaling pathways which converge on a common possible target as is Cyclin B-CDK1 (Syljuasen et al., 2006, 2007). Other cell cycle regulators required also in this context are Aurora A, WEE1, CDC25B and TLK2 (Van Vugt et al., 2004; Macurek et al., 2008; Serrano and D'Amour, 2014; Bruinsma et al., 2016).

The pathways conferring adaptation to other G2 checkpoints are less explored. In a recent study we have demonstrated that *MCPH1* function is required for the spontaneous - and induced - bypass of the decatenation checkpoint (DC), a G2 pathway that delays entry into mitosis in

response to excessive DNA catenation (Chapter III of this Thesis). Cells lacking MCPH1 function were permanently arrested at G2 during incubation with the Topoisomerase II catalytic inhibitor ICRF-193, the molecular signal that triggers the checkpoint activation. This was surprising considering that the DC is leaky and induces only a transient delay in G2 (Damelin and Bestor, 2007). Moreover, this permanent G2 arrest was not reverted even after simultaneous inhibition of ATR, the primary checkpoint effector (Deming et al., 2001). However, *MCPH1* function is dispensable for decatenation checkpoint activation. Furthermore, CHK1 function is essential for sustaining an effective DC response, and is downstream of MCPH1 in the pathway that triggers adaptation to it (Chapter III of this Thesis).

In previous studies cells treated with ICRF-193 displayed a significant although not complete inhibition of PLK1 activity (Deming et al., 2002). Moreover, overexpression of a constitutive active PLK1 variant abolished the decatenation checkpoint response (Deming et al., 2002; Luo et al., 2009). These data suggest that ICRF-193 meditated G2-arrest requires blockade of PLK1 activity. Considering these data, we have investigated here whether PLK1 activity is essential in the opposite context, that is, checkpoint adaptation. Our analyses demonstrate for the first time that PLK1 function is required for the adaptive response that bypass the checkpoint arrest in response to Topo II catalytic inhibition. Furthermore, our data provide evidences that PLK1 likely acts downstream of MCPH1 and CHK1 in a linear pathway that promote adaptation to the DC. These results are of importance to better understand the genetic requirements of cells to allow adaptation to G2 checkpoints.

METHODS

Cell cultures and treatments

We have used a modified H2B-Red1 tagged HeLa cell line. and lymphoblast cell lines (LCLs, non-transformed EBV immortalized) from one MCPH1 patient (S25X mutation) and one healthy control subject (Neitzel et al., 2002; Trimborn et al., 2004). HeLa cell lines were grown following standard conditions using DMEM medium supplemented with 10% of foetal bovine serum. LCLs were grown under usual conditions in RPMI medium supplemented with 15% foetal bovine serum.

For RNAi treatments cells were transfected with 120 nM siRNA duplexes using Lipofectamine (Invitrogen) at 50% confluency. OptiMEM medium (Invitrogen) was used for cell transfection. RNA oligos were purchased from Qiagen. The sequences of the siRNA duplexes used deplete specifically both major isoforms of MCPH1 mRNA, and were based on a previous study (Gavvovidis et al., 2012). These validated siRNA oligos knocked-down the MCPH1 protein levels efficiently (Trimborn et al., 2006; Gavvovidis et al., 2012; Arroyo et al., 2017). Synchronization of cells at G1/S was achieved by a double-thymidine protocol. The inhibitors employed were Nocodazole (final concentration 1,5 μM), ICRF-193 (final concentration 7 μM), caffeine (final concentration 2 mM), UCN-01 (final concentration 200 nM), BI2536 (final concentration 200 nM) and MK1775 (final concentration 300 nM). Untreated control cells were incubated in all cases with a similar volume of solvent.

Live-cell microscopy

The procedure was similar to the described in Arroyo et al., 2017. Cells were plated onto 35 mm tissue culture dishes fitted with glass cover-slips (MatTek Cultureware). siRNA transfection and cell synchrony was performed as described in the results section, except that upon release from the second thymidine the standard medium containing the thymidine was exchanged for DMEM without phenol red, supplemented with 10% FBS, penicillin/streptomycin and 200 mM Trolox (Calbiochem). The dishes were transferred to a microscope humidified stage incubator containing 5% CO2 at 37ºC. Cells were filmed with three to five z sections using a Nikon Biostation IM microscope fitted with 20x and 40x/0.8 n.a. objectives and coupled with Biostation IM software. Images were stacked and processed using Image J software. Timing data were

obtained after visual inspection of a minimum of 50 cells. Statistical comparisons were done using Statgraphics software.

Flow cytometry

Flow cytometry analyses were done using lymphoblast cell cultures in log-phase. One million cells approximately were recovered, washed in PBS and fixed in ice-cold Ethanol 70 overnight. Phospho-histone H3 positive cells were detected with a rabbit anti-histone H3PS10 antibody (Abcam) at a dilution of 1/250, and a donkey anti-mouse IgG FITC-conjugated secondary antibody (Santa Cruz). Propidium iodide was used as a counterstain for DNA content. Fluorescence detection was performed using an analytical flow cytometer (LSR Fortessa, BD Bioscience) equipped with BD FACSDiva™ software for data acquisition. Quantitative cell cycle analysis was done with Flowing Software v.2.5.1.

Cytogenetic analyses

Cytogenetic preparations following standard protocols were obtained in parallel from the same log-phase cell cultures analyzed by FACS. Chromosome preparations were fixed using Carnoy's solution (methanol/glacial acetic acid, 3:1), stained with Giemsa (10 %) and finally visualized by bright-field microscopy. The fraction of "prophase-like cells" (PLCs) and metaphases was determined after counting 1000 nuclei from coded slides. Microscopy images were captured with a CCD camera (Olympus DP70) coupled to a microscope (Olympus BX51) and finally managed with ImageJ software.

RESULTS AND DISCUSSION

PLK1 function is required for decatenation checkpoint adaptation in both control and MCPH1 depleted cells

We first have analyzed the cell cycle dynamics of control and MCPH1 patient cells lacking PLK1 function during undamaging conditions. In order to do that we made use of log-phase lymphoblast cultures and we assayed the dynamics of mitotic entry after incubation with nocodazole alone or combined with BI2536, a well-known PLK1 inhibitor (Steegmaier et al., 2007; Lenart et al., 2007). Mitotic cells were detected by FACS using a mitotic marker (Histone H3PS10) (Figure CIV-1A). Our data revealed that PLK1 inhibition slowed down the accumulation of mitotic cells in both control and patient cells, in comparison with the progressive accumulation observed when only nocodazole was added. In parallel to a reduced mitotic entry, the fraction of G2 cells appeared increased during prolonged incubation with BI2536 and nocodazole (Figure CIV-1B). Therefore, inhibition of PLK1 by BI2536 delays mitosis onset in control and MCPH1 patient lymphoblast cells with similar kinetics. Our results are in accordance with previous studies which demonstrated that mitotic entry is delayed but not blocked following PLK1 inhibition (Van Vugt et al., 2004; Petronczki et al., 2008). To get more evidences about the efficiency of PLK1 inhibition followed in our study we also analyzed chromosome morphology in cells after prolonged treatment with BI2536 and nocodazole. As observed in figure CIV-1E, chromosomes from both control and patients cells appeared hypercondensed and the sister chromatids retained cohesion after incubation with B12536. However, in cells treated only with nocodazole chromosomes were less compacted and the cohesion between chromatids was removed except for centromeric regions. These results are in agreement with previous descriptions about the impact of PLK1 inhibition on mitotic chromosomes (Lenart et al., 2007). Moreover, we also observed that after prolonged incubation with BI2536 alone the fraction of mitotic cells increased over the time in both control and patient cells (figure CIV-1B). This indicates that BI2536 further delays mitosis transition in lymphoblast cells as described for other cellular models (Lenart et al., 2007; Li et al., 2015).

Previous studies have showed that cells treated with ICRF-193 displayed a significant although not complete inhibition of PLK1 activity, while overexpression of a constitutive active PLK1 variant abolished the decatenation checkpoint response (Deming et al., 2002; Luo et al., 2009). These data suggest that ICRF-193 meditated G2-arrest requires blockade of PLK1 activity. How PLK1 function is exactly counteracted by other modulators of this pathway as ATR, MDC1 or Topo II alpha is still not well understood (Deming et al., 2002; Luo et al., 2009). Considering these data, we hypothesized that PLK1 activity would be an essential factor in the opposed cellular context, that is, adaptation to the decatenation checkpoint. In line with this, previous

studies have already showed that PLK1 is essential for recovery from DNA damage checkpoint (Van Vugt et al., 2004). To test our hypothesis, we assayed the dynamics of mitotic entry after simultaneous incubation with BI2536 and the Topoisomerase II inhibitor ICRF-193 during either 4h or 7h. Nocodazole was also added to trap those cells entering into mitosis, which were detected by FACS as explained above. As observed in figure CIV-1C, the rate of mitotic cells in control and patient samples slightly decreased during the time course of our experiment. In parallel, the fraction of G2 cells became increased over time (figure CIV-1D). These results are in sharp contrast to the leaky nature of the arrest mediated by the decatenation checkpoint previously noticed in control – nor in MCPH1 patient - cells (Chapter III of this Thesis). Taking together, these data indicated that PLK1 function, similarly to MCPH1, is also required for the adaptive response that spontaneously bypasses the decatenation checkpoint G2 arrest in human cells.

We also investigated the contribution of PLK1 activity during induced bypass of the decatenation checkpoint arrest. In order to do that we made use of caffeine, a well-known inhibitor of ATM/ATR kinases which override the ICRF-193-imposed G2 arrest (Deming et al., 2001; Chapter III of this Thesis). As showed in figure CIV-1 C and D, caffeine addition does not have any effect in the cell cycle dynamic of control and patient cells treated with ICRF-193 and BI2536, which remain permanently arrested at G2. This result implies that in control cells, which retain functional MCPH1, the ability of caffeine to induce adaptation in the presence of ICRF-193 requires active PLK1. Previous studies have already showed that MCPH1 depleted cells are defective in both spontaneous and caffeine-induced adaptation to the decatenation checkpoint (Chapter III of this Thesis). Therefore, both MCPH1 and PLK1 are crucial factors required for decatenation checkpoint bypass in lymphoblast cells.

Another remarkable aspect noticed in the Chapter III was the chromosome condensation dynamic of MCPH1 depleted cells arrested at G2 through decatenation checkpoint activation. MCPH1 depletion results in premature chromosome condensation during mid G2 phase of the cell cycle - and delayed decondensation after mitosis (Neitzel et al., 2002; Arroyo et al., 2017). As consequence, an elevated rate of cells containing condensed chromatin, named as “Prophase-like cells” (PLCs), are observed within a cycling population of cells lacking MCPH1 function. Interestingly, while arrested at G2 by ICRF-193 incubation PLCs arise but progressively reverse their condensation state. However, this condensation dynamic is prevented by caffeine, which suggests that ATR/ATM signaling pathways activated by the decatenation checkpoint trigger PLCs decondensation (Chapter III of this Thesis). Here we were interested in analyze how PLK1 inhibition influences the condensation dynamic of PLCs during ICRF-193-mediated G2 arrest. In order to do that we compared the fraction of G2 cells, determined by FACS, with the

frequency of "Prophase-like cells" (PLCs), determined through microscopic inspection of cytogenetic preparations made in parallel (figure CIV-1D). We observed that the frequency of PLCs increased over time during the incubation with ICRF-193 and BI2536, and a similar trend was observed if caffeine was simultaneously added. These results suggest that PLK1 inhibition prevents the decondensation of PLCs arrested at G2 during decatenation checkpoint activation. Interestingly, although with dramatically less numbers a similar tendency was also observed in control cells.

MCPH1 reinforces the contribution of PLK1 to the spontaneous and induced decatenation checkpoint adaptation in HeLa cells

In our previous study we have demonstrated that HeLa cells depleted of *MCPH1* function by siRNAs do not spontaneously override the G2 arrest triggered by ICRF-193 as do control cells (Chapter III of this Thesis). Moreover, the ability of caffeine to induce adaptation in the presence of ICRF-193 was also impaired in MCPH1-siRNA treated cells. These data were obtained using HeLa H2B-Red1 cells synchronized at G1/S with thymidine, transfected with siRNAs against *MCPH1*, and then monitored by fluorescent live-cell microscopy upon release into medium containing ICRF-193 alone or combined with caffeine. This approach was of big help to accurately compare the activation and adaptation kinetics of the decatenation checkpoint in single cells. In fact, this strategy allowed distinguishing the kinetics of the spontaneous and induced adaptation to this checkpoint. We therefore sought to compare here the activation and adaption kinetics to the decatenation checkpoint in cells with PLK1 function inhibited, and the possible impact of MCPH1 function into them. In order to do that, ICRF-193 was added 6 hours after release from the thymidine block, at the time when MCPH1 deficient cells start to prematurely condense their chromosomes during G2 (Arroyo et al., 2017), and either BI2536 alone or combined with caffeine was added to parallel samples two hours later (experimental outline in figure CIV-2A). These analyses were done in both control and MCPH1-siRNA cells. As depicted in figure CIV-2B, most control cells incubated with BI2536 arrest permanently during ICRF-193 incubation, consistent with the results obtained in lymphoblasts.

However, late adaptation to the decatenation checkpoint was still observed as some cells began to spontaneously enter into mitosis following ten hours of arrest. When caffeine was simultaneously added a similar fraction of cells finally bypassed the G2 arrest but early in time. When the same analyses were done in HeLa cells depleted of MCPH1 by RNAi we did not observe the same kinetics (figure CIV-2B). In this case spontaneous overriding was negligible (one single cell), while caffeine addition did not induced a significant increase of this rate. In order to discard that the observed responses in HeLa cells were directly consequence of the

incubation with BI2536 itself, and thus unrelated to the activation of decatenation checkpoint, we attended similar analyses in synchronized HeLa H2B-Red cells treated only with BI2536 upon release (figure CIV-3A). Our data clearly demonstrate that during undamaging conditions PLK1 inhibition delays but do not block mitosis onset neither in control nor in MCPH1-siRNA treated cells, in accordance with the findings in lymphoblast cells and with previous studies (Lenart et al., 2007; Van Vugt et al., 2004). From our results it could be concluded that PLK1 inhibition perturb but does not impair completely the capacity of HeLa cells to override the decatenation checkpoint. However, an effective permanent G2 arrest is achieved if MCPH1 function is simultaneously lacked, which demonstrate that both MCPH1 and PLK1 have synergize effects into the mechanism triggering cellular adaptation to the decatenation checkpoint.

This HeLa H2B-Red1 model was also important to unravel the chromosome decondensation dynamic of MCPH1 depleted cells upon ICRF-193 treatment (Chapter III of this Thesis). Therefore, it was of interest to monitor the timing that cells remain with condensed chromatin in the experimental setup from above, in order to analyze how PLK1 influences this dynamic. To get comparable and reliable data these measurements were done only in cells that did not attend apoptosis (Figure CIV-2C, representative stacks in figures CIV-2D and 2E, videos 1, 2, 3, 4 (CIV)). In ICRF-193 treated cells depleted of MCPH1 most PLCs were visible from the first frame of the live-cell movies and persisted for long time: when BI2536 was only added PLCs occurs during 657 ±265 minutes; however, this length was extended to 824 ±85 minutes when caffeine was simultaneously added (videos CIV-3 and CIV-4). The notorious increase in the timing of PLCs after caffeine adding could be explained by the inhibitory effect into the CDK1 activity that exhorts the ATR/ATM signaling pathways, which become inactive upon caffeine addition. The same rationale was used previously to explain the progressive decondensation of PLCs during the G2 arrest triggered by the decatenation checkpoint (Chapter III of this Thesis).

Interestingly, in control cells we also observed visible signs of chromosome condensation during long time. Thus, condensation persisted for 403 ±157 minutes when cells were incubated with BI2536, and a similar timing was also observed after simultaneous addition of caffeine (429 ±238 minutes) (Figure CIV-2 C, representative pictures in 2D and 2E). The occurrence of chromosome condensation during such a long interval was not previously observed in control G2 cells incubated with ICRF-193 (Chapter III of this Thesis). These results could indicate that PLK1 regulates the chromosome condensation dynamics of cells arrested at G2 by ICRF-193 incubation. Alternatively, the contribution of PLK1 to chromosome condensation could happen in a broader context. In line with this, cells lacking PLK1 function present hypercondensed chromosomes, a sign of abnormal chromosome condensation (Van Vugt et al., 2004; Lenart et

al., 2007; figure CIV-1E). To get more insights about the contribution of PLK1 in the chromosome condensation dynamics we analyzed undamaged HeLa H2B-Red cells treated only with BI2536 upon release from thymidine block. As presented in figures CIV-3B and C chromosome condensation was visualized for long time before cells attended nuclear envelope breakdown (NEB) in BI2536 treated control cells (109 ±88 minutes) compared with untreated cells (18 ±11 minutes). These data are in agreement with previous work (Lenart et al., 2007). A similar trend was observed in MCPH1 depleted cells. In this case, before attending NEB PLCs were visualized during 298 ±123 minutes in BI2536 treated cells while in untreated cells PLCs appeared visible during 202 ±51 minutes. As expected from cells lacking PLK1 function in all cases cells were further arrested in mitosis permanently (data not shown), a hallmark of "Polo" phenotype (Aspinall et al., 2015; Steegmaier et al., 2007; Gilmartin et al., 2009). In conclusion our data indicate that PLK1 inhibition increases the time that chromosome condensation appears visible in undamaged cells before entering into mitosis. A similar extension of the timing of chromosome condensation is also observed in cells arrested at G2 by decatenation checkpoint activation. This contribution remains also intact in cells where chromosome condensation starts prematurely during G2 as consequence of MCPH1 lack of function.

PLK1 function is required to bypass the decatenation checkpoint in cells following CHK1 inhibition

CHK1 is a key element of the ATR signaling pathway. Our previous study has proved that CHK1 function is required for an effective activation of the decatenation checkpoint (Chapter III of this Thesis), in agreement with some previous reports (Robinson et al., 2007). Moreover, we also demonstrated that the incompetence of cells lacking MCPH1 function to adapt to the decatenation checkpoint was rescued after CHK1 inhibition by UCN-01. Therefore, CHK1 could act at some point downstream of MCPH1 in the pathway that triggers recovery form the decatenation checkpoint arrest. Since our data from above demonstrate that cells also required PLK1 function to adapt to the decatenation checkpoint, we next examined how PLK1 inhibition influences the recovery capacity of cells with CHK1 inhibited. To asses that we incubated lymphoblastoid cells with ICRF-193, BI2536 and UCN-01, a well-characterized CHK1 inhibitor, during 4h and 7h in combination with nocodazole. We next determined the rate of mitotic accumulation by FACS analyses (Figure CIV-4A and B). This revealed that neither control nor MCPH1 patient cells entered into mitosis during the time course of our experiment; in fact, the mitotic rate slightly decreased during it while the fraction of G2 cells increased in parallel (Figures CIV-4A-C). Furthermore, simultaneous inhibition of ATR/ATM by caffeine addition did not abolish the G2 arrest in both control and MCPH1 patient cells (Figures CIV-4A-C). However, when PLK1 function was not inhibited the G2 arrest was efficiently bypassed

in both control and MCPH1 patient cells treated in the same conditions. In conclusion, we revealed that both caffeine- and UCN01-mediated release from an ICRF-193-mediated G2 checkpoint requires active PLK1 activity. These results clearly indicate that PLK1 is likely to act downstream of CHK1, MCPH1 and ATR in a linear pathway to promote recovery from the decatenation checkpoint arrest. The cell cycle dynamic observed was not influenced by the presence of nocodazole in our experiments as the same results were observed when nocodazole was omitted from the assays (figures CIV-4E and F). These data clearly differ from the published roles for PLK1 and CHK1 during cellular adaptation to the DNA damage checkpoint. In this case both regulators control checkpoint adaptation apparently through independent signaling pathways (Syljuasen et al., 2006). Therefore, while PLK1 is commonly required to bypass both the DNA damage and the decatenation checkpoints, other regulators specific of each pathway do exists as is the case of MCPH1, which acts upstream of PLK1 to confer adaptation to the decatenation checkpoint but not to the damage checkpoint.

We also examined the condensation dynamic of PLCs in the conditions from above. As observed in figure CIV-4 D, the frequency of PLCs increased over time in MCPH1 patient cells during simultaneous incubation with ICRF-193, BI2536, UCN-01 and nocodazole. The same tendency was observed if caffeine was simultaneously added. These results are similar to those from figure CIV-1 D, and reinforce the idea that PLK1 inhibition prevents the decondensation of PLCs arrested at G2 during decatenation checkpoint activation. In parallel samples where PLK1 function was not inhibited the PLC rate was not increased over time, which is the expected outcome after efficient bypass of the G2 arrest (noticed by a reduction in the G2 fraction in parallel to an increased mitotic frequency). In control cells we also observed an increment in the time that cells remain with visible chromosome condensation after the same treatments (figure CIV-4C). Furthermore, a similar dynamic was also observed when nocodazole was omitted from the assays in both control and MCPH1 patient cells (figures CIV-4E and 4F). Taking together these data reinforce the idea that chromosome condensation gets longer when PLK1 function is blocked during both undamaging conditions and altered chromatin topology.

Partial bypass of decatenation G2 checkpoint arrest after WEE1 inhibition depends on functional PLK1 and MCPH1

We finally were interested in analyzing the contribution of WEE1 to the decatenation checkpoint. WEE1 is a kinase that selectively phosphorylates the Y15 residue of CDK1 and promotes its inactivation. This inhibitory function is antagonized by CDC25 phosphatases, being their balances and results determinant to regulate the full activation of CDK1 (Lindqvist

et al., 2009). In order to do that we first compared if the dynamic of mitotic entry is disturbed in control and MCPH1 patient cells following WEE1 inhibition. Following the strategy previous explained lymphoblast cells were incubated during different times (1, 4 or 7 hours) with nocodazole alone or combined with MK-1775, a potent small-molecule inhibitor that aborts WEE1 function by abolishing PY15-CDK1 phosphorylation (Hirai et al., 2009). Our results clearly showed that the rate of mitotic entry is similarly accelerated during the first hours of incubation with MK-1775 in both control and MCPH1 patient cells (Figure CIV-5A). In parallel, the fraction of G2 cells was reduced during the same time compared with untreated samples (Figure CIV-5B and Figure CIV-6C). These results clearly indicate the WEE1 inhibition induces, as expected, rapid G2 progression and accelerates mitosis onset in a similar way in both control and MCPH1 patient cells. A similar dynamic has been also previously observed in another cell models after MK-1775 treatment (Hirai et al., 2009). We also observed a similar dynamic when we inhibited WEE1 in the HeLa H2B-Red1 model depleted of MCPH1 by siRNA (Supplementary Figure CIV-S1).

We next investigated if WEE1 function is required for efficient activation of the decatenation checkpoint, which remained fairly unknown. Previous studies about the role of WEE1 during DNA damage activation showed contradictory results, as some claim that WEE1 is not required to efficiently arrest cells at G2 (Van Vugt et al., 2004), while others showed that its inhibition by MK-1775 abrogates such arrest (Hirai et al., 2009). Following the same strategy as before cells were simultaneously incubated with ICRF-193, MK-1775 and nocodazole during 4h and 7h, and the rate of mitotic cells was determined by FACS. As showed in figures CIV-6A and B MK-1775 incubation abrogates only partially the ICRF-193 induced G2 arrest in control cells. Thus, the rate of mitotic cells was progressively increased over time, although with reduced kinetics compared with cells that were treated only with nocodazole. This dynamic differs from the observed in MCPH1 patient cells. In this case MK-1775 treatment produced only a minor increase in the fraction of mitotic cells over time compared with nocodazole single-treated cells (figure CIV-6A). In line with this, the fraction of G2 cells was found higher in MCPH1 patient cells compared with controls after the indicated treatments (figure CIV-6B). Taking together these results indicate for the first time that WEE1 inhibition perturbs the capacity of the decatenation checkpoint to achieve an efficient G2 arrest. However, in cells that lack simultaneously MCPH1 function this alteration was almost alleviated. Our results could be also interpreted as follows: WEE1 is another factor that restrains spontaneous adaptation to the decatenation checkpoint and this contribution is reinforced if MCPH1 function is simultaneously lacked.

We finally analyzed how WEE1 inhibition alters the response of the decatenation checkpoint in cells were PLK1 function was abolished. To do that we analyzed the mitotic rate of cells simultaneously treated with ICRF-193, MK-1775 and BI2536 for 4 and 7 hours. In these conditions both control and MCPH1 patient cells remain permanently arrested in G2 (figure CIV-6 A and B). These results indicate that in cells where WEE1 function is inhibited PLK1 inhibition restored an efficient G2 arrest after ICRF-193 treatment. This response remains unaltered independently of the presence of functional MCPH1. In other words, active PLK1 is an essential factor to allow cellular adaptation to the decatenation checkpoint and its likely located downstream of CHK1, WEE1 and MCPH1 in the pathway that controls it. Moreover, when we compared the dynamic of PLCs after the indicated treatments we observed that inhibition of PLK1 and WEE1 result in an increase of the PLC rate over time of cells while arrested at G2 by ICRF-193. However, this rate was reduced when WEE1 but not PLK1 function was abolished, which could be in line with the occurrence of a leaky G2 arrest and, consequently, a partial restore of mitotic entry.

Our results demonstrate that cellular adaptation to the decatenation checkpoint depends on a single pathway that comprises PLK1, CHK1, MCPH1, and ATR (Figure CIV-7). Interestingly, all of them are dispensable for the onset of mitosis during undamaging conditions (our data and other published work). Previous analyses have demonstrated that PLK1 is essential during cellular adaptation to the DNA damage checkpoint that responses to DSBs (Toczyski et al., 1997; Syljuasen et al., 2006; Van Vugt et al., 2004). Our study demonstrates that the signaling pathways that confer cellular adaptation are variable depending on the particular alteration that is signalized. One example is MCPH1, which is required to confer cellular adaptation in response to alterations in the topology of the DNA but not to UV- or IR- induced damage. Another difference is the contribution of WEE1 to these pathways. Inhibition of WEE1 function avoids the cellular dependence on PLK1 to abrogate the G2-arrest induced by the occurrence of DSBs, and indication that WEE1 acts downstream of PLK1 in this pathway (Van Vugt et al., 2004). Our current results suggest that PLK1 and WEE1 contribute however in a different manner to allow cell recovery from an ICRF-193-mediated G2 arrest. In this case, the inhibition of WEE1 does not alleviate the PLK1 requirement to override the G2 arrest, which is compatible with PLK1 emplaced downstream of WEE1 in the pathway triggering adaptation to the decatenation checkpoint. On the other hand, it could not be excluded that WEE1 and PLK1 contribute through independent pathways during adaptation to the decatenation checkpoint.

ACKNOWLEDGMENTS

This work was supported by Junta de Andalucía (Funding program 'Ayudas a grupos de investigación', reference BIO 220). M. Arroyo PhD is granted by University of Jaén (Spain), and was provided with travelling grants to perform short-term stays at the University of Minnesota by EMBO and "Escuela de Doctorado" (University of Jaén, Spain), respectively. The authors express their gratitude to: H. Neitzel (Berlin, Germany) for providing the lymphoblast cell lines used in this study, C. Fisher and G. Marques (University of Minnesota, US) for technical assistance. Research at laboratory of R. Kuriyama was financially supported by NSF (MCB1140033). Technical and human support provided by CICT of Universidad de Jaén (UJA, MINECO, Junta de Andalucía, FEDER) is gratefully acknowledged.

Author's contribution statement

J.A.M., D.J.C. and R.K. designed the experiments. M.A., D.K., M.T. and J.A.M. performed the experiments. M.A., M.T., A.S. and J.A.M. analyzed the results. J.A.M. and D.J.C. wrote the main manuscript text. All authors reviewed the manuscript.

Additional information

Competing financial interest statement: the corresponding author, on behalf of all authors of the paper, declares no competing financial interest.

REFERENCES

Alvarez-Fernandez M, Halim VA, Krenning L, Aprelia M, Mohammed S, Heck AJ, et al. (2010). Recovery from a DNA damage-induced G2 arrest requires Cdk-dependent activation of FoxM1. EMBO R 2010; 11:452-8.

Alvarez-Fernández M, Medema RH, Lindqvist A. (2010). Transcriptional regulation underlying recovery from a DNA damage-induced arrest. *Transcription*, 1(1), pp. 32–35.

Arroyo M, Kuriyama R, Trimborn M, Keifenheim D, Cañuelo A, Sánchez A, Clarke DJ, Marchal JA. (2017). MCPH1, mutated in primary microcephaly, is required for efficient chromosome alignment during mitosis. *Sci. Rep.* **7,** 1–12

Aspinall CF, Zheleva D, Tighe A, Taylor SS. (2015). Mitotic entry: Non-genetic heterogeneity exposes the requirement for Plk1. *Oncotarget*. doi:10.18632/oncotarget.5507

Bartek J, Lukas J. (2007). DNA damage checkpoints: from initiation to recovery or adaptation. Curr Opin Cell Biol; 19(2):238–45. PMID: 17303408.

Bruinsma W, Berg JVD, Aprelia M. (2016). Tousled-like kinase 2 regulates recovery from a DNA damage-induced G 2 arrest', 17(5), pp. 1–12.

Damelin M, Bestor TH. The decatenation checkpoint. (2007). Br J Cancer. 96(2):201-5.

Deming PB, Cistulli CA, Zhao H, Graves PR, Piwnica-Worms H, Paules RS, Downes CS, Kaufmann WK. (2001). The human decatenation checkpoint. Proc Natl Acad Sci U S A;98(21):12044-9.

Deming PB, Flores KG, Downes CS, Paules RS, Kaufmann WK. (2002). ATR enforces the topoisomerase II-dependent G2 checkpoint through inhibition of Plk1 kinase. J Biol Chem;277(39):36832-8.

Gilmartin AG, Bleam MR, Richter MC, Erskine SG, Kruger RG, Madden L, Hassler DF, Smith GK, Gontarek RR, Courtney MP, Sutton D, Diamond MA, Jackson JR, Laquerre SG. (2009). Distinct concentration-dependent effects of the polo-like kinase 1-specific inhibitor GSK461364A, including differential effect on apoptosis. Cancer research. 2009; 69:6969–6977.

Hirai H, Iwasawa Y, Okada M, Arai T, Nishibata T, Kobayashi M, Kimura T, Kaneko N, Ohtani J, Yamanaka K, Itadani H, Takahashi-Suzuki I, Fukasawa K, Oki H, Nambu T, Jiang J, Sakai T, Arakawa H, Sakamoto T, Sagara T, Yoshizumi T, Mizuarai S, Kotani H. (2009). Small-molecule inhibition of Wee1 kinase by MK-1775 selectively sensitizes p53-deficient tumor cells to DNA-damaging agents. Mol. Cancer Ther. 8, 2992–3000.

Jackson SP, Bartek J. (2009). The DNA-damage response in human biology and disease. Nature 461: 1071–1078.

Langerak P, Russell P. (2011). Regulatory networks integrating cell cycle control with DNA damage checkpoints and double-strand break repair. *Philosophical Transactions of the Royal Society B: Biological Sciences*, 366(1584), pp. 3562–3571.

Lénárt P, Petronczki M, Steegmaier M, Di Fiore B, Lipp JJ, Hoffmann M, Rettig WJ, Kraut N, Peters JM. (2007). The Small-Molecule Inhibitor BI 2536 Reveals Novel Insights into Mitotic Roles of Polo-like Kinase 1. Curr. Biol. 17, 304–315.

Li J, Karki A, Hodges KB, Ahmad N, Zoubeidi A, Strebhardt K, Ratliff TL, Konieczny SF, Liu X. (2015). Cotargeting Polo-Like Kinase 1 and the Wnt/β-Catenin Signaling Pathway in Castration-Resistant Prostate Cancer. Mol Cell Biol. 35(24):4185-98.

Lindqvist A, Rodríguez-Bravo V, Medema RH. (2009). The decision to enter mitosis: feedback and redundancy in the mitotic entry network. J Cell Biol. 185, 193-202.

Luo J, Emanuele MJ, Li D, Creighton CJ, Schlabach MR, Westbrook TF, Wong KK, Elledge SJ. (2009). A Genome-wide RNAi Screen Identifies Multiple Synthetic Lethal Interactions with the Ras Oncogene. *Cell* **137,** 835–848.

Luo K, Yuan J, Chen J, Lou Z. (2009). Topoisomerase IIalpha controls the decatenation checkpoint. Nat Cell Biol. 2009 Feb;11(2):204-10. doi: 10.1038/ncb1828. Epub 2008 Dec 21.

Macurek L, Lindqvist A, Lim D, Lampson MA, Klompmaker R, Freire R, Clouin C, Taylor SS, Yaffe MB, Medema RH. (2008). Polo-like kinase-1 is activated by aurora A to promote checkpoint recovery. Nature. 455:119–123.

Neitzel H, Neumann LM, Schindler D, Wirges A, Tonnies H, Trimborn M. (2002). Premature chromosome condensation in humans associated with microcephaly and mental retardation: a novel autosomal recessive condition. Am J Hum Genet. 70, 1015-22.

Petronczki M, Lénárt P, Peters JM. (2008). Polo on the Rise-from Mitotic Entry to Cytokinesis with Plk1. *Dev. Cell* **14,** 646–659.

Sandell LL, Zakian VA. (1993). Loss of a yeast telomere: arrest, recovery, and chromosome loss. Cell 75: 729–739.

Serrano D, D'Amours D. (2016). Checkpoint adaptation: Keeping Cdc5 in the T-loop. Cell Cycle; 15(24):3339-3340.

Steegmaier M, Hoffmann M, Baum A, Lénárt P, Petronczki M, Krššák M, Gürtler U, Garin-Chesa P, Lieb S, Quant J, Grauert M, Adolf GR, Kraut N, Peters JM, Rettig WJ. (2007). BI 2536, a Potent and Selective Inhibitor of Polo-like Kinase 1, Inhibits Tumor Growth In Vivo. Curr. Biol. 17, 316–322.

Syljuåsen RG, Jensen S, Bartek J et al. (2006). Adaptation to the ionizing radiation-induced G2 checkpoint occurs in human cells and depends on checkpoint kinase 1 and Polo-like kinase 1 kinases. Cancer Res 66:10253–10257.

Syljuåsen RG. (2007). Checkpoint adaptation in human cells. Oncogene. 26, 5833–5839.

Toczyski DP, Galgoczy DJ, Hartwell LH. (1997). CDC5 and CKII control adaptation to the yeast DNA damage checkpoint. Cell 90: 1097–1106.

Van Vugt MA, Brás A, Medema RH. (2004). Polo-like kinase-1 controls recovery from a G2 DNA damage-induced arrest in mammalian cells. Mol Cell;15(5):799-811.

Van Vugt MA, Brás A, Medema RH. (2004). Polo-like kinase-1 controls recovery from a G2 DNA damage-induced arrest in mammalian cells. Mol Cell;15(5):799-811.

Yoo HY, Kumagai A, Shevchenko A, Shevchenko A, Dunphy WG. (2004). Adaptation of a DNA replication checkpoint response depends upon inactivation of Claspin by the Polo- like kinase. Cell 117: 575–588.

FIGURES LEGEND

Figure CIV-1: (A) Rate of histone H3PS10 positive cells in control and MCPH1 patient cells, determined by FACS, after incubation with nocodazole alone or combined with BI2536 for the indicated time points. Data from two independent experiments are presented. (B) Fraction of mitotic (M) and G2 cells, determined by FACS, in control and MCPH1 patient cells after either 4h or 7h of treatment with nocodazole alone or combined with BI2536. Data from two independent experiments are presented. For each sample, we determined in parallel the fraction of PLCs (prophase-like cells) by microscopic analyses of cytogenetic preparations. More than 500 cells were scored per sample. (C) Rate of histone H3PS10 positive cells in control and MCPH1 patient cells, determined by FACS, after incubation with nocodazole alone or combined with the indicated inhibitors after either 4h or 7h. Data from two independent experiments are presented. (D) Fraction of mitotic (M) and G2 cells, determined by FACS, in control and MCPH1 patient cells after either 4h or 7h of treatment with nocodazole alone or combined with the indicated inhibitors. Data from two independent experiments are presented. For each sample, we determined in parallel the fraction of PLCs as explained in B. (E) Representative images from cytogenetic preparations of control and MCPH1 patient cells treated with nocodazole alone or simultaneously incubated with BI2536 during 4h. Scale bars, 5 μM.

Figure CIV-2: (A) Description of the experimental procedure employed: HeLa cells stably expressing fluorescent histone H2B fused to Red1 were synchronized at the G1/S border by double thymidine block. MCPH1 depletion was achieved by transfection with siRNAs during the release from the first thymidine block. ICRF-193 was added 6h after release from the second thymidine block to coincide with the occurrence of PLCs during G2 in the siRNA treated cells. BI-2536 alone or combine with caffeine were added two hours after ICRF-193 treatment. Time-lapse images were collected using "Nikon Biostation IM Cell incubator" immediately after BI2536 adding. (B) Cumulative frequency chart showing the timing (in minutes) of nuclear envelope breakdown (NEB) in control and MCPH1-siRNA treated cells incubated with BI2536, alone or simultaneously with caffeine. Time from ICRF-193 addition is shown. At least 50 cells were analyzed in each case. (C) Dot-plot showing the time (in minutes) that PLCs from control and MCPH1-siRNA treated cells required to completely decondense their chromosomes after adding BI2536 alone or combined with caffeine. The red line indicates the mean value. The analyses are only referred to cells that did not enter into apoptosis while monitored. Statistical comparisons for the mean and median data were done by T-student and Wilcoxon (W) tests respectively. ** $p<0.01$. (D-E) Selected frames of representative cells from B showing

the dynamics of PLCs in control and MCPH1-siRNA treated cells after the indicated treatments. Time after BI2536 addition is indicated in minutes.

Figure CIV-3: (A) Cumulative frequency chart showing the timing (in minutes) of nuclear envelope breakdown (NEB) in control and MCPH1-siRNA treated cells incubated with BI2536. Cells were synchronized and siRNA treated as explained in Figure 2 (A), and BI2536 was added immediately after release from the second thymidine block. At least 50 cells were analyzed in each case. Time from thymidine release is shown (B) Dot-plot showing the length of PLCs in control and MCPH1-siRNA cells untreated or incubated with BI2536. The red line indicates the mean value. The analyses are only referred to cells that did not enter into apoptosis while monitored. Statistical comparisons for the mean and median data were done by T-student and Wilcoxon (W) tests respectively. ** $p<0.01$. (C) Selected frames of representative cells from B showing the dynamics of PLCs in control and MCPH1-siRNA treated cells after the indicated treatment. Time after BI2536 addition is indicated in minutes.

Figure CIV-4: (A-B) Rate of histone H3PS10 positive cells in control (A) and MCPH1 patient cells (B), determined by FACS, after incubation with nocodazole alone or combined the indicated inhibitors for the indicated time points. Data from two independent experiments are presented. (C-D) Fraction of mitotic (M) and G2 cells, determined by FACS, in control (C) and MCPH1 patient cells (D) after either 4h or 7h of treatment with nocodazole combined with the indicated inhibitors. Data from two independent experiments are presented. For each sample, we determined in parallel the fraction of PLCs by microscopic analyses of cytogenetic preparations. More than 500 cells were scored per sample. (E-F) Same analyses as in C and D but without adding nocodazole to the cell cultures.

Figure CIV-5: (A) Rate of histone H3PS10 positive cells in control and MCPH1 patient cells, determined by FACS, after incubation with nocodazole alone or combined with MK1775 for the indicated time points. Data from two independent experiments are presented. (B) Fraction of mitotic (M) and G2 cells, determined by FACS, in control and MCPH1 patient cells after either 4h or 7h of treatment with nocodazole alone or combined MK1775 for the indicated time points. Data from two independent experiments are presented. For each sample, we determined in parallel the fraction of PLCs (prophase-like cells) by microscopic analyses of cytogenetic preparations. More than 500 cells were scored per sample.

Figure CIV-6: (A) Rate of histone H3PS10 positive cells in control and MCPH1 patient cells, determined by FACS, after incubation with nocodazole alone or combined with the indicated inhibitors after either 4h or 7h. Data from two independent experiments are presented. (B)

Fraction of mitotic (M) and G2 cells, determined by FACS, in control and MCPH1 patient cells after either 4h or 7h of treatment with nocodazole alone or combined with the indicated inhibitors. Data from two independent experiments are presented. For each sample, we determined in parallel the fraction of PLCs as explained in B. (C) Fraction of mitotic (M) and G2 cells, determined by FACS, in control and MCPH1 patient cells after either 4h or 7h of treatment with MK1775 alone or combined with ICRF-193. Data from two independent experiments are presented. For each sample, we determined in parallel the fraction of PLCs as explained in B.

Figure CIV-7: Model for the signaling pathway triggering decatenation checkpoint adaptation in human cells: both spontaneous and caffeine-induced adaptation requires MCPH1 function to block CHK1 activity, which results in a PLK1-dependent checkpoint bypass.

VIDEOS LEGEND

Video CIV-1: synchronized HeLa H2B-Red1 control cells were incubated with ICRF-193 at 6 hours and BI2536+medium (mock) at 8 hours respectively after release from the second thymidine block. Time from mock adding (in minutes) is indicated.

Video CIV-2: synchronized HeLa H2B-Red1 control cells were incubated with ICRF-193 at 6 hours and BI2536+caffeine at 8 hours after release from the second thymidine block. Time from caffeine adding (in minutes) is indicated.

Video CIV-3: synchronized HeLa H2B-Red1 MCPH1-siRNA treated cells were incubated with ICRF-193 at 6 hours and BI2536+medium (mock) at 8 hours after release from the second thymidine block. Time from mock adding (in minutes) is indicated.

Video CIV-4: synchronized HeLa H2B-Red1 MCPH1-siRNA treated cells were incubated with ICRF-193 at 6 hours and BI2536+caffeine at 8 hours respectively after release from the second thymidine block. Time from caffeine adding (in minutes) is indicated.

Figure CIV-1:

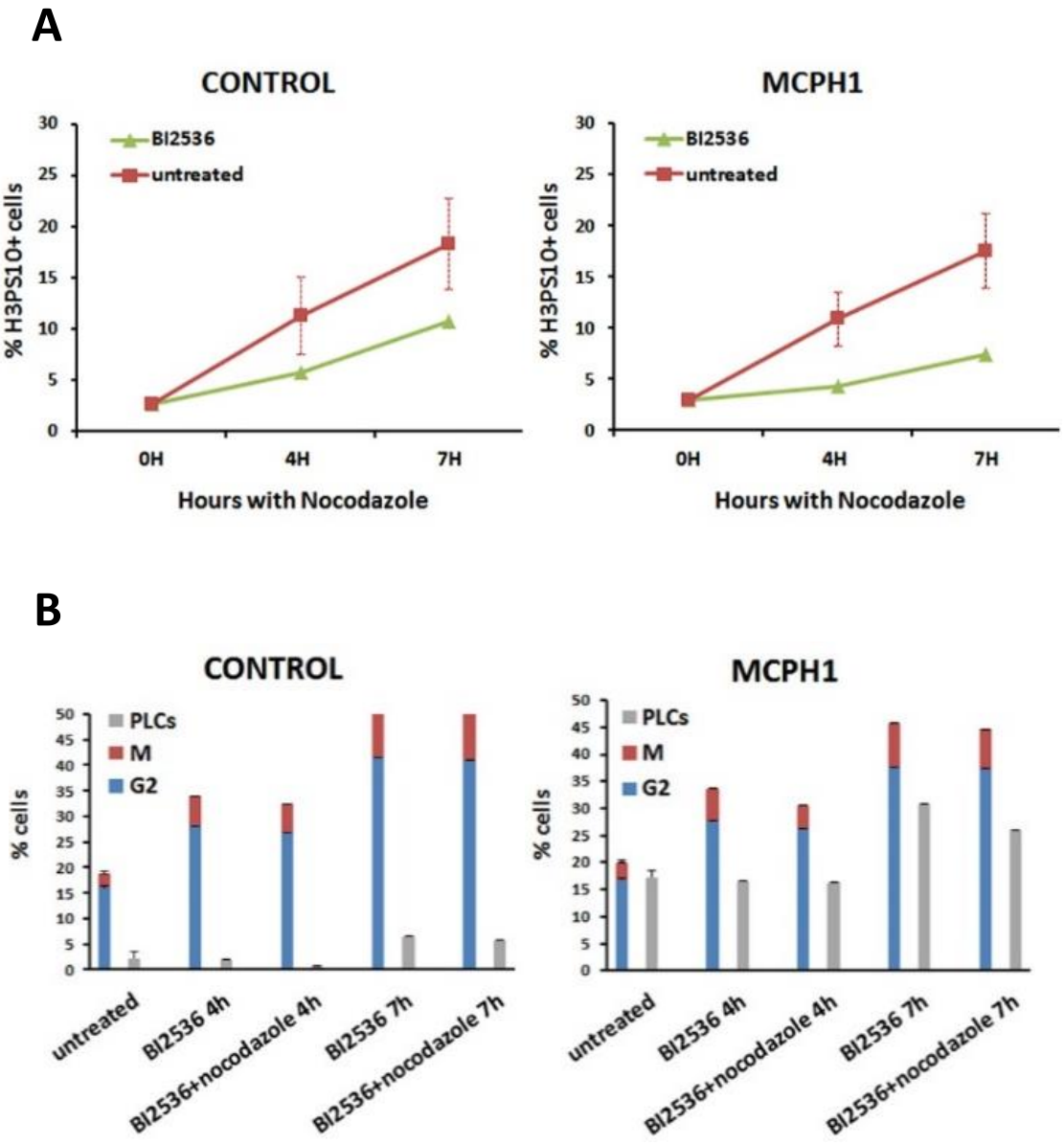
A
CONTROL
MCPH1
BI2536
untreated
% H3PS10+ cells
0
5
10
15
20
25
30
0H
4H
7H
Hours with Nocodazole
B
CONTROL
MCPH1
PLCs
M
G2
% cells
0
5
10
15
20
25
30
35
40
45
50
untreated
BI2536 4h
BI2536+nocodazole 4h
BI2536 7h
BI2536+nocodazole 7h

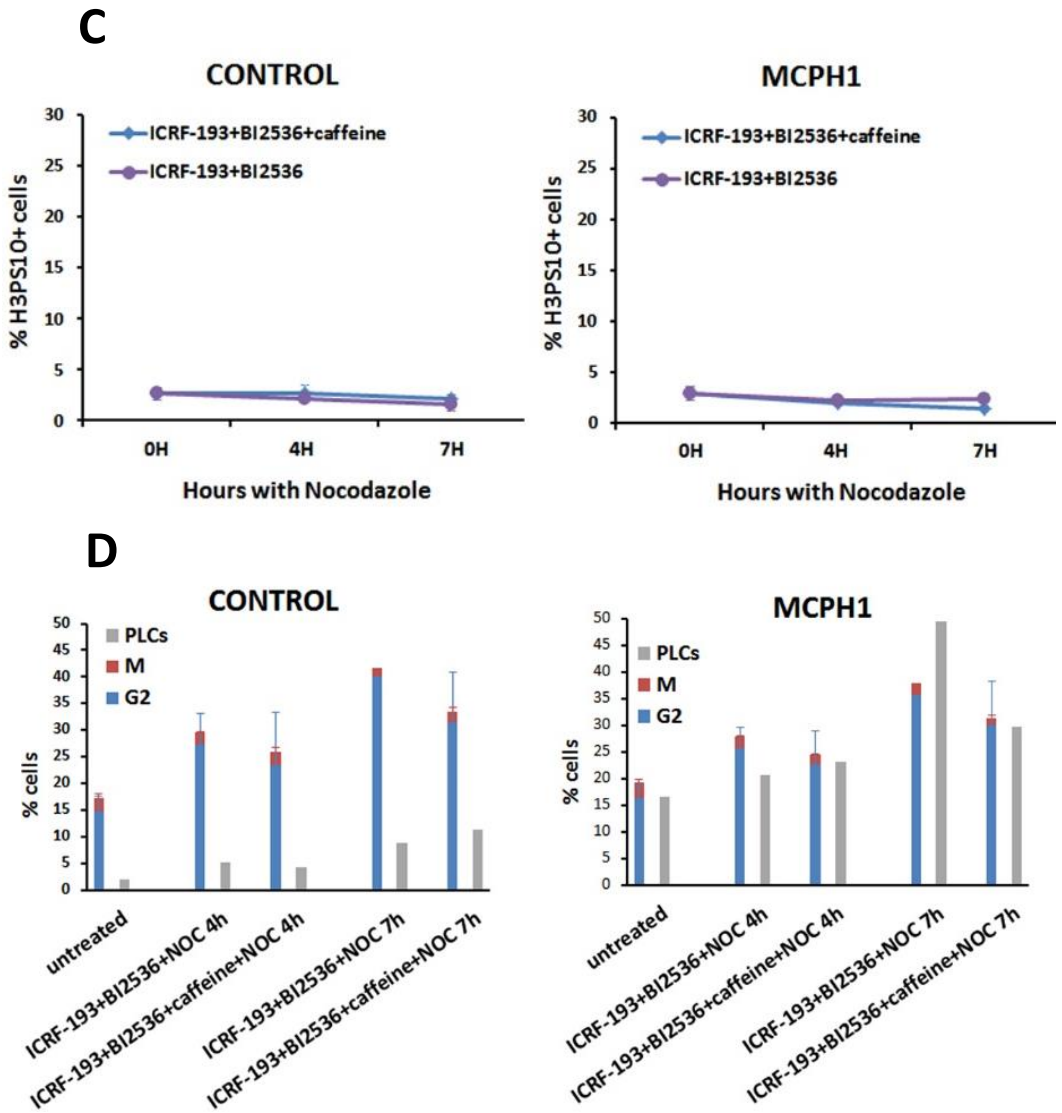
C
CONTROL
MCPH1
ICRF-193+BI2536+caffeine
ICRF-193+BI2536
% H3PS10+ cells
Hours with Nocodazole
0H
4H
7H
D
CONTROL
MCPH1
PLCs
M
G2
% cells
untreated
ICRF-193+BI2536+NOC 4h
ICRF-193+BI2536+caffeine+NOC 4h
ICRF-193+BI2536+NOC 7h
ICRF-193+BI2536+caffeine+NOC 7h

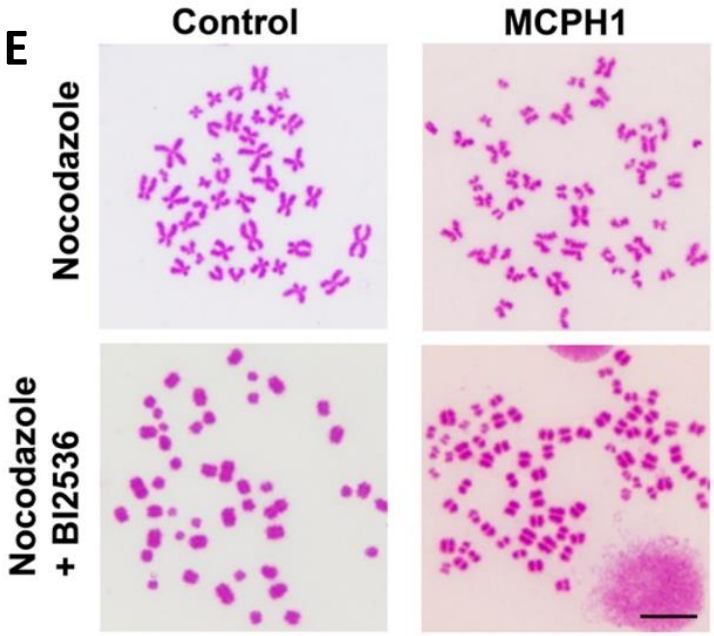
E
Control
MCPH1
Nocodazole
Nocodazole + BI2536

Figure CIV-2:

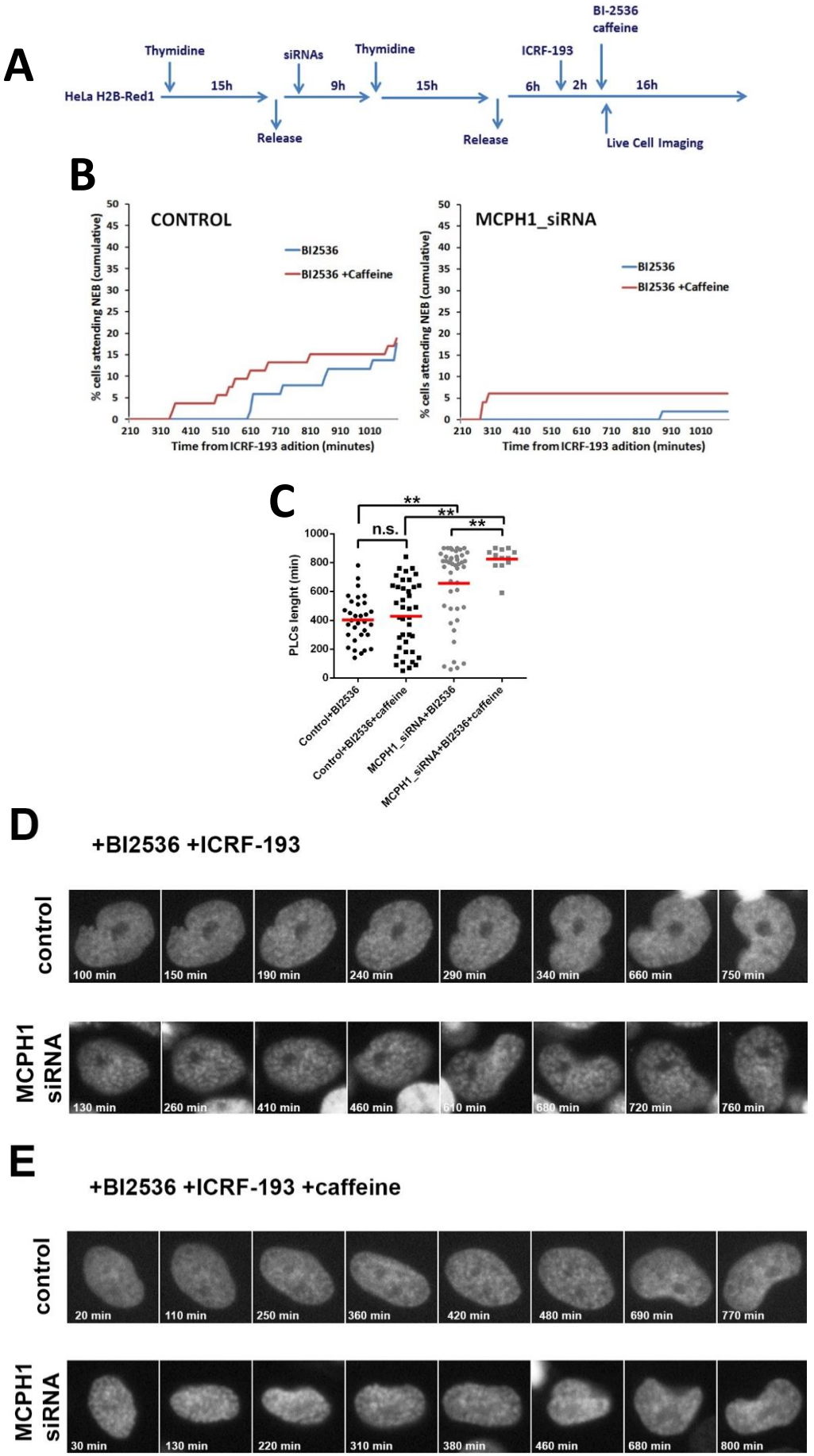
A
Thymidine
siRNAs
Thymidine
ICRF-193
BI-2536
caffeine
HeLa H2B-Red1
15h
9h
15h
6h
2h
16h
Release
Release
Live Cell Imaging
B
CONTROL
MCPH1_siRNA
BI2536
BI2536 +Caffeine
% cells attending NEB (cumulative)
Time from ICRF-193 adition (minutes)
C
n.s.
**
PLCs lenght (min)
Control+BI2536
Control+BI2536+caffeine
MCPH1_siRNA+BI2536
MCPH1_siRNA+BI2536+caffeine
D
+BI2536 +ICRF-193
control
MCPH1 siRNA
E
+BI2536 +ICRF-193 +caffeine
control
MCPH1 siRNA

Figure CIV-3:

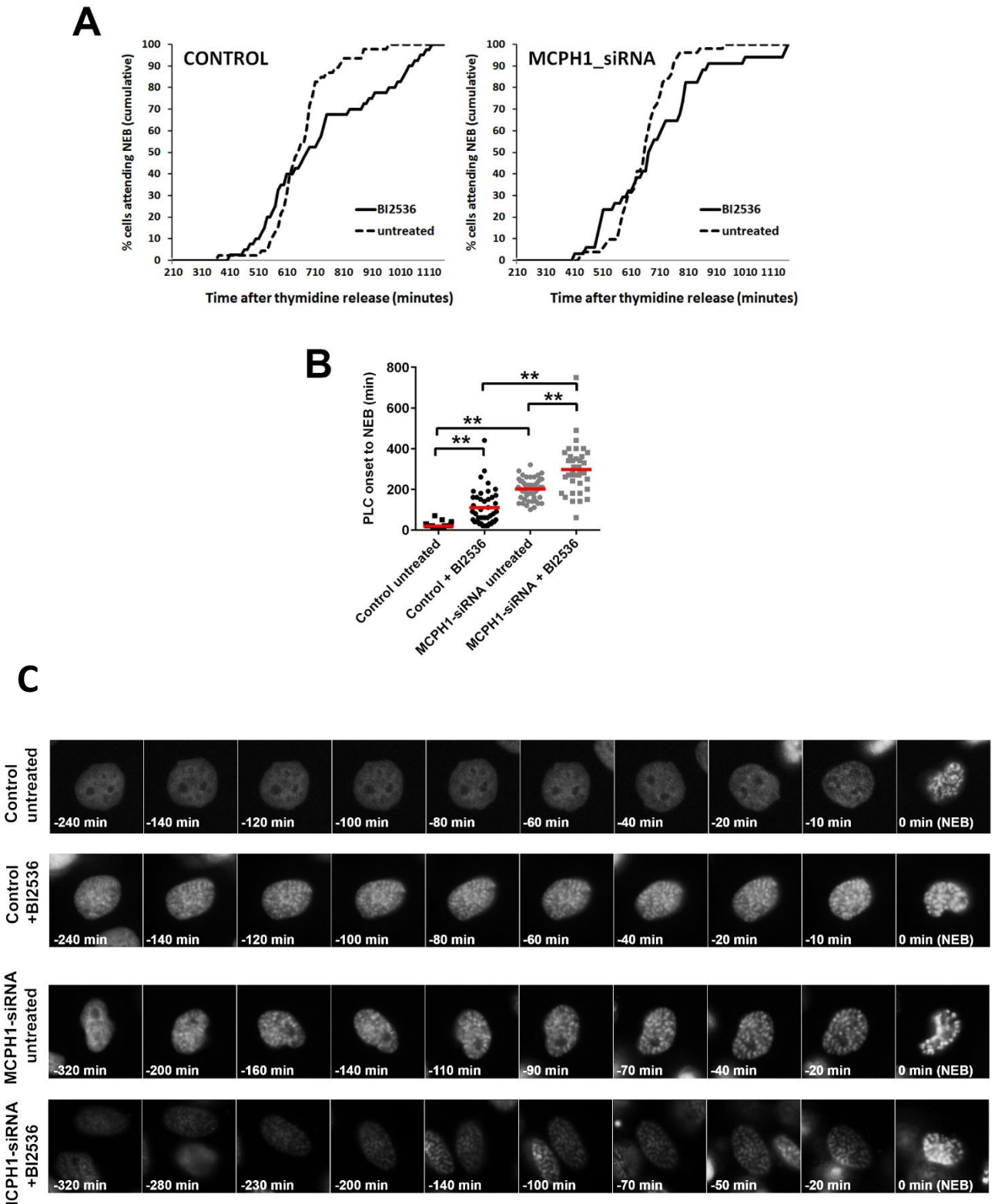
A
CONTROL
MCPH1_siRNA
% cells attending NEB (cumulative)
Time after thymidine release (minutes)
BI2536
untreated
B
PLC onset to NEB (min)
Control untreated
Control + BI2536
MCPH1-siRNA untreated
MCPH1-siRNA + BI2536
C
Control untreated
Control +BI2536
MCPH1-siRNA untreated
MCPH1-siRNA +BI2536
0 min (NEB)

Figure CIV-4:

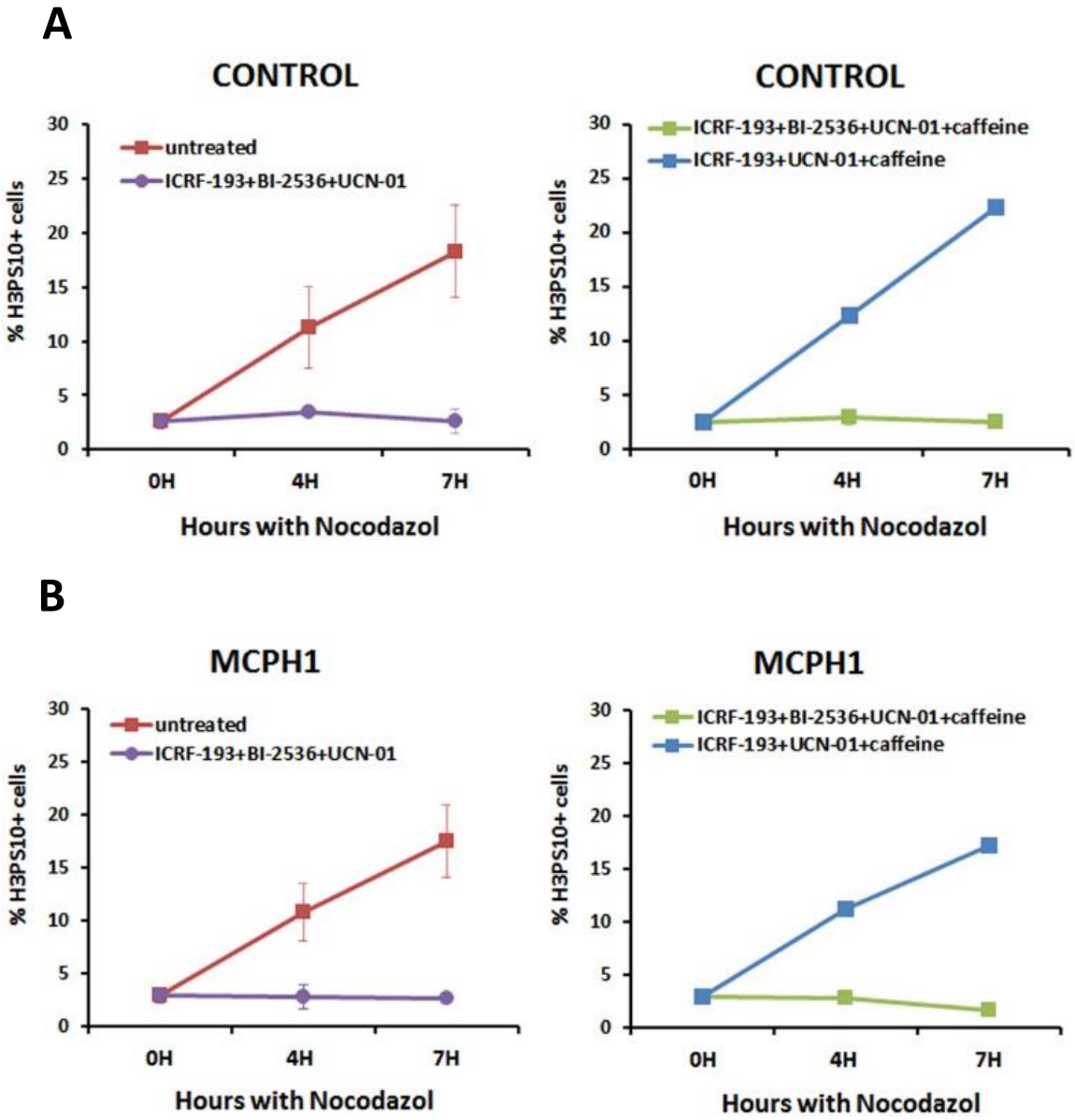
A
CONTROL
untreated
ICRF-193+BI-2536+UCN-01
% H3PS10+ cells
Hours with Nocodazol
0H
4H
7H
CONTROL
ICRF-193+BI-2536+UCN-01+caffeine
ICRF-193+UCN-01+caffeine
B
MCPH1
MCPH1

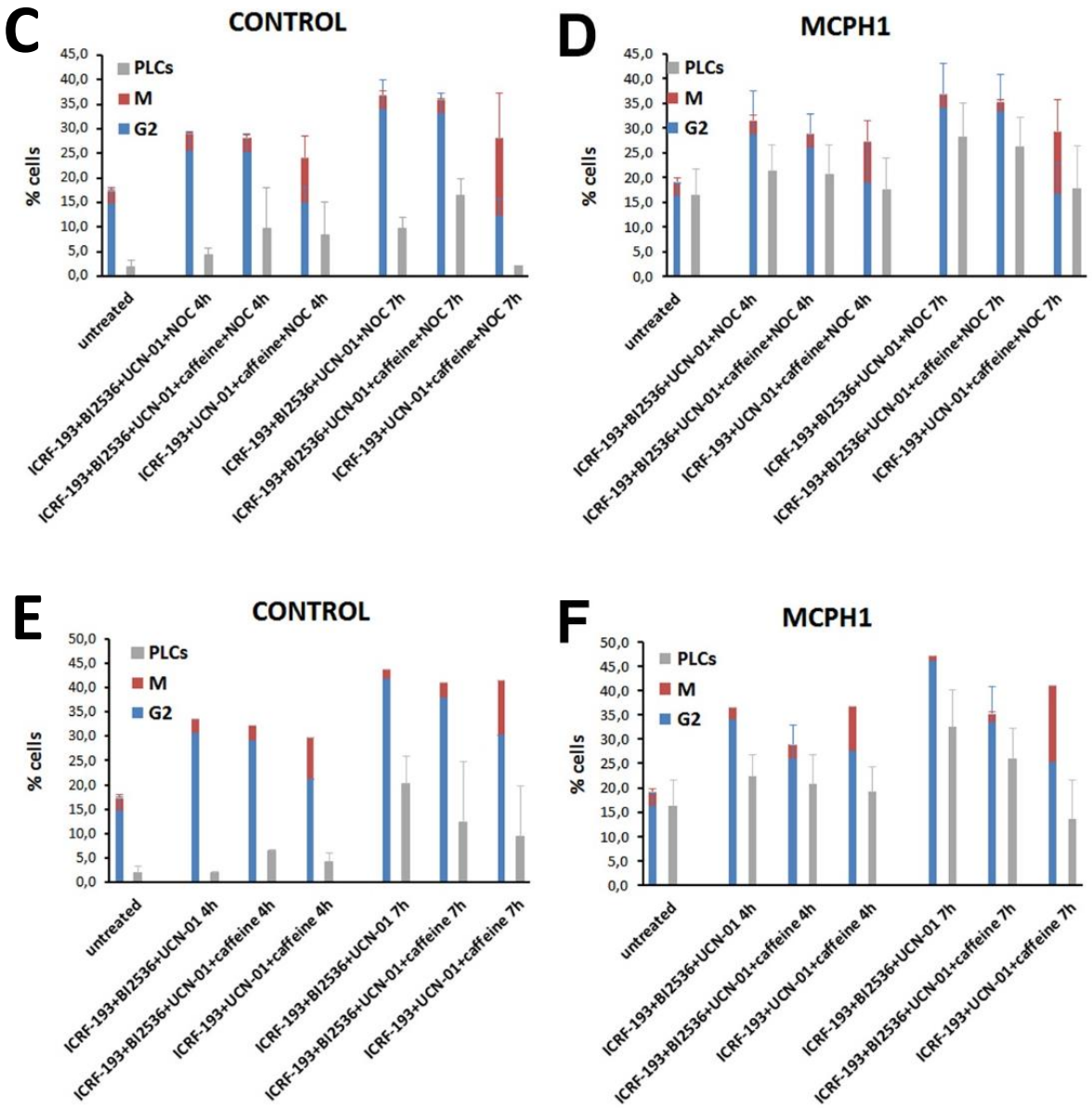
C
CONTROL
PLCs
M
G2
% cells
45,0
40,0
35,0
30,0
25,0
20,0
15,0
10,0
5,0
0,0
untreated
ICRF-193+BI2536+UCN-01+NOC 4h
ICRF-193+BI2536+UCN-01+caffeine+NOC 4h
ICRF-193+UCN-01+caffeine+NOC 4h
ICRF-193+BI2536+UCN-01+NOC 7h
ICRF-193+BI2536+UCN-01+caffeine+NOC 7h
ICRF-193+UCN-01+caffeine+NOC 7h
D
MCPH1
PLCs
M
G2
% cells
45,0
40,0
35,0
30,0
25,0
20,0
15,0
10,0
5,0
0,0
untreated
ICRF-193+BI2536+UCN-01+NOC 4h
ICRF-193+BI2536+UCN-01+caffeine+NOC 4h
ICRF-193+UCN-01+caffeine+NOC 4h
ICRF-193+BI2536+UCN-01+NOC 7h
ICRF-193+BI2536+UCN-01+caffeine+NOC 7h
ICRF-193+UCN-01+caffeine+NOC 7h
E
CONTROL
PLCs
M
G2
% cells
50,0
45,0
40,0
35,0
30,0
25,0
20,0
15,0
10,0
5,0
0,0
untreated
ICRF-193+BI2536+UCN-01 4h
ICRF-193+BI2536+UCN-01+caffeine 4h
ICRF-193+UCN-01+caffeine 4h
ICRF-193+BI2536+UCN-01 7h
ICRF-193+BI2536+UCN-01+caffeine 7h
ICRF-193+UCN-01+caffeine 7h
F
MCPH1
PLCs
M
G2
% cells
50,0
45,0
40,0
35,0
30,0
25,0
20,0
15,0
10,0
5,0
0,0
untreated
ICRF-193+BI2536+UCN-01 4h
ICRF-193+BI2536+UCN-01+caffeine 4h
ICRF-193+UCN-01+caffeine 4h
ICRF-193+BI2536+UCN-01 7h
ICRF-193+BI2536+UCN-01+caffeine 7h
ICRF-193+UCN-01+caffeine 7h

Figure CIV-5:

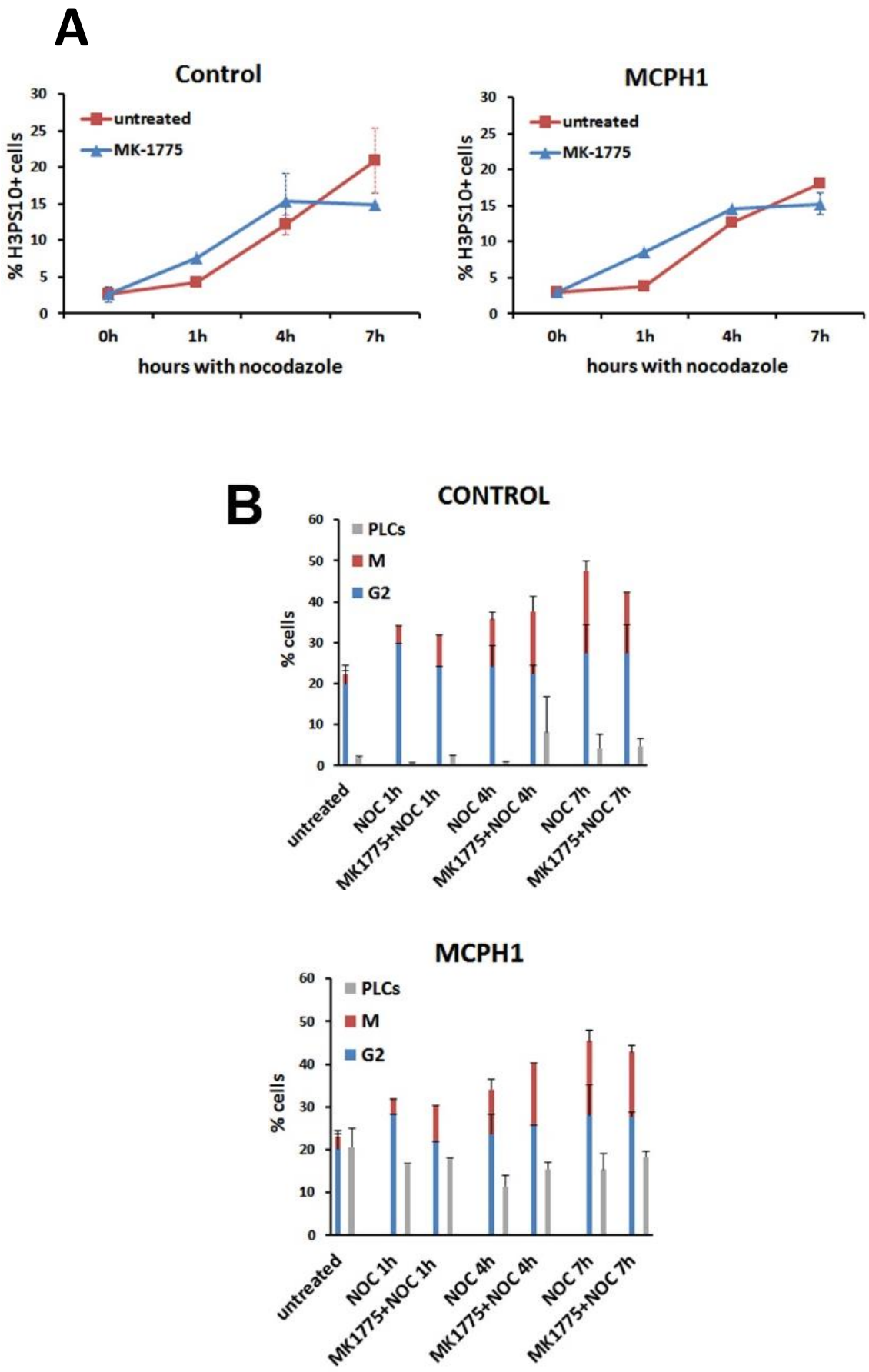
A
Control
MCPH1
untreated
MK-1775
% H3PS10+ cells
hours with nocodazole
0h
1h
4h
7h
B
CONTROL
MCPH1
PLCs
M
G2
% cells
untreated
NOC 1h
MK1775+NOC 1h
NOC 4h
MK1775+NOC 4h
NOC 7h
MK1775+NOC 7h

Figure CIV-6:

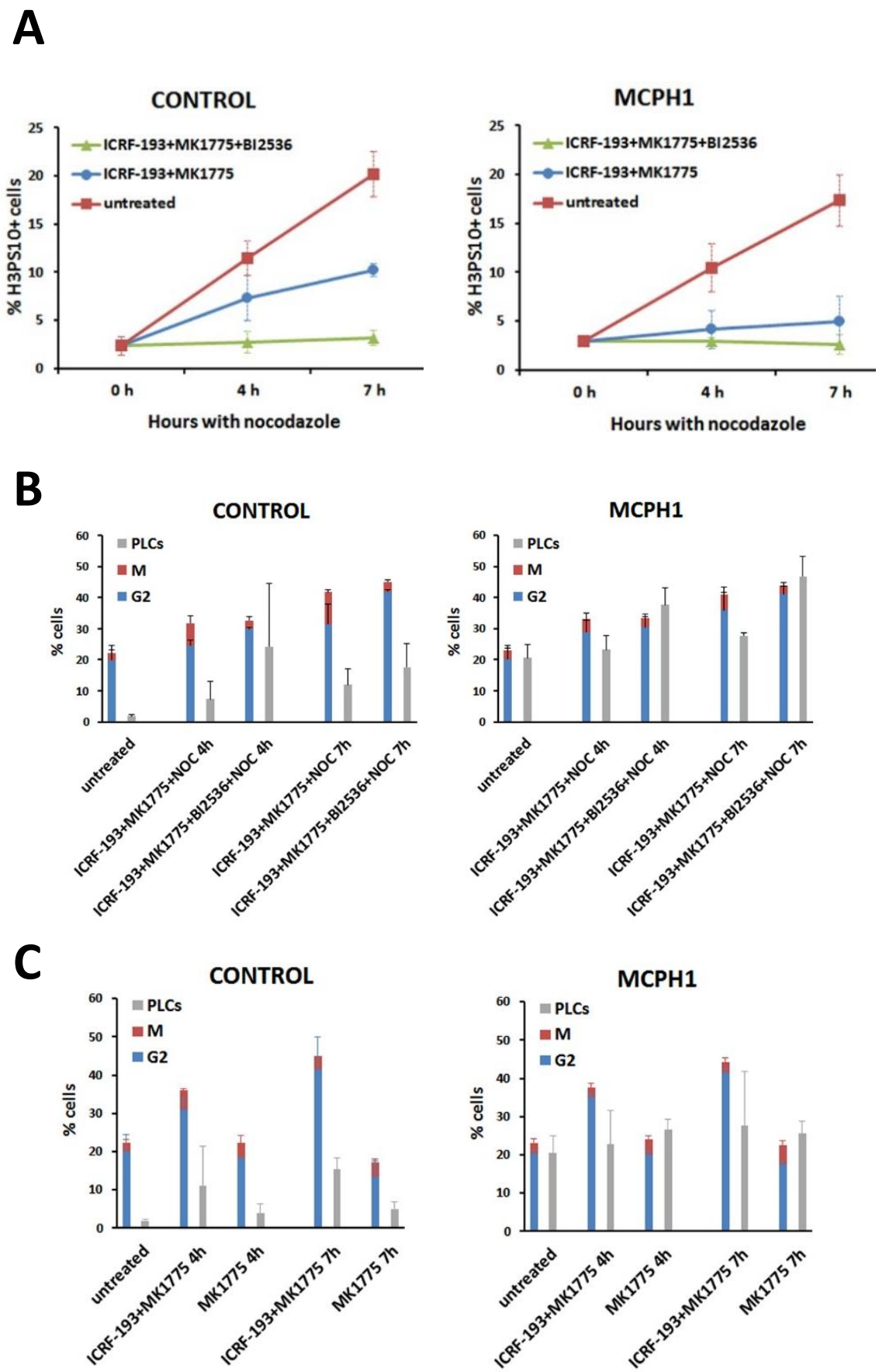
A
CONTROL
MCPH1
ICRF-193+MK1775+BI2536
ICRF-193+MK1775
untreated
% H3PS10+ cells
0 h
4 h
7 h
Hours with nocodazole
B
CONTROL
MCPH1
PLCs
M
G2
% cells
untreated
ICRF-193+MK1775+NOC 4h
ICRF-193+MK1775+BI2536+NOC 4h
ICRF-193+MK1775+NOC 7h
ICRF-193+MK1775+BI2536+NOC 7h
C
CONTROL
MCPH1
PLCs
M
G2
% cells
untreated
ICRF-193+MK1775 4h
MK1775 4h
ICRF-193+MK1775 7h
MK1775 7h

Figure CIV-7:

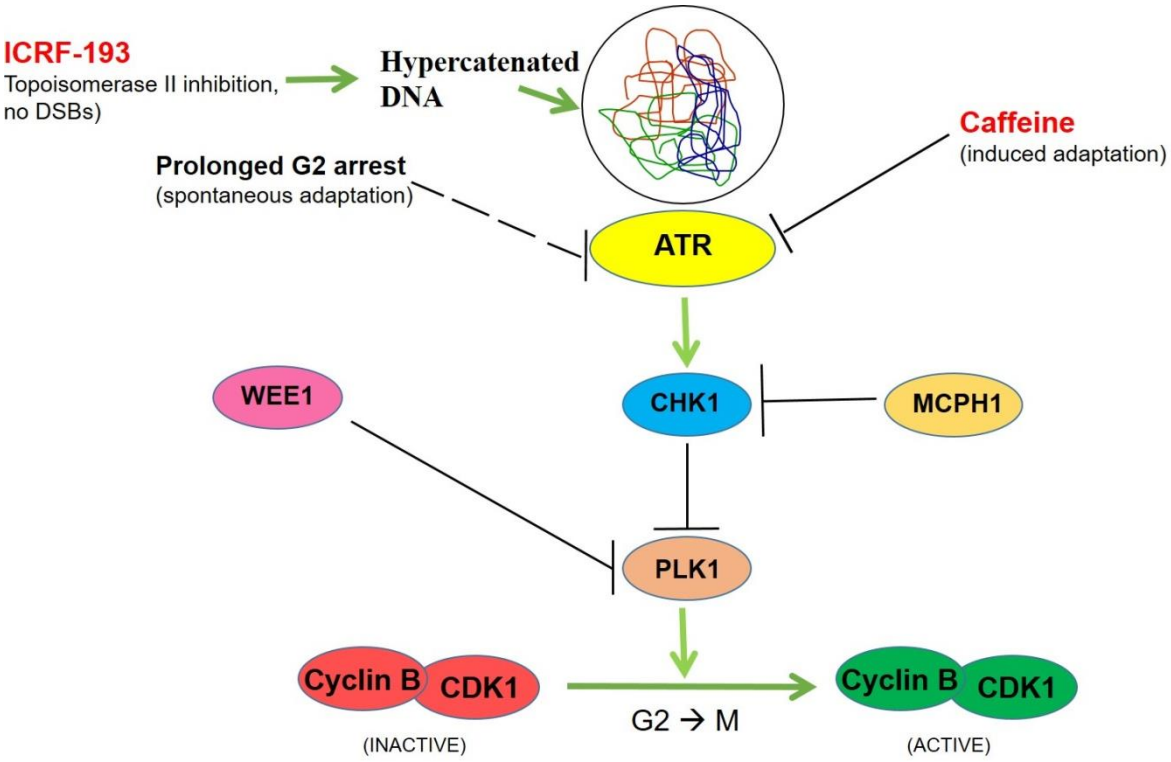
ICRF-193
Topoisomerase II inhibition, no DSBs)
Hypercatenated DNA
Caffeine
(induced adaptation)
Prolonged G2 arrest
(spontaneous adaptation)
ATR
WEE1
CHK1
MCPH1
PLK1
Cyclin B
CDK1
(INACTIVE)
G2 → M
Cyclin B
CDK1
(ACTIVE)

SUPPLEMENTARY INFORMATION

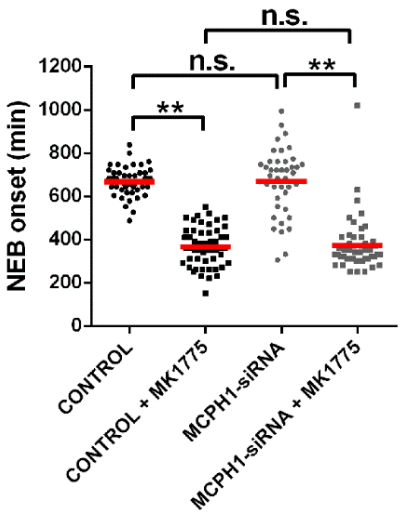

Supplementary figure CIV-S1: Dot-plot showing the timing of NEB onset in control and MCPH1 depleted cells either untreated or incubated with BI2536. Cells were synchronized and transfected with siRNAs as explained in Figure CIV-2. BI2536 was added immediately after release from the second thymidine block. At least 50 cells were analyzed in each case. Time from thymidine release is shown. The red line indicates the mean value. Statistical comparisons for the mean and median data were done by T-student and Wilcoxon (W) tests respectively. ** $p<0.01$.

DISCUSIÓN

DISCUSIÓN

Capítulo I: Deficiencias en la estructura cromosómica en el síndrome MCPH1

Los resultados presentados en el primer capítulo de este estudio demuestran que la falta de función para el gen MCPH1 produce una serie de alteraciones concretas en la estructura de los cromosomas metafásicos. En concreto, los ejes cromatídicos están hiperenrollados y la longitud de los cromosomas está en consecuencia reducida. Además, las cromátidas hermanas aparecen sin resolver muy frecuentemente. La combinación de ejes cromatídicos hiperenrollados y cromátidas sin resolver da lugar a una morfología ondulada distintiva que hemos denominado morfología "*twisted*". Por otro lado, también se ha observado una pérdida de la cohesión centromérica. Todas estas alteraciones también se observan en líneas celulares convencionales humanas (U2OS) cuando se silencia temporalmente la expresión de *MCPH1* con RNAi. Nuestro estudio es clave para entender la contribución de *MCPH1* en los mecanismos que controlan la organización y formación del cromosoma mitótico. En este sentido, las alteraciones descritas en la resolución de las cromátidas hermanas y la cohesión centromérica podrían apuntar a una nueva función molecular de este gen desconocida hasta la fecha.

La visualización de cromátidas hermanas en apariencia no resueltas podría tener implicaciones funcionales importantes. La resolución de las cromátidas hermanas es un proceso dinámico y complejo que requiere la formación de los ejes cromatídicos, la liberación de uniones entre cromatina-cohesina y la eliminación de concatenaciones entre moléculas de ADN que componen ambas cromátidas hermanas (Shintomi y Hirano, 2010; Losada et al., 2002; Miyazaki y Orr-Weaver, 1994). Este conjunto de procesos se completa durante prometafase temprana en células animales, y es fundamental para la correcta segregación anafásica (Losada et al., 2005B; Shintomi et al., 2010). Nuestros resultados sugieren que este proceso podría estar desregulado en ausencia de función para *MCPH1*.

En este sentido, destacan las semejanzas entre la morfología "*twisted*" descrita en nuestro estudio y algunos de los estadios intermedios en la organización cromosómica durante mitosis temprana descritos en estudios previos (Gimenez-Abian et al., 1995). Estos autores sugieren la existencia de asociaciones físicas entre los ejes estructurales de ambas cromátidas hermanas durante el límite profase/prometafase, que las hacen permanecer estrechamente asociadas e indistinguibles. Dichas asociaciones serían muy transitorias y extremadamente difíciles de observar debido a la rapidez con que ocurre en condiciones normales el proceso de individualización de las cromátidas hermanas (Gimenez-Abian et al., 1995). Tampoco puede descartarse que la aparición de cromosomas con

morfología "*twisted*" tenga un significado biológico diferente y que debería tenerse en cuenta en futuras investigaciones sobre los mecanismos moleculares responsables de la condensación cromosómica.

Otro resultado interesante de nuestro trabajo es el aumento en el porcentaje de cromosomas con división centromérica prematura (PCDs, *"Premature Centromeric Division"*) en células sin función para *MCPH1*. Si bien el defecto en la cohesión centromérica no es demasiado acusado – aunque significativo – bajo condiciones de choque hipotónico normales, éste es más pronunciado tras un tratamiento hipotónico más intenso. La pérdida de cohesión cromosómica es una característica común de algunos síndromes o desordenes genéticos, entre otros el Síndrome de Roberts (RBS), el síndrome de aneuploidía variegada en mosaico (MVA) o el síndrome de Cornelia-de-Lange (CdLS) (Tomkins et al., 1979; Kajii et al., 1998; Kaur et al., 2005). Mientras que RBS y CdLS son cohesinopatías, causadas directamente por mutaciones en genes que regulan la cohesión cromosómica (Vega et al., 2005; Tonkins et al., 2004), MVA representa un defecto en el punto de control del huso mitótico (Hanks et al., 2004). Sin embargo, la pérdida de cohesión en células sin función para *MCPH1* es menos dramática y más similar a la situación descrita en pacientes con el síndrome de "enanismo osteodisplásico microcefálico primordial tipo II" (MOPDII), asociado a mutaciones en el gen *PCNT* (Rauch et al., 2008), o en pacientes afectados por "alfa-Talasemia y retraso mental ligado al cromosoma X" por mutaciones en el gen *ATRX* (Ritchie et al., 2008). En ambos síndromes, al igual que hemos descrito en células de pacientes MCPH1, la cohesión centromérica se ve reducida pero no se pierde completamente, y solo es detectada tras condiciones de choque hipotónico fuertes. Tanto *PCNT* como *ATRX* son genes que codifican complejos remodeladores de cromatina que influyen en la cohesión cromatídica a través de diferentes vías: el punto de control del huso mitótico para PCNT, y la unión del complejo cohesina para ATRX (Rauch et al., 2008; Ritchie et al., 2008).

Alteraciones en factores remodeladores de la cromatina también están involucradas en la patogénesis del síndrome MCPH, ya que mutaciones en el gen *PCH1*, un factor remodelador de cromatina, fueron identificadas en una familia afectada por microcefalia primaria (Awad et al., 2013). Sin embargo, los pacientes con este síndrome no mostraban ningún defecto en la cohesión cromosómica. Como conclusión, nuestros resultados podrían indicar que *MCPH1* regula directamente la cohesión centromérica. Alternativamente, las PCDs podrían ser consecuencia indirecta de alteraciones estructurales relacionadas asociadas a la hipercondensación de la cromatina.

Hasta la fecha no hay estudios que describan incrementos en los niveles de aneuploidía en células de pacientes MCPH1, por lo que la reducción en la cohesión centromérica no parece alterar la segregación cromosómica posterior en células sin función para *MCPH1*, aunque faltan estudios más detallados al respecto (ver sección siguiente). A pesar de que el número de pacientes MCPH1 es extremadamente pequeño, la inexistencia de aneuploidías se ve reforzada al no haber evidencias que indiquen una incidencia elevada de casos de cáncer entre ellos. Tampoco se ha encontrado una mayor predisposición a cáncer en los síndromes CdLS (Liu y Krantz, 2008), RBS (Van den Berg y Francke, 1993), MOPDII (Rauch et al., 2008) o ATRX (Gibbons et al., 1995). Sin embargo, si se ha observado un incremento en los niveles de aneuploidía en los síndromes RBS y MOPDII, pero la incidencia es muy baja comparada con pacientes afectados por el síndrome MVA, muchos de los cuales sufren cáncer durante la infancia (Callier et al., 2005).

A pesar de estos datos previos, la correlación entre mutaciones en *MCPH1* y cáncer debe ser investigada en mayor profundidad, ya que la desregulación de su expresión ha sido descrita en algunos tipos de tumores en los últimos años (Venkatesh y Suresh, 2014). Además, estudios recientes en un modelo de ratón muestran que la deficiencia de *Mcph1* promueve la inestabilidad genómica e incrementa la susceptibilidad a cáncer (Liang et al., 2014).

Capítulo II: MCPH1 controla el proceso de alineamiento cromosómico durante mitosis

En la segunda parte de nuestro estudio hemos analizado como están coordinadas la condensación cromosómica y la progresión del ciclo celular en células humanas sin función para el gen *MCPH1*. Los resultados obtenidos demuestran en primer lugar que cuando falta la función de este gen la progresión a través de la fase G2 del ciclo celular y la posterior entrada en mitosis no se ve retrasada. Esto concuerda también con otros resultados que muestran que la mayoría de PLCs en pacientes MCPH1 no son positivas para marcadores mitóticos – H3PS10, H3PS28 y ciclina B – algo descrito previamente y confirmado en nuestro trabajo (Trimborn et al., 2006; Alderton et al., 2006). Además, la tasa de entrada en mitosis sigue dinámicas similares tanto en controles sanos como en células de pacientes MCPH1. En conjunto, estos resultados confirman que las PLCs corresponden a células en las fases G2 o G1 del ciclo, que surgirían como consecuencia de una descoordinación entre la condensación cromosómica y la progresión normal del ciclo celular (O´Driscoll et al., 2006). A pesar de esta descoordinación, las vías moleculares que regulan la transición G2/M son robustas en ausencia de función para este gen, y determinan que la mitosis se inicie según el patrón temporal establecido y no prematuramente.

Se ha propuesto que el inicio de la condensación cromosómica prematura en el síndrome MCPH1 es consecuencia de la activación precoz de CDK1 durante fase G2 (Alderton et al., 2006; Gruber et al., 2011). Nuestros resultados confirman esta implicación, ya que si se impide la activación de CDK1 en células sin función para *MCPH1* no se visualizan PLCs. El papel exacto de MCPH1 en la regulación de CDK1 es por el momento desconocido, aunque parece ocurrir de forma independiente a la vía de señalización de ATR (Alderton et al., 2006; Vassiley et al., 2014). La activación completa del complejo ciclina B-CDK1 es el evento clave para la entrada en mitosis, y está controlada por diferentes vías, redundantes entre sí, organizadas en bucles de retroalimentación que garantizan la activación coordinada de los diferentes eventos mitóticos (Lindqvist et al., 2009). Aunque la mayor parte de CDK1 es activada en el límite G2/M, también se detectan niveles bajos de su forma activa en fase G2 temprana (Lindqvist et al., 2009). En este contexto, nuestros datos podrían indicar que *MCPH1* previene, a través de una vía de señalización desconocida, la condensación cromosómica durante todo G2 al mantener el nivel de activación del complejo ciclina B-CDK1 por debajo del mínimo requerido para el inicio de la condensación. Alternativamente, MCPH1 y CDK1 podrían regular la condensación cromosómica a través de vías independientes, ya que a día de hoy no se ha identificado una asociación directa entre ambos durante este proceso.

Por otro lado, nuestros resultados han identificado una nueva función para el gen *MCPH1* durante mitosis. Así, las células sin función para este gen emplean más tiempo en alinear completamente todos los cromosomas en la placa metafásica en comparación con controles. Esta alteración, no descrita previamente, indica que *MCPH1* tiene función específica en prometafase controlando el alineamiento de los cromosomas. Además, como consecuencia de esta alteración se produce un incremento en la duración de la prometafase y, por extensión, en la duración total de la mitosis. Estudios previos sugerían que la falta de función para este gen daba lugar a un inicio prematuro de la mitosis. Esta conclusión se apoyaba principalmente en el incremento en la frecuencia de mitosis en células sin función para *MCPH1* (Gruber et al., 2011; Tibelius et al., 2009). Sin embargo, nuestros datos revelan claramente que este incremento en el índice mitótico, que también hemos observado en nuestro estudio, se explicaría por la mayor duración global de la mitosis que hemos descrito - producto de una prometafase de mayor duración- y no por un inicio prematuro. Además, tal y como se ha comentado previamente, la transición G2/M en células sin función para *MCPH1* sigue una dinámica similar a la de células control, lo que tampoco estaría de acuerdo con un supuesto inicio prematuro de la mitosis.

Los análisis de inmunofluorescencia en células neuroprogenitoras de un modelo de ratón Mcph1 -/- muestran un incremento en la frecuencia de husos mitóticos bipolares con cromosomas sin alinear (Gruber et al., 2011). Estos errores se explican por una descoordinación entre la maduración centrosómica y el resto de procesos mitóticos. Teniendo en cuenta nuestros resultados y los estudios previos (Gruber et al., 2011), resulta evidente que el proceso de alineamiento cromosómico durante prometafase se ve alterado por la falta de *MCPH1*. Además, el aumento en la duración global de la mitosis es un dato de interés para la discusión científica sobre los mecanismos patogénicos en el síndrome MCPH1 (Woods y Basto, 2014). Así, un incremento en la duración de mitosis tan sutil como el aquí descrito, podría tener un gran impacto en la neurogénesis y afectar a la producción final de neuronas, mientras que en otros tipos celulares dicha alteración no tendría consecuencias tan importantes.

Por el momento se desconocen las bases moleculares que subyacen al defecto en el proceso de alineamiento cromosómico que hemos descrito. Entre otras, podría ser consecuencia de alteraciones menores que afecten a la dinámica de unión cinetocoro-microtúbulos y/o a la dinámica de movimientos cromosómicos a través del huso mitótico hacia el ecuador de la célula. Los defectos en la maduración centrosómica descritos en las células de ratón Mcph1-/- podrían ser otro de los factores subyacentes críticos (Gruber et al., 2011). Además, también deben contemplarse en este escenario las alteraciones en la estructura cromosómica asociadas a la falta de función de *MCPH1*

(descritas en el capítulo I). En particular, el defecto en la resolución de las cromátidas hermanas, al ser éste un proceso crítico que asegura la correcta segregación cromosómica. En este sentido, un estudio reciente concluye que fallos en la resolución de las concatenaciones en el ADN durante la mitosis son el mecanismo patogénico responsable de la aparición de microcefalia en pacientes con mutaciones en el complejo condensina II (Martin et al., 2016). Dada la interacción entre condensina II y MCPH1 (Trimborn et al., 2006; Yamashita et al., 2011), la presencia de cromátidas hermanas sin resolver, y el incremento en la duración de prometafase en células humanas defectivas para *MCPH1*, una hipótesis atractiva es que el proceso de resolución de concatenaciones y superenrollamientos en el ADN durante mitosis está alterado en pacientes MCPH1 y contribuye directamente a la aparición de microcefalia primaria. El ligero incremento en los errores durante la segregación anafásica que hemos observado es un dato en favor de esta hipótesis, ya que la presencia de concatenaciones sin resolver en el ADN es uno de los mecanismos principales que provocan errores en anafase como puentes de ADN y cromosomas retrasados (Germann et al., 2014; Brownlow et al., 2014).

Capítulos III-IV: MCPH1 es esencial en la adaptación celular al "Decatenation Checkpoint" en fase G2 del ciclo celular

La investigación sobre el papel de *MCPH1* en la vía de señalización de G2 denominada "*decatenation checkpoint*" (DC) responde a algunos datos previos. Tal y como se ha comentado en el capítulo anterior, la falta de función para *MCPH1* en células HeLa y Hct116 origina un leve incremento en los errores durante la segregación cromosómica, lo que podría ser consecuencia de un defecto en el proceso que monitoriza este punto de control, esto es, la resolución de concatenaciones en el ADN. Por otro lado, la vía de señalización dependiente de ATR requiere de la función de *MCPH1* para inducir una parada eficiente del ciclo celular en respuesta a la irradiación UV (Alderton et al., 2006). Curiosamente, la vía ATR también es esencial para la activación del "*decatenation checkpoint"* (Damelin y Bestor, 2007).

En primer lugar, nuestros resultados demuestran que el DC se activa en respuesta a la inhibición de Topoisomerasa II en ausencia de función para *MCPH1*, dando lugar a una parada celular en G2 y evitando la entrada en mitosis. Esta activación normal se evidenció tanto en líneas celulares de pacientes MCPH1 como en células HeLa con silenciamiento temporal de *MCPH1* por RNAi. Estos datos concuerdan con estudios previos que muestran la existencia de un *DC* eficiente en líneas celulares de linfoblastos humanos (Deming et al., 2001; Bower et al., 2010A), y sugieren que la función de *MCPH1* es dispensable para su activación. Sin embargo, es destacable que la respuesta de este punto de control a largo plazo mostró diferencias interesantes entre células control y células sin función para *MCPH1*. La capacidad del DC para mantener el ciclo celular detenido en G2 es solo temporal, de modo que generalmente las células terminan entrando en mitosis a pesar de presentar alteraciones graves en la topología cromosómica (Damelin y Bestor, 2007; Lee et al., 1997; Downes et al., 1994; Gorbsky, 1994; Ishida et al., 1994). Esta dinámica también fue observada en nuestro estudio en células control que tienen *MCPH1* funcional (Figura CIII-1A y Figura CIII-2B). Sin embargo, cuando carecen de la función de este gen las células no son capaces de adaptarse espontáneamente al punto de control e iniciar la división celular, permaneciendo paradas en G2 de modo permanente.

Este descubrimiento nos llevó a estudiar más a fondo el fenómeno de adaptación celular al DC, para lo que analizamos la dinámica del ciclo celular en presencia de ICRF-193 y tras la inactivación forzada de este punto de control. Con ese fin se empleó cafeína, un conocido inhibidor de las quinasas ATM/ATR que anula la respuesta celular del DC, determinando así una adaptación celular forzada muy rápida al punto de control (Deming et al., 2001). De nuevo se observaron resultados sorprendentes. Mientras que en estas condiciones las células control entran en mitosis sin retraso

alguno en G2, las células sin función para *MCPH1* permanecen detenidas en G2 largo tiempo. Cuando se analizó la estructura cromosómica en células control tratadas con ICRF-193 y cafeína se observó un elevado número de mitosis con cromosomas muy alterados, consecuencia directa de la falta de actividad de Topoisomerasa II (Downes et al., 1994; Deming et al., 2002; Gimenez-Abian et al., 2000; Bower et al., 2010B). Sin embargo, en células sin *MCPH1* tratadas en las mismas condiciones no se observaron dichas alteraciones cromosómicas; por el contrario, en este caso aumentaba la frecuencia de PLCs. Por tanto, la adaptación celular espontánea al DC está severamente alterada cuando falta *MCPH1*, y la habilidad de cafeína para inducir una adaptación forzada en presencia de ICRF-193 también está comprometida.

Estos resultados fueron confirmados en dos modelos experimentales distintos, células HeLa con *MCPH1* silenciado por RNAi y linfoblastos de pacientes, y sugieren que *MCPH1* forma parte de la vía de señalización que regula la respuesta adaptativa al DC. Sin embargo, su función no es imprescindible en la cascada de reacciones que controlan su activación. El DC implica la vía de señalización de ATR (Deming et al., 2001), vía molecular que requiere la función de *MCPH1* para bloquear de forma eficiente el ciclo celular en respuesta al daño en el ADN por radiación UV (Alderton et al., 2006). Por tanto, la demostración de una activación eficiente del DC en ausencia de *MCPH1* funcional es un resultado llamativo e inesperado. En conjunto, estos resultados refuerzan la idea de que ambas vías de señalización, las que responden a la radiación UV y a la inhibición catalítica de Topoisomerasa II, difieren en sus mecanismos de activación y en algunos componentes de las rutas de señalización, si bien ambas dependen en origen de la activación de ATR.

Otro aspecto interesante que hemos analizado es si la activación del DC influye sobre la condensación cromosómica alterada característica de células sin función para MCPH1. Nuestros análisis demuestran que el tratamiento prolongado con ICRF-193 induce la descondensación de la cromatina en las células que muestran el fenotipo PLC. Dado que el inicio prematuro y el mantenimiento prolongado de condensación cromosómica en células deficientes para *MCPH1* depende de la activación prematura de CDK1 (Alderton et al., 2006) (resultados capítulo II de este trabajo), la descondensación observada podría ser consecuencia directa de la vía de señalización ATR, al producir la inactivación de CDK1. Esto también explicaría la dinámica contraria observada para las PLCs tras adicionar cafeína. En este caso la condensación no es revertida, probablemente porque CDK1 no se inactiva al estar inhibida la vía de señalización de ATR.

Por otro lado, las observaciones podrían ser consecuencia directa de la actividad de otro punto de control del ciclo celular denominado "*antephase checkpoint*". Este punto de control actúa al final de G2 en respuesta a diferentes tipos de estrés celular como shock hipotónico, radiación UV o

perturbaciones topológicas de la cromatina (Rieder y Cole, 2000; Mikhailov et al., 2004; Ching y Yeong, 2010). Su nombre "antefase" hace referencia a la manifestación citológica que se visualiza tras su activación, esto es, la descondensación cromosómica en células que se encuentran en profase temprana. Su vía de señalización no requiere de la actividad de ATM/ATR; sin embargo, es críticamente dependiente de la señalización de P38 MAPK (Matsusaka y Pines, 2004; Mikhailov et al., 2004). Por tanto, si nuestros resultados fueran consecuencia directa de la activación del "*antephase checkpoint"*, el silenciamiento del mismo con inhibidores específicos de P38 MAPK debería restaurar la progresión celular en células sin función para *MCPH1*. Sin embargo, esto no fue lo observado en nuestro estudio, ya que las células *MCPH1* continuaban paradas en G2, lo que sugiere que dicha respuesta es independiente de la señalización de P38 MAPK (Figura CIII-3). Por tanto, parece poco probable que P38 MAPK participe en la vía de señalización que responde a la inhibición catalítica de Topoisomerasa II, lo que concuerda con algunos estudios previos (Damelin y Bestor, 2007). Sin embargo, otros autores si consideran que el antephase checkpoint es el punto de control que responde a la inhibición de Topoisomerasa II (Mikhailov et al., 2004), por lo que estudios adicionales serían de interés para elucidar esta cuestión.

Dada la implicación de *MCPH1* en la adaptación celular al DC, también hemos investigado si la función de este gen es importante en la respuesta adaptativa en otros puntos de control del ciclo celular, como el que responde al daño en el ADN durante G2. Mientras que ICRF-193 es un inhibidor catalítico de Topoisomerasa II que no causa daño en el ADN, existen inhibidores químicos que bloquean este enzima en una conformación que genera DSBs masivamente (Damelin y Bestor, 2007) (Figura CIII-4). Según esto, los inhibidores químicos de Topoisomerasa II inducen una parada del ciclo celular en G2 debido a la activación del punto de control por daño en el ADN, que requiere de ATM/ATR (Clarke et al., 2006; Luo et al., 2009; Bower et al., 2010B). De acuerdo con estos datos, era de interés definir si la función de *MCPH1* es requerida en la respuesta al tratamiento con etoposido, un inhibidor químico de Topoisomerasa II, o durante la adaptación celular al mismo. La dinámica observada fue similar en células con y sin función para *MCPH1*: en presencia de etoposido las células no entran en mitosis y quedan paradas en G2; sin embargo, este bloqueo es omitido eficientemente cuando se adiciona cafeína.

Por tanto, en células sin función para *MCPH1* la respuesta al daño en el ADN inducida tras la inhibición química de Topoisomerasa II es eficiente y sensible a cafeína. De este modo, mientras que *MCPH1* es esencial para la adaptación al punto de control en G2 en presencia de ICRF-193 (DC), su función no es necesaria durante la adaptación al punto de control dependiente de ATM que responde a la presencia de DSBs. Estos resultados concuerdan con análisis previos de irradiación en

células de pacientes MCPH1 (Gavvovidis et al., 2010), y con otros estudios que muestran una respuesta canónica del punto de control regulado por ATM en células sin función para este gen (Brown et al., 2010; Gruber et al., 2011; Zhou et al., 2013). Hay que destacar que las diferentes dinámicas de adaptación celular observadas en respuesta a los diferentes tratamientos con inhibidores específicos de Topoisomerasa II, ICRF-193 o etoposido, están de acuerdo con la idea de que el punto de control por daño en el ADN y el DC son vías de señalización diferentes que regulan la entrada en mitosis (Damelin y Bestor, 2007; Bower et al., 2010B). Aunque ambos puntos de control comparten la dependencia de ATR, otros componentes son únicos para cada vía de señalización.

Los resultados de este estudio permiten avanzar en la comprensión sobre la vía de señalización del DC, aún bastante desconocida. Dado que MCPH1 regula la función centrosómica de CHK1 durante la progresión normal del ciclo celular (Tibelius et al., 2009) y que esta última es un elemento clave en la vía de señalización de ATR, hemos examinado el papel potencial de la quinasa CHK1 en el DC, donde existe cierta controversia acerca de su contribución (Deming et al., 2001; Robinson et al., 2007). Nuestros resultados indican con claridad que CHK1 participa en el DC, ya que su inhibición tanto en células control como en células sin función para *MCPH1* elimina la parada del ciclo en G2 que impone ICRF-193. En línea con esto, estudios previos muestran que células DT40 Chk1 -/- exhiben un DC ineficiente (Robinson et al., 2007). El papel exacto de CHK1 en este punto de control está por determinar, y no parece estar relacionado con un incremento en los niveles de CHK1 fosforilada en S345, que es considerada la forma activa de esta quinasa (Deming et al., 2001; Bower et al., 2010A) (Figura CIII-6). Por otro lado, las células sin función para *MCPH1* recuperan su capacidad de adaptación al DC cuando se inhibe CHK1, lo que sugiere que MCPH1 se localiza por encima de CHK1 – y por debajo de ATR – en la ruta de señalización que controla la adaptación celular al DC, dónde regularía negativamente su función (Figura D-1).

Estudios previos han demostrado que la parada del ciclo celular en respuesta a ICRF-193 requiere la inactivación de la quinasa PLK1 (Deming et al., 2002). Aún está por definir cómo su función es regulada durante la activación del DC, aunque se han identificado algunos moduladores potenciales como ATR, MDC1 y Topoisomerasa IIα (Deming et al., 2002; Luo et al., 2000). Considerando estos datos, hemos analizado en nuestro estudio si PLK1 es un factor esencial en el contexto celular opuesto, es decir, en la adaptación al DC. Nuestro estudio demuestra con claridad que la función de PLK1, de forma similar a MCPH1, también es necesaria en el proceso de adaptación celular que previene la parada del ciclo tras la activación del DC. Además, la inhibición simultánea tanto de ATR como de CHK1 no parece tener ningún efecto en la respuesta celular al tratamiento con ICRF-

193 y un inhibidor de PLK1 (BI2536), permaneciendo las células, tanto control como con *MCPH1* no funcional, bloqueadas de manera permanente en G2. Estos resultados sugieren que PLK1 actúa por debajo de CHK1, MCPH1 y ATR dentro de la vía de señalización que controla la adaptación a la activación del DC (Figura D-1).

Nuestros resultados en conjunto, han permitido avanzar en la comprensión de la vía de señalización que controla la adaptación celular al DC, que comprende, entre otros, PLK1, CHK1, MCPH1 y ATR. Curiosamente, todos ellos son dispensables para la entrada en mitosis en ausencia de alteraciones en el ADN (Pines y Rieder, 2001; Lindqvist et al., 2009; Alderton et al., 2006; Brown y Baltimore, 2003) pero se vuelven esenciales en la adaptación celular al DC. Esta dependencia refuerza las ideas previas de algunos autores, que establecen que mientras que la entrada en mitosis puede ocurrir por diferentes vías alternativas redundantes en condiciones normales, en un contexto de alteraciones en el ADN pasa a depender críticamente de una sola de ellas (Lindquvist et al., 2009). Estudios previos habían demostrado que la función de PLK1 es esencial en la adaptación celular al punto de control que responde a la presencia de DSBs en el ADN (Toczyski et al., 1997; Syljuasen et al., 2006; Van Vugt et al., 2004).

Nuestro estudio demuestra que las vías de señalización que inducen adaptación celular están integradas por diferentes componentes según el tipo concreto de alteración que se produce. Por ejemplo, *MCPH1* no es necesario para la adaptación celular en respuesta a la radiación ionizante, pero si frente a alteraciones en la topología del ADN. También encontramos diferencias en relación con la actividad de la quinasa WEE1 en estas vías de señalización. Mientras que WEE1 actúa por debajo de PLK1 en la respuesta adaptativa que responde a la presencia de DSBs (Van Vugt et al., 2004), la situación parece ser la contraria en la vía que regula la adaptación al DC, estando PLK1 por debajo de WEE1 (Figura D-1). Por otro lado, tampoco podemos excluir que WEE1 y PLK1 regulen la capacidad de adaptación celular al DC a través de diferentes vías.

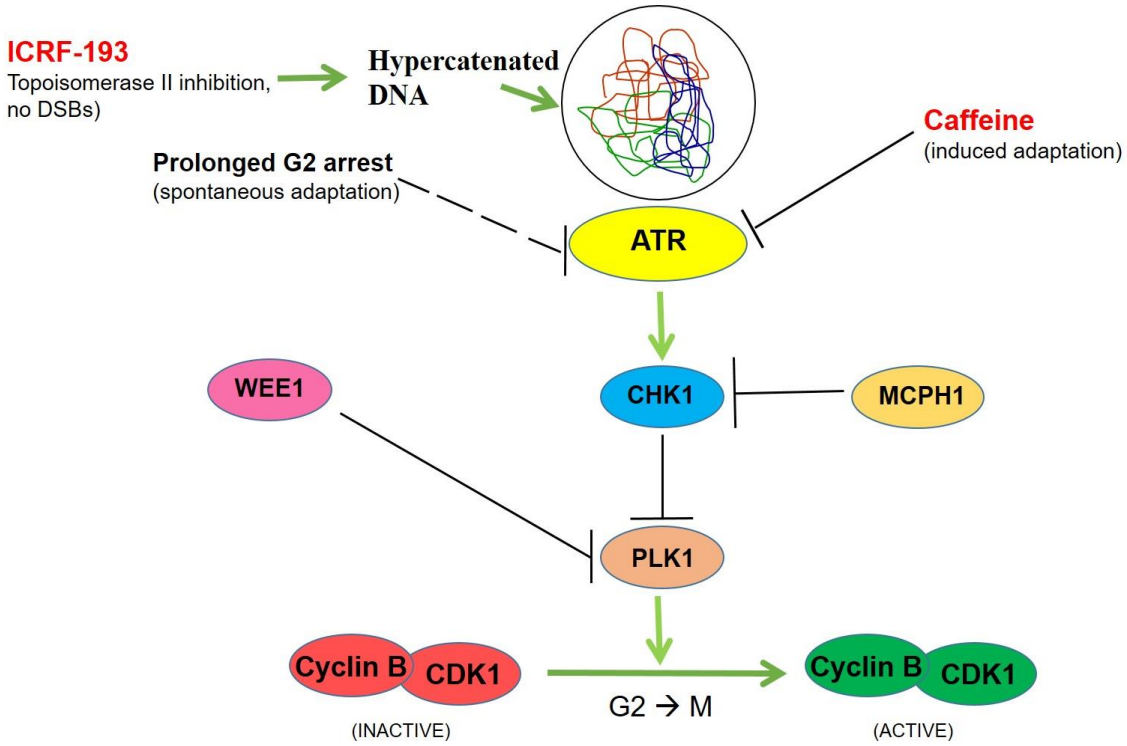

Figura D-1: Esquema simplificado del modelo propuesto para la vía de señalización que regula la adaptación al *"decatenation checkpoint"* Las flechas verdes indican activación, las líneas negras inactivación. Las versiones activa e inactiva del complejo ciclina B-CDK1 se indica con los colores verde y rojo respectivamente.

CONCLUSIONES

CONCLUSIONES

1. La falta de función de MCPH1 altera la morfología de los cromosomas mitóticos de forma específica. Así, los ejes cromatídicos están hiperenrollados y las cromátidas hermanas aparecen frecuentemente sin resolver, lo que da lugar a una morfología ondulada distintiva denominada "*twisted*".
2. En ausencia de MCPH1 los cromosomas mitóticos muestran una pérdida de cohesión centromérica, lo que podría indicar una función desconocida hasta la fecha para este gen en el proceso que determina la cohesión cromosómica.
3. En condiciones fisiológicas normales (ausencia de daño en el ADN), las células con falta de función para MCPH1 progresan a través de la fase G2 del ciclo celular e inician mitosis sin retraso comparadas con células que si tienen funcional este gen.
4. El fenotipo PLC ("Prohase-like cells") se corresponde con células en fase G2 o G1 del ciclo celular en las que la condensación cromosómica es visible, como consecuencia de una descoordinación entre la ejecución de este proceso y la mitosis.
5. La inhibición de la actividad de CDK1 impide el inicio y/o el mantenimiento de la condensación cromosómica en las PLCs que se originan durante la fase G2. Según esto, la actividad de MCPH1 sería necesaria para regular los niveles mínimos de CDK1 activo requeridos para el inicio del proceso de condensación.
6. MCPH1 regula el proceso de alineamiento cromosómico durante prometafase. Las células sin función para MCPH1 necesitan más tiempo en comparación con controles para alinear completamente sus cromosomas en la placa metafásica.
7. Debido a la extensión en los tiempos de alineamiento cromosómico durante prometafase, la duración total de mitosis en células carentes de función de MCPH1 está incrementada. Esta alteración es de importancia para el mecanismo patogénico responsable de la aparición de microcefalia primaria.
8. La función de MCPH1 no es necesaria para la activación del "*decatenation checkpoint"* (DC), punto de control que funciona durante la fase G2 del ciclo celular en respuesta a la inhibición de Topoisomerasa II.
9. MCPH1 es imprescindible en la respuesta adaptativa al DC. Así, la adaptación celular espontánea a este punto de control está severamente alterada cuando falta MCPH1, y la habilidad de cafeína para inducir una adaptación forzada en presencia ICRF-193, un inhibidor catalítico de Topoisomerasa II, también está comprometida.

10. La actividad de MCPH1 es por el contrario dispensable tanto para el funcionamiento como en la adaptación al punto de control que se activa por roturas de cadena doble en el ADN. Esto demuestra que el punto de control por daño en el ADN y el DC son vías de señalización diferentes que regulan la entrada en mitosis. Si bien ambos comparten la dependencia de ATR, otros componentes son únicos para cada vía de señalización.
11. El bloqueo permanente en G2 e insensible a cafeína que muestran células sin función para MCPH1 tras la incubación con el inhibidor de Topo II ICRF-193 no se revierte tras la inhibición de P38 MAPK, principal regulador del "*antephase checkpoint"*. Este punto de control no está por tanto implicado en el bloqueo celular observado.
12. La actividad de CHK1 es necesaria para el mantenimiento de un bloqueo eficiente en G2 por activación del DC. En la vía de señalización que regula la respuesta de adaptación a este punto de control CHK1 actúa aguas abajo de MCPH1, ya que la parada permanente en G2 que induce ICRF-193 en células sin función para MCPH1 se revierte tras la inhibición simultánea de CHK1.
13. La función de PLK1 también es necesaria para la adaptación celular al DC. PLK1 actúa por debajo de CHK1, MCPH1 y ATR dentro de la vía de señalización que controla esta respuesta.
14. WEE1 contribuye parcialmente en la respuesta adaptativa al DC. En esta vía de señalización estaría situada aguas arriba de PLK1; alternativamente WEE1 y PLK1 podrían regular la capacidad de adaptación a este punto de control a través de vías independientes.

CONCLUSIONS

1. MCPH1 loss of function results in altered shaping of mitotic chromosomes. Thus, chromatid axes are hypercoiled and sister chromatids appears frequently unresolved, giving rise to a distinctive wavy morphology referred to as "twisted".
2. Chromosomes from cells lacking MCPH1 function show loss of centromeric cohesion. This alteration might point towards a so far unknown function of MCPH1 in the mechanism regulating chromosome cohesion.
3. Under undamaging conditions cells lacking MCPH1 progress through G2 phase of cell cycle and start mitosis on schedule.
4. PLCs ("Prophase-like cells") are either G2 or G1 cells that arise as consequence of premature chromosome condensation and delayed decondensation respectively.
5. Inhibition of CDK1 activity prevents chromosome condensation onset and its maintenance thereafter in G2 PLCs. According to this, MCPH1 seems to maintain the levels of active CDK1 during G2 below the minimum levels required for chromatin condensation onset.
6. MCPH1 regulates the process of chromosome alignment during prometaphase. Cells lacking MCPH1 function employ more time than control cells to fully align all their chromosomes at the metaphase plate.
7. As consequence of lengthened prometaphase, the timing of mitosis is increased in cells without MCPH1 function. Such mitotic delay could potentially contribute to the pathogenic mechanism of MCPH1 primary microcephaly.
8. MCPH1 function is not required for the activation of the decatenation checkpoint (DC), a molecular pathway that delays mitosis onset in response to Topoisomerase II inhibition.
9. MCPH1 function is required to allow cellular adaptation to the DC. Both, spontaneous and caffeine-induced adaptation to this checkpoint is severely altered when MCPH1 function is loss.
10. MCPH1 is not involved in the pathways controlling either activation or cellular adaptation to the G2 checkpoint that responds to double strand breaks in the DNA (DSBs). This result supports the notion that DNA damage and decatenation checkpoints are different G2 pathways regulating mitosis entry.
11. The permanent caffeine-insensitive G2 arrest observed in MCPH1 cells after inhibition of Topoisomerase II by ICRF-193 incubation is not bypassed if P38 MAPK, modulator of the antephase checkpoint, is simultaneously inhibited. This checkpoint is thus not involved in the ICRF-193-related G2 cell arrest.

12. CHK1 activity is required by the DC for establishing an efficient G2 arrest. Since the permanent G2 arrest induced by the DC in MCPH1 cells is abolished after simultaneous inhibition of CHK1, CHK1 is likely acting downstream of MCPH1 in the pathway regulating adaptation to it.
13. PLK1 function is also required to allow cellular adaptation to the DC. PLK1 likely acts downstream of CHK1, MCPH1 and ATR in this signaling pathway.
14. WEE1 contributes partially in the adaptive response to the DC. Within this pathway, WEE1 might act upstream of PLK1 or, alternatively, both might control DC adaptation through different pathways.

BIBLIOGRAFÍA DE LA INTRODUCCIÓN Y DE LA DISCUSIÓN

BIBLIOGRAFÍA DE LA INTRODUCCIÓN Y DE LA DISCUSIÓN

Abe S, Nagasaka K, Hirayama Y, Kozuka-Hata H, Oyama M, Aoyagi Y, Obuse C, Hirota T. (2011). The initial phase of chromosome condensation requires Cdk1-mediated phosphorylation of the CAP-D3 subunit of condensin II. Genes Dev. **25,** 863-74.

Abraham RT. (2001). Cell cycle checkpoint signaling through the ATM and ATR kinases. Genes Dev. 15, 2177–2196.

Ahmad I, Baig SM, Abdulkareem AR, Hussain MS, Sur I, Toliat MR, Nürnberg G, Dalibor N, Moawia A, Waseem SS, Asif M, Nagra H, Sher M, Khan MM., Hassan I, Rehman Su, Thiele H, Altmüller J, Noegel AA and Nürnberg P. (2017). Genetic heterogeneity in Pakistani microcephaly families revisited. Clin Genet, 92: 62-68.

Akimitsu N, Adachi N, Hirai H, Hossain MS, Hamamoto H, Kobayashi M et al. (2003). Enforced cytokinesis without complete nuclear division in embryonic cells depleting the activity of DNA topoisomerase IIalpha. Genes Cells 8: 393–402.

Alakbarzade V, Hameed A, Quek DQY, Chioza BA, Baple EL, Cazenave-Gassiot A, Nguyen LN, Wenk MR, Ahmad AQ, Sreekantan-Nair A, Weedon MN, Rich P, Patton MA, Warner TT, Silver DL, Crosby AH. (2015). A partially inactivating mutation in the sodium-dependent lysophosphatidylcholine transporter MFSD2A causes a non-lethal microcephaly syndrome. Nature Genet. 47: 814-817.

Alderton GK, Galbiati L, Griffith E, Surinya KH, Neitzel H, Jackson AP. (2006). Regulation of mitotic entry by microcephalin and its overlap with ATR signalling. Nat Cell Biol. 8, 725-33.

Alvarez-Fernández M, Halim VA, Krenning L, Aprelia M, Mohammed S, Heck AJ, et al. (2010). Recovery from a DNA damage-induced G2 arrest requires Cdk-dependent activation of FoxM1. EMBO R 2010; 11:452-8.

Alvarez-Fernández M, Medema RH. (2010). Transcriptional regulation underlying recovery from a DNA damage-induced arrest. *Transcription*, 1(1), pp. 32–35.

Antonczak AK, Mullee LI, Wang Y, Comartin D, Inoue T, Pelletier L, Morrison CG. (2016). Opposing effects of pericentrin and microcephalin on the pericentriolar material regulate CHK1 ctivation in the DNA damage response. Oncogene. 14;35(15):2003-10.

Arnaud L, Pines J, Nigg EA. (1998). GFP tagging reveals human Polo-like kinase 1 at the kinetochore/centro- mere region of mitotic chromosomes. Chromosoma 107: 424–429.

Asencio C, Davidson IF, Santarella-Mellwig R, Ly-Hartig TB, Mall M, Wallenfang MR, Mattaj IW, Gorjanacz M. (2012). Coordination of Kinase and Phosphatase Activities by Lem4 Enables Nuclear Envelope Reassembly during Mitosis. Cell 150, 122–135.

Austin CA, and Marsh KL. (1998). topoisomerase II, pp. 215–226.

Awad S, Al-Dosari MS, Al-Yacoub N, Colak D, Salih MA, Alkuraya FS, Poizat C. (2013) Mutation in PHC1 implicates chromatin remodeling in primary microcephaly pathogenesis. Hum Mol Genet. 22(11):2200-13. doi: 10.1093/hmg/ddt072.

Baniahmad A, Steiner C, Kohne AC, and Renkawitz R. (1990). Modular structure of a chicken lysozyme silencer: involvement of an unusual thyroid hormone receptor binding site. Cell, 61(3): 505–514. doi:10.1016/0092-8674(90)90532-J. PMID:2159385.

Barbelanne M, Tsang WY. (2014). Molecular and cellular basis of autosomal recessive primary microcephaly. Biomed Res Int. 2014:547986. doi: 10.1155/2014/547986 (2014).

Barr AR, and Gergely F. (2007). Aurora-A: the maker and breaker of spindle poles. J. Cell Sci. 120:2987–2996.

Bartek J, Lukas J. (2001A). Mammalian G1- and S-phase checkpoints in response to DNA damage, Curr. Opin. Cell Biol. 13 738–747.

Bartek J, Lukas J. (2001B). Pathways governing G1/S transition and their response to DNA damage, FEBS Lett. 490 (2001) 117–122.

Bartek J, Lukas J. (2007). DNA damage checkpoints: from initiation to recovery or adaptation. Curr Opin Cell Biol; 19(2):238–45. PMID: 17303408.

Belmont AS. (2006). Mitotic chromosome structure and condensation. Curr. Opin. Cell Biol. 18:632–638.

Berger JM, Gamblin SJ, Harrison SC, Wang JC. (1996). Structure and mechanism of DNA topoisomerase II. *Nature*, pp. 225–232.

Biersack H, Jensen S, Gromova I, Nielsen IS, Westergaard O, Andersen AH. (1996). Active heterodimers are formed from human DNA topoisomerase IIa and IIb isoforms. Proc Natl Acad Sci USA 93: 8288–8293.

Bilguvar K, Ozturk AK, Louvi A, Kwan KY, Choi M, Tatli B, Yalnizoglu D, Tuysuz B, Caglayan AO, Gokben S, Kaymakcalan H, Barak T, Bakircioglu M, Yasuno K, Ho W, Sanders S, Zhu Y, Yilmaz S, Dincer A, Johnson MH, Bronen RA, Kocer N, Per H, Mane S, Pamir MN, Yalcinkaya C, Kumandas S, Topcu M, Ozmen M, Sestan N, Lifton RP, State MW, Gunel M. (2010). Whole-exome sequencing identifies recessive WDR62 mutations in severe brain malformations. Nature 467:207–210.

Blasina A, Price BD, Turenne GA, and McGowan CH. (1999). Caffeine inhibits the checkpoint kinase ATM. Curr. Biol. Res. *50*, 353–366.

Bond J, Roberts E, Mochida GH, Hampshire DJ, Scott S, Askham JM, Springell K, Mahadevan M, Crow YJ, Markham AF, et al. (2002). ASPM is a major determinant of cerebral cortical size. Nat. Genet. 32, 316-320.

Bond J, Scott S, Hampshire DJ, Springell K, Corry P, Abramowicz MJ, Mochida GH, Hennekam RC, Maher ER, Fryns JP, Alswaid A, Jafri H, Rashid Y, Mubaidin A, Walsh CA, Roberts E, Woods CG. (2003). Protein-Truncating Mutations in ASPM Cause Variable Reduction in Brain Size. *The American Journal of Human Genetics*, 73(5), pp. 1170–1177.

Bond J, Roberts E, Springell K, Lizarraga SB, Scott S, Higgins J, et al. (2005). A centrosomal mechanism involving CDK5RAP2 and CENPJ controls brain size, Nat. Genet. 37; 353e355.

Bower JJ, Zhou Y, Zhou T, Simpson DA, Arlander SJ, Paules RS, Cordeiro-Stone M, Kaufmann WK. (2010A). Revised genetic requirements for the decatenation G2 checkpoint: the role of ATM. Cell Cycle. 9(8):1617-28.

Bower JJ, Karaca GF, Zhou Y, Simpson DA, Cordeiro-Stone M, Kaufmann WK. (2010B). Topoisomerase IIalpha maintains genomic stability through decatenation G (2) checkpoint signaling. Oncogene. 29(34):4787-99.

Brooks K, Ranall M, Spoerri L, Stevenson A, Gunasingh G, Pavey S, Meunier F, Gonda TJ, Gabrielli B. (2014). Decatenation checkpoint-defective melanomas are dependent on PI3K for survival. *Pigment cell & melanoma research*, 27(5), pp. 813–821.

Brown JA, Bourke E, Liptrot C, Dockery P, Morrison CG. (2012). MCPH1/BRIT1 limits ionizing radiation-induced centrosome amplification. Oncogene. 2010 Oct 7;29(40):5537-44.

Brown EJ, Baltimore D. (2003). Essential and dispensable roles of ATR in cell cycle arrest and genome maintenance. *Genes and Development*, 17(5), pp. 615–628.

Brownlow N, Pike T, Zicha D, Collinson L, Parker PJ. (2014). Mitotic catenation is monitored and resolved by a PKCε-regulated pathway. Nat Commun 5, 5685.

Bruinsma W, Berg JVD, Aprelia M. (2016). Tousled-like kinase 2 regulates recovery from a DNA damage-induced G 2 arrest', 17(5), pp. 1–12.

Brüning-Richardson A, Bond J, Alsiary R, Richardson J, Cairns DA, McCormack L, Hutson R, Burns P, Wilkinson N, Hall GD, Morrison EE, Bell SM. (2011). ASPM and microcephalin expression in epithelial ovarian cancer correlates with tumour grade and survival. *British Journal of Cancer*, 104(10), pp. 1602–1610. doi: 10.1038/bjc.2011.117.

Brunk K, Vernay B, Griffith E, Reynolds NL, Strutt D, Ingham PW, et al. (2007). Microcephalin coordinates mitosis in the syncytial Drosophila embryo. J Cell Sci; 120:3578-88.

Burden DA. and Osheroff N. (1998) Mechanism of action of eukaryotic topoisomerase II and drugs targeted to the enzyme. Biochim. Biophys. Acta, 1400, 139–154.

Callier P, Faivre L, Cusin V, Marle N, Thauvin-Robinet C, Sandre D, Rousseau T, Sagot P, Lacombe E, Faber V, Mugneret F. (2005). Microcephaly is not mandatory for the diagnosis of mosaic variegated aneuploidy syndrome. Am J Med Genet A. 137(2), 204-7.

Chen CC, Dechassa ML, Bettini E, Ledoux MB, Belisario C, Heun P, Luger K, Mellone BG. (2014). CAL1 is the Drosophila CENP-A assembly factor. J. Cell Biol. 204:313–329. http://dx.doi.org/10.1083/ jcb.201305036.

Chen T, Sun Y, Ji P, Kopetz S, Zhang W. (2015). Topoisomerase IIα in chromosome instability and personalized cancer therapy. *Oncogene*, 34(31), pp. 4019–4031.

Chin CF, Yeong FM. (2010) Safeguarding entry into mitosis: the antephase checkpoint. Mol Cell Biol 30:22–32.

Clarke DJ, Johnson RT, and Downes CS. (1993) Topoisomerase II inhibition prevents anaphase chromatid segregation in mammalian cells independently of the generation of DNA strand breaks. J. Cell Sci., 105, 563–569.

Clarke DJ, Vas AC, Andrews CA, Díaz-Martínez LA, Giménez-Abián JF. (2006). Topoisomerase II checkpoints: universal mechanisms that regulate mitosis. Cell Cycle. 5(17):1925-8.

Clausen TH, Lamark T, Isakson P, Finley K, Larsen KB, Brech A, Overvatn A, Stenmark H, Bjorkoy G, Simonsen A, Johansen T. (2010). p62/SQSTM1 and ALFY interact to facilitate the formation of p62 bodies/ALIS and their degradation by autophagy. Autophagy 6: 330-344.

Coelho PA, Queiroz-Machado J, Carmo AM, Moutinho-Pereira S, Maiato H, Sunkel CE. (2008). Dual role of topoisomerase II in centromere resolution and aurora B activity. PLoS Biol 6:e207.

Cortes F, Pastor N, Mateos S, Dominguez I. (2003). Roles of DNA topoisomerases in chromosome segregation and mitosis. Mutat Res 543: 59–66.

Damelin M, Sun YE, Sodja VB, Bestor TH. (2005). Decatenation checkpoint deficiency in stem and progenitor cells. Cancer Cell 8: 479–484.

Damelin M, Bestor TH. The decatenation checkpoint. (2007). Br J Cancer. 96(2):201-5.

Darvish H, Esmaeeli-Nieh S, Monajemi GB, Mohseni M, Ghasemi-Firouzabadi S, Abedini SS, Bahman I, Jamali P, Azimi S, Mojahedi F, Dehghan A, Shafeghati Y, Jankhah A, Falah M, Soltani Banavandi MJ, Ghani-Kakhi M, Garshasbi M, Rakhshani F, Naghavi A, Tzschach A, Neitzel H, Ropers HH, Kuss AW, Behjati F, Kahrizi K, Najmabadi H. (2010). A clinical and molecular genetic study of 112 Iranian families with primary microcephaly. *Journal of Medical Genetics*, 47(12), pp. 823–828.

De Laat WL, Jaspers NG, Hoeijmakers JH. (1999). Molecular mechanism of nucleotide excision repair. Genes Dev; 13(7):768–85. PMID: 10197977.

De Souza CPC, Ellem KAO, Gabrielli BG. (2000). Centrosomal and cy- toplasmic Cdc2/cyclin B1 activation precedes nuclear mitotic events. Exp. Cell Res. 257:11–21.

Deming PB, Cistulli CA, Zhao H, Graves PR, Piwnica-Worms H, Paules RS, Downes CS, Kaufmann WK. (2001). The human decatenation checkpoint. Proc Natl Acad Sci U S A;98(21):12044-9.

Deming PB, Flores KG, Downes CS, Paules RS, Kaufmann WK. (2002). ATR enforces the topoisomerase II-dependent G2 checkpoint through inhibition of Plk1 kinase. J Biol Chem;277(39):36832-8.

Diaz-Martinez LA, Gimenez-Abian JF, Azuma Y, Guacci V, Gimenez-Martin G, Lanier LM et al. (2006). PIASgamma is required for faithful chromosome segregation in human cells. PLoS ONE 1: e53.

DiStasio A, Driver A, Sund K, Donlin M, Muraleedharan RM, Pooya S, Kline-Fath B, Kaufman KM, Prows CA, Schorry E, Dasgupta B, Stottmann RW. (2017). Copb2 is essential for embryogenesis and hypomorphic mutations cause human microcephaly. Hum. Molec. Genet. 26: 4836-4848.

Do Carmo Avides M, and Glover DM. (1999). Abnormal spindle protein, Asp, and the integrity of mitotic centrosomal microtubule organizing centers. Science 283, 1733- 1735.

Do Carmo-Avides M, Tavares A, and Glover DM. (2001) 'Polo kinase and Asp are needed to promote the mitotic organizing activity of centrosomes', *Nature Cell Biology*, 3(4), pp. 421–424.

Doherty SC, McKeown SR, McKelvey-Martin V, Downes CS, Atala A, Yoo JJ et al. (2003). Cell cycle checkpoint function in bladder cancer. J Natl Cancer Inst 95: 1859–1868.

Doll R, Peto R. (1981). The causes of cancer in the United States today. J. Natl Cancer Inst. 66, 1192–1308.

Downes CS, Clarke DJ, Mullinger AM, Gimenez-Abian JF, Creighton AM, Johnson RT. (1994). A topoisomerase II-dependent G2 cycle checkpoint in mammalian cells.

Earnshaw WC, Laemmli UK. (1983) Architecture of metaphase chromosomes and chromosome scaffolds. J Cell Biol. 96(1):84-93.

Elia AE, Cantley LC, Yaffe MB. (2003A). Proteomic screen finds pSer/ pThr-binding domain localizing Plk1 to mitotic substrates. Science. 299:1228–1231. (A).

Elia AE, Rellos P, Haire LF, Chao JW, Ivins FJ, Hoepker K, Mohammad D, Cantley LC, Smerdon SJ, Yaffe MB. (2003B). The molecular basis for phosphodependent substrate targeting and regulation of Plks by the Polo-box domain. Cell. 115:83–95. (B).

Evans PD, Anderson JR, Vallender EJ, Choi SS, Lahn BT. (2004A). Reconstructing the evolutionary history of microcephalin, a gene controlling human brain size. Hum. Mol. Genet. 13, 1139–1145.

Evans PD, Anderson JR, Vallender EJ, Gilbert SL, Malcom CM, Dorus S, et al. (2004B). Adaptive evolution of ASPM, a major determinant of cerebral cortical size in humans. Hum. Mol. Genet. 13, 489–494.

Evans PD, Gilbert SL, Mekel-Bobrov N, Vallender EJ, Anderson JR, Vaez-Azizi LM, et al. (2005). Microcephalin, a gene regulating brain size, continues to evolve adaptively in humans. Science 309 (5741), 1717– 1720.

Farooq M, Baig S, Tommerup N, Kjaer KW. (2010). Craniosynostosis-microcephaly with chromosomal breakage and other abnormalities is caused by a truncating MCPH1 mutation and is allelic to premature chromosomal condensation syndrome and primary autosomal recessive microcephaly type 1. Am J Med Genet A, 152A:495-497.

Farr CJ, Antoniou-Kourounioti M, Mimmack ML, Volkov A, Porter A. (2014). The α isoform of topoisomerase II is required for hypercompaction of mitotic chromosomes in human cells. *Nucleic Acids Research*, 42(7), pp. 4414–4426.

Finlay BL, Darlington RB (1995). Linked regularities in the development and evolution of mammalian brains. Science, 268(5217):1578-1584.

Fish JL, Kosodo Y, Enard W, Pabo S, Huttner WB. (2006). Aspm specifically maintains symmetric proliferative divisions of neuroepithelial cells. Proc. Natl. Acad. Sci. USA 103, 10438-10443.

Forbes SA, Bindal N, Bamford S, Cole C, Kok CY, Beare D, Jia M, Shepherd R, Leung K, Menzies A, Teague JW, Campbell PJ, Stratton MR, Futreal PA. (2011). COSMIC: mining complete cancer genomes in the catalogue of somatic mutations in cancer. Nucleic Acids Res. 39, D945–D950.

Franchitto A, Oshima J, Pichierri P. (2003). The G2-phase decatena- tion checkpoint is defective in Werner syndrome cells. Cancer Res 63: 3289–3295.

Furniss KL, Tsai HJ, Byl JAW, Lane AB, Vas AC, Hsu WS, Osheroff N, Clarke DJ. (2013). Direct Monitoring of the Strand Passage Reaction of DNA Topoisomerase II Triggers Checkpoint Activation. *PLoS Genetics*, 9(10).

Garshasbi M, Motazacker MM, Kahrizi K, Behjati F, Abedini SS, Nieh SE, et al. (2006). SNP array-based homozygosity mapping reveals MCPH1 deletion in family with autosomal recessive mental retardation and mild microcephaly. Hum. Genet. 118, 708--715.

Gasser SM, Laroche T, Falquet J, Boy de la Tour E, Laemmli UK. (1986) Metaphase chromosome structure. Involvement of topoisomerase II. J Mol Biol. 188(4):613-29.

Gavvovidis I, Pöhlmann C, Marchal JA, Stumm M, Yamashita D, Hirano T, Schindler D, Neitzel H, Trimborn M. (2010). MCPH1 patient cells exhibit delayed release from DNA damage-induced G2/M checkpoint arrest. Cell Cycle. 9(24):4893-9.

Gavvovidis I, Rost I, Trimborn M, Kaiser FJ, Purps J, et al. (2012). A novel MCPH1 isoform complements the defective chromosome condensation of human MCPH1-deficient cells. PLoS One. 7, e40387.

Genin J, Desir N, Lambert M, Biervliet N, Van Der Aa, Pierquin G, et al. (2012). Kinetochore KMN network gene CASC5 mutated in primary microcephaly, Hum. Mol. Genet. 21 5306e5317.

Germann SM, Schramke V, Pedersen RT, Gallina I, Eckert-Boulet N, Oestergaard VH, Lisby M. (2014). TopBP1/Dpb11 binds DNA anaphase bridges to prevent genome instability. J Cell Biol. **204,** 45-59.

Ghafouri-Fard S, Fardaei M, Gholami M, Miryounesi M. (2015). A case report: autosomal recessive microcephaly caused by a novel mutation in MCPH1 gene. Gene, 571: 149–150.

Ghani-Kakhki M, Robinson PN, Morlot S, Mitter D, Trimborn M, Albrecht B, Varon R, Sperling K, Neitzel H. (2012). Two missense mutations in the primary autosomal recessive microcephaly gene MCPH1 disrupt the function of the highly conserved n-terminal BRCT domain of microcephalin. *Molecular Syndromology*, 3(1), pp. 6–13.

Gharshasbi M, Motazacker MM, Kahrizi K, Behjati F, Abedini SS, Nieh SE, et al. (2006). SNP array-based homozygosity mapping reveals MCPH1 deletion in family with autosomal recessive mental retardation and mild microcephaly. Hum Genet. 118:708–15.

Gibbons RJ, Picketts DJ, Villard L, Higgs DR. (1995). Mutations in a putative global transcriptional regulator cause X-linked mental retardation with alpha-thalassemia (ATR-X syndrome). Cell. 80(6):837-45.

Giménez-Abián JF, Clarke DJ, Mullinger AM, Downes CS, Johnson RT. (1995). A postprophase topoisomerase II-dependent chromatid core separation step in the formation of metaphase chromosomes. *J. Cell Biol.* 131, 7–17.

Gimenez-Abian JF, Clarke DJ, Devlin J, Gimenez-Abian MI, De la Torre C, Johnson RT, Mullinger AM, Downes CS. (2000). Premitotic chromosome individualization in mammalian cells depends on topoisomerase II activity. Chromosoma 109: 235–244.

Gorbsky GJ. (1994). Cell cycle progression and chromosome segregation in mammalian cells cultured in the presence of the topoisomerase II inhib- itors ICRF-187 [(+)-1,2-bis(3,5-dioxopiperazinyl-1-yl) propane; ADR-529] and ICRF-159 (Razoxane). Cancer Res. 54, 1042–1048.

Goswami PC, Roti Roti JL, Hunt CR. (1996). The cell cycle-coupled expression of topoisomerase IIa during S phase is regulated by mRNA stability and is disrupted by heat shock or ionizing radiation. Mol Cell Biol 16: 1500–1508.

Green LC, Kalitsis P, Chang TM, Cipetic M, Kim JH, Marshall O, Turnbull L, Whitchurch CB, Vagnarelli P, Samejima K, Earnshaw WC, Choo KH, Hudson DF. (2012). Contrasting roles of condensin I and condensin II in mitotic chromosome formation', *Journal of Cell Science*, 125(6), pp. 1591–1604.

Greer Card DA, Sierant ML, Davey S. (2010). Rad9A is required for G2 decatenation checkpoint and to prevent endoreduplication in response to topoisomerase II inhibition. *Journal of Biological Chemistry*, 285(20), pp. 15653–15661.

Gressens P, Hill JM, Gozes I, Fridkin M, Brenneman DE. (1993). Growth factor function of vasoactive intestinal peptide in whole cultured mouse embryos. Nature;362(6416):155–158.

Gressens P, Hill JM, Paindaveine B, Gozes I, Fridkin M, Brenneman DE. (1994). Severe microcephaly induced by blockade of vasoactive intestinal peptide function in the primitive neuroepithelium of the mouse. J Clin Invest. 94(5):2020–2027.

Griffith JD, Lindsey-Boltz LA, Sancar A. (2002). Structures of the Human Rad17-Replication Factor C and Checkpoint Rad 9-1-1 Complexes Visualized by Glycerol Spray/Low Voltage Microscopy J. Biol.Chem.277, 15233–15236.

Gromova I, Biersack H, Jensen S, Nielsen OF, Westergaard O, Andersen AH. (1998). Characterization of DNA topoisomerase II a/b heterodimers in HeLa cells. Biochemistry 37: 16645–16652.

Gruber R, Zhou Z, Sukchev M, Joerss T, Frappart PO, Wang ZQ. (2011). MCPH1 regulates the neuroprogenitor division mode by coupling the centrosomal cycle with mitotic entry through the Chk1-Cdc25 pathway. Nat Cell Biol. 13, 1325-34.

Guacci V, Koshland D, Strunnikov A. (1997). A direct link between sister chromatid cohesion and chromosome condensation revealed through the analysis of MCD1 in S. cerevisiae. Cell 91:47–57.

Guemez-Gamboa A, Nguyen LN, Yang H, Zaki MS, Kara M, Ben-Omran T, Akizu N, Rosti RO, Rosti B, Scott E, Schroth J, Copeland B, et al. (2015). Inactivating mutations in MFSD2A, required for omega-3 fatty acid transport in brain, cause a lethal microcephaly syndrome. Nature Genet. 47: 809-813.

Guernsey DL, Jiang H, Hussin J, Arnold M, Bouyakdan K, Perry S, Babineau-Sturk T, Beis J, Dumas N, Evans SC, Ferguson M, Matsuoka M, Macgillivray C, Nightingale M, Patry L, Rideout AL, Thomas A, Orr A, Hoffmann I, Michaud JL, et al. (2010). Mutations in centrosomal protein CEP152 in primary micro- cephaly families linked to MCPH4. Am J Hum Genet 87: 40–51.

Hachet V, Canard C, Gonczy P. (2007). Centrosomes promote timely mitotic entry in C. elegans embryos. Dev. Cell. 12:531–541.

Hagting A, Karlsson C, Clute P, Jackman M and Pines J. (1998). MPF local- ization is controlled by nuclear export. EMBO J., 17, 4127–4138.

Hagting A, Jackman M, Simpson K, Pines J. (1999). Translocation of cy- clin B1 to the nucleus at prophase requires a phosphorylation-dependent nuclear import signal. Curr. Biol. 9:680–689.

Hanks S, Coleman K, Reid S, Plaja A, Firth H, Fitzpatrick D, Kidd A, Méhes K, Nash R, Robin N, Shannon N, Tolmie J, Swansbury J, Irrthum A, Douglas J, Rahman N. (2004). Constitutional aneuploidy and cancer predisposition caused by biallelic mutations in BUB1B. Nat Genet. 36(11):1159-61.

Harding B, Moccia N, Drunat A, Soukarieh S, Tubeuf O, Chitty H, Verloes LS, Gressens A, El Ghouzzi P, Joriot V, Di Cunto S, Martins F, Passemard A, Bielas S. (2016). Mutations in citron kinase cause recessive microlissencephaly with multinucleated neurons. Am. J. Hum. Genet. 99: 511-520.

Harper JW, Burton JL, Solomon MJ. (2002) The anaphase-promoting complex: it's not just for mitosis any more. Genes Dev. 16, 2179–2206.

Harrison JC, Haber JE. (2006). Surviving the breakup: the DNA damage checkpoint. Annu Rev Genet 40: 209–235.

Hartwell LH, Kastan MB. (1994). Cell cycle control and cancer. Science. 266:1821–1828.

Hassan MJ, Khurshid M, Azeem Z, John P, Ali G, Chishti MS, Ahmad W. (2007). Previously described sequence variant in CDK5RAP2 gene in a Pakistani family with autosomal recessive primary microcephaly. BMC Med Genet, 8:58-64.

Heck MM, Hittelman WN, Earnshaw WC. (1988). Differential expression of DNA topoisomerases I and II during the eukaryotic cell cycle. *Proc. Natl. Acad. Sci. U. S. A.* 85, 1086–90.

Hemmat M, Rumple MJ, Mahon LW, Morrow M, Zach T, Anguiano A, Elnaggar MM, Wang BT, Boyar FZ. (2017). CMA analysis identifies homozygous deletion of MCPH1 in 2 brothers with primary Microcephaly-1. *Molecular Cytogenetics*. Molecular Cytogenetics, 10(1), p. 33.

Hirano T, Mitchison TJ (1994). A heterodimeric coiled-coil protein required for mitotic chromosome condensation in vitro. Cell 79(3):449-58.

Hirano T, Kobayashi R, Hirano M. (1997). Condensins, chromosome condensation protein complexes containing XCAP-C, XCAP-E and a Xenopus homolog of the Drosophila Barren protein. Cell 89(4):511-21.

Hirano T. (2006). At the heart of the chromosome: SMC proteins in action. *Nature Reviews Molecular Cell Biology*, 7(5), pp. 311–322.

Hirota T. (2004). Distinct functions of condensin I and II in mitotic chromosome assembly. *Journal of Cell Science*, 117(26), pp. 6435–6445.

Hussain MS, Baig SM, Neumann S, Nürnberg G, Farooq M, Ahmad I, et al. (2012). A truncating mutation of CEP135 causes primary microcephaly and disturbed centrosomal function. Am. J. Hum. Genet. 90, 871--878.

Hussain MS, Baig SM, Neumann S, Peche VS, Szczepanski S, Nurnberg G, et al. (2013). CDK6 associates with the centrosome during mitosis and is mutated in a large Pakistani family with primary microcephaly, Hum. Mol. Genet. 5199e5214.

Huyton T, Bates PA, Zhang X, Sternberg MJ, Freemont PS. (2000). The BRCA1 C-terminal domain: structure and function. Mutat Res 2000, 460:319-332.

Iliakis G, Wang Y, Guan J, Wang H. (2003). DNA damage checkpoint control in cells exposed to ionizing radiation. Oncogene; 22:5834–5847.

Insolera R, Bazzi H, Shao W, Anderson KV, Shi SH. (2014). Cortical neurogenesis in the absence of centrioles. Nat Neurosci 17: 1528–1535.

Ishida R, Sato M, Narita T, Utsumi KR, Nishimoto T, Morita T, Na- gata H, Andoh T. (1994). Inhibition of DNA topoisomerase II by ICRF- 193 induces polyploidization by uncoupling chromosome dynamics from other cell cycle events. J. Cell Biol. 126, 1341–1351.

Jackman M, Lindon C, Nigg EA, Pines J. (2003). Active cyclin B1-Cdk1 first appears on centrosomes in prophase. Nat. Cell Biol. 5, 143–148.

Jackson AP, Eastwood H, Bell SM, Adu J, Toomes C, Carr IM, Roberts E, Hampshire, DJ, Crow YJ, Mighell AJ, Karbani G, Jafri H, Rashid Y, Mueller RF, Markham AF and Woods CG. (2002). Identification of microcephalin, a protein implicated in determining the size of the human brain. Am J Hum Genet 71:136-42.

Jackson SP, Bartek J. (2009). The DNA-damage response in human biology and disease. Nature 461: 1071–1078.

Jain CK, Roychoudhury S, Majumder HK. (2015). Selective killing of G2 decatenation checkpoint defective colon cancer cells by catalytic topoisomerase II inhibitor. *Biochimica et Biophysica Acta - Molecular Cell Research*. Elsevier B.V., 1853(5), pp. 1195–1204.

Jamieson CR, Govaerts C, Abramowicz MJ. (1999). Primary autosomal recessive microcephaly: homozygosity mapping of MCPH4 to chromosome 15. (Letter) Am. J. Hum. Genet. 65: 1465-1469.

Jeffers LJ, Coull BJ, Stack SJ, Morrison CG. (2008). Distinct BRCT domains in Mcph1/Brit1 mediate ionizing radiation-induced focus formation and centrosomal localization. Oncogene. 27(1):139-44.

Jo YH, Kim HO, Lee J, Le, SS, Cho CH, Kang IS, et al. (2013). MCPH1 protein expression and polymorphisms are associated with risk of breast cancer. Gene 517, 184--190.

Jo YS, Kim SS, Kim MS, Yoo NJ, Lee SH. (2017). Candidate tumor suppressor gene MCPH1 is mutated in colorectal and gastric cancers. *International Journal of Colorectal Disease*. International Journal of Colorectal Disease, 32(1), pp. 161–162.

Ju B-G, Solum D, Song EJ, Lee K-J, Rose DW, et al. (2004). Activating the PARP-1 sensor component of the groucho/TLE1 corepressor complex mediates a CaMKinaseIIdelta-dependent neurogenic gene activation pathway.

Ju B-G, Lunyak VV, Perissi V, Garcia-Bassets I, Rose DW, et al. (2006). A Topoisomerase IIβ-Mediated dsDNA Break Required for Regulated Transcription. Science 312: 1798–1802.

Kadir R, Harel T, Markus B, Perez Y, Bakhrat A, Cohen I, Volodarsky M, Feintsein-Linial M, Chervinski E, Zlotogora J, Sivan S, Birnbaum RY, Abdu U, Shalev S, Birk OS. (2016). ALFY-

controlled DVL3 autophagy regulates Wnt signaling, determining human brain size. PLoS Genet. 12: e1005919.

Kaindl AM, Passemard S, Kumar P, Kraemer N, Issa L, Zwirner A, Gerard B, Verloes A, Mani S, Gressens P. (2010). Many roads lead to primary autosomal recessive microcephaly. Prog. Neurobiol. 90, 363–383.

Kajii T, Kawai T, Takumi T, Misu H, Mabuchi O, Takahashi Y, Tachino M, Nihei F, Ikeuchi T. (1998). Mosaic variegated aneuploidy with multiple congenital abnormalities: homozygosity for total premature chromatid separation trait. Am J Med Genet. 78(3):245-9.

Kalwinsky DK, Look AT, Ducore J, Fridland A. (1983). Effects of the epipodophyllotoxin VP-16-213 on cell-cycle traverse, DNA-synthesis and DNA strand size in cultures of human-leukemic lymphoblasts. Cancer Res. 43, 1592-1597.

Kastan MB, Bartek J. (2004) Cell-cycle checkpoints and cancer. Nature 432:316–323.

Kaufmann WK, Kies PE. (1998). DNA signals for G2 checkpoint response in diploid human fibroblasts. Mutat Res 400: 153–167.

Kaur M, DeScipio C, McCallum J, Yaeger D, Devoto M, Jackson LG, Spinner NB and Krantz ID. (2005). Precocious sister chromatid separation (PSCS) in Cornelia de Lange syndrome. Am J Med Genet A 138:27-31.

Khan MA, Rupp VM, Orpinell M, Hussain MS, Altmüller J, Steinmetz MO, Enzinger C, Thiele H, Höhne W, Nürnberg G, Baig SM, Ansar M, Nürnberg P, Vincent JB, Speicher MR, Gönczy P, Windpassinger C. (2014). A missense mutation in the PISA domain of HsSAS-6 causes autosomal recessive primary microcephaly in a large consanguineous Pakistani family. Hum Mol Genet. 23, 5940-9.

Kimura K, Rybenkov VV, Crisona NJ, Hirano T, Cozzarelli NR. (1999). 13S condensin actively reconfigures DNA by introducing global positive writhe: implications for chro- mosome condensation. Cell 98:239–248.

Kitagawa H, Fujiki R, Yoshimura K, Mezaki Y, Uematsu Y, et al. (2003). The chromatin-remodelling complex WINAC targets a nuclear receptor to promoters and is impaired in Williams syndrome. Cell 113: 905–917.

Kitajima TS, Sakuno T, Ishiguro K, et al. (2006). Shugoshin collaborates with protein phosphatase 2A to protect cohesin. Nature 441:46–52.

Klingseisen A, Jackson AP. (2011). Mechanisms and pathways of growth failure in primordial dwarfism. Genes Dev 25: 2011–2024.

Koonin EV, Altschul SF, Bork P. (1996). BRCA1 protein products . . . Functional motifs . . . Nat. Genet. 13, 266--268.

Kouprina N, Pavlicek A, Collins NK, et al., (18 co-authors). (2005). The microcephaly ASPM gene is expressed in proliferating tissues and encodes for a mitotic spindle protein. Hum Mol Genet. 14(15):2155–2165.

Kramer A, Mailand N, Lukas C, Syljuasen RG, Wilkinson CJ, Nigg EA, Bartek J, Lukas J. (2004). Centrosome-associated Chk1 prevents pre- mature activation of cyclin-B-Cdk1 kinase. Nat. Cell Biol. 6:884–891.

Krauss MJ, Morrissey AE, Winn HN, Amon E, Leet TL. (2003). Microcephaly: an epidemiologic analysis. Am J Obstet Gynecol, 188:1484-1490.

Kumar A, Markandaya M, Girimaji SC. (2002). Primary microcephaly: micro- cephalin and ASPM determine the size of the human brain. J. Biosci. 27, 629–632.

Kumar SC, Girimaji MR, Duvvari SH. Blanton (2009). Mutations in STIL, encoding a pericentriolar and centrosomal protein, cause primary microcephaly, Am. J. Hum. Genet. 84 286-290.

Laemmli UK. (1978). Levels of organization of the DNA in eucaryotic chromosomes. Pharmacol Rev. 30(4):469-76.

Laemli UK, Kas E, Poljak L, Adachi Y. (1992). Scaffold-associated regions: cis-acting determinants of chromatin structural loops and functional domains. Curr. Opin. Genet. Dev., 2, 275–285.

Lancaster MA, Renner M, Martin CA, Wenzel D, Bicknell LS, Hurles ME, et al. (2013). Cerebral organoids model human brain development and microcephaly. Nature 501, 373--379.

Lane AB, Giménez-Abián JF, Clarke DJ. (2013). A novel chromatin tether domain controls topoisomerase II?? dynamics and mitotic chromosome formation', *Journal of Cell Biology*, 203(3), pp. 471–486.

Langerak P, Russell P. (2011). Regulatory networks integrating cell cycle control with DNA damage checkpoints and double-strand break repair. *Philosophical Transactions of the Royal Society B: Biological Sciences*, 366(1584), pp. 3562–3571.

Lee C, Wevrick R, Fisher RB, Ferguson-Smith MA, Lin CC. (1997). Human centromeric DNAs. Hum Genet 100:291– 304

Leroy JG, Frias JL. (2005). Nonsydromic microcephaly: An overview. Advances in Pediatrics, 52, 261–293.

Leung JW, Leitch A, Wood JL, Shaw-Smith C, Metcalfe K, Bicknell LS, Jackson AP, Chen J. (2011). SET nuclear oncogene associates with microcephalin/MCPH1 and regulates chromosome condensation. J. Biol. Chem. 286, 21393–21400.

Li H, Bielas SL, Zaki MS, Ismail S, Farfara D, Um K, Rosti RO, Scott EC, Tu S, Chi NC, Gabriel S, Erson-Omay EZ, Ercan-Sencicek AG, Yasuno K, Caglayan AO, Kaymakcalan H, Ekici B, Bilguvar K, Gunel M, Gleeson JG. (2016). Biallelic mutations in citron kinase link mitotic cytokinesis to human primary microcephaly. Am. J. Hum. Genet. 99: 501-510, 2016.

Li J, Meyer AN, Donoghue DJ. (1997). Nuclear localization of cyclin B1 mediates its biological activity and is regulated by phosphorylation. Proc. Natl. Acad. Sci. USA. 94:502–507.

Liang Y, Gao H, Lin SY, Peng G, Huang X, Zhang P, Goss JA, Brunicardi FC, Multani AS, Chang S, Li K. (2010). BRIT1/MCPH1 is essential for mitotic and meiotic recombination DNA repair and maintaining genomic stability in mice. PLoS Genet. 6(1):e1000826.

Liang Y, Gao H, Lin SY, Goss JA, Du C, Li K. (2014). Mcph1/Brit1 deficiency promotes genomic instability and tumor formation in a mouse model. Oncogene doi: 10.1038/onc.2014.367.

Lin SY, Rai R, Li K, Xu ZX, Elledge SJ. (2005). BRIT1/MCPH1 is a DNA damage responsive protein that regulates the Brca1-Chk1 pathway, implicating checkpoint dysfunction in microcephaly. Proc Natl Acad Sci U S A. 102(42):15105-9.

Lin SY, Liang Y, Li K. (2010). Multiple Roles of BRIT1/MCPH1 in DNA Damage Response, DNA Repair, and Cancer Suppression. *Yonsei Med. J.* 51, 295.

Lindqvist A, van Zon W, Karlsson Rosenthal C, Wolthuis RM. (2007). Cyclin B1-Cdk1 activation continues after centrosome separation to control mitotic progression. PLoS Biol. 5,e123.

Lindqvist A, Rodríguez-Bravo V, Medema RH. (2009). The decision to enter mitosis: feedback and redundancy in the mitotic entry network. J Cell Biol. 185, 193-202.

Liu J, Krantz ID. (2008). Cohesin and human disease. Annu Rev Genomics Hum Genet. 9:303-20. doi: 10.1146/annurev.genom.9.081307.164211.

Liu X, Zhou ZW, Wang ZQ. (2016). The DNA damage response molecule MCPH1 in brain development and beyond. *Acta Biochimica et Biophysica Sinica*, 48(7), pp. 678–685. doi: 10.1093/abbs/gmw048.

Lizarraga SB, Margossian SP, Harris MH, Campagna DR, Han AP, Blevins S, et al. (2010). Cdk5rap2 regulates centrosome function and chromosome segregation in neuronal progenitors. Development 137, 1907--1917.

Lobanenkov VV, Nicolas RH, Adler VV, Paterson H, Klenova EM, Polotskaja AV, Goodwin GH. (1990). A novel sequence-specific DNA binding protein which interacts with three regularly spaced direct repeats of the CCCTC-motif in the 5′- flanking sequence of the chicken c-myc gene. Oncogene, 5(12): 1743–1753. PMID:2284094.

Losada A, Hirano M, Hirano T. (1998). Identification of Xenopus SMC protein complexes required for sister chromatid cohesion. Genes Dev 12:1986–1997.

Losada A, Hirano M, Hirano T. (2002). Cohesin release is required for sister chromatid resolution, but not for condensin-mediated compaction, at the onset of mitosis. Genes Dev. 16(23):3004-16.

Losada A, Hirano T. (2005A). Dynamic molecular linkers of the genome: the first decade of SMC proteins. Genes Dev 19:1269–1287.

Losada A, Yokochi T, Hirano T. (2005B). Functional contribution of Pds5 to cohesin-mediated cohesion in human cells and Xenopus egg extracts. J Cell Sci 118:2133–2141.

Lukas J, Lukas C, Bartek J. (2004). Mammalian cell cycle checkpoints: Signalling pathways and their organization in space and time. *DNA Repair*, 3(8–9), pp. 997–1007.

Luo K, Yuan J, Chen J, Lou Z. (2008). Topoisomerase IIalpha controls the decatenation checkpoint. Nat Cell Biol. 11(2):204-10.

Lynn R, Giaever G, Swanberg SL, Wang JC. (1986). Tandem regions of yeast DNA topoisomerase II share homology with different subunits of bacterial gyrase. Science, 233, 647–649.

Macurek L, Lindqvist A, Lim D, Lampson MA, Klompmaker R, Freire R, Clouin C, Taylor SS, Yaffe MB, Medema RH. (2008). Polo-like kinase-1 is activated by aurora A to promote checkpoint recovery. Nature. 455:119–123.

Madaule P, Furuyashiki T, Reid T, Ishizaki T, Watanabe G, Morii N, Narumiya S. (1995). A novel partner for the GTP-bound forms of rho and rac. FEBS Lett. 377: 243-248.

Maeshima K, Laemmli UK. (2003) A two-step scaffolding model for mitotic chromosome assembly. Dev Cell. 4(4):467-80.

Maeshima K, Eltsov M, Laemmli UK. (2005). Chromosome structure: improved immunolabeling for electron microscopy. Chromosoma 114: 365–375.

Mahmood S, Ahmad W, Hassan MJ. (2011). Autosomal Recessive Primary Microcephaly (MCPH): clinical manifestations, genetic heterogeneity and mutation continuum. Orphanet J Rare Dis. 6, 39.

Makrythanasis P, Maroofian R, Stray-Pedersen A, Musaev D, Zaki MS, Mahmoud IG, Selim L, Elbadawy A, Jhangiani SN, Coban Akdemir ZH, Gambin T, Sorte HS, et al. (2018). Biallelic variants in KIF14 cause intellectual disability with microcephaly. Europ. J. Hum. Genet. 26: 330-339.

Malumbres M, Barbacid M. (2005). Mammalian cyclin-dependent kinases. 30(11).

Mantere T, Winqvist R, Kauppila S, Grip M, Jukkola-Vuorinen A, Tervasmaki A, Rapakko K, et al. (2016). Targeted next-generation sequencing identifies a recurrent mutation in MCPH1 associating with hereditary breast cancer susceptibility. PLoS Genet, 12: e1005816.

Marko JF. (2008). Micromechanical studies of mitotic chromosomes. Chromosome Res. 16:469–497.

Martin CA, Murray JE, Carroll P, Leitch A, Mackenzie KJ, et al. (2016). Mutations in genes encoding condensin complex proteins cause microcephaly through decatenation failure at mitosis. Genes Dev. **30,** 2158-2172.

Matsusaka T, Pines J. (2004). Chfr acts with the p38 stress kinases to block entry to mitosis in mammalian cells. J Cell Biol.166(4):507-16.

Michaelis C, Ciosk R, Nasmyth K. (1997). Cohesins: chromosomal proteins that prevent premature separation of sister chromatids. Cell 91, 35-45.109.

Mikhailov A, Shinohara M, Rieder CL. (2004). Topoisomerase II and histone deacetylase inhibitors delay the G2/M transition by triggering the p38 MAPK checkpoint pathway. J Cell Biol. 166(4):517-26.

Mirzaa GM, Vitre B, Carpenter G, Abramowicz I, Gleeson JG, Paciorkowski AR, et al. (2014). Mutations in CENPE define a novel kinetochore- centromeric mechanism for microcephalic primordial dwarfism, Hum. Genet. 133 (2014) 1023e1039.

Miyazaki WY, Orr-Weaver TL. (1994). Sister-chromatid cohesion in mitosis and meiosis. Annu Rev Genet 28: 167–187.

Mochida GH, Walsh CA. (2001). Molecular genetics of human microcephaly. Curr Opin Neurol, 14:151-156.

Morris-Rosendahl DJ, Kaindl AM. (2015). What next-generation sequencing (NGS) technology has enabled us to learn about primary autosomal recessive microcephaly (MCPH). *Molecular and Cellular Probes*. Elsevier Ltd, 29(5), pp. 271–281.

Murray A, Hunt T. (1993). The cell cycle: An introduction. New York, NY: W.H. Freeman and Company.

Kakar N, Ahmad J, Morris-Rosendahl DJ, Altmuller J, Friedrich K, Barbi G, et al. (2015). STIL mutation causes autosomal recessive microcephalic lobar hol- oprosencephaly, Hum. Genet. 134 45e51.

Nakagawa T, Hayashita Y, Maeno K, Masuda A, Sugito N, Osada H et al. (2004). Identification of decatenation G2 checkpoint impair- ment independently of DNA damage G2 checkpoint in human lung cancer cell lines. Cancer Res 64: 4826–4832.

Nasmyth K, Haering CH. (2005). The structure and function of SMC and kleisin complexes. Annu Rev Biochem 74:595–648.

Natale F, Rapp A, Yu W, Maiser A, Harz H, Scholl A, Grulich S, Anton T, Horl D, Chen W, Durante M, Taucher-Scholz G, Leonhardt H, Cardoso MC. (2017). Identification of the elementary structural units of the DNA damage response. *Nature Communications*, 8.

Neitzel H, Neumann LM, Schindler D, Wirges A, Tonnies H, Trimborn M. (2002). Premature chromosome condensation in humans associated with microcephaly and mental retardation: a novel autosomal recessive condition. Am J Hum Genet. 70, 1015-22.

Nicholas AK, Khurshid M, Desir J, Carvalho OP, Cox JJ, Thornton G, Kausar R, Ansar M, Ahmad W, Verloes A, Passemard S, Misson JP, LindsayS, Gergely F, Dobyns WB, Roberts E, Abramowicz M, Woods CG. (2010). WDR62is associated with the spindle poleandismutatedinhuman microcephaly. Nat Genet 42:1010–1014.

Nitiss JL. (2009). DNA topoisomerase II and its growing repertoire of biological functions. Nat. Rev. Cancer 2009, 9, 327–337.

Nurse P. 1990. Universal control mechanism regulating onset of M-phase. Nature 344: 503–508.

Nurse P. 1994. Ordering S phase and M phase in the cell cycle. Cell 79: 547–550.

Nurse P. 1997. Checkpoint pathways come of age. Cell 91: 865– 867.

O'Driscoll M, Jackson AP, Jeggo PA. (2006). Microcephalin: a causal link between impaired damage response signaling and microcephaly. Cell Cycle 5, 2339-44.

O'Driscoll M, Jeggo PA. (2008). The role of the DNA damage response pathways in brain development and microcephaly: Insight from human disorders. *DNA Repair*, 7(7), pp. 1039–1050.

O'Farrell PH. (2001). Triggering the all-or-nothing switch into mitosis. Trends Cell Biol. 11:512–519.

Ong CT, Corces VG. (2014). CTCF: an architectural protein bridging genome topology and function. Nat. Rev. Genet. 15, 234–246.

Ono T, Losada A, Hirano M, Myers MP, Neuwald AF, Hirano T. (2003). Differential contributions of condensin I and condensin II to mitotic chromosome architecture in vertebrate cells. Cell 115, 109-121.

Ono T, Fang Y, Spector DL, Hirano T. (2004). Spatial and temporal regulation of Condensins I and II in mitotic chromosome assembly in human cells. Mol. Biol. Cell 15, 3296-3308.

Osborn A, Elledge S, Zou L. (2002). Checking on the fork: the DNA- replication stress-response pathway. Trends Cell Biol. 12, 509–516.

Pagnamenta AT, Murray JE, Yoon G, Sadighi Akha E, Harrison V, Bicknell LS, Ajilogba K, Stewart H, Kini U, Taylor JC, Keays DA, Jackson AP, Knight SJ. (2012). A novel nonsense CDK5RAP2 mutation in a Somali child with primary microcephaly and sensorineural hearing loss. Am J Med Genet A;158A:2577-82.

Park I, Avraham HK. (2006). Cell cycle-dependent DNA damage signaling induced by ICRF-193 involves ATM, ATR, CHK2, and BRCA1. Exp Cell Res 312: 1996–2008.

Passemard S, Titomanlio L, Elmaleh M, Afenjar A, Alessandri JL, Andria G, de Villemeur TB, Boespflug-Tanguy O, Burglen L, Del Giudice E, Guimiot F, Hyon C, Isidor B, Megarbane A, Moog U, Odent S, Hernandez K, Pouvreau N, Scala I, Schaer M, Gressens P, Gerard B, Verloes A. (2009). Expandingthe clinicalandneuroradiologic phenotype ofprimary micro- cephaly due to ASPM mutations. Neurology 73:962–969.

Passemard S, Kaindl AM, Titomanlio L, Gerard B, Gressens P, Verloes A. (2011A). Primary Autosomal Recessive Microcephaly. Gene Reviews. Medical Genetics Information Resource.

Passemard S, El Ghouzzi V, Nasser H, Verney C, Vodjdani G, Lacaud A, et al. (2011B). VIP blockade leads to microcephaly in mice via disruption of Mcph1-Chk1 signaling. J. Clin. Invest. 121, 3071--3087.

Paulson JR, Laemmli UK (1977). The structure of histone-depleted metaphase chromosomes. Cell. 12(3):817-28.

Peng G, Yim EK, Dai H, Jackson AP, Burgt Iv, Pan MR, Hu R, Li K, Lin SY. (2009) BRIT1/MCPH1 links chromatin remodelling to DNA damage response. Nat Cell Biol. 11(7):865-72.

Peng G, Lin SY. (2009). BRITI/MCPHI is a multifunctional DNA damage responsive protein mediating DNA repair- associated chromatin remodeling. Cell Cycle, vol.8, no. 19, pp. 3071–3072.

Pfaff KL, Straub CT, Chiang K, Bear DM, Zhou Y, Zon LI. (2007). The zebra fish cassiopeia mutant reveals that SIL is required for mitotic spindle organization. Mol. Cell Biol. 27, 5887–5897.

Pfau RB, Thrush DL, Hamelberg E, Bartholomew D, Botes S, Pastore M, et al. (2013). MCPH1 deletion in a newborn with severe microcephaly and premature chromosome condensation. Eur. J. Med. Genet. 56, 609--613. doi: 10. 1016/j.ejmg.2013.09.007.

Pines J, Rieder CL. (2001) Re-staging mitosis: a contemporary view of mitotic progression. Nat Cell Biol 3: E3–E6.

Piskadlo E, Oliveira RA. (2017). A topology-centric view on mitotic chromosome architecture. *International Journal of Molecular Sciences*, 18(12), pp. 1–21.

Ponting C, Jackson, AP. (2005). Evolution of primary microcephaly genes and the enlargement of primate brains. Curr. Opin. Genet. Dev. 15, 241–248.

Portier N, Audhya A, Maddox PS, Green RA, Dammermann A, Desai A, Oegema K. (2007). A microtubule-independent role for centrosomes and aurora a in nuclear envelope breakdown. Dev. Cell. 12:515–529.

Rai R, Dai H, Multani AS, Li K, Chin K, Gray J, Lahad JP, Liang J, Mills GB, Meric-Bernstam F, Lin SY. (2006). BRIT1 regulates early DNA damage response, chromosomal integrity, and cancer. Cancer Cell. 10(2):145-57.

Rai R, Phadnis A, Haralkar S, Badwe RA, Dai H, Li K et al. (2008). Differential regulation of centrosome integrity by DNA damage response proteins. Cell Cycle 7: 2225–2233.

Rakic P. (1988). Specification of cerebral cortical areas. Science 1988, 241(4862):170-176.

Rauch A, Thiel CT, Schindler D, Wick U, Crow YJ, Ekici AB, van Essen AJ, Goecke TO, Al-Gazali L, Chrzanowska KH, Zweier C, Brunner HG, Becker K, Curry CJ, Dallapiccola B, Devriendt K, Dörfler A, Kinning E, Megarbane A, Meinecke P, Semple RK, Spranger S, Toutain A, Trembath RC, Voss E, Wilson L, Hennekam R, de Zegher F, Dörr HG, Reis A. (2008). Mutations in the pericentrin (PCNT) gene cause primordial dwarfism. Science. 319:816-9.

Ray A, Milum K, Battu A, Wani G, Wani AA. (2013). NER initiation factors, DDB2 and XPC, regulate UV radia- tion response by recruiting ATR and ATM kinases to DNA damage sites. DNA Repair (Amst); 12(4):273–83.

Ray A, Mir SN, Wani G, Zhao Q, Battu A, Zhu Q, et al. (2009). Human SNF5/INI1, a component of the human SWI/SNF chromatin remodeling complex, promotes nucleotide excision repair by influencing ATM recruitment and downstream H2AX phosphorylation. Mol Cell Biol; 29(23):6206–19.

Ray A, Blevins C, Wani G, Wani AA. (2016). ATR- and ATM-Mediated DNA damage response is dependent on excision repair assembly during G1 but not in S phase of cell cycle', *PLoS ONE*, 11(7), pp. 1–20.

Rickmyre JL, Dasgupta S, Ooi DL, Keel J, Lee E, Kirschner MW et al. (2007). The Drosophila homolog of MCPH1, a human microcephaly gene, is required for genomic stability in the early embryo. J Cell Sci 120: 3565–3577.

Rieder CL, Cole R. Microtubule disassembly delays the G2-M transition in vertebrates. (2000). Curr Biol;10(17):1067-70.

Ritchie K, Seah C, Moulin J, Isaac C, Dick F, Bérubé NG. (2008) Loss of ATRX leads to chromosome cohesion and congression defects. J Cell Biol. 180(2):315-24.

Roberts E, Hampshire DJ, Pattison L, Springell K, Jafri H, Corry P, Woods CG. (2002). Autosomal recessive primary microcephaly: An analysis of locus heterogenity and phenotypic variation. Journal of Medical Genetics, 39, 718–721.

Robinson HM, Bratlie-Thoresen S, Brown R, Gillespie DA. (2007). Chk1 is required for G2/M checkpoint response induced by the catalytic topoisomerase II inhibitor ICRF-193. Cell Cycle;6(10):1265-7.

Roca J. (1995): The mechanisms of DNA topoisomerases. Trends Biochem. Sci. 20, 156 ± 160.

Roca J, Wang JC. (1994) DNA transport by a type II DNA topoisomerase: evidence in favor of a two-gate mechanism. Cell, 77, 609–616.

Rogakou EP, Pilch DR, Orr AH, Ivanova VS, Bonner WM. (1998). DNA double-stranded breaks induce histone H2AX phosphorylation on serine 139. J. Biol. Chem. 273, 5858–5868.

Rushton JP, Vernon PA, Bons TA. (2007). No evidence that polymorphisms of brain regulator genes Microcephalin and ASPM are associated with general mental ability, head circumference or altruism. Biol. Lett. 3, 157--160.

Saitoh N, Goldberg IG, Wood ER, Earnshaw WC. (1994). ScII: an abundant chromosome scaffold protein is a member of a family of putative ATPases with an unusual predicted tertiary structure. J Cell Biol. 127(2):303-18.

Sandell LL, Zakian VA. (1993). Loss of a yeast telomere: arrest, recovery, and chromosome loss. Cell 75: 729–739.

Santamaria A, Neef R, Eberspacher U, Eis K, Husemann M, Mumberg D et al. (2007). Use of the novel Plk1 inhibitor ZK- Thiazolidinone to elucidate functions of Plk1 in early and late stages of mitosis. Mol Biol Cell 18: 4024–4036.

Shen T, Kaya N, Zhao FL, Lu SG, Cao Y, Herness S, (2005). Co-expression patterns of the neuropeptides vasoactive intestinal peptide and cholecystokinin with the transduction molecules α-gustducin and T1R2 in rat taste receptor cells. Neuroscience; Volume 130, Issue 1, Pages 229-238.

Shi L, Lin Q, Su B. (2015). Estrogen regulation of microcephaly genes and evolution of brain sexual dimorphism in primates Speciation and evolutionary genetics. *BMC Evol. Biol.* 15, 1–10.

Shiloh Y, Kastan MB. (2001). ATM: genome stability, neuronal development, and cancer cross paths. Adv. Cancer Res. 83, 209–254.

Shintomi K, Hirano T. (2010) 'Sister chromatid resolution: A cohesin releasing network and beyond', *Chromosoma*, 119(5), pp. 459–467.

Skoufias DA, Lacroix FB, Andreassen PR, Wilson L, Margolis RL. (2004). Inhibition of DNA decatenation, but not DNA damage, arrests cells at metaphase. Mol Cell 15: 977–990.

St Onge RP, Udell CM, Casselman R, Davey S. (1999). The human G2 checkpoint control protein hRAD9 is a nuclear phosphoprotein that forms complexes with hRAD1 and hHUS1. Mol. Biol. Cell 10: 1985–1995.

Stubblefield E, Wray W. (1971). Architecture of the Chinese hamster metaphase chromosome. Chromosoma. 32(3):262-94.

Stucki M, Jackson SP. (2006). GammaH2AX and MDC1: anchoring the DNA-damage-response machinery to broken chromosomes. DNA Repair 5, 534–543.

Suri M. (2003). What's new in neurogenetics? Focus on 'primary microcephaly. *Eur. J. Paediatr. Neurol.* 7, 389–392.

Swedlow JR, Hirano T. (2003). The making of the mitotic chromosome: modern insights into classical questions. Mol. Cell. 11:557–569.

Syljuåsen RG. (2007). Checkpoint adaptation in human cells. Oncogene. 26, 5833–5839.

Syljuåsen RG, Jensen S, Bartek J et al. (2006). Adaptation to the ionizing radiation-induced G2 checkpoint occurs in human cells and depends on checkpoint kinase 1 and Polo-like kinase 1 kinases. Cancer Res 66:10253–10257.

Tang Z, Shu H, Qi W, Mahmood NA, Mumby MC, Yu H (2006). PP2A is required for centromeric localization of Sgo1 and proper chromosome segregation. Dev Cell 10, 575–585.

Tassan JP, Schultz SJ, Bartek J, Nigg EA. (1994). Cell cycle analysis of the activity, subcellular localization, and subunit composition of human CAK (CDK-activating kinase). J. Cell Biol. 127:467–478.

Terzoudi GI, Manola KN, Pantelias GE, Iliakis G. (2005). Checkpoint abrogation in G2 compromises repair of chromosomal breaks in ataxia telangiectasia cells. *Cancer Research*, 65(24), pp. 11292–11296.

Thornton GK, Woods CG. (2009). Primary microcephaly: do all roads lead to Rome? Trends Genet 25: 501–510.

Tibelius A, Marhold J, Zentgraf H, Heilig CE, Neitzel H, Ducommun B, et al. (2009). Microcephalin and pericentrin regulate mitotic entry via centrosome-associated Chk1. J Cell Biol. 185, 1149-57.

Toczyski DP, Galgoczy DJ, Hartwell LH. (1997). CDC5 and CKII control adaptation to the yeast DNA damage checkpoint. Cell 90: 1097–1106.

Tomkins D, Hunter A, Roberts M. (1979) Cytogenetic findings in Roberts-SC phocomelia syndrome(s). Am J Med Genet. 4(1):17-26.

Tommerup N, Mortensen E, Morten H, Nielsen H, Wegner R-D, Schindler D, Mikkelsen M. (1993). Chromosomal breakage, endomitosis, endoreduplication, and hypersensi- tivity toward radiomimetric and alkylating agents: a possible new autosomal recessive mutation in a girlwith craniosynos- tosis and microcephaly. Hum Genet 92:339–346.

Tonkin ET, Wang TJ, Lisgo S, Bamshad MJ and Strachan T. (2004). NIPBL, encoding a homolog of fungal Scc2-type sister chromatid cohesion proteins and fly Nipped-B, is mutated in Cornelia de Lange syndrome. Nat Genet 36:636-41.

Toyoshima F, Moriguchi T, Wada A, Fukuda M, Nishida E. *et al.* (1998). Nuclear export of cyclin B1 and its possible role in the DNA damage-induced G2 checkpoint. *The EMBO journal*, 17(10), pp. 2728–35.

Toyoshima-Morimoto F, Taniguchi E, Nishida E (2002) Plk1 promotes nuclear translocation of human Cdc25C during prophase. EMBO Rep 3: 341-348.

Toyoshima-Morimoto F, Taniguchi E, Shinya N, Iwamatsu A, Nishida E (2001) Polo-like kinase 1 phosphorylates cyclin B1 and targets it to the nucleus during prophase. Nature 410: 215-220. doi:10.1038/35065617. PubMed: 11242082.

Trimborn M, Bell SM, Felix C, Rashid Y, Jafri H, Griffiths PD, Neumann LM, Krebs A, Reis A, Sperling K, Neitzel H and Jackson AP. (2004). Mutations in microcephalin cause aberrant regulation of chromosome condensation. Am J Hum Genet 75:261-6.

Trimborn M, Richter R, Sternberg N, Gavvovidis I, Schindler D, et al. (2005). The first missense alteration in the MCPH1 gene causes autosomal recessive microcephaly with an extremely mild cellular and clinical phenotype. Hum Mutat 26, 496.

Trimborn M, Schindler D, Neitzel H, Hirano T. (2006). Misregulated chromosome condensation in MCPH1 primary microcephaly is mediated by condensin II. Cell Cycle 5, 322-6.

Trimborn M, Ghani M, Walther DJ, Dopatka M, Dutrannoy V, et al. (2010). Establishment of a mouse model with misregulated chromosome condensation due to defective Mcph1 function. PLoS One 5, e9242.

Tuck C, Zhang T, Potapova T, Malumbres M, Novák B. (2013). Robust mitotic entry is ensured by a latching switch. *Biology Open*, 2(9), pp. 924–931. doi:10.1242/bio.20135199.

Vallender EJ, Lahn BT. (2004). How mammalian sex chromosomes acquired their peculiar gene content. Bioessays 26: 159Y169.

Van Den Berg DJ, Francke U. (1993). Roberts syndrome: a review of 100 cases and a new rating system for severity. Am J Med Genet. 47(7):1104-23.

Van Den Bosch J. (1959). Microcephaly in The Netherlands: a clinical and genetical study. Ann. Hum. Genet. 23, 91–116.

Van Vugt MA, Bras A, Medema RH. (2005). Restarting the cell cycle when the checkpoint comes to a halt. Cancer Res 65: 7037–7040.

Van Vugt MA, Brás A, Medema RH. (2004). Polo-like kinase-1 controls recovery from a G2 DNA damage-induced arrest in mammalian cells. Mol Cell;15(5):799-811.

Vassilev LT, Tovar C, Chen S, Knezevic D, Zhao X, Sun H, Heimbrook DC, Chen L. (2006). Selective small-molecule inhibitor reveals critical mitotic functions of human CDK1. Proc Natl Acad Sci U S A. **103,** 10660-5.

Vega H, Waisfisz Q, Gordillo M, Sakai N, Yanagihara I, Yamada M, van Gosliga D, Kayserili H, Xu C, Ozono K, Jabs EW Inui K, Joenje H. (2005). Roberts syndrome is caused by mutations in ESCO2, a human homolog of yeast ECO1 that is essential for the establishment of sister chromatid cohesion. Nat Genet 37, 468-70.

Venkatesh T, Suresh PS. (2014). Emerging roles of MCPH1: expedition from primary microcephaly to cancer. Eur J Cell Biol. 93(3):98-105.

Volkmer E, Karnitz LM. (1999). Human homologs of Schizosaccharomyces pombe rad1, hus1, and rad9 form a DNA damage-responsive protein complex. J. Biol. Chem. 274: 567–570.

Vos SM, Tretter EM, Schmidt BH, Berger JM. (2011). All tangled up: how cells direct, manage and exploit topoisomerase function. Nat Rev Mol Cell Biol 12: 827–841.

Waizenegger IC, Hauf S, Meinke A, Peters JM. (2000). Two distinct pathways remove mammalian cohesin from chromosome arms in prophase and from centromeres in anaphase. Cell 103, 399-410.

Wang JC. (2002). Cellular roles of DNA topoisomerases: a molecular perspective. *Nature reviews. Molecular cell biology*; 3:430–440.

Wang N, Lu H, Chen W, Gan M, Cao X, Zhang J, Chen L. (2014). Primary microcephaly gene MCPH1 shows a novel molecular biomarker of human renal carcinoma and is regulated by miR-27a. Int J Clin Exp Pathol. 2014 Jul 15;7(8):4895-903.

Wang LH, Schwarzbraun T, Speicher MR, Nigg EA. (2008). Persistence ofDNAthreads in human anaphase cells suggests late completion of sister chromatid decatenation. Chromosoma 117, 123–135.

Watt PM, Hickson ID. (1994). Structure and function of type II DNA topoisomerases. *The Biochemical journal*; 303:681–695.

Wood JL, Singh N, Mer G, Chen J. (2007). MCPH1 functions in an H2AX-dependent but MDC1-independent pathway in response to DNA damage. J Biol Chem. 2007 Nov 30;282(48):35416-23.

Woods CG. (2004). Human microcephaly. Curr Opin Neurobiol 14:112-7.

Woods CG, Basto R. (2014). Microcephaly. *Current Biology*, 24(23), pp. R1109–R111.

Woods CG, Bond J, Enard W. (2005). Autosomal recessive primary microcephaly (MCPH): a review of clinical, molecular, and evolutionary findings. Am J Hum Genet. 76,717-28.

Wray W, Stubblefield E. (1970) A new method for the rapid isolation of chromosomes, mitotic apparatus, or nuclei from mammalian fibroblasts at near neutral pH. Exp Cell Res. 59(3):469-78.

Xiao Z, Chen Z, Gunasekera AH, Sowin TJ, Rosenberg SH, Fesik S, et al. (2003). Chk1 mediates S and G2 arrests through Cdc25A degradation in response to DNA-damaging agents. J Biol Chem 2; 278(24):21767–73. PMID: 12676925.

Xu X, Lee J, Stern DF. (2004). Microcephalin is a DNA damage response protein involved in regulation of CHK1 and BRCA1. J Biol Chem. 279(33):34091-4.

Yajima H, Lee KJ, Zhang S, Kobayashi J, Chen BP. (2009). DNA double-strand break formation upon UV- induced replication stress activates ATM and DNA-PKcs kinases. J Mol Biol; 385(3):800–10.

Yamamoto S, Jaiswal M, Charng WL, Gambin T, Karaca E, Mirzaa G, Wiszniewski W, Sandoval H, Haelterman NA, Xiong B, Zhang K, Bayat V, et al. (2014). A Drosophila genetic resource of mutants to study mechanisms underlying human genetic diseases. Cell 159: 200-214, 2014.

Yamashita D, Shintomi K, Ono T, Gavvovidis I, Schindler D, Neitzel H, Trimborn M, Hirano T. (2011). MCPH1 regulates chromosome condensation and shaping as a composite modulator of condensin II. J Cell Biol. 194, 841-54.

Yang J, Bardes ESG, Moore JD, Brennan J, Power MA, Kornbluth S. (1998). Control of cyclin B1 localization through regulated binding of the nuclear export factor CRM1. Genes Dev. 12, 2131-2143.

Yang YJ, Baltus AE, Mathew RS, Murphy EA, Evrony GD, Gonzalez DM, Wang EP, Walker Marshall, Barry CA, Murn BJ, Tatarakis J, Mahajan A, Samuels MA, Shi HH, Golden Y, Mahajnah JA, Shenhav M, Walsh R. (2012). Microcephaly gene links trithorax and REST/NRSF to control neural stem cell proliferation and differentiation. Cell 151, 1097–1112.

Yoo HY, Kumagai A, Shevchenko A, Shevchenko A, Dunphy WG. (2004). Adaptation of a DNA replication checkpoint response depends upon inactivation of Claspin by the Polo- like kinase. Cell 117: 575–588.

Yu TW, Mochida GH, Tischfield DJ, Sgaier SK, Flores-Sarnat L, Sergi CM, Topcu M, McDonald MT, Barry BJ, Felie JM, Sunu C, Dobyns WB, Folkerth RD, Barkovich AJ, Walsh CA. (2010). Mutations in WDR62, encoding a centrosome-associated protein, cause microcephaly with simplified gyri and abnormal cortical architecture. Nat Genet 42: 1015–1020.

Yuan K, Li N, Huo Y, Yan F, Yang Y, Ward T, et al. (2009). Recruitment of separase to mitotic chromosomes is regulated by Aurora B. Cell Cycle; 8:1433-43.

Yuan JF, Eckerdt J, Bereiter-Hahn E, Kurunci-Csacsko M, Kaufmann, Strebhardt K. (2002). Cooperative phosphorylation including the activity of polo-like kinase 1 regulates the subcellular localization of cyclin B1. Oncogene. 21:8282–8292.

Zhong X, Pfeifer GP, Xu X. (2006). Microcephalin encodes a centrosomal protein. Cell Cycle 5, 457-458.

Zhou ZW, Tapias A, Bruhn C, Gruber R, Sukchev M, Wang ZQ. (2013). DNA damage response in microcephaly development of MCPH1 mouse model. DNA Repair, 12: 645–655.

CURRICULUM VITAE

CURRICULUM VITAE

María de la Cabeza Arroyo López

marroyo@ujaen.es

Licenciada en Biología por la Universidad de Jaén (2012). Máster en Biotecnología y Biomedicina por la Universidad de Jaén (2013). Estudios de Doctorado llevados a cabo en el Programa de Doctorado en Biología Molecular y Celular de la Universidad de Jaén, bajo la supervisión de los Doctores Juan Alberto Marchal Ortega y Antonio Sanchez Baca, contratada con una beca predoctoral del Plan Propio de esta Universidad (Acción 15, ayudas predoctorales para la incentivación del doctorado, 2015-actualidad). Investigadora asociada en laboratorio de Genética en el Departamento de Biología Experimental de la Universidad de Jaén (2012-actualidad), y miembro del grupo de investigación Genética Molecular Humana y Animal (BIO220), Universidad de Jaén. Dos estancias de investigación realizadas en la Universidad de Minnesota, en el "*College of Biological Sciences*, department of *Genetics, Cell Biology and Development"* (Minneapolis, Estados Unidos) bajo la supervisión del Doctor Duncan Clarke: una en 2015, gracias a una ayuda de la Escuela de Doctorado para la realización de estudios de doctorado en Cotutela internacional (seis meses de duración), y otra en 2016, con una ayuda EMBO short-term fellowships (tres meses). Dos artículos publicados como primera autora en revistas internacionales (en 2015 y 2017), cuatro artículos de coautora, y participación en más de 10 congresos y seminarios nacionales e internacionales. Su actividad docente queda reflejada al haber participado como profesora asociada en diversas asignaturas del Grado en Biología de la Universidad de Jaén durante los cursos 2015-2016, 2016-2017 y 2017-2018. Participación en Proyectos de Innovación Docente (planes y equipos de trabajo relacionados con EEES: proyecto titulado "Transferencia de prácticas docentes de trabajo cooperativo del ámbito pre-universitario a la docencia práctica de asignaturas de Grado y Postgrado en la Universidad de Jaén".